



Joule Project JIRP106/03

Oct 2006 – Dec 2008

## **Tapping the Tidal Power Potential of the Eastern Irish Sea**

### **FINAL REPORT**

**March 2009**

**Richard Burrows, Ian Walkington, Nick Yates, Terry Hedges,  
Daoyi Chen, Ming Li, Jianguo Zhou**

Department of Engineering, University of Liverpool, Liverpool L69 3GQ

**Judith Wolf, Roger Proctor, Jason Holt**

Proudman Oceanographic Laboratory, Liverpool L3 5DA

**David Prandle**

Consultant

**[www.liv.ac.uk/engdept/tidalpower](http://www.liv.ac.uk/engdept/tidalpower)**



## CONTENTS

	Page
<b>LIST OF FIGURES</b>	<b>iv</b>
<b>LIST OF TABLES</b>	<b>ix</b>
<b>ACKNOWLEDGEMENTS (and Definition)</b>	<b>xiii</b>
<b>EXECUTIVE SUMMARY</b>	<b>ES.1</b>
<b>1. INTRODUCTION</b>	<b>1.1</b>
1.1 Terms of reference	1.1
1.2 Background	1.1
1.3 Project aims and objectives	1.3
<b>2. PRELIMINARY STUDIES</b>	<b>2.1</b>
2.1 Initial appraisals of barrage potential based on Prandle's approach	2.1
2.2 Reassessment of the 1980s Department of Energy barrage scheme energy estimates	2.2
2.2.1 Conjunctive operation	2.3
<b>3. ENERGY FROM MAJOR BARRAGE SCHEMES (0-D MODELLING)</b>	<b>3.1</b>
3.1 0-D modelling context	3.1
3.2 Dee Estuary and Dee-Wirral Lagoon	3.2
3.2.1 Initial appraisal (ebb generation only)	3.3
3.2.2 Investigating different operating modes	3.5
3.2.2.1 Effect of pumping	3.6
3.2.3 Turbine conditioning	3.7
3.2.3.1 Changing generator capacity	3.7
3.2.3.2 Increasing turbine diameter	3.8
3.2.3.3 Conclusion	3.8
3.2.4 Increasing installed turbine capacity and cost implications arising	3.10
3.2.4.1 Comment and discussion	3.12
3.2.5 Increasing installed sluice capacity and cost implications arising	3.13
3.2.6 Dee Outer Barrage (Dee-Wirral Lagoon)	3.14
3.2.7 Dee Offshore Lagoon	3.15
3.3 Mersey Estuary	3.16
3.3.1 Initial appraisal (ebb generation only)	3.17
3.3.2 Investigating different operating modes	3.17
3.3.2.1 Effect of pumping	3.18
3.3.3 Turbine conditioning	3.19
3.3.3.1 Changing generator capacity	3.19
3.3.4 Increasing installed turbine capacity and cost implications arising	3.21
3.3.4.1 Effect on generation window	3.22
3.3.5 Increasing installed sluice capacity and cost implications arising	3.23
3.3.6 Intertidal area	3.24
3.4 Ribble Estuary	3.28
3.5 Morecambe Bay	3.29
3.5.1 Initial appraisal (ebb generation only)	3.31
3.5.2 Investigating different operating modes	3.31
3.5.2.1 Effect of pumping	3.32
3.5.3 Turbine conditioning	3.33
3.5.3.1 Changing generator capacity	3.33

3.5.4	Increasing installed turbine capacity and cost implications arising	3.35
3.5.5	Increasing installed sluice capacity and cost implications arising	3.36
<b>3.6</b>	<b>Solway Firth</b>	<b>3.36</b>
3.6.1	Initial appraisal (ebb generation only)	3.38
3.6.2	Investigating different operating modes	3.38
3.6.2.1	Effect of pumping	3.39
3.6.3	Turbine conditioning	3.40
3.6.3.1	Changing generator capacity	3.40
3.6.4	Increasing installed turbine capacity and cost implications arising	3.42
3.6.5	Increasing installed sluice capacity and cost implications arising	3.43
3.6.6	Conclusion	3.44
<b>4.</b>	<b>CONJUNCTIVE (MULTI-SCHEME) ENERGY CAPTURE (2-D MODELLING)</b>	<b>4.1</b>
<b>4.1</b>	<b>Introduction</b>	<b>4.1</b>
<b>4.2</b>	<b>Present climate scenario</b>	<b>4.3</b>
4.2.1	Base configuration (1xDoEn)	4.3
4.2.1.1	One-way (ebb) mode operation	4.3
4.2.1.2	Two-way (dual) mode operation	4.5
4.2.2	Tidal stream turbine farm energy capture	4.7
4.2.3	Enhanced energy capture from tripling turbine capacity (3xDoEn)	4.9
4.2.3.1	One-way (ebb) mode operation	4.9
4.2.3.2	Two-way (dual) mode operation	4.11
4.2.4	Combined tidal range (1xDoEn barrages, ebb mode) and tidal stream extraction	4.13
4.2.4.1	Tidal range	4.13
4.2.4.2	Tidal stream	4.14
4.2.5	Summary	4.15
<b>4.3</b>	<b>Future climate scenario</b>	<b>4.16</b>
4.3.1	Tidal range	4.17
4.3.1.1	One-way (ebb) mode operation (1xDoEn)	4.17
4.3.1.2	Two-way (dual) mode operation (3xDoEn)	4.18
4.3.2	Tidal stream	4.20
4.3.3	Combined tidal range (3xDoEn barrages, dual mode) and tidal stream extraction	4.21
4.3.3.1	Tidal range	4.21
4.3.3.2	Tidal stream	4.21
4.3.4	Summary	4.22
<b>5.</b>	<b>ENVIRONMENTAL IMPLICATIONS</b>	<b>5.1</b>
<b>5.1</b>	<b>Introduction</b>	<b>5.1</b>
5.1.1	Generic impacts of tidal power schemes	5.2
5.1.1.1	Physical changes	5.2
5.1.1.2	Environmental and ecological impacts	5.2
5.1.1.3	Human, economic, aesthetic and amenity impacts	5.3
5.1.2	Modelling studies: far-field effects	5.3
<b>5.2</b>	<b>Present hydrodynamics in the Irish Sea (base run)</b>	<b>5.4</b>
<b>5.3</b>	<b>Impact of changes in tide-induced circulation</b>	<b>5.6</b>
5.3.1	One-way (ebb) mode operation (1xDoEn)	5.6
5.3.2	Two-way (dual) mode operation (3xDoEn)	5.8
5.3.3	Environmental implications	5.10
<b>5.4</b>	<b>Impacts on the estuarial waters and intertidal regime</b>	<b>5.11</b>
5.4.1	Introduction	5.11
5.4.2	Case study for the Mersey Estuary	5.13

5.4.2.1	2-D modelling	5.14
5.4.2.2	Environmental implications	5.16
<b>5.5</b>	<b>Impact on sediment regime and induced morphological changes</b>	<b>5.17</b>
<b>5.6</b>	<b>Water quality issues from reduced exchange and sediment disturbance</b>	<b>5.22</b>
5.6.1	Surface water quality	5.22
5.6.2	Contaminated sediments	5.23
<b>5.7</b>	<b>Flood defence</b>	<b>5.25</b>
5.7.1	Flood risk in the estuaries and protection offered by barrages	5.25
5.7.2	Global warming and coastal vulnerability	5.28
5.7.3	Conclusion	5.28
<b>6.</b>	<b>CONCLUSIONS AND RECOMMENDATIONS</b>	<b>6.1</b>
<b>6.1</b>	<b>Conclusions</b>	<b>6.1</b>
<b>6.2</b>	<b>Recommendations</b>	<b>6.2</b>
<b>7.</b>	<b>REFERENCES AND BIBLIOGRAPHY</b>	<b>7.1</b>
<b>APPENDICES</b>		
<b>1.</b>		<b>A.1</b>
A.1.1	The research team	
A.1.2	House of Commons evidence	
A.1.3	Tidal stream energy extraction from estuaries	
<b>2.</b>		<b>A.2</b>
A.2.1	Theoretical background to energy computations (0-D modelling)	
A.2.2	Implication of entry and exit losses in turbine conduits	
A.2.3	Validation of Turgency/Generation Matlab computational routines	
A.2.4	Preliminary studies – potential from barrages on major UK estuaries	
A.2.5	Constructional aspects	
<b>3.</b>		<b>A.3</b>
A.3.1	Barrage lines, cross sections and bathymetries	
A.3.2	Energy computation spreadsheets	
A.3.3	Costing calculations	
<b>4.</b>		<b>A.4</b>
A.4.1	ADCIRC background	
A.4.2	Barrage operation in ADCIRC	
A.4.3	Tidal stream farms in ADCIRC	
A.4.4	Validation of simulation grid	

## LIST OF FIGURES

		<b>Page</b>
Figure 1:	Different modes of operation of a tidal barrage.	ES.2
Figure 2:	The 0-D modelling interface: example for Dee scheme.	ES.3
Figure 3:	ADCIRC tidal modelling domain showing bathymetry and unstructured grid (North West barrages shown inset).	ES.3
Figure 4:	Illustration of power pulses and basin levels for schemes on the Dee.	ES.5
Figure 5:	Intertidal area retained in the Mersey.	ES.6
Figure 6:	1xDoEn schemes in ebb-mode operation (spring output shown inset).	ES.7
Figure 7:	1xDoEn schemes in dual-mode operation (spring output shown inset).	ES.8
Figure 1.3.1:	Schematic illustration of potential barrages initially envisaged.	1.3
Figure 2.2.1.1:	Power output of all barrages with maximum generation window (preliminary studies).	2.4
Figure 2.2.1.2:	Power output of all barrages during spring tides with maximum generation window (preliminary studies).	2.4
Figure 2.2.1.3:	Power output of all barrages during neap tides with maximum generation window (preliminary studies).	2.5
Figure 2.2.1.4:	Power output of all barrages for maximum energy generation (preliminary studies).	2.5
Figure 2.2.1.5:	Power output of all barrages during spring tides for maximum energy generation (preliminary studies).	2.6
Figure 2.2.1.6:	Power output of all barrages during neap tides for maximum energy generation (preliminary studies).	2.6
Figure 3.1.1:	Screen image showing: top – turbine performance characteristics; middle – tidal (green) and basin (blue) level variations; and bottom – power outputs.	3.1
Figure 3.2.1:	Sketch showing the location of a Dee Barrage.	3.2
Figure 3.2.2:	Dee basin area (km <sup>2</sup> ) as a function of water level (mAOD).	3.3
Figure 3.2.1.1:	Illustration of the ebb generating cycle.	3.4
Figure 3.2.1.2:	Effect of delays on annual ebb energy output from Dee Barrage (initial appraisal).	3.4
Figure 3.2.2.1:	Dee Barrage water levels for different operating modes (samples from the spring tidal phase; external tide level in green, basin water level in blue).	3.6
Figure 3.2.3.3.1:	Dee Barrage water levels and power output for 6m diameter turbines; ebb mode.	3.9
Figure 3.2.3.3.2:	Dee Barrage water levels and power output for 8m diameter turbines; ebb mode.	3.9
Figure 3.2.4.1:	Dee Barrage dual mode operation with 80 8m x 10MW turbines.	3.10
Figure 3.2.4.2:	Annual energy output from Dee Barrage operating in ebb and dual modes as a function of number of turbines.	3.11
Figure 3.2.4.3:	Unit cost of energy from Dee Barrage as a function of number of turbines; ebb and dual modes.	3.11
Figure 3.2.4.4.1:	Power output and water levels for different Dee Barrage configurations.	3.12
Figure 3.2.5.1:	Annual energy output and unit cost of energy from Dee Barrage operating in ebb and dual modes with 40 turbines as a function of number of sluices.	3.13

Figure 3.2.5.2:	Annual energy output and unit cost of energy from Dee Barrage operating in ebb and dual modes with 120 turbines as a function of number of sluices.	3.14
Figure 3.2.6.1:	Sketch showing the location of a Dee Outer Barrage (creating a Dee-Wirral Lagoon).	3.14
Figure 3.2.7.1:	Indicative scale of a Dee Offshore Lagoon relative to a Dee-Wirral Lagoon.	3.16
Figure 3.3.1:	Sketch showing the location of a Mersey Barrage.	3.16
Figure 3.3.2:	Mersey basin area (km <sup>2</sup> ) as a function of water level (mAOD).	3.17
Figure 3.3.2.1:	Mersey Barrage water levels for different operating modes (samples from the spring tidal phase; external tide level in green, basin water level in blue).	3.18
Figure 3.3.3.1.1:	Mersey Barrage water levels and power output for 7.6m diameter 23MW turbines; ebb mode.	3.19
Figure 3.3.3.1.2:	Mersey Barrage water levels and power output for 7.6m diameter 11MW turbines; ebb mode.	3.20
Figure 3.3.4.1:	Annual energy output from Mersey Barrage operating in ebb mode, both with and without pumping, as a function of number of turbines.	3.21
Figure 3.3.4.2:	Unit cost of energy from Mersey Barrage as a function of number of turbines; ebb mode.	3.21
Figure 3.3.4.1.1:	Average generation window per tide for Mersey Barrage as a function of operating mode and number of turbines.	3.23
Figure 3.3.5.1:	Annual energy output from Mersey Barrage operating in ebb mode as a function of number of sluices.	3.23
Figure 3.3.5.2:	Unit cost of energy from Mersey Barrage with 27 turbines as a function of number of sluices.	3.23
Figure 3.3.6.1:	Intertidal area retained in the Mersey for 1xDoEn and 2xDoEn schemes in ebb and dual modes with varying time delays for an average (M <sub>2</sub> ) tide.	3.24
Figure 3.3.6.2:	Unmodified tides in the Mersey during the spring to neap to spring cycle.	3.25
Figure 3.3.6.3:	Mersey basin wet area (km <sup>2</sup> , blue) and exposed sediment area (km <sup>2</sup> , red) as a function of water level (mAOD).	3.25
Figure 3.3.6.4:	Intertidal area retained in the Mersey basin by tide with varying time delays; ebb mode, 27 turbines.	3.25
Figure 3.3.6.5:	Intertidal area retained in the Mersey basin by tide with varying time delays; dual mode, 27 turbines.	3.26
Figure 3.3.6.6:	Intertidal area retained in the Mersey basin by tide with varying time delays; ebb mode, 54 turbines.	3.26
Figure 3.3.6.7:	Intertidal area retained in the Mersey basin by tide with varying time delays; dual mode, 54 turbines.	3.26
Figure 3.3.6.8:	Tide and basin water levels in the Mersey for a 27 turbine ebb scheme, 2 hour delay.	3.27
Figure 3.3.6.9:	Tide and basin water levels in the Mersey for a 54 turbine ebb scheme, 0 hour delay.	3.27
Figure 3.3.6.10:	Tide and basin water levels in the Mersey for a 54 turbine ebb scheme; 4 hour delay.	3.28
Figure 3.4.1:	Sketch showing a possible location for a Ribble Barrage.	3.28
Figure 3.4.2:	Ribble basin area (km <sup>2</sup> ) as a function of water level (mAOD).	3.29
Figure 3.5.1:	Sketch showing the location of the Morecambe Bay Outer Barrage.	3.30
Figure 3.5.2:	Morecambe Bay basin area (km <sup>2</sup> ) as a function of water level (mAOD).	3.30

Figure 3.5.2.1:	Morecambe Bay Barrage water levels for different operating modes (samples from the spring tidal phase; external tide level in green, basin water level in blue).	3.32
Figure 3.5.3.1.1:	Morecambe Bay Barrage water levels and power output for 9m diameter 50MW turbines; ebb mode.	3.34
Figure 3.5.3.1.2:	Morecambe Bay Barrage water levels and power output for 9m diameter 16MW turbines; ebb mode.	3.34
Figure 3.5.4.1:	Annual energy output from Morecambe Bay Barrage operating in ebb mode, with and without pumping, as a function of number of turbines.	3.35
Figure 3.5.4.2:	Unit cost of energy from Morecambe Bay Barrage as a function of number of turbines; ebb mode.	3.35
Figure 3.5.5.1:	Annual energy output from Morecambe Bay Barrage operating in ebb mode as a function of number of sluices.	3.36
Figure 3.5.5.2:	Unit cost of energy from Morecambe Bay Barrage with 120 turbines as a function of number of sluices.	3.36
Figure 3.6.1:	Sketch showing the location of a Solway Barrage.	3.37
Figure 3.6.2:	Solway Firth basin area (km <sup>2</sup> ) as a function of water level (mAOD).	3.37
Figure 3.6.2.1:	Solway Firth Barrage water levels for different operating modes (samples from the spring tidal phase; external tide level in green, basin water level in blue).	3.39
Figure 3.6.3.1.1:	Solway Firth Barrage water levels and power output for 9m diameter 40MW turbines; ebb mode.	3.41
Figure 3.6.3.1.2:	Solway Firth Barrage water levels and power output for 9m diameter 16MW turbines; ebb mode.	3.41
Figure 3.6.4.1:	Annual energy output from Solway Firth Barrage operating in ebb mode, both with and without pumping, as a function of the number of turbines.	3.42
Figure 3.6.4.2:	Unit cost of energy from Solway Firth Barrage as a function of number of turbines; ebb mode.	3.42
Figure 3.6.5.1:	Annual energy output from Solway Firth Barrage operating in ebb mode as a function of number of sluices (BODC and DoEn bathymetries).	3.43
Figure 3.6.5.2:	Unit cost of energy from Solway Firth Barrage for 180 turbines as a function of number of sluices.	3.43
Figure 4.1.1:	Total grid used to model the tides in the Irish Sea.	4.1
Figure 4.1.2:	Model grid representation of the Irish Sea.	4.2
Figure 4.1.3:	Model grid in the Dee Estuary.	4.2
Figure 4.2.1.1.1:	Power output from barrages with 1xDoEn capacity operated in ebb mode (typical spring and neap tidal power outputs are shown in the upper and lower right panels, respectively).	4.4
Figure 4.2.1.2.1:	Power output from barrages with 1xDoEn capacity operated in dual mode (typical spring and neap tidal power outputs are shown in the upper and lower right panels, respectively).	4.6
Figure 4.2.2.1:	The locations of the four simulated tidal stream farms: Mersey (blue); Skerries (yellow); West Wales (green); Lynmouth (red).	4.7
Figure 4.2.2.2:	Power output from tidal stream farms.	4.8
Figure 4.2.3.1.1:	Power output from barrages with 3xDoEn capacity operated in ebb mode.	4.10
Figure 4.2.3.2.1:	Power output from barrages with 3xDoEn capacity operated in dual mode.	4.11

Figure 4.2.4.1.1:	Power output from barrages with 1xDoEn capacity operated in ebb mode in conjunction with tidal stream farms.	4.13
Figure 4.2.4.2.1:	Power output from tidal stream farms operated in conjunction with barrages with 1xDoEn capacity in ebb mode.	4.15
Figure 4.3.1.1.1:	Power output from barrages with 1xDoEn capacity operated in ebb mode in future climate scenario.	4.17
Figure 4.3.1.2.1:	Power output from barrages with 3xDoEn capacity operated in dual mode in future climate scenario.	4.19
Figure 4.3.2.1:	Power output from tidal stream farms operated in conjunction with barrages with 3xDoEn capacity in dual mode in future climate scenario.	4.20
Figure 4.3.3.2.1:	Power output from tidal stream farms operated in conjunction with barrages with 3xDoEn capacity in dual mode in future climate scenario.	4.21
Figure 5.2.1:	$M_2$ and $S_2$ co-tidal charts (amplitudes are plotted in green, with contour steps of 20cm and 10cm in left and right charts, respectively, and the phase is plotted in red, with contour steps of $20^\circ$ in both charts).	5.4
Figure 5.2.2:	Plots of (a) stratification parameter and (b) bottom stress magnitude (the contours shown in plot (a) are the stratification parameter values of 2.4, 2.7 and 3.0 moving from black to light grey).	5.5
Figure 5.2.3:	Present residual currents (m/s) in the Irish Sea.	5.6
Figure 5.3.1.1:	Changes induced by barrages installed with 1xDoEn capacity operating in ebb mode to (a) $M_2$ tidal amplitude and (b) bottom stress.	5.7
Figure 5.3.1.2:	Changes due to barrages installed with 1xDoEn capacity operating in ebb mode to (a) stratification parameter and (b) tidal mixing frontal locations.	5.7
Figure 5.3.1.3:	Residual currents (m/s) with 1xDoEn ebb mode operation.	5.8
Figure 5.3.2.1:	Changes due to barrages installed with 3xDoEn capacity operating in dual mode to (a) $M_2$ tidal amplitude and (b) bottom stress.	5.9
Figure 5.3.2.2:	Changes due to barrages installed with 3xDoEn capacity operating in dual mode to (a) stratification parameter and (b) tidal mixing front locations.	5.9
Figure 5.3.2.3:	Residual currents (m/s) with 3xDoEn dual mode operation.	5.10
Figure 5.4.1.1:	Variation in intertidal area exposed through several tidal cycles in the Severn Barrage basin for: (a) spring tide; (b) neap tide.	5.11
Figure 5.4.1.2:	Variation in intertidal area exposed through several tidal cycles in the Mersey Barrage basin for: (a) spring tide; (b) neap tide.	5.12
Figure 5.4.1.3:	Variation in intertidal area exposed through several tidal cycles in the Dee Barrage basin for: (a) spring tide; (b) neap tide.	5.12
Figure 5.4.1.4:	Intertidal area in each basin: (a) tidal-averaged maximum extent; (b) average available. (Note the difference in vertical scales.)	5.13
Figure 5.4.2.1.1:	Present residual currents and bathymetry (m below mean sea level) in the Mersey.	5.15
Figure 5.4.2.1.2:	Residual currents in the Mersey with barrage in 1xDoEn ebb mode operation.	5.15
Figure 5.4.2.1.3:	Residual currents in the Mersey with barrage in 3xDoEn dual mode operation.	5.16
Figure 5.4.2.2.1:	Mudflats in the Mersey Estuary (in green) with present spring tide simulation at (a) low water and (b) high water.	5.17

Figure 5.4.2.2.2:	Mudflats in the Mersey estuary (in green) with 1xDoEn ebb mode, spring tide simulation at (a) low water and (b) high water.	5.17
Figure 5.4.2.2.3:	Mudflats in the Mersey Estuary (in green) with 3xDoEn dual mode, spring tide simulation at (a) low water and (b) high water.	5.17
Figure 5.5.1:	Comparison of observed (HRW) and predicted velocity and sediment flux at the Narrows for mean spring tide.	5.19
Figure 5.5.2:	Variations in water level downstream and upstream of Mersey Barrage.	5.19
Figure 5.5.3:	Velocity residuals near the barrage location.	5.20
Figure 5.5.4:	Comparison of bed-load residuals (a) in an open river and (b) with a barrage.	5.20
Figure 5.5.5:	Bedload transport at the mouth of the Mersey Estuary due to waves with a significant height of 5m and from a dominant north-westly direction in Liverpool Bay.	5.21
Figure 5.6.1.1:	Typical dissolved oxygen levels in the Mersey Estuary (Source: North West Environment Agency Website).	5.22
Figure 5.6.1.2:	Sites around the Mersey for water quality data collection.	5.22
Figure 5.6.2.1:	Sampling sites for sediment quality (indicated by green squares); British Geological Survey.	5.24
Figure 5.7.1.1:	Areas (in blue) in North West England below highest recorded tide level.	5.26
Figure 5.7.1.2.:	Environment Agency flood maps for (a) Solway Firth; (b) Morecambe Bay; and (c) Liverpool Bay.	5.26
Figure 5.7.1.3:	Current Shoreline Management Plans for the North West.	5.27

## LIST OF TABLES

		<b>Page</b>
Table 1:	Energy outputs and unit costs (in pence/kWh) from the 0-D study (Dee Outer Barrage shown inset).	ES.5
Table 2:	Change in tidal amplitude at barrages with 1xDoEn ebb-mode operation.	ES.7
Table 3:	Summary of 2-D modelling results.	ES.9
Table 2.1.1:	Extractable ebb-phase energy according to Prandle's approach, compared with earlier DoEn studies.	2.1
Table 2.2.1:	Total annual output of each barrage according to Turgency/Generation routines and DoEn reports.	2.2
Table 3.2.1.1:	Results of the corroboration calculations for Dee Barrage in ebb mode using 6m diameter 21MW turbines with 40 8m x 12m sluices; minimum water depth at turbines = 20m.	3.3
Table 3.2.1.2:	Effect of varying delay on ebb energy output from Dee Barrage (initial appraisal).	3.5
Table 3.2.1.3:	Revised ebb annual energy output from Dee Barrage using LIDAR bathymetry and 80% as overall efficiency in Turgency/Generation (initial appraisal).	3.5
Table 3.2.2.1:	Annual energy output from Dee Barrage as a function of operating mode.	3.5
Table 3.2.2.1.1:	Annual energy output from Dee Barrage as a function of operating mode, with positive head pumping and optimum delays.	3.7
Table 3.2.3.1.1:	Dee Barrage turbine characteristics as a function of generator capacity (turbine diameter = 6m; hub diameter = 3m).	3.7
Table 3.2.3.1.2:	Annual energy output from Dee Barrage as a function of generator capacity (turbine diameter = 6m; hub diameter = 3m).	3.7
Table 3.2.3.2.1:	Dee Barrage turbine characteristics as a function of generator capacity (turbine diameter = 8m; hub diameter = 3m).	3.8
Table 3.2.3.2.2:	Annual energy output from Dee Barrage as a function of operating mode (turbine diameter = 8m; hub diameter = 3m).	3.8
Table 3.2.3.2.3:	Effect on annual energy from Dee Barrage of changing generator capacity (8m turbines).	3.8
Table 3.2.6.1:	Annual energy output and cost of energy from Dee Outer Barrage.	3.15
Table 3.3.1.1:	Results of the corroboration calculations for Mersey Barrage in ebb mode using 7.6m diameter 23MW turbines with 18 12m x 12m sluices; minimum water depth at turbines = 13m.	3.17
Table 3.3.2.1:	Annual energy output from Mersey Barrage as a function of operating mode.	3.17
Table 3.3.2.1.1:	Annual energy output from Mersey Barrage as a function of operating mode, with positive head pumping and optimum delays.	3.18
Table 3.3.3.1.1:	Mersey Barrage turbine characteristics as a function of generator capacity.	3.19
Table 3.3.3.1.2:	Annual energy output from Mersey Barrage as a function of operating mode with conditioned turbine.	3.19
Table 3.3.3.1.3:	Annual energy output and cost of energy from Mersey Barrage for 7.6m 23MW turbines; 12m x 12m sluices.	3.20
Table 3.3.3.1.4:	Annual energy output and cost of energy from Mersey Barrage for 7.6m 11MW turbines; 12m x 12m sluices.	3.20
Table 3.3.4.1:	2xDoEn scheme - annual energy output and cost of energy from Mersey Barrage for 54 7.6m 23MW turbines; 18 12m x 12m sluices.	3.22

Table 3.3.4.2:	3xDoEn scheme - annual energy output and cost of energy from Mersey Barrage for 81 7.6m 23MW turbines; no separate sluices.	3.22
Table 3.4.1:	Annual energy output from Ribble Barrage as a function of operating mode (11 4m diameter 6.5MW turbines).	3.29
Table 3.4.2:	Cost of energy from Ribble Barrage operating in ebb mode.	3.29
Table 3.5.1.1:	Results of the corroboration calculations for Morecambe Bay Barrage in ebb mode using 9m diameter 50MW turbines with 140 12m x 12m sluices; minimum water depth at turbines = 26m.	3.31
Table 3.5.2.1:	Annual energy output from Morecambe Bay Barrage as a function of operating mode.	3.31
Table 3.5.2.1.1:	Annual energy output from Morecambe Bay Barrage as a function of operating mode, with positive head pumping and optimum delays.	3.32
Table 3.5.3.1.1:	Morecambe Bay Barrage turbine characteristics as a function of generator capacity.	3.33
Table 3.5.3.1.2:	Annual energy output from Morecambe Bay Barrage as a function of operating mode with conditioned turbine.	3.33
Table 3.5.3.1.3:	Annual energy output and cost of energy from Morecambe Bay Barrage for 9m 50MW turbines; 140 12m x 12m sluices.	3.33
Table 3.5.3.1.4:	Annual energy output and cost of energy from Morecambe Bay Barrage for 9m 16MW turbines; 140 12m x 12m sluices.	3.33
Table 3.5.4.1:	Annual energy output and cost of energy from Morecambe Bay Barrage for 360 9m 50MW turbines; 140 12m x 12m sluices (DoEn bathymetry).	3.36
Table 3.6.1.1:	Results of the corroboration calculations for Solway Firth Barrage in ebb mode using 9m diameter 40MW turbines with 200 12m x 12m sluices; minimum water depth at turbines = 23m.	3.38
Table 3.6.2.1:	Annual energy output from Solway Firth Barrage as a function of operating mode.	3.38
Table 3.6.2.1.1:	Annual energy output from Solway Firth Barrage as a function of operating mode, with positive head pumping and optimum delays.	3.39
Table 3.6.3.1.1:	Solway Firth Barrage turbine characteristics as a function of generator capacity.	3.40
Table 3.6.3.1.2:	Annual energy output from Solway Firth Barrage as a function of operating mode with conditioned turbine.	3.40
Table 3.6.3.1.3:	Annual energy output and cost of energy from Solway Firth Barrage for 9m 40MW turbines; 200 12 x 12m sluices.	3.40
Table 3.6.3.1.4:	Annual energy output and cost of energy from Solway Firth Barrage for 9m 16MW turbines; 200 12 x 12m sluices.	3.40
Table 3.6.4.1:	Annual energy output and cost of energy from Solway Firth Barrage for 540 9m 40MW turbines; 200 12m x 12m sluices (DoEn bathymetry).	3.43
Table 4.1.1:	Present tidal component amplitudes at each barrage location.	4.3
Table 4.1.2:	Maximum annual energy available at each barrage line using undisturbed tidal amplitudes, as predicted by the 0-D model.	4.3
Table 4.2.1.1:	Number of turbines, total installed capacity and sluice gate area for each modelled barrage (1xDoEn).	4.3
Table 4.2.1.1.1:	Annual energy outputs from barrages operating in ebb mode (1xDoEn).	4.4
Table 4.2.1.1.2:	Changes in $M_2$ and $S_2$ tidal amplitudes at the barrages operating in ebb mode (1xDoEn).	4.5

Table 4.2.1.1.3:	Predicted annual energy outputs of barrages operating in ebb mode (1xDoEn) from 0-D and ADCIRC models using ADCIRC predictions for tidal regime.	4.5
Table 4.2.1.2.1:	Annual energy outputs from barrages operating in dual mode (1xDoEn).	4.6
Table 4.2.1.2.2:	Changes in $M_2$ and $S_2$ tidal amplitudes at the barrages operating in dual mode (1xDoEn).	4.6
Table 4.2.1.2.3:	Predicted annual energy outputs of barrages operating in dual mode (1xDoEn) from 0-D and ADCIRC models using ADCIRC predictions for tidal regime.	4.7
Table 4.2.2.1:	The installed capacity and rated speed of each tidal stream farm.	4.8
Table 4.2.2.2:	Annual energy production and utilisation rate for the tidal stream farms.	4.9
Table 4.2.2.3:	Annual energy production and utilisation rates for the tidal stream farms with an initial generation velocity of 1m/s.	4.9
Table 4.2.3.1:	Number of turbines, total installed capacity and sluice gate area for each modelled barrage (3xDoEn).	4.9
Table 4.2.3.1.1:	Annual energy outputs from barrages operating in ebb mode (3xDoEn).	4.10
Table 4.2.3.1.2:	Changes in $M_2$ and $S_2$ tidal amplitudes at the barrages operating in ebb mode (3xDoEn).	4.10
Table 4.2.3.1.3:	Predicted annual energy outputs of barrages operating in ebb mode (3xDoEn) from 0-D and ADCIRC models using ADCIRC predictions for tidal regime.	4.11
Table 4.2.3.2.1:	Annual energy outputs from barrages operating in dual mode (3xDoEn).	4.12
Table 4.2.3.2.2:	Changes in $M_2$ and $S_2$ tidal amplitudes at the barrages operating in dual mode (3xDoEn).	4.12
Table 4.2.3.2.3:	Predicted annual energy outputs of barrages operating in dual mode (3xDoEn) from 0-D and ADCIRC models using ADCIRC predictions for tidal regime.	4.12
Table 4.2.4.1.1:	Annual energy outputs from barrages operating in ebb mode (1xDoEn) in conjunction with tidal stream farms.	4.13
Table 4.2.4.1.2:	Changes in $M_2$ and $S_2$ tidal amplitudes at the barrages operating in ebb mode (1xDoEn) in conjunction with tidal stream farms.	4.14
Table 4.2.4.1.3:	Predicted annual energy outputs of barrages operating in ebb mode (1xDoEn) in conjunction with tidal stream farms from 0-D and ADCIRC models.	4.14
Table 4.2.4.1.4:	Differences in annual energy production of barrages operating in ebb mode (1xDoEn) without and with tidal stream farms.	4.14
Table 4.2.4.2.1:	Annual energy outputs from tidal stream farms when operating in ebb mode (1xDoEn) in conjunction with barrages; and the changes from operating alone.	4.15
Table 4.2.5.1:	Annual energy production for each barrage, installed turbine capacity and operating mode.	4.15
Table 4.3.1:	Changes in $M_2$ and $S_2$ tidal amplitudes at the barrages due to the increase in sea level.	4.16
Table 4.3.2:	Maximum annual energy available at each barrage line in present and future climate scenarios, as predicted from 0-D model.	4.17
Table 4.3.1.1.1:	Annual energy output, maximum potential energy and percentage of energy extracted at each barrage operating in ebb mode (1xDoEn) in future climate scenario.	4.18
Table 4.3.1.1.2:	Changes in $M_2$ and $S_2$ tidal amplitudes at the barrages operating in ebb mode (1xDoEn) in future climate scenario.	4.18

Table 4.3.1.1.3:	Predicted annual energy outputs of barrages operating in ebb mode (1xDoEn) from 0-D and ADCIRC models in future climate scenario.	4.18
Table 4.3.1.2.1:	Annual energy output, maximum potential energy and percentage of energy extracted at each barrage operating in dual mode (3xDoEn) in future climate scenario.	4.19
Table 4.3.1.2.2:	Changes in $M_2$ and $S_2$ tidal amplitudes at the barrages operating in dual mode (3xDoEn) in future climate scenario.	4.19
Table 4.3.1.2.3:	Predicted annual energy outputs of barrages operating in dual mode (3xDoEn) from 0-D and ADCIRC models in future climate scenario.	4.20
Table 4.3.2.1:	Annual energy production and utilisation rate for the tidal stream farms in future climate scenario.	4.21
Table 4.3.3.2.1:	Annual energy outputs from tidal stream farms when operating in dual mode (3xDoEn) in conjunction with barrages; and the changes from operating alone in future climate scenario.	4.22
Table 4.3.4.1:	Annual energy output from each barrage in future climate scenario.	4.22
Table 5.4.1.1:	Tidal-averaged maximum intertidal area within each basin.	5.12
Table 5.4.1.2:	Average intertidal area within each basin.	5.13
Table 5.5.1:	Sediment transport rate in the Narrows integrated over a spring tide (range = 8.4m) and a neap tide (range = 4.6m) in both open estuary and barrage scenarios. The values are from the Port Advisory Service (PAS) Mersey Barrage feasibility study (1990) and the present work.	5.21
Table 5.6.1.1:	The River Ecosystem Classification for 2007.	5.23
Table 5.7.1.1:	Average annual equivalent replacement costs of tidal and coastal flood defences.	5.27

## ACKNOWLEDGEMENTS

The work reported herein has been undertaken as part of project JIRP 106/03 funded over the period 2006-2008 by the Northwest Regional Development Agency through the Joule Centre. The views expressed are, however, those of the authors and do not necessarily reflect those of the sponsors or the host institutions in which the work was conducted.

The contribution of the following students in their preliminary appraisal of the software developments and preparatory energy generation investigations is gratefully acknowledged: undergraduates - Russell Butcher, Tom Fitzpatrick, Stuart Robinson, Tim Bradshaw, Stephen Brammer, Sam Whitehurst, Michael Carter and Tom Davies; master's students – Liz Roe and Hui Li; also master's students, Alan Maher and Peter Johnson for their early literature gathering and preliminary evaluations. Thanks to Ben Carroll for contributions from his ongoing computational PhD studies on sediment regime change from barrages on the Dee and Mersey, using complementary 2-D modelling with TELEMAC.

Thanks also to the following individuals approached, directly or otherwise, on this or related matters during the timeframe of the project: George Aggidis (Lancaster University), Dr Stuart Anderson (Conwy District Councillor), Robert Ayres (Faber Maunsell), Hazel Broatch (Bridge-over-the-Bay), Nigel Catterson (Utopia, NB21c), Dr Yiping Chen (Atkins), Professor Roger Falconer (Cardiff University), Anthony Hatton (Peel Holdings), Dr David Howard (CEH), Dr Peter Jones (EA, RSK, POL), Dr Robert Kirby (Severn Tidal Power Group), Ian Leaper (Buro Happold), Peter Nears (Peel Holdings), Professor Stephen Salter (University of Edinburgh), Dr Tom Shaw (Severn Tidal Power Group), David Watson (RSK), Mike Young (Natural England); and to the offices of the Environment Agency for the supply of LIDAR and flood risk data.

### Definition

In what follows later, a 'DoEn' or '1xDoEn' barrage installation is taken as one with installed turbine capacity (and complementary sluicing) consistent with the outcomes of the UK Department of Energy's 1980s studies, with the characteristics of extracting about half the available ebb-phase energy, in a scheme where the basin in ebb-mode of operation drains only to near mean tide (sea) level. This was found from these early studies to yield electricity at minimum cost.

The 'DoEn' or '1xDoEn' installation is adopted as a baseline here because, later, schemes of multiples of this turbine capacity (ie 2xDoEn, 3xDoEn, etc) are considered as alternatives, operating in either ebb mode or in dual (two-way) generation mode.

## EXECUTIVE SUMMARY

### 1 Introduction

The geographical location of the United Kingdom and the seas that surround it provide internationally enviable renewable resources. Technologies for wind power extraction are now mature and an increasing role for the opportunistic capture of this intermittent energy source for the electricity grid is firmly established. Marine wave energy offers even greater scope for the future, with somewhat slower temporal variability but with necessary technological advances still outstanding. Even more exclusive, however, is the potential for tidal energy extraction from around the UK coastline. The most attractive locations for harnessing tidal power are estuaries with a high tidal range for barrages, and other areas with strong tidal currents (e.g. straits and headlands) for free-standing tidal stream devices. Barrage schemes, drawing on established low-head hydropower technology, are fully proven. The La Rance plant in France has now passed its 40<sup>th</sup> year of operation.

Of about 500-1000TWh/year of tidal energy potentially available worldwide (Baker, 1991), Hammons (1993) estimated the UK to hold 50TWh/year, representing 48% of the European resource, and few sites worldwide are as close to electricity users and the transmission grid as those in the UK. Following from a series of government-funded studies commissioned by UKAEA in the 1980s, 8 major estuaries were identified where tidal barrages would be capable of procuring over 40TWh/year. In rank order of scale, they were the Severn, Solway Firth, Morecambe Bay, Wash, Humber, Thames, Mersey and Dee (see UKAEA, 1980 and 1984, Baker, 1991). Thus, about half of this energy was located in the North West of England (House of Commons, 2008).

Also within the Eastern Irish Sea, exploitable tidal stream resources have been identified to the north of Anglesey and to the north of the Isle of Man, with more localised resources in the approaches to Morecambe Bay and the Solway Firth (DTI, 2004). Note, however, that in estuaries it is unlikely that tidal stream options can come close to the energy yield of barrage alternatives. Recent assessments for the Mersey offer estimates of 40-100GWh/year for tidal stream arrays, contrasting with 1200GWh/year estimated for a barrage at an equivalent location (RSK Environmental Ltd, 2007). In a similar vein, whilst tidal lagoons are often mooted as a viable alternative to estuary barrages, offering a similar operational function, it is highly unlikely that they could be realised at a comparable scale and remain competitive on cost against the major barrage schemes cited above.

It should be noted that a barrage merely delays the flux of water as the tidal level changes: holding back the release of water as the tide level subsides under 'ebb generation' so that the 'head' (water level) difference is sufficient for turbine operation; deferring the entry of rising tidal flow to the inner estuary basin for 'flood generation'. In 'dual mode', there is a combination of both. Each mode has some restricting effect as energy is extracted from the tide, so reducing the range of tidal variation within the basin: ebb generation generally uplifts low water levels; flood generation generally reduces high water levels; and dual mode results in smaller changes but to both high and low water levels (see Figure 1). Therefore, a degree of environmental modification is inevitable, but this does not necessarily imply degradation from a physical or ecological perspective, though issues related to protection of habitats need to be confronted.

It is also important to recognise that barrage schemes are unique amongst power installations, being inherently multi-functional infrastructure, offering flood protection, road and rail crossings and significant amenity/leisure opportunities, amongst other features. Thus, a fully holistic treatment of overall cost-benefit is imperative for robust decision-making. It is suggested that, to date, this position has been inadequately addressed, especially in respect of barrages' potential strategic roles in flood defence and transportation planning. It follows, therefore, that apart from the direct appraisal of energy capture, other complementary investigations must be sufficiently advanced to allow proper decision-making

in respect of these 'secondary' functions (as well as the various adverse issues, such as sediment regime change, impact on navigation and environmental modification).

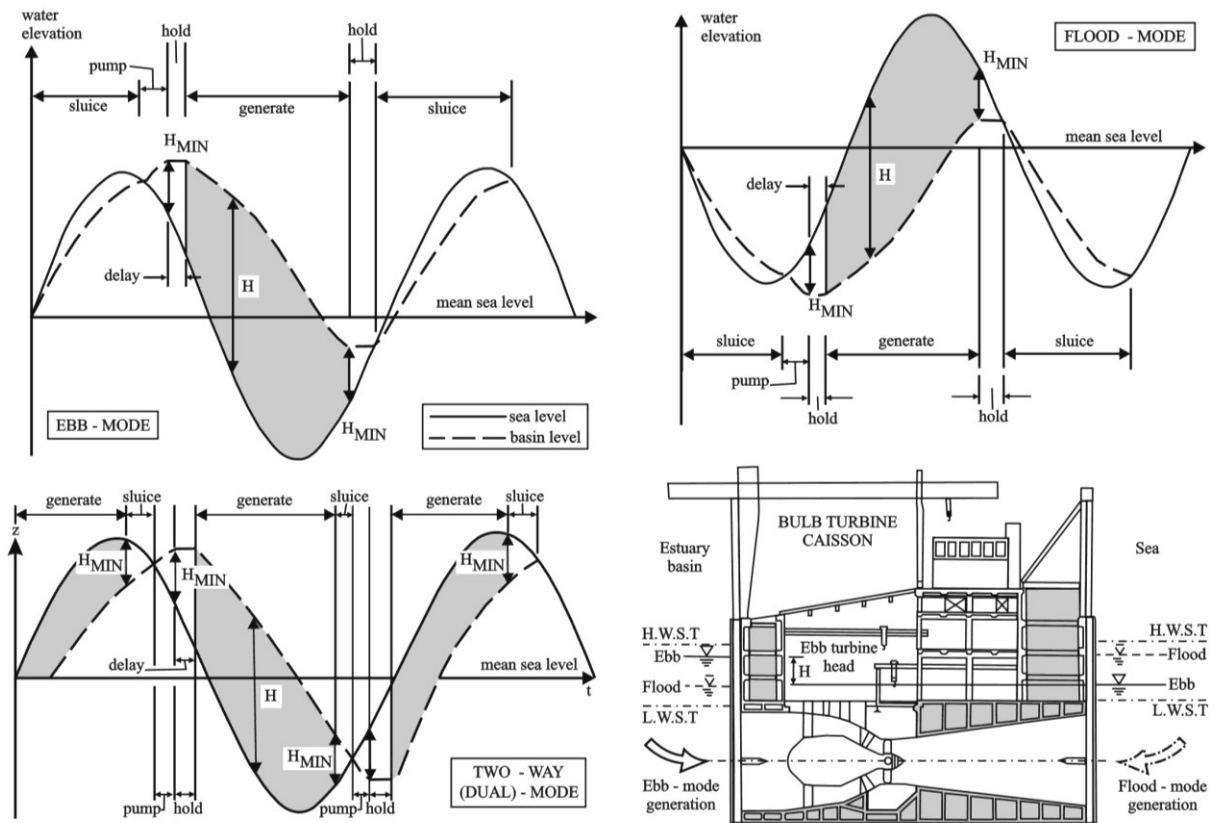


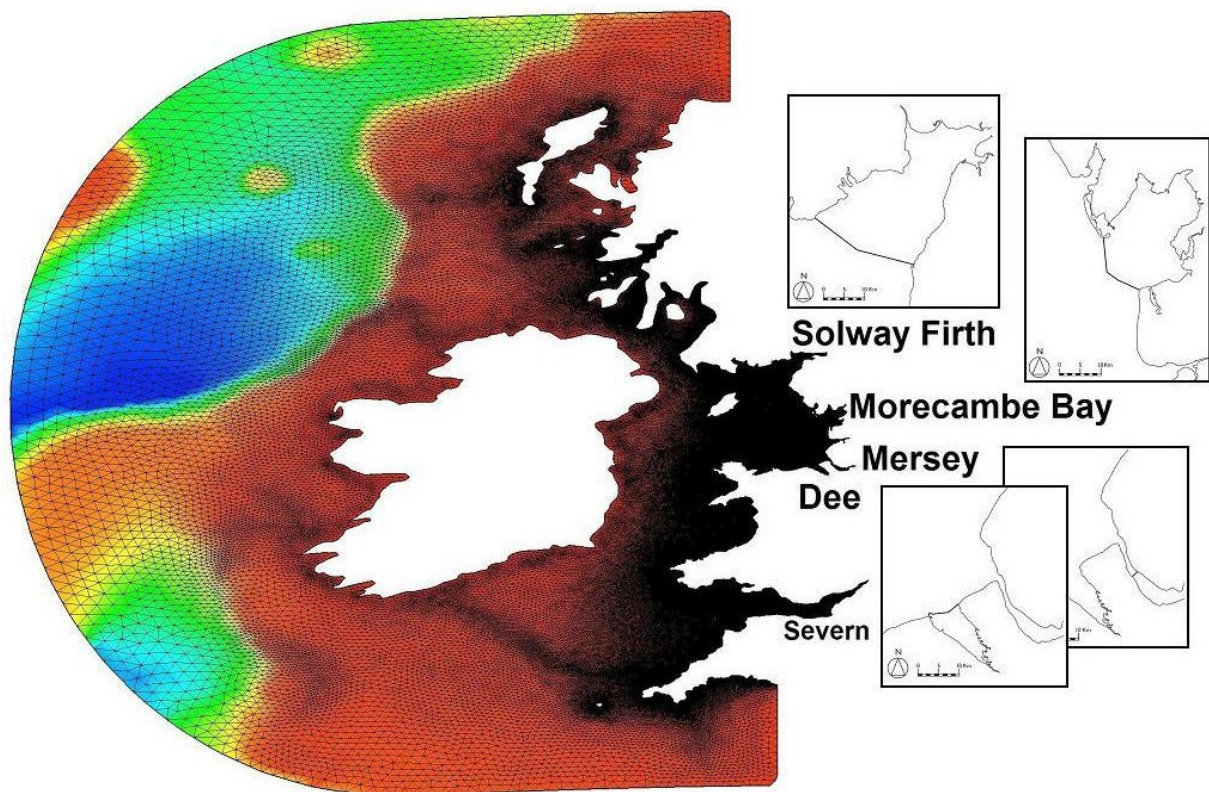
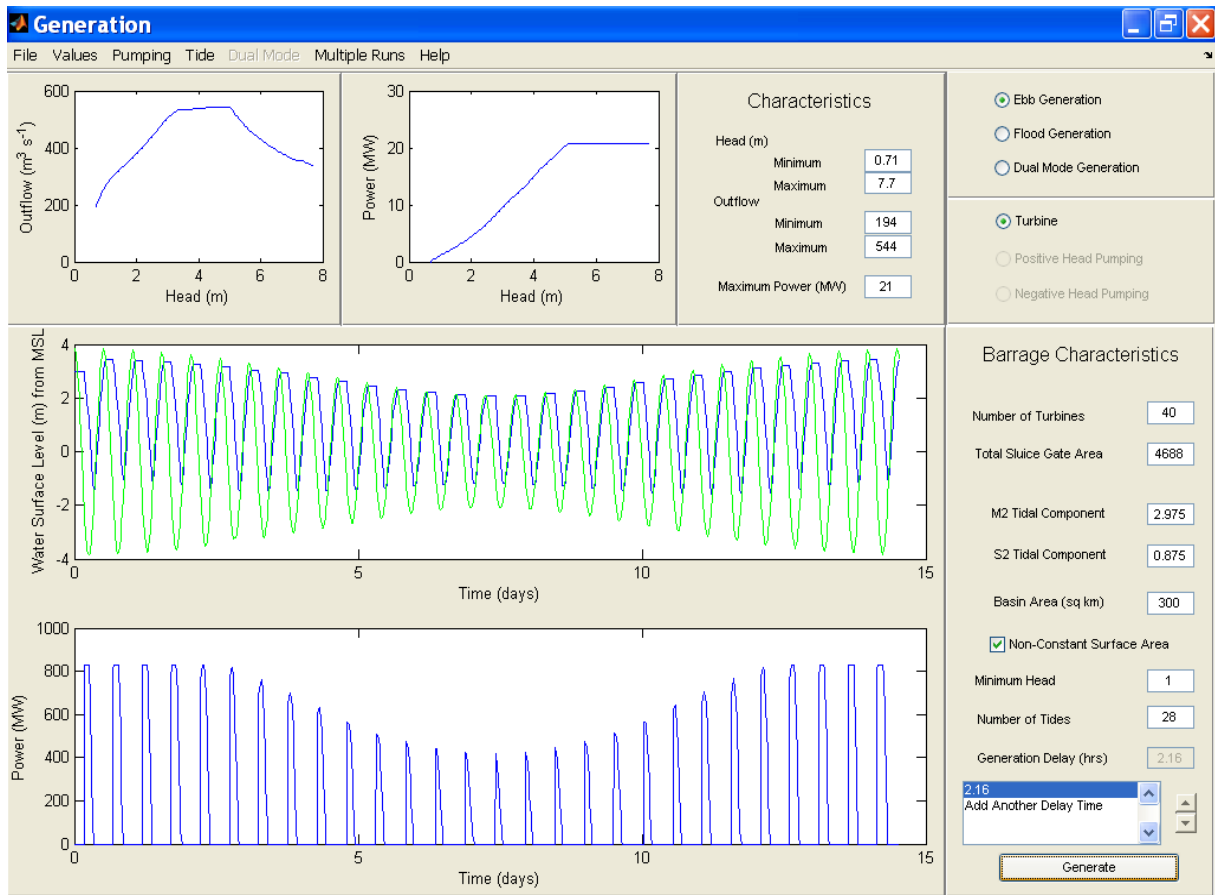
Figure 1: Different modes of operation of a tidal barrage.

## 2 Modelling

The present study aimed to re-appraise the earlier estimates of the potential energy yield from North West barrages and to further this detailed technical scrutiny with assessment of the various operational mode options (ebb, flood or dual) and the broader effects arising from their conjunctive action. To this end, two levels of technical evaluation were explored.

### 2.1 Zero-dimensional (0-D) modelling

Zero-dimensional modelling (employing the  $M_2$ , lunar semi-diurnal, and  $S_2$ , solar semi-diurnal, tidal constituents) was used to synthesise the local behaviour of a barrage with turbine and sluicing systems, assuming flat water levels either side (sometimes referred to as a 'flat-estuary/basin' or 'two-tank' model). This approach rigorously treated the hydraulics and energy generation from the double-regulated bulb turbine systems considered here, but made no allowance for the hydrodynamics of flows arriving at and passing from the barrage. Alternative turbine characteristics could be assimilated, potentially to represent tidal 'fence' or 'reef' systems. The bespoke software routines were developed using MATLAB, with the user interface shown in Figure 2.



## 2.2 Two-dimensional (2-D) modelling

Two-dimensional modelling (employing the 5 major tidal constituents for the region:  $M_2$ ,  $S_2$ ,  $N_2$ ,  $O_1$  and  $K_1$ ) was used to account for the hydrodynamics of the flows arriving at and passing from the barrage structures, and thereby account for energy dissipation by bed friction throughout the modelling domain. Since multiple estuary sites were included, a model domain extending over the whole Irish Sea and beyond was required. In order to incorporate any likely impacts from the operation of a potential Severn barrage in the Bristol Channel, the model domain was extended to cover this region also. The ADCIRC modelling platform adopted employed almost 750,000 cells forming the unstructured finite element grid to be subjected to 2-D depth-averaged modelling of the tidal hydrodynamics, as shown in Figure 3. The model allowed the examination of both the undisturbed and disturbed systems, with the option of including various tidal power schemes.

## 3 Discussion of Results

In the following discussion, a 'DoEn' (or 1xDoEn) barrage installation is taken as one with installed turbine capacity (and complementary sluicing) consistent with the outcomes of the UK Department of Energy's 1980s studies, with the characteristics of extracting about half of the available energy during ebb generation. This arrangement was found in these early studies to yield electricity at minimum cost. Here it is adopted as a baseline because schemes of multiples of this turbine capacity (i.e. 2xDoEn, 3xDoEn, etc) are considered later as alternatives, operating in either ebb mode or for dual (two-way) generation.

### 3.1 Zero-dimensional (0-D) modelling

The 0-D modelling routines consistently under-predicted the DoEn energy generation figures by approximately 15%, this being attributable to different assumptions in the treatment of sluicing characteristics, unquantifiable departures in turbine performance characteristics, and the different levels of tide-to-tide control on the selected optimal generation window. Nevertheless, the work described here confirms the scale of resource predicted by DoEn in the 1980s for ebb-only power generation. These 1xDoEn arrangements are also confirmed as generally leading to the lowest cost of energy produced over a 120-year operating lifetime.

Use of positive head pumping, to uplift the basin water level immediately after flood-phase sluicing has finished, is found to increase energy capture, generally by somewhat less than 10% in ebb-mode operations, and the gain is found to be sensitive to barrage configuration and estuary bathymetry. Higher returns in energy with pumping are found to be achievable from dual (two-way) generation and for schemes of higher installed capacity.

In the 0-D studies, different turbine sizes, generator ratings and sluice capacities were investigated; and the 'best' options selected in summarising outcomes are shown in Table 1 and Figure 4. Whilst these figures are considered to be reasonable estimates of potential energy returns, further turbine conditioning (choice of diameter, generator rating and rated head, etc) and increased sluice capacity might be expected to further enhance energy capture. At the same time, the detailed hydraulic design of turbine ducts and sluice passageways might give rise to minor (entry/exit) head losses, so reducing the turbine driving head and hence the energy production. As a result of these contrasting factors, an uncertainty range in the region of  $\pm 10\%$  would seem appropriate.

Table 1: Energy outputs and unit costs (in pence/kWh) from the 0-D study (Dee Outer Barrage shown inset).

Barrages	1xDoEn Ebb-Mode Energy (TWh/year)		1xDoEn Dual-Mode Energy (TWh/year)		3xDoEn Dual-Mode Energy (TWh/year)	
	Cost (p/kWh)	Cost (p/kWh)	Cost (p/kWh)	Cost (p/kWh)	Cost (p/kWh)	Cost (p/kWh)
Solway Firth	8.44	5.83	7.78	6.71	17.84	5.86
Morecambe Bay	5.83	6.04	5.75	6.46	11.45	7.39
Mersey	1.07	4.28	0.98	5.12	1.72	6.16
Dee	1.35	6.81	1.30	8.15	2.21	10.20
Dee Outer	4.60	8.15				

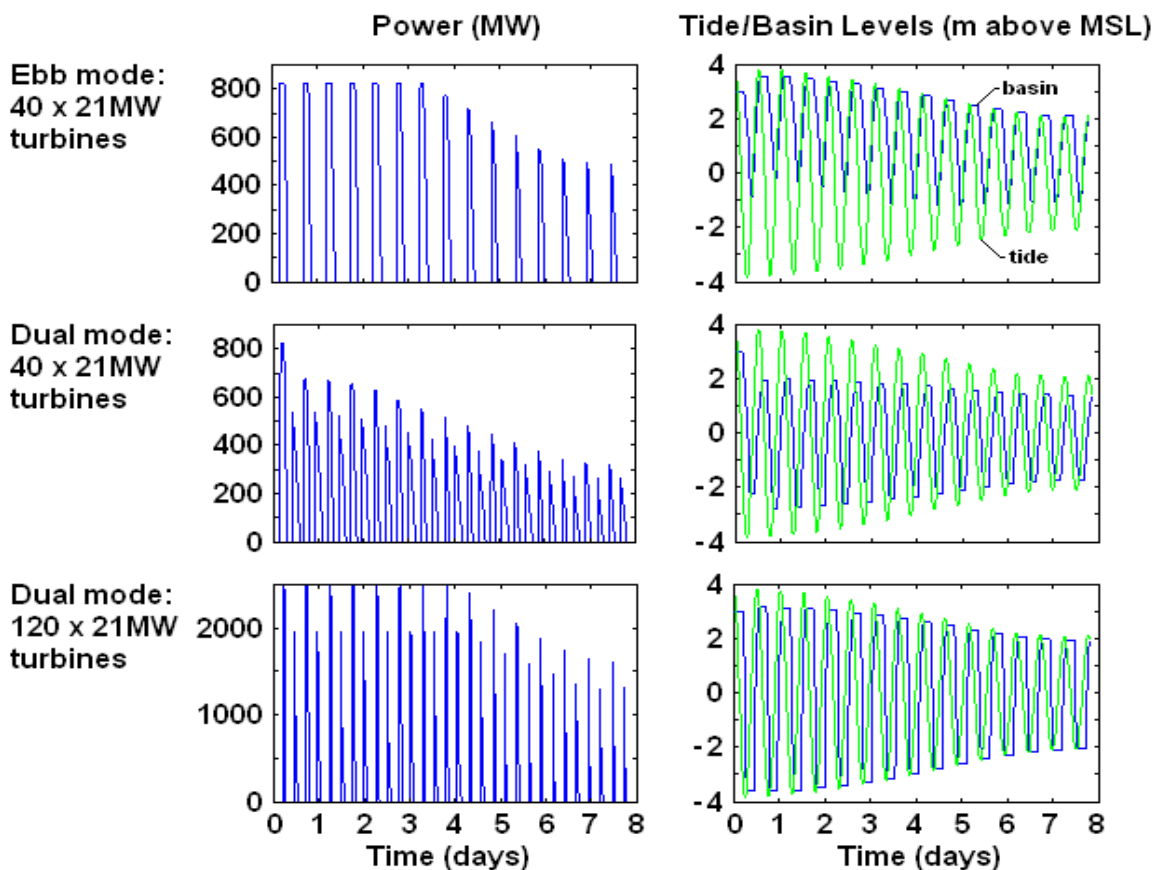
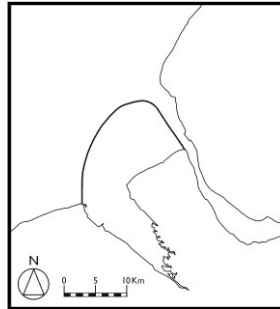


Figure 4: Illustration of power pulses and basin levels for schemes on the Dee.

The figures in Table 1 suggest that ebb-only generation schemes in the North West with 1xDoEn turbine provision could meet about 5% of UK demand at the lowest unit cost of electricity produced, this including the Dee Outer Barrage shown inset. With further scheme optimisation and refined representation of pumping efficiencies, a figure closer to 6% might be achieved.

Dual-mode operation with 1xDoEn turbine installations is typically found to yield energy in the range 78-98% of that achieved from the equivalent ebb mode, and at a cost penalty in the region of 20% on the basis of the turbine having a relative efficiency in the 'reverse' mode of about 80%.

By adopting the relatively more expensive 3xDoEn system installations (3 times the number of turbines) and dual (two-way) generation, with suitably conditioned turbines, the renewable energy capture would theoretically increase to more than 9% of UK consumption. This would be achieved without substantial increase in the unit cost of electricity, according to the assessment made here (but see the outcome of 2-D modelling, below, which finds that these energy returns may not be fully achieved). Adopting higher installed capacity in dual-mode operation mobilises a larger proportion of the tidal prism, as can be seen in Figure 4, so preserving more of the intertidal zone. Such an arrangement would result in a much reduced impact on the environment. In the example of a 3xDoEn scheme on the Mersey, about 90% of the intertidal area would be retained, against about 65% for 1xDoEn ebb operation, as shown in Figure 5 (the curves representing different 'delays' before generation, with that offering maximum energy return shown in the legend). Positive head pumping after flood-phase sluicing would add further to the intertidal zone. Again, these results arise from the 0-D analysis but may not be fully recaptured when accounting for the 2-D hydrodynamics, as discussed later.

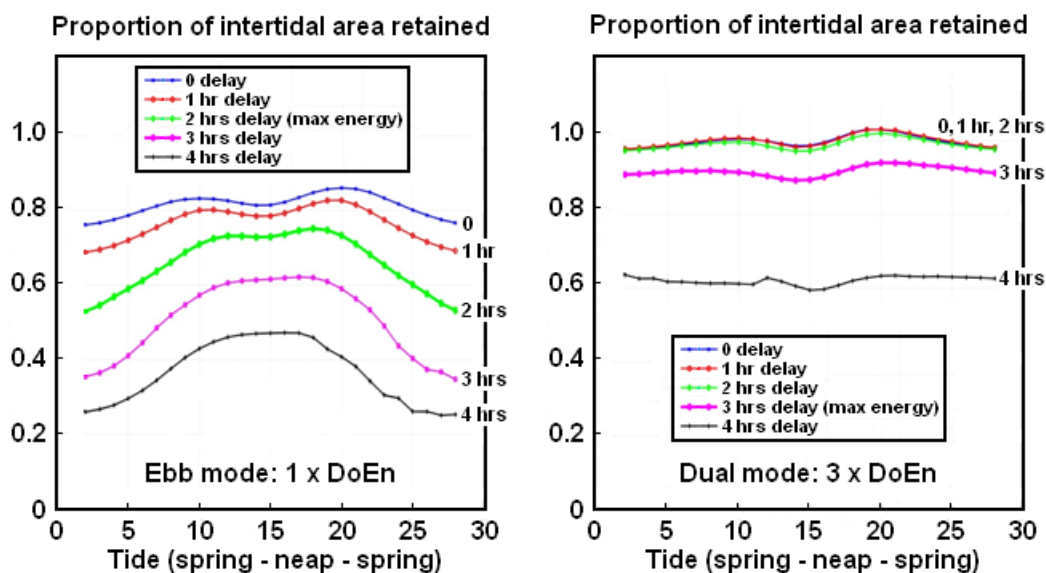


Figure 5: Intertidal area retained in the Mersey.

In the North West estuaries, a combination of ebb-mode and flood-mode operation could provide an extended daily energy generation window. It could only be achieved, however, at the sacrifice of cost effectiveness, since flood-mode operation is found to be typically only 60-70% as efficient as ebb generation. This reduction in efficiency is a result of the reduced volume of the tidal prism which is mobilised, combined with lower turbine driving heads.

### 3.2 Two-dimensional (2-D) modelling

2-D modelling provided an accurate representation of the hydrodynamics of the tidal circulation whilst incorporating the operational behaviour of tidal range devices. It was achieved by introducing the barrage turbine and sluice characteristics as internal boundary conditions in ADCIRC, together with the definition of operational controls via MATLAB routines. Extraction of barrage water levels and turbine flows for energy output was also achieved through routines developed in MATLAB.

Only a limited number of 2-D runs have so far been completed and, for ease of application, unified operational controls were applied (i.e. constant time delay before generation commences across all barrages in the system). As a result, no attempt has been made to replicate the best performance achieved in the 0-D modelling of each individual scheme. Nevertheless, power predictions for the Solway Firth, Morecambe Bay, Mersey, Dee and Severn have been made under conjunctive operation in a number of operating modes, for which changes in tidal amplitude (see Table 2) and timings are directly modelled and are included in the power predictions. Changes in regional hydrodynamics were observed, demonstrating the necessity of modelling all the barrages in conjunction. As a consequence, location specific effects were revealed which altered the power predictions significantly from the 0-D modelling. Furthermore, the 2-D modelling allowed possible changes in local circulation patterns caused by tidal stream farms to be explored.

Figure 6 summarises energy outputs from the 2-D analysis for 1xDoEn ebb-mode generation (with conditions during spring tides shown as an inset). The 2-D modelling demonstrates that the Eastern Irish Sea resources are highly synchronised in tidal phase. They are, however, out of phase with the resource of roughly equivalent scale on the Severn Estuary (potentially supplemented by those on the Wash and the Humber Estuary), making possible extended (about 20 hours) input to the grid from ebb-mode operation.

Table 2: Change in tidal amplitude at barrages with 1xDoEn ebb-mode operation.

Barrages	M <sub>2</sub> component (m)		S <sub>2</sub> component (m)	
	Amplitude	Difference	Amplitude	Difference
Solway Firth	2.50	-0.14	0.80	-0.02
Morecambe Bay	2.84	-0.15	0.92	-0.03
Mersey	2.82	-0.36	0.86	-0.13
Dee	2.32	-0.56	0.68	-0.21
Severn	3.10	-0.80	1.18	-0.19

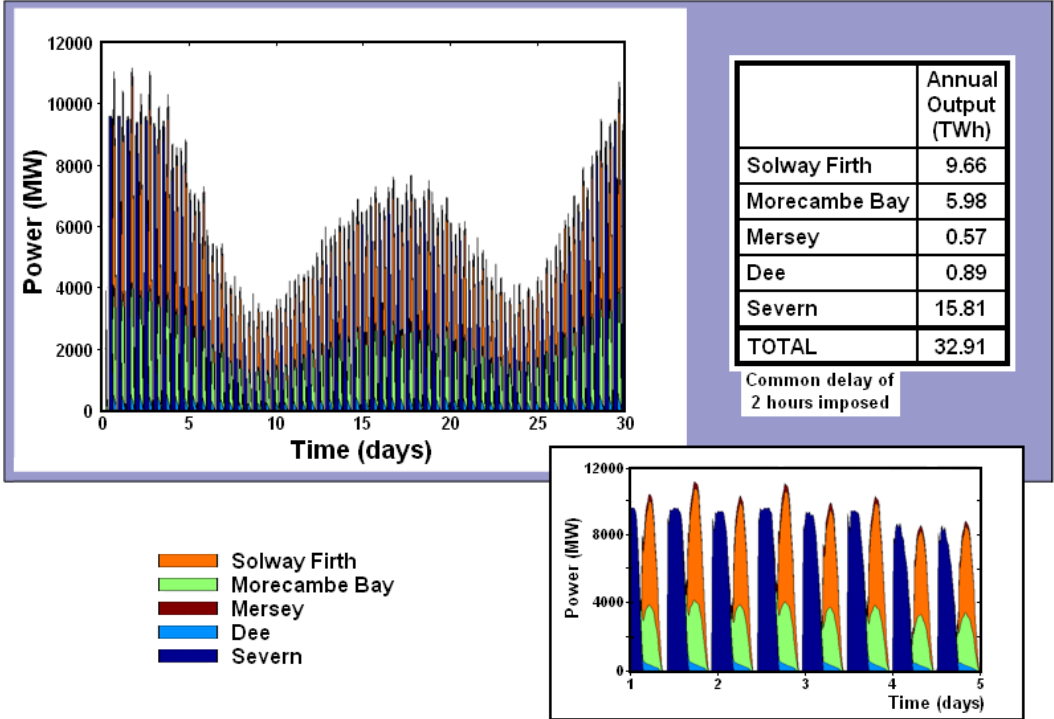


Figure 6: 1xDoEn schemes in ebb-mode operation (spring output shown inset).

Comparing the energy generation from the 2-D model with those from the 0-D modelling for the 1xDoEn schemes, it is seen that predictions are in fair agreement for the Solway Firth and Morecambe Bay, but are significantly lower for the Dee and Mersey. The Dee and Mersey, together with the Severn, suffer a proportionally larger reduction in  $M_2$  and  $S_2$  tidal amplitudes under the conjunctive actions simulated (see Table 2) and this may go some way to explaining the apparent inconsistencies.

For the estuaries with constrained outlets (the Mersey by way of the down river ‘Narrows’ and the Dee by its constrained deep channel and associated skewed turbine/slucice arrangement), the hydraulic flow capacity might also be compromised under enhanced local releases and further exploratory study is called for.

Figure 7 summarises the energy outputs from the 2-D analysis for 1xDoEn dual-mode operation. It confirms that dual-mode operation for schemes sized at the 1xDoEn level are less effective in energy generation (and hence cost) than one-way ebb-mode generation. Furthermore, in this mode the power pulses give rise to higher peaks likely to be more difficult to assimilate into the electricity grid.

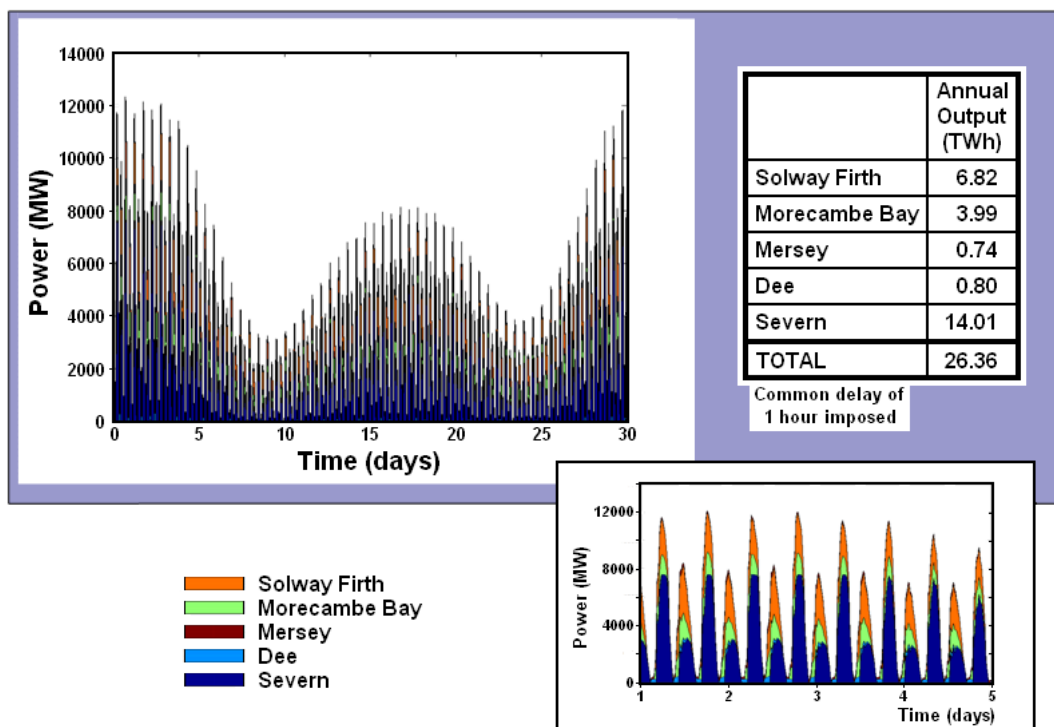


Figure 7: 1xDoEn schemes in dual-mode operation (spring output shown inset).

In contrast to the 1xDoEn schemes, Table 3 indicates that for dual-mode operation with high installed capacity (3xDoEn), the expected payback in energy extraction predicted from 0-D modelling does not materialise. The full explanation for this is unclear, beyond the effect of the reduction in  $M_2$  and  $S_2$  tidal amplitudes experienced at the barrages. The hydrodynamic requirement to shift higher flows to and from the barrages with 3xDoEn installations compared with 1xDoEn capacity is a likely additional factor, resulting in the possibility of transient motions and resonant effects. Computational instabilities and ill-configuration also remain plausible causes.

Table 3: Summary of 2-D modelling results.

Barrages	1xDoEn Ebb-Mode Energy (TWh/year)		1xDoEn Dual-Mode Energy (TWh/year)		3xDoEn Dual-Mode Energy (TWh/year)	
	Solway Firth	9.66		6.82		10.80
Morecambe Bay	5.98		3.99		7.13	
Mersey	0.57		0.74		0.97	
Dee	0.89		0.80		1.35	
	Total Energy (TWh/year)	UK (%)	Total Energy (TWh/year)	UK (%)	Total Energy (TWh/year)	UK (%)
North West	17.10	4.5	12.35	3.2	20.25	5.3
Severn	15.81	4.2	14.01	3.7	20.01	5.3
Total	32.91	8.7	26.36	6.9	40.26	10.6

Notwithstanding these unresolved power generation issues, it seems inevitable that local scour will be a feature beneath the concentrated flow streams arriving at and emerging from both the sluices and the turbine outlets. Physically, these might be designed for in the dredging operations during construction or else will subsequently emerge as self-scour features. Local deepening was embedded in the computational grid for the 2-D modelling in order to avoid computational instabilities. Nevertheless, it may be necessary to investigate a wider scale of deepening to better represent the likely scour induced by the emerging flow jets in order to ensure that hydraulic resistance in this near-field region is suitably represented.

With a reported 64GW mean tidal energy input to the Irish Sea and installed turbine energy extraction capacity in the region of 20GW for 1xDoEn ebb-mode barrage operations in the North West estuaries and in the Severn (giving rise to a mean extraction rate in the region of 5-6GW), some change to tidal circulation might be envisaged. This was one of the main questions to be investigated in the study. The 2-D modelling outcomes for conjunctive operation of the 5 major estuary barrages (Solway Firth, Morecambe Bay, Mersey, Dee and Severn) do manifest discernible changes. At all the barrage locations, the mean tidal amplitudes are reduced (see Table 2) and an increase is experienced on the east coast of Ireland, which whilst small (< 200mm), would need to be fully investigated for impacts on flood risk. Furthermore, the small changes observed to tidal residual currents, bottom stress and stratification parameter within the Irish Sea must be evaluated for their likely influence on such factors as sediment drift, benthic conditions and eutrophication risk, with the associated potential influences on biodiversity and fisheries, etc.

As a result of the inevitable local changes to the flow distribution across the line of a barrage, morphological readjustment by means of new channel formations, etc, will result in a transient state of enhanced sediment mobilisation and potential contaminant release for some time (perhaps several years) before water quality reaches a new dynamic equilibrium. Where this might be an issue, as in industrialised estuaries such as the Mersey, with heavily contaminated sediments, novel approaches might be called for to suppress plume dispersal and for the utilisation or disposal of dredged material.

Tidal-stream devices, in the form of single turbines or multiple units in arrays, or cross-river fences installed in estuaries are unlikely to exploit a significant proportion of the tidal range resource extractable by barrages. A theoretical study conducted within this project suggests that only single figure percentage returns on the equivalent barrage figures are achievable. In the light of this, no concerted attempt has been made to produce a detailed study of tidal stream exploitation in the North West estuaries. However, in the 2-D modelling, tidal-stream farms have been investigated at an exploratory level at sites under consideration for such developments within the modelling domain, including within the Mersey Estuary and the Skerries off the Isle of Anglesey. Installed capacity and turbine rated flow characteristics have been chosen to match those published in recent reports for the various farms. The

principal observation from the indicative tests completed is that the scale of these resources is dwarfed by the estuarial barrage potential, so that Irish Sea tidal stream farm deployments are unlikely to have (other than very local) discernable additional effects on the tidal hydrodynamics compared to those displayed by the conjunctive barrage operations. As an additional cautionary note, it is evident in the 2-D modelling that the tendency for flows to divert around a tidal-stream farm, as a consequence of the blockage, is likely to reduce the fraction of incident energy which is extractable. This is a factor that may not have been properly accounted for in a number of the earlier assessments of tidal stream resources.

#### **4 Other General Comments**

Flood risk benefits from the installation of barrages are likely to be significant, though the review conducted here was not sufficiently focused to provide quantitative data in support of this assertion. Most readily perceived is the protection afforded against tidal flooding, which is likely to increase over the coming century as a result of sea level rise.

Similarly, though less widely appreciated, proactive operation of a barrage scheme should be capable of reducing fluvial (river) flood risk and thereby alleviate the adverse effects of increased river flows arising from climate change. This protection would extend from the estuary shore up-river to the tidal limit and beyond to the furthestmost reach affected by 'backwater' surcharge during the superposition of peak river flow discharge upon high-tide receiving levels. The benefit would be achieved by draining the basin at low tide (and closure of the barrage's sluice/turbine ducts) preceding the arrival of flood water in order to provide a maximum storage volume to absorb the flood. During extreme events, the full turbine complement could forego power generation and instead be operated to pump water from the basin in order to lower the levels until the flood has subsided.

At the time of writing, it remains unconfirmed from the 2-D studies that the substantially greater energy predicted by the 0-D modelling can be achieved from more expensive 3xDoEn turbine installations.

Most unit energy costs arising from the schemes discussed here fall below 10p/kWh on the basis of the low discount rate of 3.5% applied. These costs are likely to be competitive against alternative energy sources, as illustrated in the SDC (2007) report, and will inevitably become increasingly competitive against fossil fuels as the drawdown in these reserves takes place over coming decades. The SDC report goes further and suggests that Treasury rules would permit lower figures of 2.5% to be set in support of infrastructure with 100+ year operational lives, such as those envisaged for tidal barrage installations.

The outcomes presented in this paper provide an outline of what might be achievable in renewable energy procurement from the Eastern Irish Sea. It does not include the further potential for tidal-range energy procurement, of similar major scale, from the shore-attached lagoons suggested for the North Wales coast (Anderson, 2008). From a technical perspective, the work completed merely provides a guide for detailed engineering designs to follow at such time that the national need for additional renewable energy dictates.

#### **5 Concluding Remarks**

1. Barrages on the Solway Firth, Morecambe Bay, Mersey and Dee, operating in ebb-only generation with 1xDoEn turbine provision could meet about 5% of UK demand. With further scheme optimisations and refined representation of pumping efficiencies, a figure close to 6% might be achieved. Based on the scale of the North West's 'economy' at approximately 12% of the UK total, this energy capture should supply about half the North West's present electricity needs.

2. In economic terms, this study has shown that the North West schemes should be no more than 70% more expensive in unit cost of energy produced when compared to that achievable from the Severn with, in each case, lowest costs arising from installations consistent with the Department of Energy's 1980s studies (1xDoEn turbine installations).
3. Increasing turbine provision substantially (to up to 3 times the default provision) would increase energy capture and enable retention of more of the intertidal area in the estuarial basin, so alleviating some of the environmental concerns, but at extra cost of electricity produced.
4. 2-D modelling significantly alters the energy predictions from the 0-D modelling, so demonstrating the necessity of the more rigorous approach.
5. As a consequence of 4 above, further investigation is required to determine how much of the substantial energy increases predicted from 0-D modelling of 3xDoEn installations can be realised in the 2-D modelling. Presently, only about a 20% enhancement has been achieved, in part because of the reduction of tidal amplitudes at the barrage locations.
6. Whilst power production between the North West estuaries and the Severn is fully complementary in ebb-mode operation, dual-mode (two-way) operation would give rise to synchronised and higher peak power pulses for the electricity grid to handle.
7. Earlier studies (DoEn, 1989) reported the potential for an outer line for the Severn barrage producing an additional 6.80TWh/year and barrages on the Wash, Humber and Thames capable of yielding 3.75, 1.65 and 1.37TWh/year, respectively (UKAEA, 1980). Combining these with the 33TWh/year obtained herein for the North West barrages and the Cardiff-Weston Severn barrage scheme (for similar 1xDoEn ebb-mode operation) would achieve a total of about 46.5TWh/year. This should be capable of uplift to around 50TWh/year by addition of positive head pumping, representing 13% of the UK (2005) electricity consumption of 387TWh/year.
8. Further energy capture from other small barrage schemes in estuaries or embayments (DoEn, 1989, Anderson, 2008) should enable tidal range energy extraction to meet 15% of UK energy consumption.
9. Adding an extractable UK tidal stream resource of about 5% (SDC, 2007), would uplift the potential for tidal energy to meet up to 20% of the nation's (present) electricity consumption.
10. Outline studies have been conducted to investigate modest tidal stream generator array deployments, as a demonstration of this capability, within the domain of the 2-D ADCIRC model developed in this project.

## **Acknowledgements**

The work reported herein has been undertaken as part of project JIRP 106/03 funded over the period 2006-2008 by the Northwest Regional Development Agency through the Joule Centre. The views expressed are those of the authors and do not necessarily reflect those of the sponsors or the host institutions in which the work was conducted.

## **References**

- Anderson S (2008). The Resurgam Project: Feasibility Study Brief for a Pilot Commercial Offshore Tidal Energy Storage and Release (TESAR) Scheme and Exhibition Centre on the North Wales Coast, <e-mail cle.dr.stuart.anderson@conwy.gov.uk>.
- Baker AC (1991). Tidal Power, IEE Energy Series 5, Peter Peregrinus Ltd, London.

- Department of Energy (DoEn) (1989). The UK Potential for Tidal Energy from Small Estuaries, ETSU TID 4048-P1, Binnie & Partners, London.
- Department of Trade and Industry (DTI) (2004). Atlas of Marine Renewable Energy Resources: Technical Report, Report no. R1106, ABP Marine Environmental Research Ltd, Southampton.
- Fells Associates (2008). A Pragmatic Energy Policy for the UK, <[www.fellsassociates.com](http://www.fellsassociates.com)>.
- Hammons TJ (1993). Tidal Power, Proceedings of the Institute of Electrical and Electronics Engineers, 81(3), 419-433.
- House of Commons (2008). Renewable Electricity-Generation Technologies. Innovation, Universities, Science and Skills Committee Report, Volume II, HC 216-II, Memorandum 4, Ev 86-91, The Stationery Office, London.
- RSK Environmental Ltd (2007). Mersey Tidal Power Study: an Exploration of the Potential for Renewable Energy, Full Report, <[www.merseytidalpower.co.uk](http://www.merseytidalpower.co.uk)>.
- Sustainable Development Commission (SDC) (2007). Turning the Tide: Tidal Power in the UK, Sustainable Development Commission, London, <[www.sd-commission.org.uk](http://www.sd-commission.org.uk)>.
- United Kingdom Atomic Energy Authority (UKAEA) (1980). Preliminary Survey of Tidal Energy of UK Estuaries, Severn Tidal Power Report STP-102, Binnie & Partners, London.
- United Kingdom Atomic Energy Authority (UKAEA) (1984). Preliminary Survey of Small Scale Tidal Energy, Severn Tidal Power Report STP-4035 C, Binnie & Partners, London.

# 1. INTRODUCTION

## 1.1 Terms of reference

This project, JIRP106/03, running over the period October 2006 - December 2008, was awarded under the first call for proposals on 'Offshore Renewables' by the Joule Centre for Energy Research, a then newly-established partnership of North West Universities, commercial organisations and other stakeholders, with funding from the North West Development Agency.

The study outcomes aimed to place on a firm footing the potential of the North West to achieve electricity contributions (in terms of generating capacity, daily generation window and predictability) towards renewable energy targets by exploitation of its substantial tidal resources. It was hoped that the successful outcome of this study will prompt similar investigations for the coastline in the other regions of the UK, so that a comprehensive portfolio of practically achievable tidal energy reserves and energy generation expectations can be firmly established. Upon implementation, the benefits will fall to both the government and UK population at large by the realisation of a significant, inherently secure and non-climate-damaging component to its energy mix. With full exploitation of tidal power opportunities, both across the UK and worldwide, the global community would make an important advance towards sustainable energy production.

## 1.2 Background

The medium to long-term procurement of energy and the related issue of climate change is set to remain at the top of government and public agendas, both nationally and internationally, for some time to come. No clear perception has yet emerged for a sustainable global energy future and the combination of rapid growth in both economies and populations in the developing world are set to place extreme pressure on fossil fuel reserves. It seems inevitable, therefore, that as the 21<sup>st</sup> century evolves, ever greater utilisation of renewable energy resources must be made if the means for modern living are to be preserved. From the perspective of the global community, it will ultimately become an obligation for all societies to properly and fully exploit the natural energy resources at their disposal for the common good.

The geographical location of the United Kingdom and the seas that surround it provide internationally enviable renewable resources. Technologies for wind power extraction are now mature and an increasing role for the opportunistic capture of this intermittent energy source for the electricity grid is firmly established. Marine wave energy offers even greater scope for the future with a somewhat slower temporal variability but with necessary technological advances still outstanding. Even more exclusive, however, is the potential for tidal energy extraction from around the UK coastline. Crucial here is the fact that tidal barrage solutions, drawing on established low-head hydropower technology, are fully proven. The Rance tidal power plant in France has now passed its 40<sup>th</sup> year of operation (Cottillon, 1978; Frau, 1993).

Suitable sites are relatively few globally. Of about 500-1000TWh/year of energy potentially available worldwide (Baker, 1991), Hammons (1993) estimates the UK to hold 50TWh/year, representing 48% of the European resource; and few sites worldwide are as close to electricity users and the transmission grid as those in the UK. DoEn (1989) identified 16 UK estuaries where tidal barrages would be capable of procuring 44TWh/year and further sites suitable for small-scale installations.

In the context of the future UK energy mix, it is worth noting that the earlier estimates of UK tidal barrage potential amounted to approximately 20% of UK electricity need in the late 1980s and today in the region of 13%, far exceeding the realistic scope of wind sources and

with the added benefit of absolute reliability. In addition to barrage solutions to tidal energy capture, there is also more modest scope for tidal-stream energy generation using submerged rotors, either free standing or as part of a 'tidal fence', these extracting from the kinetic energy of the tidal flows. Although all tidal energy generation is intermittent locally, covering ~10-11 hours per day, tidal lag around the coastline provides an opportunity for the grid input window to be extended to closer to 24 hours. With its complete predictability, and operating in a mix with thermal, hydropower and nuclear production as well as thermal renewables, a fully effective base-load role should be attainable in close proximity to centres of population.

The most attractive locations for harnessing tidal power are estuaries with a high tidal range for barrages and other areas with large tidal currents (e.g. straits and headlands) for free-standing tidal stream turbines. The NW of England is well provided for; it has the estuaries of the Dee, Mersey, Ribble, Wyre, Morecambe Bay and Solway Firth with a macro-tidal range. Based on earlier studies (Baker, 1991), a total installed capacity of 12GW has been estimated (Ribble excluded), with a potential energy yield of at least 17.5TWh/year, approximately 6% of UK national need and by inference in the region of half the North West's electricity demand. Of all potential UK sites, the Mersey with a very narrow mouth, and therefore needing a relatively short barrage length (MBC, 1992), offers power production at the lowest unit cost of all UK sites (DoEn, 1989). Exploitable tidal stream resources have been identified to the north of Anglesey and to the north of the Isle of Man, with more localised resources in Morecambe Bay and the Solway Firth (DTI, 2004).

It should be of crucial strategic value at the highest level for technically robust estimates of the realisable UK tidal energy reserves to be established so that they can properly be assimilated into future energy planning (accepting the 10-15 year time horizons necessary). Thereby, rational implementation might be initiated as and when concerns over energy price or security, or carbon emissions dictate. Furthermore, it is considered paramount that this energy potential be fully appreciated when planning application is received for alternative schemes, which might compromise maximum exploitation of the renewable resource. Such instances might arise, for example, should a tidal stream array or tidal fence installation be promoted where the barrage option remains viable and for which a substantially increased energy capture might be expected.

It should be noted that a barrage solution attempts merely to delay the natural motion of the tidal flux as sea level changes: deferring the entry of rising tidal flow into the inner estuary basin, for so-called 'flood-flow' generation when head (water level difference) is sufficient for turbine operation; holding back the release of water as tide level subsides – 'ebb-flow' generation; or 'dual mode', a combination of both. Each mode has some restricting effect, so reducing the range of tidal variation within the basin, ebb generation uplifting mean water levels, flood flow reducing mean levels and dual mode resulting in little change. A degree of environmental modification is, therefore, inevitable but this does not necessarily imply any serious degradation. Following this line of argument, there now remains a need to re-appraise with detailed technical scrutiny the earlier study estimates of potential barrage energy yield and to further this with assessment of the various operational mode options (ebb, flood or dual) and in conjunctive action, to firmly establish the scope for an extended (near 24 hour) generation window. Focus on the North West of England's estuaries, and supplementing the assessment with evaluation of complementary tidal stream generation as proposed here, provides an ideal starting point.

Tidal-stream devices, in the form of single turbines or multiple units in arrays or cross-river fences, installed in estuaries are unlikely to be able to exploit a significant proportion of the tidal range resource extractable by barrages. A theoretical study (Appendix A.1.3) conducted within this project suggests that only single figure percentage returns on the equivalent barrage figures are achievable. In the light of this, no concerted attempt has been made to produce a detailed study into tidal stream exploitation in the estuaries considered here.

Of course, tidal energy development cannot be considered in isolation, even from the purely maritime perspective. The Eastern Irish Sea is already being used for offshore hydrocarbons and wind energy, with more windfarms planned. Further exploitation of marine renewable energy will have to be managed in conjunction with other uses of this semi-enclosed sea such as waste disposal, fisheries, transport and recreation, as well as oil and gas exploration and marine aggregate extraction. In consequence, impacts of tidal energy extraction upon such matters as the general tidal dynamic of the Irish Sea, and thereby on estuarial sediment fluxes and estuary water retention times, as well as fish migration and spawning conditions, need careful consideration. These needs are in addition to the pursuance of issues relating to ecology, navigation and potential benefits in respect of flood protection, transport and amenity interests when barrage construction is contemplated.

### 1.3 Project aims and objectives

This project aimed to establish a generic regional modelling approach to study the practicable exploitation of tidal energy and potential hydrological, morphological and environmental impacts in the Eastern Irish Sea.

Its principal study objectives, therefore, each with distinctive deliverable outcomes, were:

1. To evaluate the realisable tidal energy potential of the coasts of the North West of England, stretching from the Dee Estuary to the Solway Firth, with regard to the installation of estuary barrages, tidal fence structures or tidal stream rotor arrays, or combinations thereof. The possible barrages are depicted in Figure 1.3.1.
2. To establish the potential daily generation window from optimal conjunctive operation of such devices, taking account of the different possible modes of operation (ebb, flood or dual phase generation) in the case of barrages.
3. To evaluate any impact on the overall tidal dynamics of the Irish Sea as a consequence of this energy extraction and the associated modifications by time lag in estuary momentum exchange.
4. Arising from 3, above, to assess the implications, if any, of biophysical coupling in the marine ecosystem, manifesting water quality or ecological consequences.
5. To ascertain the scale of flood protection benefit likely to accrue from proactive operation of barrages, fully accounting for the worsening effects of sea level rise and change in catchment rainfall regimes as a consequence of climate change, so affecting fluvial flood magnitudes and frequencies.

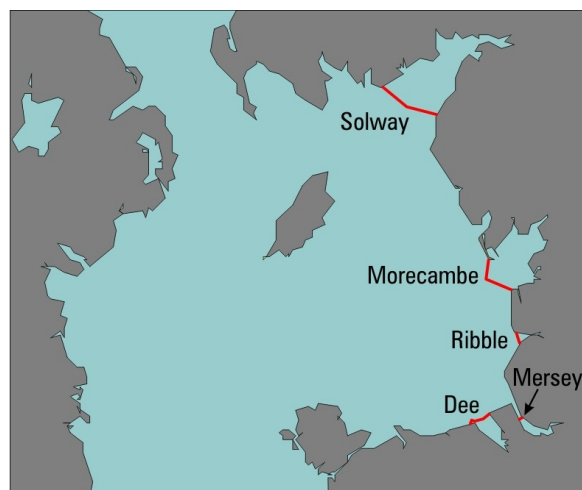


Figure 1.3.1: Schematic illustration of potential barrages initially envisaged.

## 2. PRELIMINARY STUDIES

### 2.1 Initial appraisals of barrage potential based on Prandle's approach

Prandle (1984) presented a simple parametric approach for evaluating the potential energy capture from barrage schemes operated in both ebb and two-way (dual) modes. This approach provides a speedy means of establishing the likely scale of the resource at a given site. Application to the adopted barrage lines at all five of the North West's major estuaries are given below after first giving a résumé of the context and assumptions underpinning the approach.

Prandle's assumptions:

- constant turbine throughflow rate (inconsistent with intended operations; see Appendix A.2.1);
- consider tides of mean amplitude  $A$  (usually taken as  $M_2$ , the lunar semi-diurnal component) only, i.e. no explicit account for spring-neap variations;
- based upon use of fixed basin area  $S$ ;
- operations simulated upon the basis of setting basin 'start level', 'finish level' and 'minimum generating head' as independent variables, with the energy extracted, the installed capacity and the sluicing requirements being the computed dependent variables.

The maximum theoretical energy representing the instantaneous release of water from the basin at high water level to low water level during the ebb phase and the reverse on the flood phase, yields:

$$E_{MAX} = 4\rho g A^2 S \quad (1)$$

where  $g = 9.81\text{m/s}^2$  and  $\rho = 1025\text{kg/m}^3$ .

Prandle's simulations then suggest that the extractable ebb-phase energy per tidal cycle will be:

$$E \approx 0.27 E_{MAX} \quad (2)$$

Table 2.1.1: Extractable ebb-phase energy according to Prandle's approach, compared with earlier DoEn studies.

	$A = M_2$ (m)	$S^{\wedge}$ ( $\text{km}^2$ )	Prandle's Annual Energy (TWh)	DoEn* (1980,1984)	Difference (%)
Solway Firth	2.74	~820	13.10	~12.0	~-8
Morecambe Bay	3.07	~330	6.62	~6.62	~0
Ribble	2.83	~31	0.53		
Mersey	3.23	~62	1.38	~1.54	~12
Dee	2.98	~58	1.10	~1.50	~36

\* Note that the Department of Energy (DoEn) figures given here are those excluding the allowance for losses, taken as 5% for generator efficiency and 10% for machine and transmission outages, subsequently applied to yield their published figures (UKAEA, 1980, 1984).

$\wedge$   $S$  is taken as the surface area at the mid-elevation between  $+1.0 \times M_2$  and  $-0.3 \times M_2$ , i.e.  $+0.35 \times M_2$ .

These simple calculations show a surprisingly close approximation to the much more rigorous and detailed computer-based computations completed as part of the Department of Energy's studies of the 1980s. It is interesting to note that the methodology adopted for the earlier study was based on operating the basin to extract about half the energy available during the ebb phase of the tide only, this being equivalent to 0.25 of the potential energy of the full cycle, and so closely comparable to Prandle's figure of 0.27.

From hereon, a ‘DoEn’ installation is taken as one with installed turbine capacity consistent with the outcomes of the 1980s studies, with the characteristics of extracting half the available ebb-phase energy, in a scheme where the basin in ebb mode of operation drains only to near mean tide (sea) level. This is adopted because, later, schemes of multiples of this turbine capacity (i.e. 2xDoEn, 3xDoEn, etc) are considered as alternatives operating in either ebb mode or in dual (two-way) generation mode.

## 2.2 Reassessment of the 1980s Department of Energy barrage scheme energy estimates

To facilitate the present study, a suite of computational tools was developed for both 0-D (zero-dimensional) modelling (i.e. a ‘flat estuary/basin’ approach to barrage function) and 2-D modelling, capable of treating in detail the hydrodynamics external to the barrage structures. The latter is considered in chapter 4.

For the 0-D approach, the methodology adopted was that presented in the text ‘Tidal Power’ by Baker (1991), as the culmination of his central role in the studies conducted by Binnie & Partners for the Department of Energy through the 1980s. This text offered a speedy means of making progress on the computational components of the study whilst broader literature searches continued. The methodology leading to the Matlab based routines ‘Turgency’ and ‘Generation’ is outlined in Appendix A.2.1. Appendix A.2.2 offers reassurance that minor head losses associated with entry to, and exit from the turbine ducts (not incorporated into the computations, since these would generally be quantified only later through the detailed hydraulic design) contribute only marginally to the uncertainty range of predictions (potentially reducing energy predictions by figures in the region of 3-12%). Appendix A.2.3 provides initial independent validation testing of the software against the earlier Department of Energy commissioned studies (UKAEA, 1984) for two potential small UK barrage schemes.

Notwithstanding a ~10% disparity arising, the Turgency/Generation routines were then applied to the possible barrage schemes at the eight major estuary locations in the UK having the greatest tidal power potential, see Appendix A.2.4.

The comparison of total annual energy produced from each barrage, see Appendix A.2.4, between the Generation program and that produced from previous studies (UKAEA, 1980, 1984; DoEn, 1989) is shown in Table 2.2.1.

Table 2.2.1: Total annual output of each barrage according to Turgency/Generation routines and DoEn reports.

	Turgency/Generation (TWh)	DoEn reports (TWh)	Difference (%)
Solway Firth	9.81	11.99	18.2
Morecambe Bay	4.28	5.42	21.0
Mersey	1.34	1.54	13.0
Dee	1.29	1.36	5.1
Severn	11.12	15.09	26.3
Thames	1.30	1.60	18.8
Wash	3.24	4.39	26.2
Humber	1.55	1.93	19.7
			Average = 18.5%

The under-prediction of energy capture from the Turgency/Generation routines, as applied herein, by an average of 18.5% arising from the validity checks is loosely consistent with the outcomes from the main body of testing (for the Dee, Mersey, Morecambe Bay and Solway Firth) presented later in Chapter 3. Whilst the Turgency (turbine characteristics) program

could be validated directly against the example given by Baker (1991), it has not been possible to conduct more in-depth validation checking of the Generation program outcomes, due to the lack of detailed information provided in the available literature on the technical details of the earlier studies.

The most conspicuous cause of the discrepancy is likely to be in the treatment of the sluicing effect where Turgency/Generation has taken the actual area of the openings (sluices plus turbine ducts) as the effective area, whilst the earlier DoEn studies imposed discharge coefficients ( $\sim 1.8$ ) arising from specific design assumptions. Exploratory runs (applied as part of the studies in Chapter 3 and incorporated in Appendix A.3.1) suggest that the resulting increase in sluicing flows can explain between 5 and 10% of the under-prediction. Furthermore, and also of particular note, is the fact that all of the DoEn studies (UKAEA, 1980, 1984; DoEn, 1981, 1989) were based on a single-regulated bulb turbine adopted for the Severn study, and turbine operation characteristics were scaled from this machine. The present work using Turgency/Generation utilises a 'hill chart' characterising turbine performance (see Appendix A.2.1) taken from Baker (1991) and representing a double-regulated bulb turbine unit, but normalised such that the maximum machine efficiency is not disclosed. In the above validation studies using Turgency/Generation, maximum efficiencies in a range up to 97% were used in these preliminary tests, high figures being selected partially to constrain the rated head arising from the turbine/generator combinations under investigation.

Another difference in implementation is that the Turgency/Generation routines attempt only to select generator start times to achieve maximum energy capture by means of a fixed delay (after the minimum generating head is reached) over all tides in the spring to neap cycle. In contrast, the DoEn study enacted a more refined optimisation process, where the start of generation was optimised sequentially for each tide. It might, therefore, be expected that this more rigorous approach will also account for some of the remaining disparity between the approaches.

Whilst the lack of close agreement in the validation checks is unfortunate, it is considered that the Turgency/Generation routines provide a sufficiently consistent (and perhaps slightly pessimistic) energy prediction platform upon which to base the more detailed studies to be reported in Chapters 3 and 4. Furthermore, the preliminary computations discussed above can also be employed to offer an insight into the wider contribution of tidal energy to the electricity grid.

### 2.2.1 Conjunctive operation

One of the perceived drawbacks of using tidal energy is the lack of continuous power output and the difficulty of incorporating the electricity into the national grid. Of course, intermittency is not a problem of tidal power alone. Most renewable sources suffer from this problem, but the power output from tidal barrage schemes is much greater than from all other renewable intermittent sources. One possible way to overcome this perceived difficulty is to consider tidal barrages operating in conjunction to provide a wider power generation window. The major question that must then be answered is whether tidal barrages could be operated continuously over a 24 hour cycle to provide base load to the national grid. There are other reasons for considering conjunctive operation, not least to see how much power is achievable through renewable energy and when that power is available.

Two regimes are examined here. The first is the greatest generation window available for all barrage sites, and thus the greatest generation window available for the full daily output. The second is the greatest energy output produced from all the barrage sites, and thus a reduced generation window.

Figure 2.2.1.1 shows that there is a large variation in the energy produced from the spring tides to the neap tides. It is also clear that there is not 24-hour coverage for any of the tides

within the spring-neap cycle. Figure 2.2.1.2 shows the power output from the spring tides. It is apparent that there is a significant base load produced, of about 4GW, across 20 hours of the day. There are two peaks of power, which are the Severn, Humber and Wash barrages and the Mersey, Dee, Solway Firth and Morecambe Bay barrages.

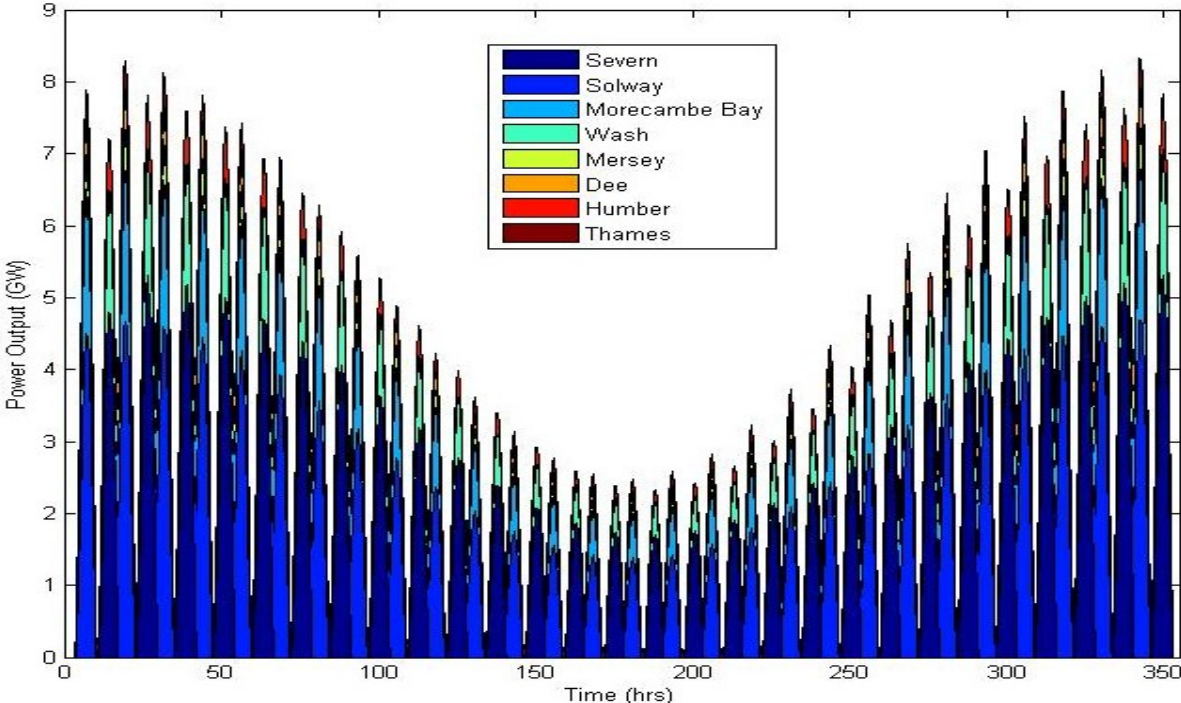


Figure 2.2.1.1: Power output of all barrages with maximum generation window (preliminary studies).

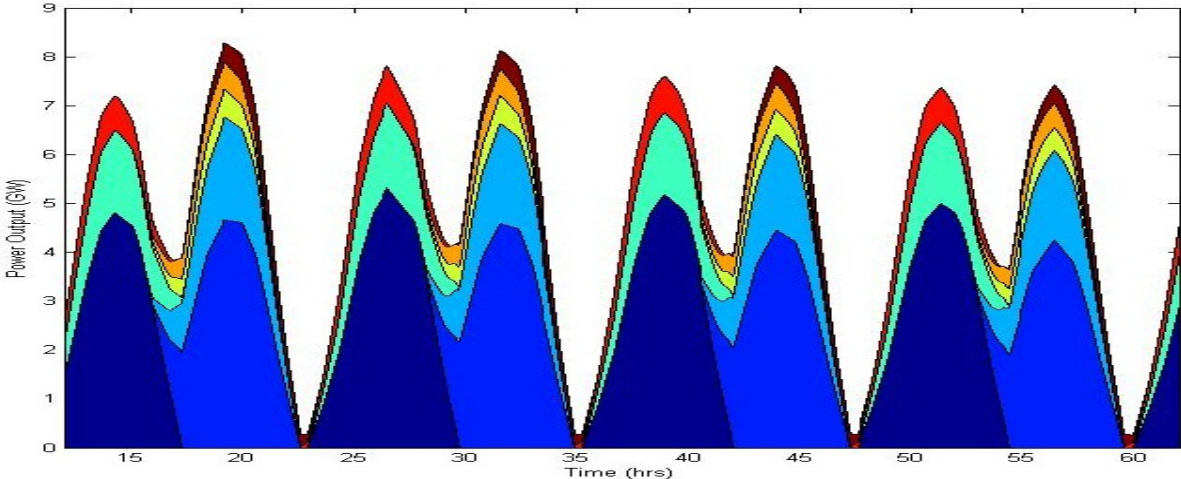


Figure 2.2.1.2: Power output of all barrages during spring tides with maximum generation window (preliminary studies).

These pairs of schemes are almost completely out of phase and so the possibility of using flood operation at some of the barrages in order to close the gap is not available. The same bi-modal distribution is seen in the neap tides, shown in Figure 2.2.1.3, although the total power output is a lot less. Now the base load is under 1GW, although the generation window is still almost 20 hours per day. The total annual output from the 8 barrage schemes, utilising the largest generation window, is 29.4TWh.

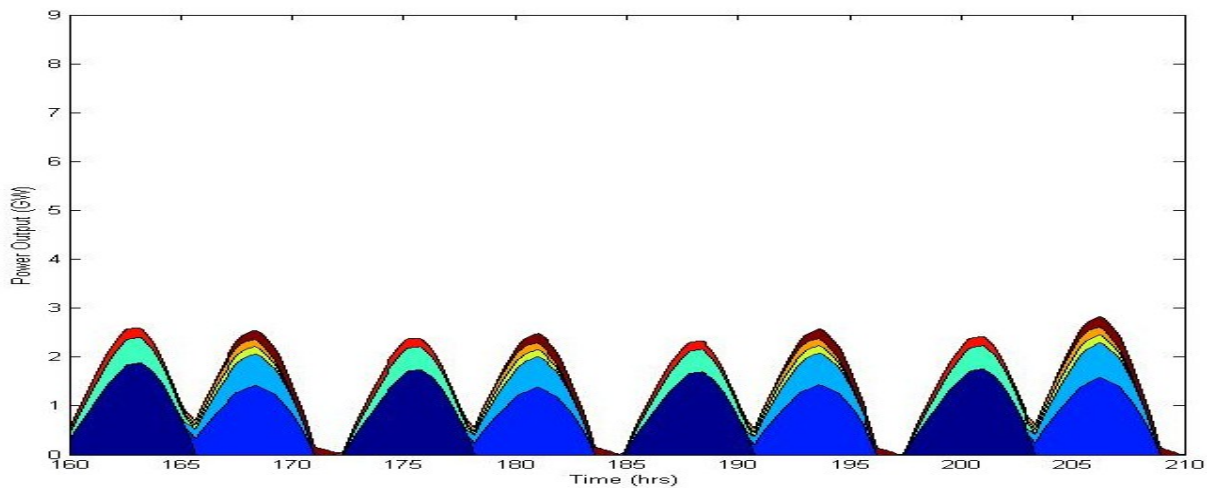


Figure 2.2.1.3: Power output of all barrages during neap tides with maximum generation window (preliminary studies).

A similar sequence of power distribution is seen when maximum energy output is required from the barrages; see Figure 2.2.1.4. Now, however, there is less of a window over which a base load is produced. In Figure 2.2.1.5, the same bi-modal power distribution can be seen, although now clearly there is not the same coverage in terms of time. The neap tides provide the same difficulties as the largest window case. Here again, Figure 2.2.1.6, the power output is dramatically reduced, by over 50 %, from the spring tides. The total power output available from the barrage schemes, when maximising power output, is 36.1TWh.

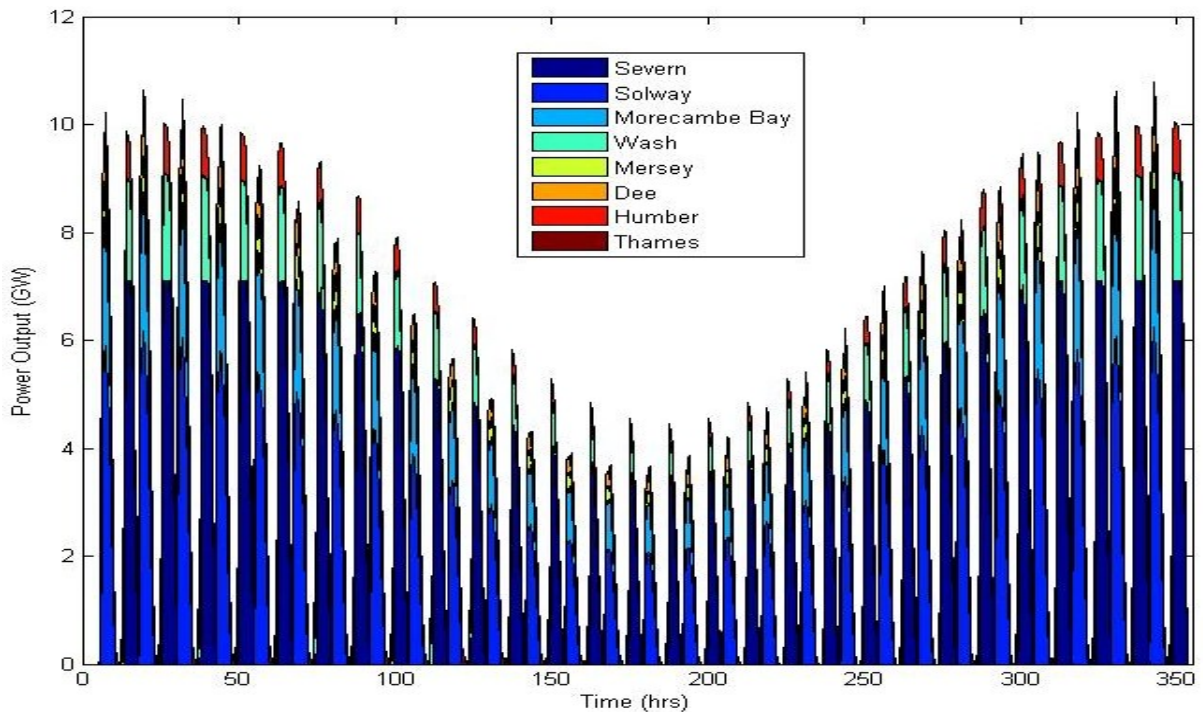


Figure 2.2.1.4: Power output of all barrages for maximum energy generation (preliminary studies).

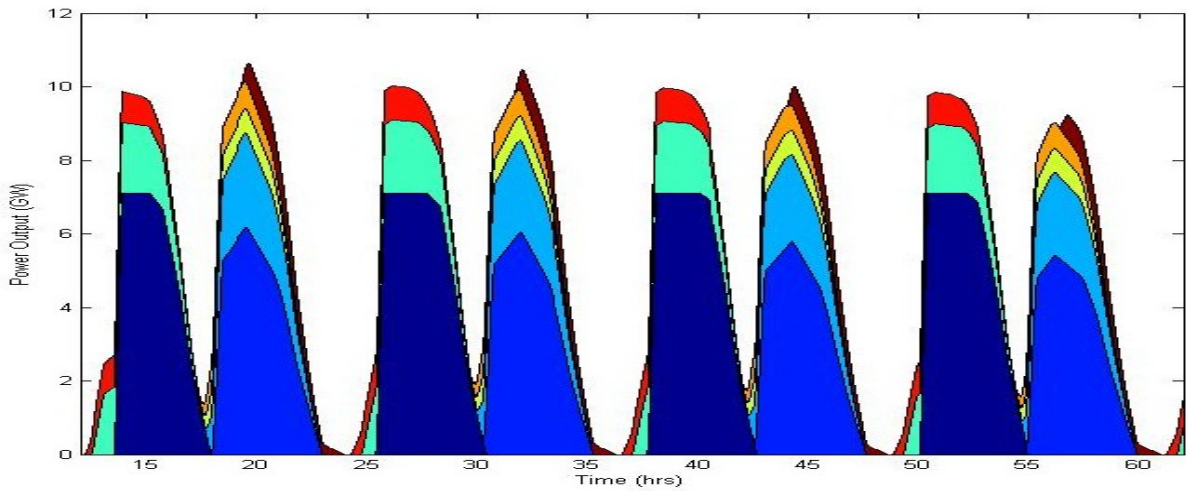


Figure 2.2.1.5: Power output of all barrages during spring tides for maximum energy generation (preliminary studies).

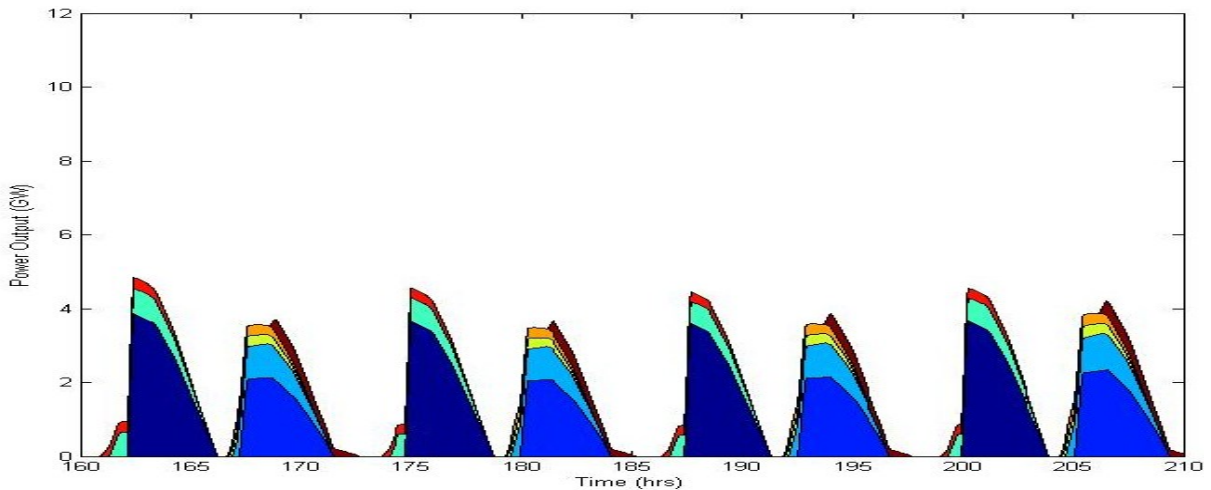


Figure 2.2.1.6: Power output of all barrages during neap tides for maximum energy generation (preliminary studies).

When considering the potential of tidal barrages, the total power available is considerable. The maximum annual energy output represents close to 10% of the total annual electricity consumption within the UK. At present, only 4.5% of electricity generation is through renewable sources, and the government has a binding target of 20% by 2020. If tidal barrages were utilised across the above 8 sites alone, then over half of the target, under current usage, would be met. This does not take into account the drive to reduce electricity demand over the coming years, which would uplift the percentage contributions.

### 3. ENERGY FROM MAJOR BARRAGE SCHEMES (0-D MODELLING)

#### 3.1 0-D modelling context

A 0-D (flat-estuary or two-tank) model has been employed in the project to synthesise barrage operation, with realistic turbine characteristics relating flow rate  $Q$ , diameter  $D$  and head  $H$  to the efficiency and power  $P$ , as defined by the hill chart introduced in Section 2.2 and described in Appendix A.2.1. This form of assessment is consistent with that used in earlier studies (UKAEA, 1980, 1984; Baker, 1991) and has been formulated in Matlab-based routines, depicted in Figure 3.1.1, illustrating ebb generation for a scheme of 40 6m diameter 21MW turbines on the Dee Estuary. The barrage alignments proposed in the earlier studies (UKAEA, 1980) have been adopted for the studies completed herein. The alignments are depicted in the introduction to each barrage in the following sections.

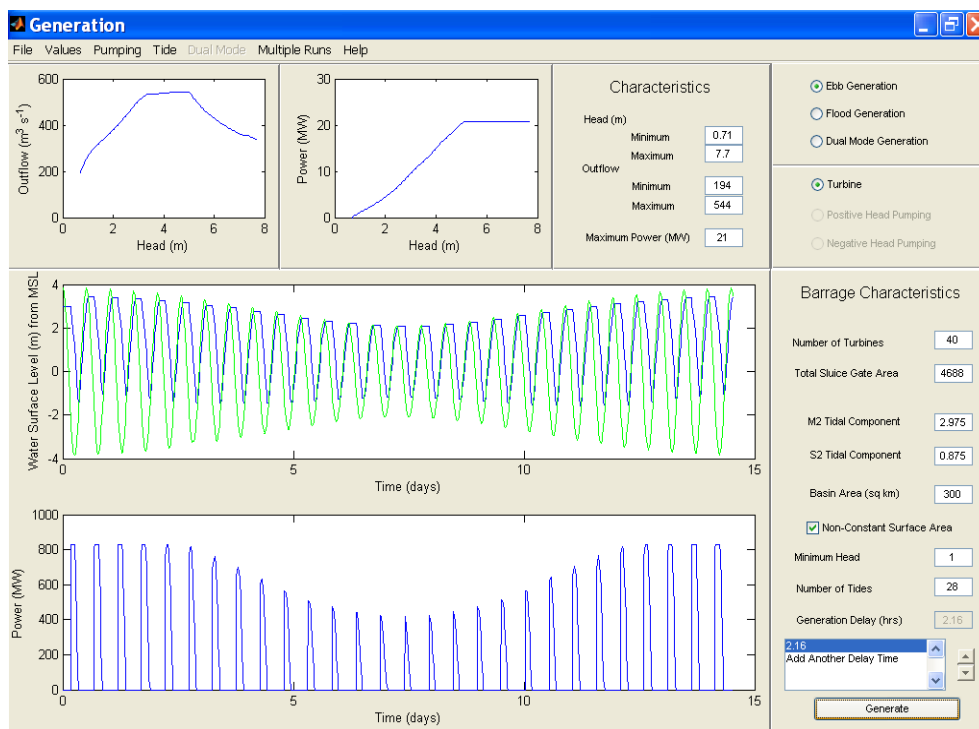


Figure 3.1.1: Screen image showing: top – turbine performance characteristics; middle – tidal (green) and basin (blue) level variations; and bottom – power outputs.

- In the routines, energy capture can be maximised by choosing a suitable 'delay' after the chosen minimum generation head is reached (these figures being 1m and 2.16h, respectively, in Figure 3.1.1).
- The routine ensures that cavitation is avoided by controlling the chosen speed of revolution of the turbines.
- When considering the potential for pumped storage once basin levels have filled to the maximum under gravity sluicing, a delivery flow rate matching the turbine flow at 1m head has been arbitrarily taken in these studies when operating the turbines as pumps; and the pump efficiency is conservatively assumed to be 40% in allowing for the energy cost of pumping.
- Similar pumping characteristics are assumed when attempting to further drain the basin following sluicing in preparation for flood phase generation during studies of dual mode operation.

Before proceeding, note the following terminology:

A DoEn (or 1xDoEn) installation is here taken as one with installed turbine capacity (and complementary sluicing) consistent with the outcomes of the UK Department of Energy's 1980s studies, with the characteristics of extracting about half the available ebb phase energy, in a scheme where the basin in ebb mode operation drains only to near mean tide (sea) level. This arrangement was found from these early studies to yield electricity at minimum unit cost.

A DoEn (or 1xDoEn) configuration is adopted as a baseline because later schemes of multiples of this turbine capacity (i.e. 2xDoEn, 3xDoEn, etc) are considered as alternatives, operating in either ebb mode or in dual (two-way) generation mode.

### 3.2 Dee Estuary and Dee-Wirral Lagoon

The alignment for a barrage on the Dee Estuary is that proposed in the DoEn report (UKAEA, 1980). It is depicted in Figure 3.2.1. Appendix A.3.1 contains extracts from the 1980 document showing both the alignment and the cross-section of the estuary.

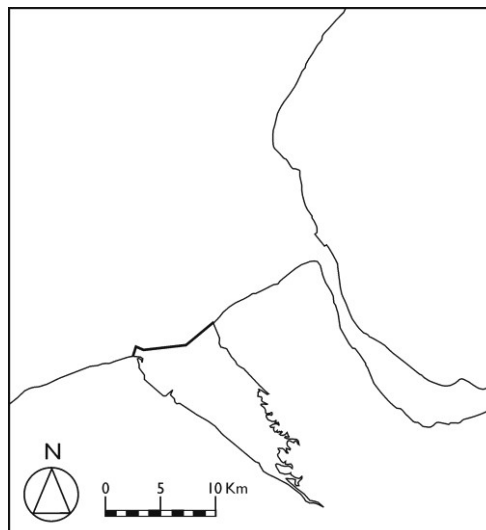


Figure 3.2.1: Sketch showing the location of a Dee Barrage.

For the Dee, the tidal conditions for the 0-D analysis can be defined by the  $M_2$  and  $S_2$  tidal constituents, 2.975m and 0.875m, respectively, at this location close to the Hilbre Island tide gauge. Water depths in the deep channel location for the turbines adopted in the earlier study are approximately 20m at low water spring tide level. This depth is critical to cavitation avoidance as part of the turbine selection process.

In the studies that follow, some turbine selection and energy calculations have been undertaken for shallower depth (13m), to give more options in the placement of turbines along the line of the barrage, avoiding extensive dredging (see the spreadsheet computation summaries in Appendix A.3.2). In fact, turbine performance is not highly sensitive, in most cases, to the assumed depth of water and so a depth of 13m was adopted for most runs of the Turgency/Generation 0-D energy modelling (see Appendix A.2.1). For this study, the bathymetry within the impounded area behind the barrage was established from LIDAR data collected by the Environment Agency in 2003. The resulting relationship between water surface area and water level is presented in Figure 3.2.2 (with estimated values used in the 1980 DoEn study also shown). Tabular values are given in Appendix A.3.1.

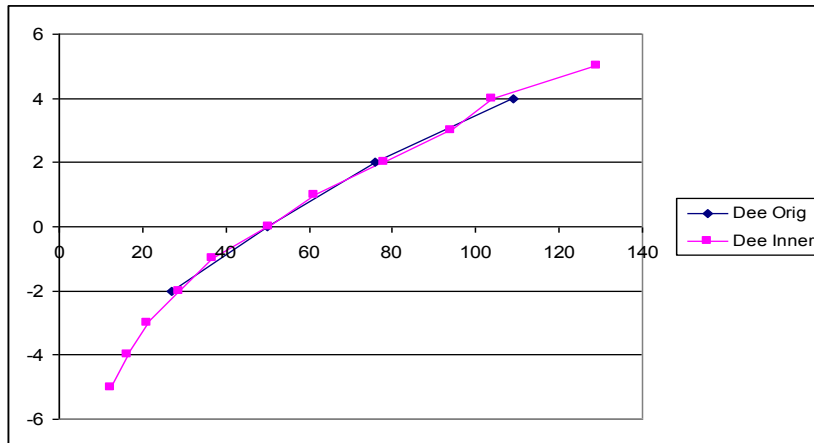


Figure 3.2.2: Dee basin area (km<sup>2</sup>) as a function of water level (mAOD).

### 3.2.1 Initial appraisal (ebb generation only)

The initial aim here was to corroborate the 1980 Department of Energy study findings for the Dee, as further validation of the 0-D Turgency/Generation model. For this reason, the initial studies employed a turbine diameter of 6m and the estuary bathymetry from the earlier study, depicted as ‘Dee Orig’ in Figure 3.2.2.

As discussed earlier in Chapter 2 and in Appendix A.2.4, the precise treatment of the turbine characteristics in the earlier DoEn (UKAEA, 1980) studies, purportedly from a single-regulated axial flow (bulb) turbine, could not be fully reconciled against the hill chart (see Appendix A.2.1) of a double-regulated device taken from Baker (1991), so perfect agreement could not be expected. Furthermore, the maximum efficiency to be applied in the present approach was undefined, since such information might be expected to be commercially sensitive and so was not released by Baker. In reality, maximum efficiencies of ~90%+ might be expected for such turbines, widely used in conventional hydropower. Additionally, in drawing comparisons, it was to be noted that the published DoEn figures included allowances for losses of 5% for generator efficiency, and 10% for machine and transmission outages. Consequently, in the preparatory tests in Turgency/Generation, two approaches were taken: firstly, a (default) maximum efficiency of 80% was used, but with no subsequent reduction for losses; and secondly, a more realistic 95% maximum efficiency, together with 5% and 10% energy reductions (see the note accompanying Table 2.1.1). Table 3.2.1.1 presents the maximum annual energy predictions achieved by assuming a 1.0m minimum generating head ( $H_{min}$ ), together with the ‘best’ delay.

Table 3.2.1.1: Results of the corroboration calculations for Dee Barrage in ebb mode using 6m diameter 21MW turbines with 40 8m x 12m sluices; minimum water depth at turbines = 20m.

Number of Turbines	DoEn 1980 Annual Energy (TWh)	Present Study – 80% Maximum Turbine Efficiency			Present Study – 95% Maximum Turbine Efficiency			
		Energy (TWh)	% of DoEn	Delay (hrs)	Energy (TWh)	Losses (TWh)	% of DoEn (including losses)	Delay (hrs)
40	1.16	0.997	86.0	2.26	1.029	0.174	88.7	2.24
50	1.28	1.092	85.3	2.58	1.127	0.191	88.1	2.56

Figure 3.2.1.1 provides a schematic illustration of the approach used in the calculations and Figure 3.2.1.2 shows the effect of differing delays for the 40 turbine, 80% maximum efficiency case. It can be seen that the energy output can be boosted by over 20% through the use of delays.

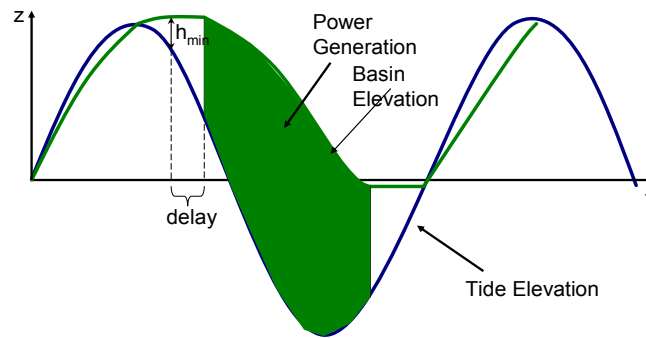


Figure 3.2.1.1: Illustration of the ebb generating cycle.

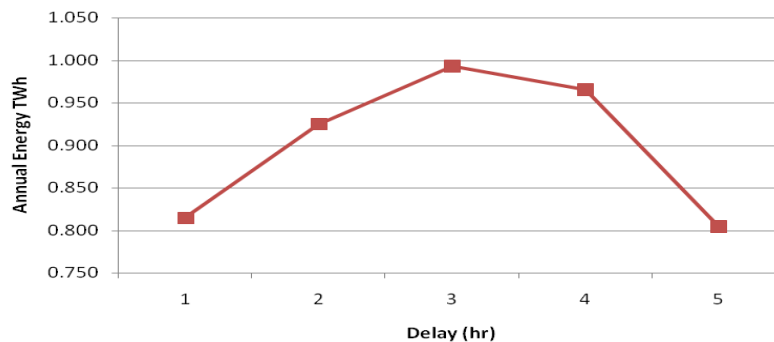


Figure 3.2.1.2: Effect of delays on annual ebb energy output from Dee Barrage (initial appraisal).

It can be seen (Table 3.2.1.1) that the present study routines produce predictions within 15% of the earlier DoEn studies when using 80% efficiency as the maximum turbine efficiency with no subsequent losses. The agreement is close to 10% using a more likely combination of machine efficiency (95%) combined with expected losses (15%).

An additional level of optimisation was employed in the earlier DoEn studies, with the suitable delay being established on a tide-by-tide basis through the spring-neap cycle, as opposed to the 'best' fixed delay employed in Turgency/Generation. Further tests were undertaken by evaluating the best delays for spring, neap and mean (intermediate) tides. The results in Table 3.2.1.2 show the outcome of applying a linear variation of these delay values across the individual tides in the spring-neap sequence (and noting that the 8m diameter turbine is an option to be proposed later). As can be seen, there is only a small percentage uplift in the figures, suggesting that the additional rigour in setting the time for first generation is unlikely to explain more than 1-2% of the near 15% under-prediction arising from Turgency/Generation. This is consistent with the preliminary study findings discussed earlier in Section 2 and in Appendices A.2.3 and A.2.4. Therefore, the remaining disparity (of approximately 10-15%) between the present study outcomes (80% maximum efficiency) and 1980 DoEn studies must be attributed, at this point, to differences in turbine characteristics and their assimilation into the respective computational routines, as well as the differing assumption on sluice characteristics discussed in Section 2.2. Nevertheless, given the general consistency across the full range of validation studies, the Turgency/Generation routines can be taken to offer acceptable and conservative estimates of the exploitable energy at the feasibility level considered herein. Thus, having concluded that a default figure of 80% turbine efficiency applied in Turgency/Generation provides a conservative estimate of energy capture, making implicit allowance for losses, this default is used in all subsequent calculations.

Table 3.2.1.2: Effect of varying delay on ebb energy output from Dee Barrage (initial appraisal).

Type of Turbine	Spring Delay (hrs)	Mean Delay (hrs)	Neap Delay (hrs)	Energy (TWh)	% change*
6m 21MW (x40)	2.2	2.26	2.28	1.006	0.178
8m 21MW (x40)	2.2	2.94	3.04	1.373	1.366
Tide	$M_2+S_2$	$M_2$	$M_2-S_2$		

\* % change is relative to the ebb power output obtained using an 80% maximum efficiency with a single non-varying delay.

The final element of the initial appraisal is then to update the figures from Table 3.2.1.1 using the higher quality LIDAR-based bathymetric characteristics of the basin. These are given in Table 3.2.1.3 and, as Figure 3.2.2 shows good agreement between the two data sets, the revised bathymetry provides only a small uplift to the energy figures.

Table 3.2.1.3: Revised ebb annual energy output from Dee Barrage using LIDAR bathymetry and 80% as overall efficiency in Turgency/Generation (initial appraisal).

Number of Turbines	Energy (TWh) with original DoEn 1980 Bathymetry	Energy (TWh) with Bathymetry from LIDAR Data	% change
40	0.997	1.004	0.7
50	1.092	1.100	0.7

### 3.2.2 Investigating different operating modes

In this section, the three alternative operating modes of ebb, flood and dual (two-way) energy generation are investigated. Outline consideration is also given to the addition of 'positive' pumping (pumping before turbinning). In ebb mode, positive pumping uplifts the basin water level at the end of filling on the flood tide (through sluices and turbine ducts). The reverse is the case for flood mode. For dual mode, positive pumping lowers the basin level before turbinning on the flood tide, and raises it before ebb turbinning.

As indicated above, calculations from here onwards are based on the imposition of 80% maximum turbine efficiency to provide conservative estimates implicitly incorporating at least 15% allowance for losses and outages. The figures derived in this section relate to a scheme of 40 6m diameter turbines of 21MW generator capacity (with 20m minimum water depth) and 40 12m x 12m sluices consistent with the DoEn 1980 scheme specification.

Table 3.2.2.1: Annual energy output from Dee Barrage as a function of operating mode.

Operating Mode	Energy Output: LIDAR Bathymetry (TWh)	Energy Output for LIDAR Bathymetry: % of ebb figure	Energy Output: constant basin area (TWh)	Energy Output for constant basin area: % of ebb figure
Ebb	1.004		1.054*	
Dual	0.786	78.2	0.823	78.1
Flood	0.597	59.5	1.056*	100.0

\* The difference between the ebb and flood mode figures is simply a rounding error.

It is clear from the results in Table 3.2.2.1 that for the LIDAR bathymetry (as distinct from assuming a constant basin area), the ebb mode produces the highest total energy output. Flood mode is conceptually the same as ebb mode; the difference in energy yield is due to the reduced tidal prism mobilised, arising from the bathymetry of the estuary, as the mean basin level is lowered rather than raised.

Dual mode also gives a lower energy output but, in this case, the explanation is more complex. The lower output is due to lower head differences during generation (see Figure 3.2.2.1), a lower tidal prism mobilised compared to ebb (as the mean basin level remains

close to mean tide level), and reduced energy generation efficiency in reverse (flood generation) mode. This last factor is due to the reduced hydraulic efficiency of the flow conduits and the turbine blade/guide vane systems. In this study, the reverse (flood) efficiency of dual mode operation has been taken to be approximately 80% of that in the ebb (positive) direction (AEA Technology, 2006).

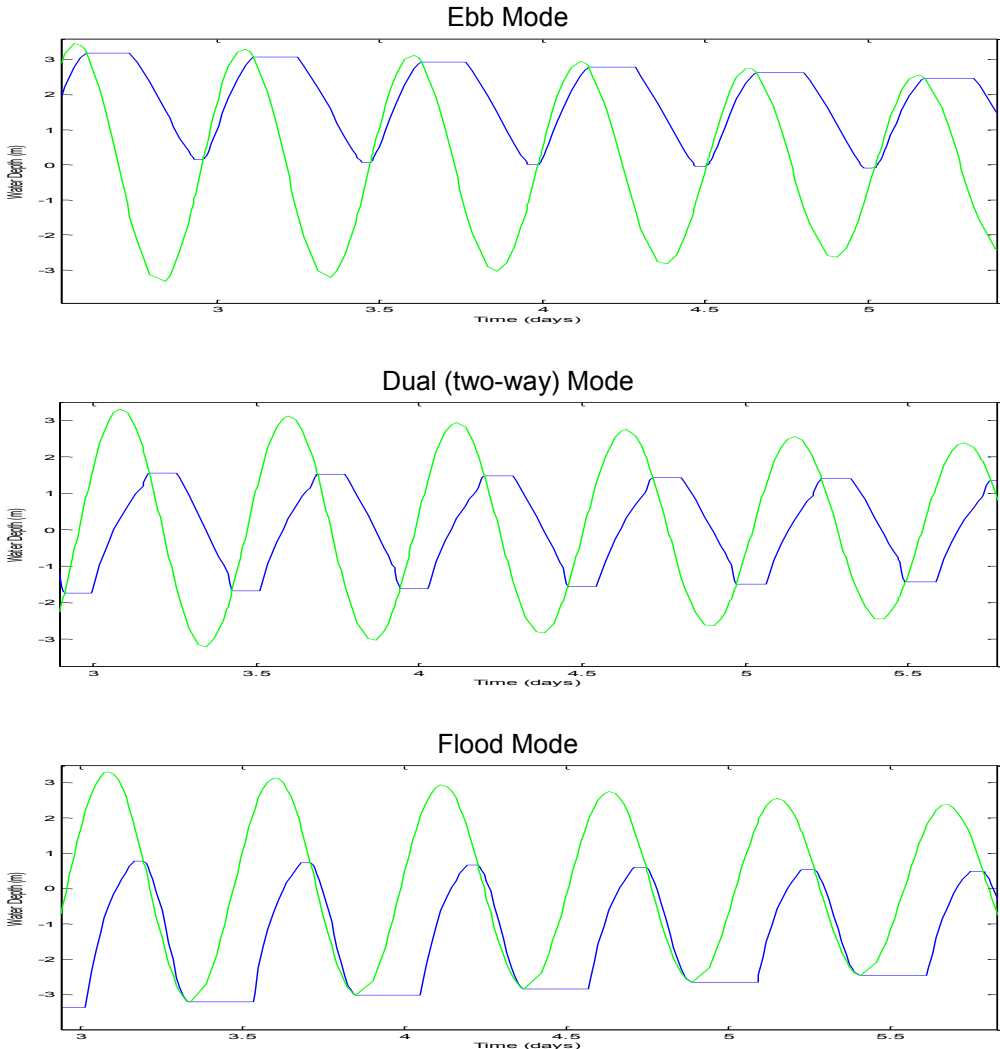


Figure 3.2.2.1: Dee Barrage water levels for different operating modes (samples from the spring tidal phase; external tide level in green, basin water level in blue).

3.2.2.1 Effect of pumping

La Rance has reported (Hillairet and Weisrock, 1986) a 10% increase in the amount of net energy produced as a result of pumping water before energy generation begins (positive head pumping). Shaw and Watson (2003) predict a similar level of benefit for the Severn Barrage. Little information is available relating to the precise performance characteristics of a turbine operating in reverse, i.e. in pumping mode. For the purposes of the present study, the Turgency/Generation computer model was provided with a simple linear pumping model, presently set with an assumed pumping efficiency of 40%. It operated only over heads up to  $H_{min}$  (taken herein as 1.0m) and with constant flow taken from the turbine characteristic at this head.

The calculations above were repeated with the addition of pumping to ascertain its effect. The figures in Table 3.2.2.1.1 indicate that pumping, whilst generally proving beneficial, does

not prove so consistently across the differing modes of operation. It is likely that greater gain might be achieved by extending the 'pumped-storage' effect to a higher limiting 'lift' than the 1.0m applied here. Hillairet and Weisrock (1986) indicated use up to 2.5m at La Rance and Shaw and Watson (2003) suggested 3.0m for the higher tidal ranges prevailing at the Severn. There is little virtue in pursuing this issue further until a better definition of pump characteristics is forthcoming. The effects of pumping on different station configurations are considered in more detail in Section 3.2.4.

Table 3.2.2.1.1: Annual energy output from Dee Barrage as a function of operating mode, with positive head pumping and optimum delays.

Mode	Without Pumping (TWh)	With Pumping (TWh)	% change
Ebb	1.004	1.0539	+4.93
Dual	0.786	0.886	+12.68
Flood	0.597	0.674	+12.73

### 3.2.3 Turbine conditioning

#### 3.2.3.1 Changing generator capacity

It was noted that the present version of the original 21MW turbine selected in the DoEn study produced a rated head of 7.83m (from the application of the adopted hill chart within Turgency). This figure is higher than that arising in the DoEn study; and it is excessive, given the spring tidal amplitude of 3.85m and, hence, a spring tidal range (high water to low water) of 7.7m. The implication is that the turbines are unlikely to run at full capacity during most generation cycles, as might be inferred from Figure 3.2.2.1, where driving heads are significantly lower than the tidal range. Consequently, and noting that the situation will be worse for dual mode (two-way) operation than for ebb and flood modes, two further turbine generator capacities were considered: 15MW and 10MW. As before, the calculations were performed with a 40 turbine configuration (turbine diameter = 6m; hub diameter = 3m) using the LIDAR bathymetry. Table 3.2.3.1.1 shows the operational characteristics of the machines.

Table 3.2.3.1.1: Dee Barrage turbine characteristics as a function of generator capacity (turbine diameter = 6m; hub diameter = 3m).

Generator (MW)	Rated Head (m)	Speed (rpm)
21	7.83	88.24
15	5.79	86.96
10	4.53	83.33

Table 3.2.3.1.2 presents the annual energy outputs arising, where it can be seen that there is little sensitivity to the installed generator capacity. The better conditioning of the machine with a smaller generator has a positive effect for the flood and dual mode operations.

Table 3.2.3.1.2: Annual energy output from Dee Barrage as a function of generator capacity (turbine diameter = 6m; hub diameter = 3m).

Mode	21MW	15 MW	% change relative to 21MW	10MW	% change relative to 21MW
Ebb	1.0043	1.0038	-0.05	0.9776	-2.65
Dual	0.7861	0.7861	0.00	0.8058	+2.51
Flood	0.5975	0.5978	+0.05	0.6173	+3.32

### 3.2.3.2 Increasing turbine diameter

Given the presence of depths at low water of spring tides of nearly 20m in the main channels of the Dee, it was considered appropriate to investigate a larger turbine diameter than that considered in the earlier study. Therefore, the 6m unit was replaced by an 8m unit whilst retaining a 3m hub size. Table 3.2.3.2.1 gives the new operational characteristics. The rated heads (the heads at which full power is generated) are now seen to be better related to the likely driving heads, as might again be deduced from Figure 3.2.2.1. Furthermore, the rotation speeds are now seen to fall close to 50rpm, which was favoured during the DoEn studies.

Table 3.2.3.2.1: Dee Barrage turbine characteristics as a function of generator capacity (turbine diameter = 8m; hub diameter = 3m).

Generator (MW)	Rated Head (m)	Speed (rpm)
21	5.19	54.55
15	4.04	54.55
10	3.05	51.28

The energy figures shown in Table 3.2.3.2.2 are grouped by size of generator for the 8m turbine, and percentages are given relative to the output achieved using the same generator capacity in the 6m diameter turbines.

Table 3.2.3.2.2: Annual energy output from Dee Barrage as a function of operating mode (turbine diameter = 8m; hub diameter = 3m).

Mode	Energy (TWh): 21MW	% change relative to 6m / 21MW	Energy (TWh): 15MW	% change relative to 6m / 15MW	Energy (TWh): 10MW	% change relative to 6m / 10MW
Ebb	1.354	+34.8	1.004	+28.6	1.142	+16.8
Dual	1.303	+65.8	1.293	+64.5	1.214	+54.4
Flood	0.794	+32.8	0.598	+32.7	0.769	+24.5

A significant gain in energy capture is immediately apparent in using the larger turbines. Having improved the turbine conditioning (in terms of rated head) for the conditions experienced, the smaller generators are now disadvantageous, as seen from the figures relative to the 21MW units presented in Table 3.2.3.2.3.

Table 3.2.3.2.3: Effect on annual energy from Dee Barrage of changing generator capacity (8m turbines).

Mode	15 MW % change	10MW % change
Ebb	-4.70	-15.64
Dual	-0.80	-6.86
Flood	-0.05	-3.17

### 3.2.3.3 Conclusion

It was found that changing the generator capacity of the 6m diameter turbine used in the present study had only a small effect on the total energy output, at most 3.32%. A far larger effect was obtained by increasing the turbine diameter to 8m (up to 65.8%), which also had the effect of reducing the rotation speed. This change in size is considered to be practically achievable as extra depth can be made available by dredging.

The significant energy increases with the 8m turbine are largely due to the additional flow

capacity of the larger turbine, as is apparent in the Figures 3.2.3.3.1 and 3.2.3.3.2. These plots, for a configuration of 40 21MW turbines running in ebb mode, show both the variations in water levels and the corresponding power pulses for the 6m and 8m units, respectively. What is of potential interest from an environmental viewpoint is that the larger turbine draws more water, and hence a larger tidal prism is mobilised, with a larger tidal range created within the basin, thereby increasing the intertidal zone retained. This line of discussion will be picked up again later.

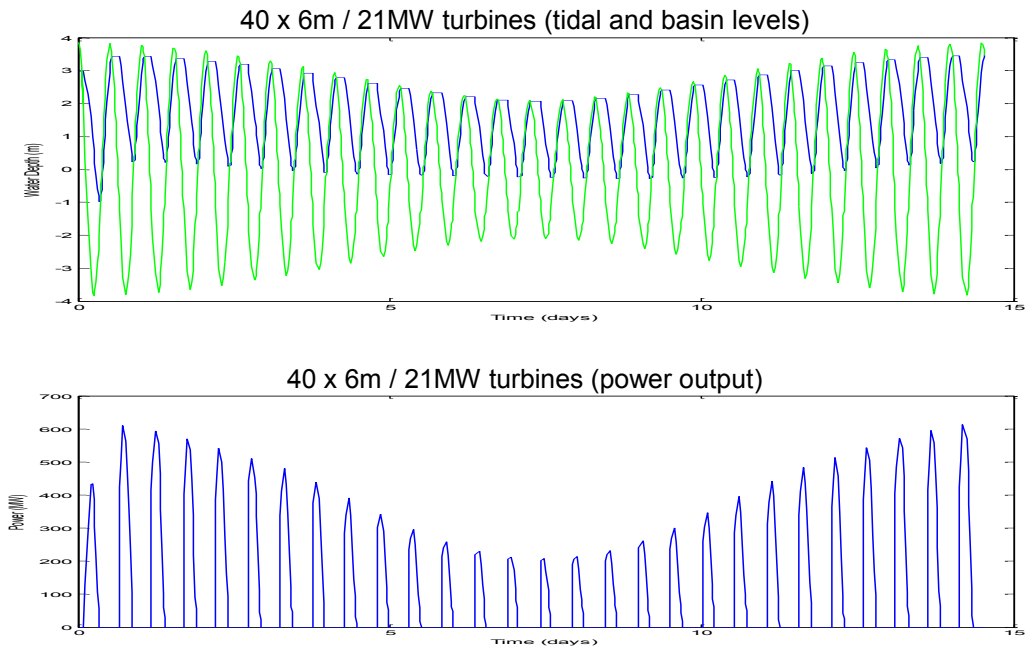


Figure 3.2.3.3.1: Dee Barrage water levels and power output for 6m diameter turbines; ebb mode.

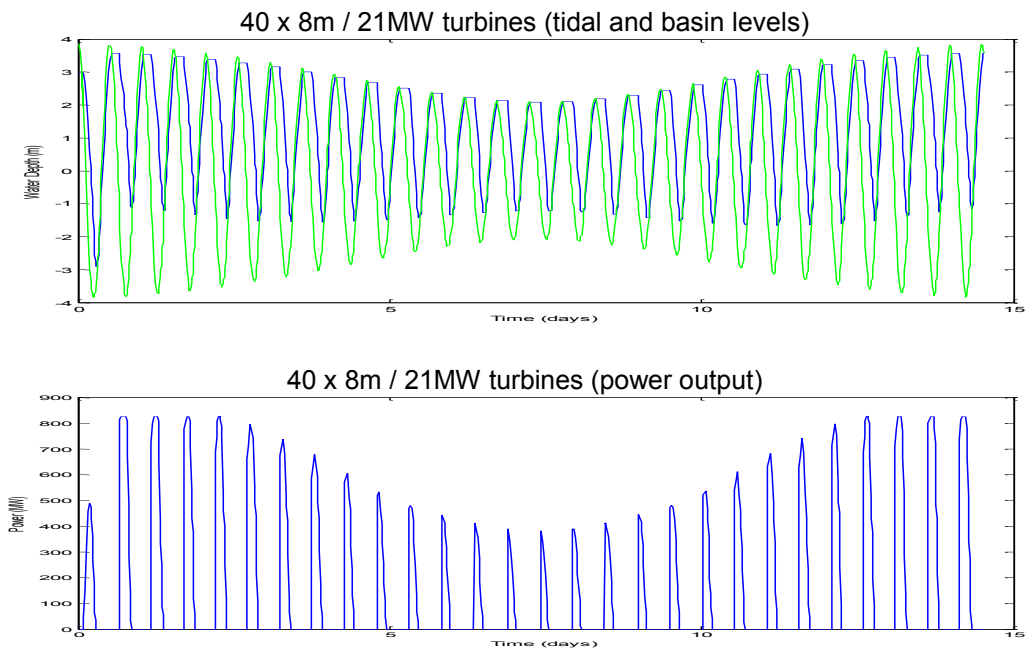


Figure 3.2.3.3.2: Dee Barrage water levels and power output for 8m diameter turbines; ebb mode.

### 3.2.4 Increasing installed turbine capacity and cost implications arising

Prandle (1984) has shown theoretically that dual mode operation should give rise to an increased energy capture. In practice, the energy captured is reduced by the loss of hydraulic efficiency under reverse flow through the turbine and passageway. It is also lowered by the reduced tidal prism mobilised in the basin, centred close to mean water level, as compared to the larger prism activated over the uplifted elevations in ebb mode.

The above findings imply that larger flow rates are required to compensate for the lower driving heads generated in comparison to ebb mode. This observation means that a larger number of turbine units are required for a dual mode (two-way) scheme than for an ebb scheme, if the resource is to be fully exploited. In addition, dual mode operation with a larger number of turbine units has the potential to more fully maintain the internal tidal regime.

In two-way operation, the priority is to pass through the turbines as much as possible of the tidal prism mobilised each cycle. As the number of turbines is increased, flow through the sluices is of reducing significance compared to sluicing through the turbines. For this reason, the area of the sluices was arbitrarily reduced to half that of the DoEn studies. Figure 3.2.4.1 clearly shows how the tidal regime in the basin can be preserved, in this case for 80 8m x10MW machines, without resorting to pumping.

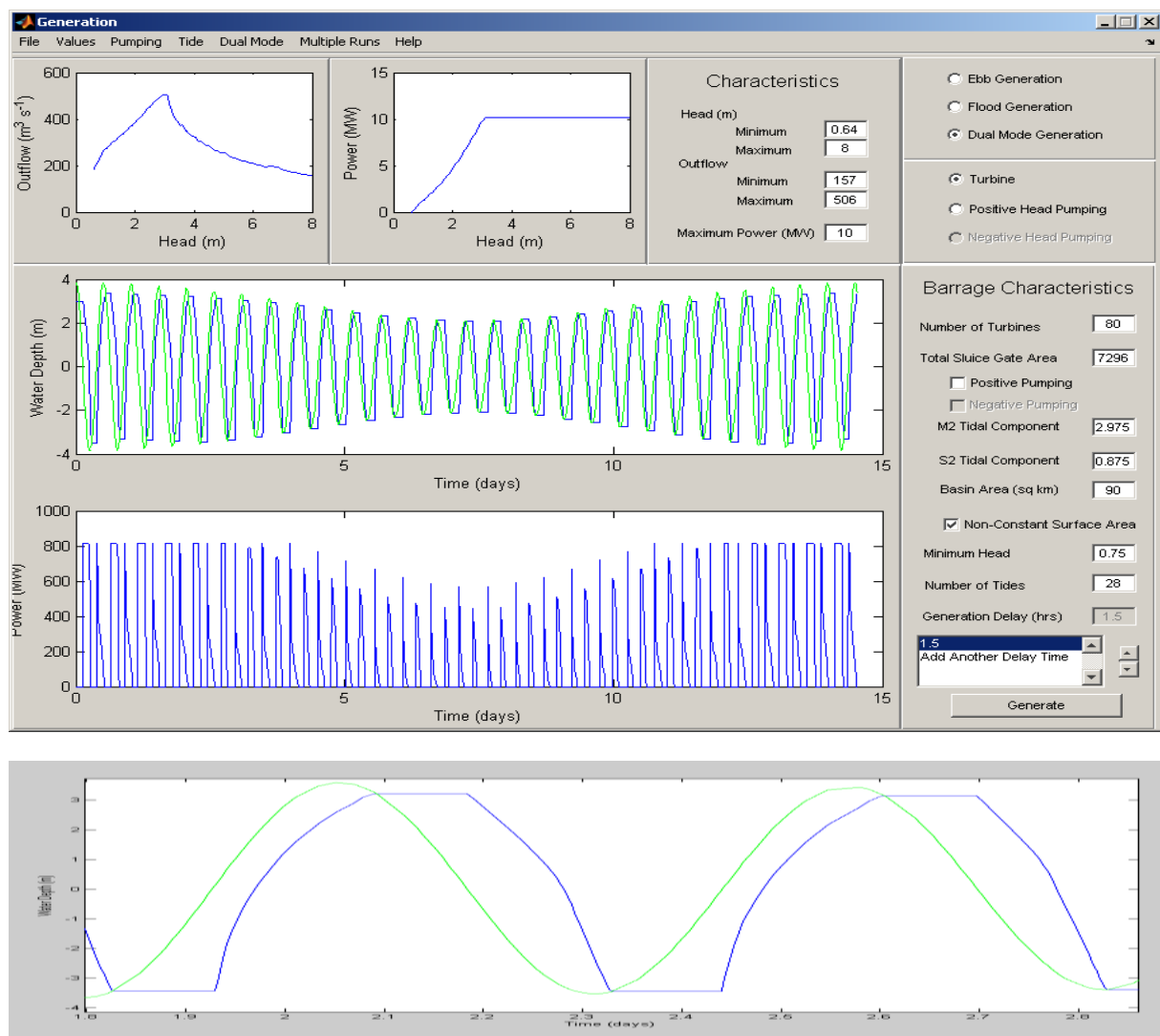


Figure 3.2.4.1: Dee Barrage dual mode operation with 80 8m x 10MW turbines.

A number of 'extreme' runs were performed with 21MW / 8m turbines, increasing the turbine numbers up to eight times those in the DoEn studies. (Note, however, that this extends conditions some way beyond the limits of practicability.) Delays and pumping were also used to fully optimise the power output for the number of turbines used. For comparison purposes, these runs were performed for both ebb and dual mode configurations.

21MW / 8m turbines were used in the 'extreme' runs as they gave increased output for both ebb and dual modes. However, turbines with a lower rated head (lower generator capacity) might offer better value for money if the generator cost savings are larger than the reduced value of the energy yield. (See Appendix A.3.3 for an outline of the costing basis adopted.)

Figure 3.2.4.2 shows the total power output for both ebb and dual modes, both with and without pumping, as a function of the number of turbines.

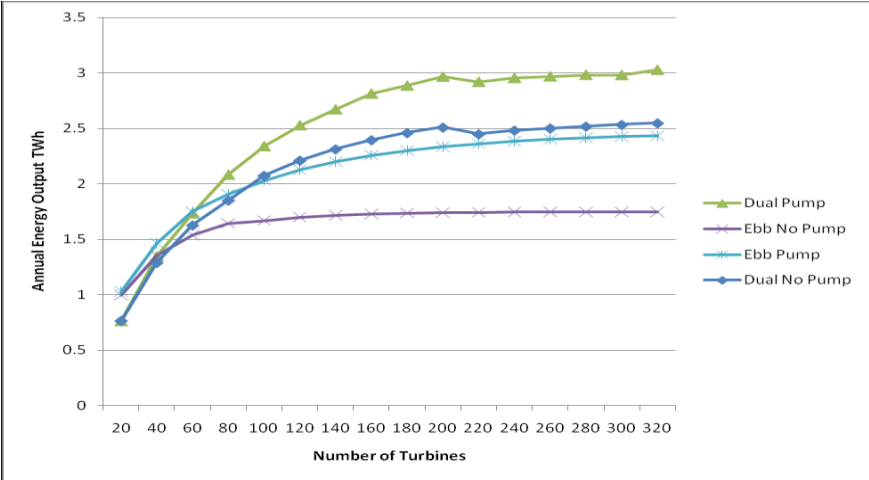


Figure 3.2.4.2: Annual energy output from Dee Barrage operating in ebb and dual modes as a function of number of turbines.

In addition to the energy runs, indicative costs were calculated by linear scaling of the 1980 DoEn costs (see Appendix A.3.3) and used to derive the unit cost of the electricity produced. These costs were updated to 2007 using figures given in the SDC (2007) report, assuming a low discount rate of 3.5%. The results are presented in Figure 3.2.4.3.

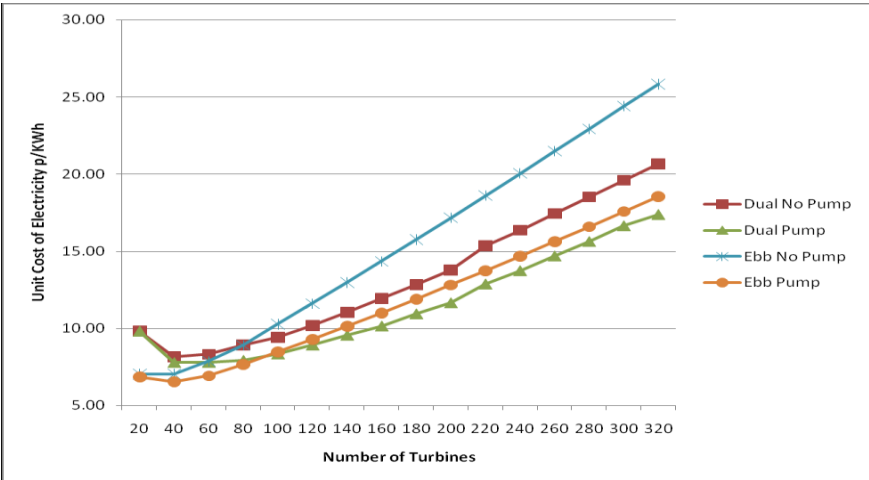


Figure 3.2.4.3: Unit cost of energy from Dee Barrage as a function of number of turbines; ebb and dual modes.

### 3.2.4.1 Comment and discussion

It is clear from the diagrams above that the 1980 DoEn study found the configuration for the Dee which produced the lowest unit cost of energy, which was their remit. It is also interesting to note that dual mode operation captures more energy than ebb mode operation at higher turbine numbers, and this is what is to be expected from theory. Dual mode operation is expected to give more energy as it involves capturing the potential energy from both emptying and filling the basin. Ebb mode, by contrast, is only capturing the potential energy from emptying the basin.

It is also clear from Figure 3.2.4.2 that pumping can increase the energy gain. At high turbine numbers, the energy gain is around 20% for dual mode and 40% for ebb mode. In practice, there will be a number of limits on what can be gained from pumping, not least of which will be the water level at spring tides, when water uplift may be inappropriate due to flood risk.

Whilst the lowest costs were derived from ebb mode with 20 or 40 turbines, these may not yet be the most economical configurations. As Figure 3.2.2.1 made clear, this ebb mode configuration will lead to the tidal range being reduced, and the average water level being uplifted. If scheme costs arise from the need to mitigate environmental change under the EU Habitats Directive, then higher installed capacities in dual mode may be more cost effective, as they lead to less modification of the tidal regime. It is also worth noting that the dual mode cost of electricity for 40 turbines is 15% higher than the ebb-only cost, which is in agreement with the detailed findings of the 1981 Severn Study (DoEn, 1981).

The issue with water levels is made clearer in Figure 3.2.4.4.1 which shows basin water levels for 40 turbines (1xDoEn) operating in ebb and dual modes, and for an installed capacity of 120 turbines (3xDoEn) in dual mode.

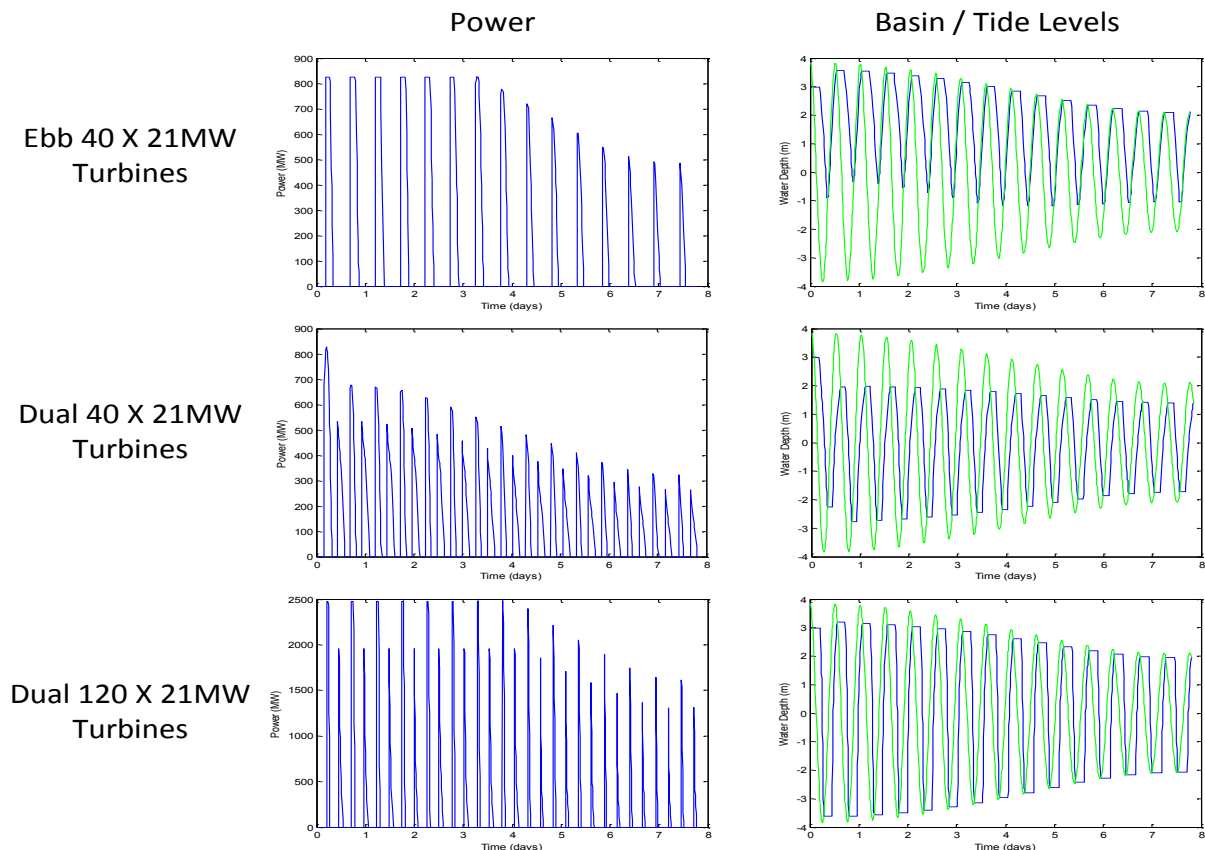


Figure 3.2.4.4.1: Power output and water levels for different Dee Barrage configurations.

Figure 3.2.4.4.1 also makes clear that whilst higher installed capacities have positive effects in reducing tidal modification, they are likely to create issues in integration with the electricity grid, as the power is produced in larger, shorter pulses. It will be interesting to see how this issue is addressed in the current UK Government Department of Energy and Climate Change (DECC) study of the Severn Estuary.

### 3.2.5 Increasing installed sluice capacity and cost implications arising

Calculations similar to the above were performed, again using 8m diameter 21MW turbines (with a minimum water depth at the turbines of 13m), but this time varying the sluicing area. The number of sluices was varied for both a 40 (1xDoEn) and a 120 (3xDoEn) turbine barrage configuration, in both ebb and dual modes. The results are summarised in Figures 3.2.5.1 and 3.2.5.2.

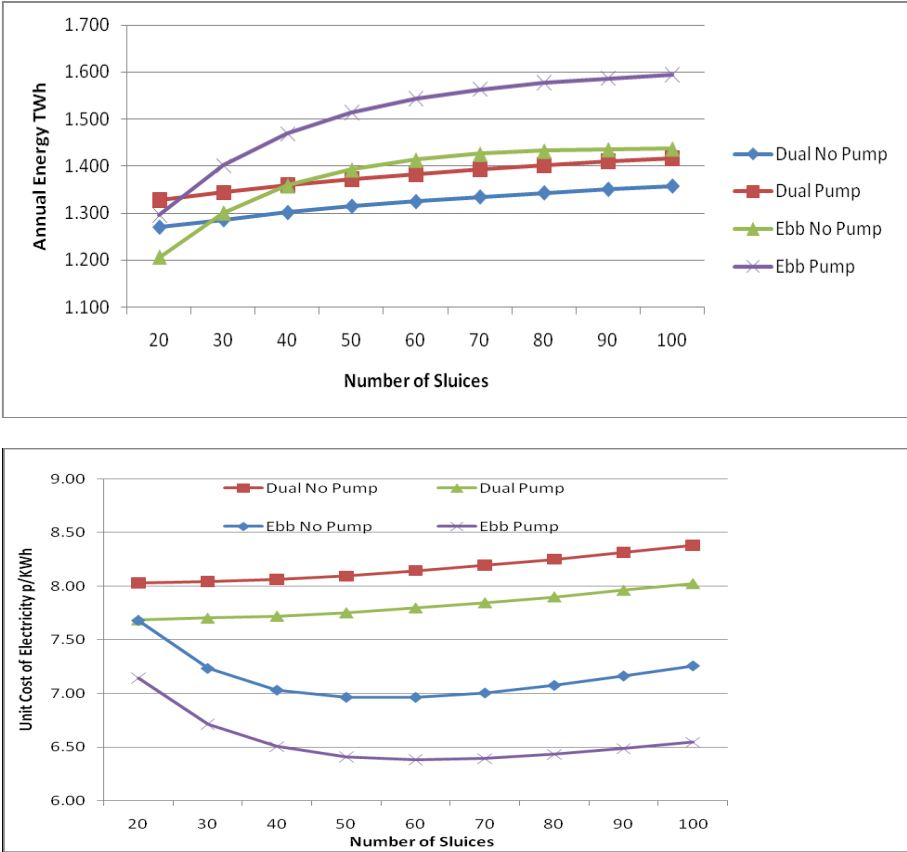


Figure 3.2.5.1: Annual energy output and unit cost of energy from Dee Barrage operating in ebb and dual modes with 40 turbines as a function of number of sluices.

The graphs for 40 turbines illustrate that dual mode operation is less sensitive than ebb mode operation to the degree of sluicing, as has already been mentioned. The 40 sluice configuration chosen in the DoEn study is not quite the optimum found here, but this is unsurprising given the difference in energy output found.

With 120 turbines, both the energy and cost are much less sensitive to changes in sluicing, regardless of mode. For this configuration, the turbines represent a significant sluicing area in their own right, and sluices represent a much smaller proportion of the total costs.

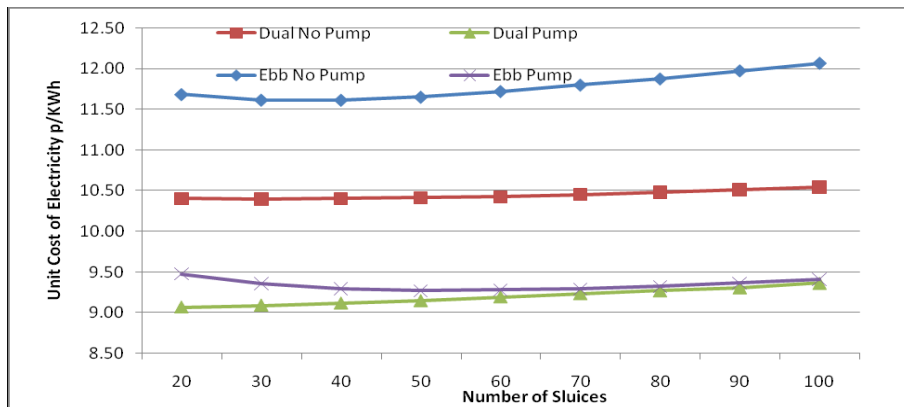
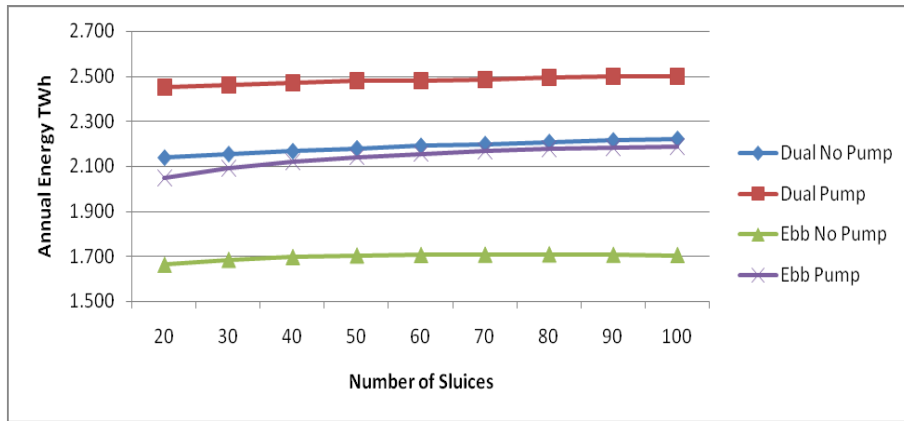


Figure 3.2.5.2: Annual energy output and unit cost of energy from Dee Barrage operating in ebb and dual modes with 120 turbines as a function of number of sluices.

### 3.2.6 Dee Outer Barrage (Dee-Wirral Lagoon)

The scope for barrages located across embayments was considered in earlier studies (DoE 1989) and, more recently, there has been interest (Anderson, 2008) in the concept of a coastal impoundment. This arrangement uses barrages to generate energy but also to protect large stretches of coastline from the direct action of the sea.

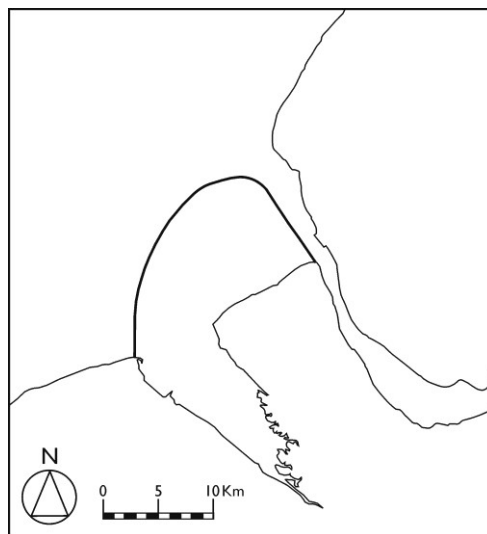


Figure 3.2.6.1: Sketch showing the location of a Dee Outer Barrage (creating a Dee-Wirral Lagoon).

The Dee Outer Barrage, creating a Dee-Wirral Lagoon, which follows the extensive Great Burbo Bank, was chosen to investigate such an impoundment, as it would provide flood defence for the low-lying North Wirral shore. The possible line of a Dee Outer Barrage is shown in Figure 3.2.6.1.

Indicative calculations for ebb mode operation have been performed for a Dee Outer Barrage (Table 3.2.6.1) using the Solway Firth costing data from the 1980 DoEn study, as the Solway Barrage alignment has comparable water depths and length.

Table 3.2.6.1: Annual energy output and cost of energy from Dee Outer Barrage.

Mode	Energy Output (TWh)	Cost of Energy (p/kWh)	% change in Cost of Energy relative to DoEn Dee Study
No Pumping	4.601	8.15	+15.5
Pumping	5.037	7.45	+14.1

The calculations were performed for a configuration of 150 x 8m 21MW turbines and 120 x 8m x 12m sluices – a scaling factor of three relative to the DoEn 1980 study (derived from the relative scale of the basin area). The interesting aspect of these results is that the cost of energy is not significantly greater than for the shorter inner line.

Although not investigated in this study, the Dee Outer line could also be modified to terminate at Formby Point at significant cost-benefit, thereby offering flood protection for the Dee, Mersey and Alt estuaries in a single structure. The barrage would only be practicable if shipping interests could be satisfactorily met via locks installed within it.

### 3.2.7 Dee Offshore Lagoon

There has also been recent interest in the concept of tidal lagoons or offshore tidal impoundments (OTIs). As the name implies, the idea is to build the barrage away from the shore as a standalone enclosure. The concept is an attempt to gain the better energy yields of tidal barrages, whilst not incurring opposition on environmental grounds from changes to the internal tidal regime.

Indicative calculations have been performed to establish the cost of energy for such a lagoon, using the storage characteristics of the Dee Outer Barrage as a model. The energy output was taken to be the same, and costs were adjusted linearly to take account of the length difference between a circular ‘free standing’ structure and a structure using the coastline as part of the boundary (for the same basin area). It was found that the unit cost of energy would increase by 39%, and that the length of the tidal lagoon perimeter would be 54.1km, compared to a Dee Outer Barrage length of 30km. These findings are broadly in line with those found for the Swansea Lagoon scheme (AEA Technology, 2006).

It is likely that the cost of energy from a tidal lagoon would be even higher than this estimate. Costs might be expected to scale with volume instead of length if the structure is generally sitting in deeper water than the equivalent estuary barrage. In addition, construction costs are likely to be higher as embankment construction cannot start from shore. It is also worth noting that such large offshore structures are likely to have significant impacts on local tides, wave patterns, sediment transport, wildlife and shipping. Thus, the positioning in Figure 3.2.7.1 is purely for illustrative purposes. The blue circle in the figure is simply to illustrate the scale of an offshore lagoon relative to a Dee-Wirral Lagoon.

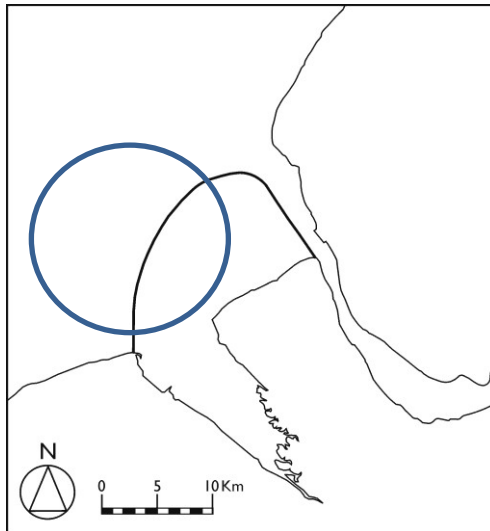


Figure 3.2.7.1: Indicative scale of a Dee Offshore Lagoon relative to a Dee-Wirral Lagoon.

### 3.3 Mersey Estuary

The alignment for a barrage in the Mersey Estuary, considered here, is that proposed in the DoEn report (UKAEA, 1984). It is depicted in Figure 3.3.1. Appendix A.3.1 contains extracts from the 1980 document showing the alignment of the barrage in more detail.

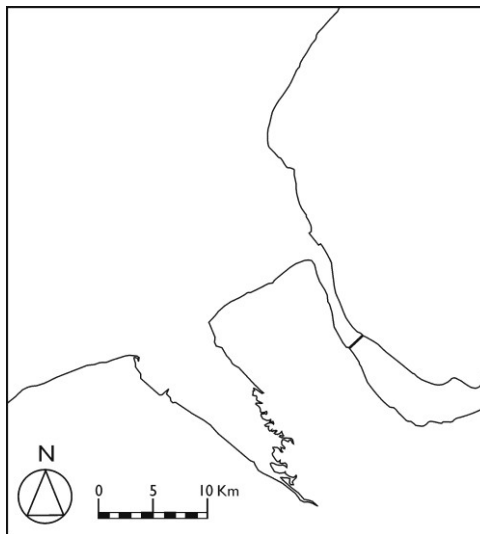


Figure 3.3.1: Sketch showing the location of a Mersey Barrage.

For the Mersey, the tidal conditions for the 0-D analysis were defined by the  $M_2$  and  $S_2$  tidal constituents, 3.23m and 0.98m, respectively. Water depths in the deep channel location for the turbines adopted in the earlier study are approximately 13m at low water spring tide level. This water depth was used for turbine selection and the energy calculations that follow.

For this study, the bathymetry within the impounded area of the barrage was established from LIDAR data collected by the Environment Agency in 2003. The resulting relationship between surface area and water level is presented in Figure 3.3.2 and is compared with the estimates used in the 1984 DoEn study. Tabular values are given in Appendix A.3.1.

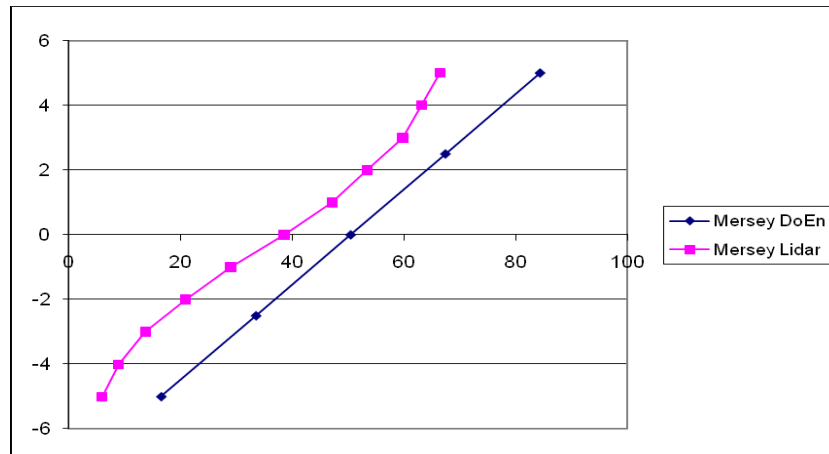


Figure 3.3.2: Mersey basin area (km<sup>2</sup>) as a function of water level (mAOD).

### 3.3.1 Initial appraisal (ebb generation only)

The aim here was to corroborate the 1984 DoEn findings for the Mersey. This was for a scheme of 27 7.6m diameter 23MW turbines and 18 12m x 12m sluices. The double-regulated turbine considered here has a rated head of 6.1m and a rotation speed of 57.7rpm. Since both the head and speed are higher than is preferred, an alternative configuration employing 11MW turbines has also been considered in Section 3.3.3. A figure of 80% was taken as the maximum turbine efficiency, with no subsequent losses, as adopted in Section 3.2. Table 3.3.1.1 presents the maximum energy predictions achieved by assuming a 1.0m minimum generating head ( $H_{min}$ ) together with the 'best' delay.

Table 3.3.1.1: Results of the corroboration calculations for Mersey Barrage in ebb mode using 7.6m diameter 23MW turbines with 18 12m x 12m sluices; minimum water depth at turbines = 13m.

Number of Turbines	DoEn Annual Energy (TWh)	Calculated Annual Energy (TWh)	% of DoEn*	Delay (hrs)
27	1.32	1.07	80.7	2.34

\* Percentage figures are a percentage of the figure reported in the 1984 DoEn study.

The results are comparable to those found earlier (Section 3.2.1 and in the preliminary studies, being approximately 15% less than the DoEn values), and are thought to arise from the difference in the specified turbine compared to that used in the 1984 study and to potential inconsistencies in the application of sluice characteristics, as discussed previously.

### 3.3.2 Investigating different operating modes

The figures derived in this section relate to a scheme of 27 7.6m diameter turbines of 23MW generator capacity (with 13m minimum water depth) and 18 12m x 12m sluices, consistent with the DoEn 1984 scheme specification.

Table 3.3.2.1: Annual energy output from Mersey Barrage as a function of operating mode.

Operating Mode	Energy Output (TWh) LIDAR Baythmetry	Energy Output % of ebb figure
Ebb	1.07	
Dual	0.98	91.8
Flood	0.64	59.9

Ebb mode produces the highest total energy output, with flood mode hindered by the bathymetry of the Mersey. Dual mode gives nearly 92% of the ebb total, which is the highest proportion for any of the estuaries studied, using the DoEn 'base' barrage configurations.

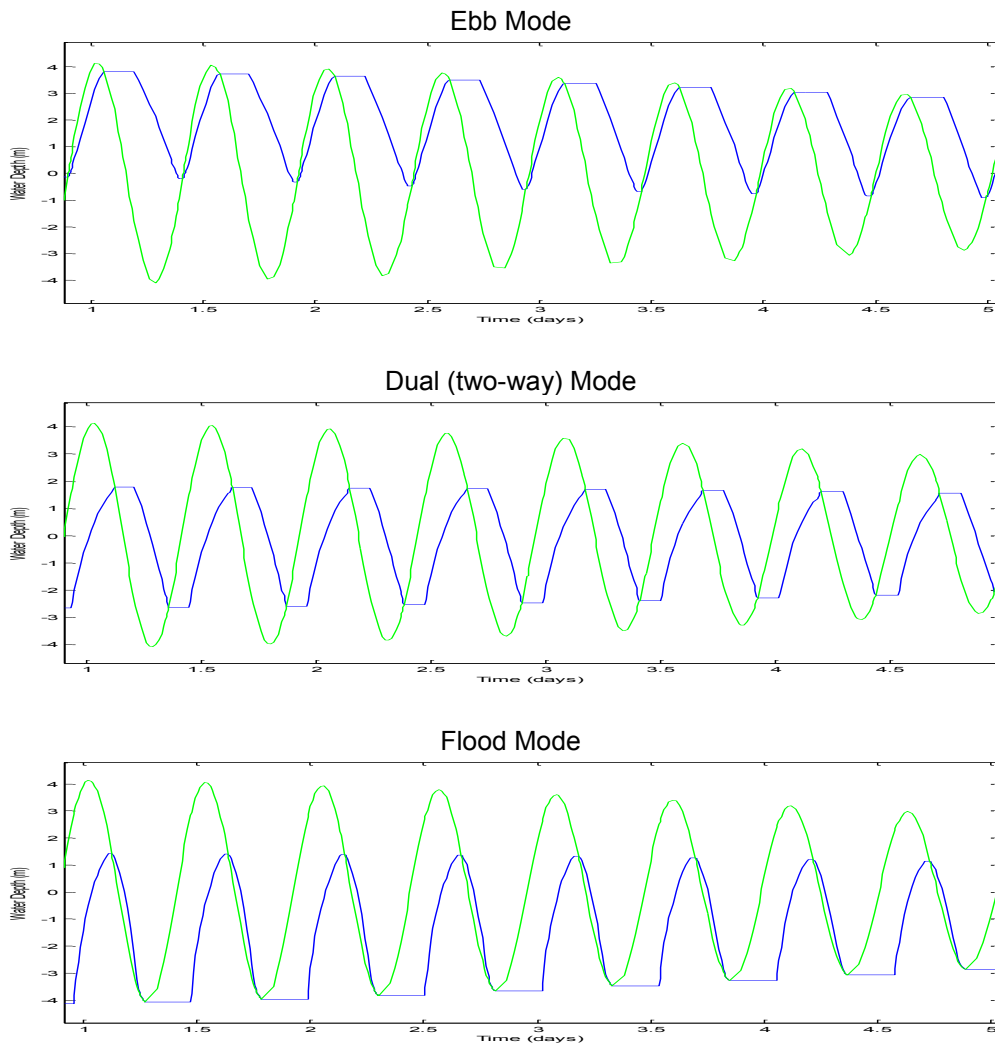


Figure 3.3.2.1: Mersey Barrage water levels for different operating modes (samples from the spring tidal phase; external tide level in green, basin water level in blue).

### 3.3.2.1 Effect of pumping

The above calculations were repeated with the addition of positive head pumping (before turbinning) to ascertain its effect. Pumping used the simple linear model described previously (Section 3.2), with a minimum head of 1m. Table 3.3.2.1.1 shows that pumping is once again generally beneficial, dual mode showing the smallest increase due to the shorter generation window and lower average head. The effects of pumping on different station configurations are considered in more detail later in Section 3.3.4.

Table 3.3.2.1.1: Annual energy output from Mersey Barrage as a function of operating mode, with positive head pumping and optimum delays.

Mode	Without Pumping (TWh)	With Pumping (TWh)	% change
Ebb	1.07	1.13	+6.35%
Dual	0.98	1.01	+3.45%
Flood	0.64	0.69	+8.70%

### 3.3.3 Turbine conditioning

#### 3.3.3.1 Changing generator capacity

As in the case of the Dee, an attempt was made to condition the turbines by reducing the generator capacity and hence its rated head, with a target of around the average tidal amplitude (approximately 3m). This was considered especially important for dual mode operation, where the driving head is expected to be lower.

Table 3.3.3.1.1: Mersey Barrage turbine characteristics as a function of generator capacity.

Generator (MW)	Rated Head (m)	Speed (rpm)
11	3.48	57.14

Table 3.3.3.1.2 presents the annual energy outputs arising, where it can be seen that this conditioning has been unsuccessful, with lower energy output in all operating modes.

Table 3.3.3.1.2: Annual energy output from Mersey Barrage as a function of operating mode with conditioned turbine.

Mode	23MW	11 MW	% change relative to 23MW
Ebb	1.07	0.87	-18.5
Dual	0.98	0.93	-5.16
Flood	0.64	0.60	-5.41

Figures 3.3.3.1.1 and 3.3.3.1.2 illustrate this further, where it can be seen that the 23MW generator is well conditioned, and the 11MW generator is too small for ebb mode operation, with extensive clipping of the power output (turbines working at maximum output).

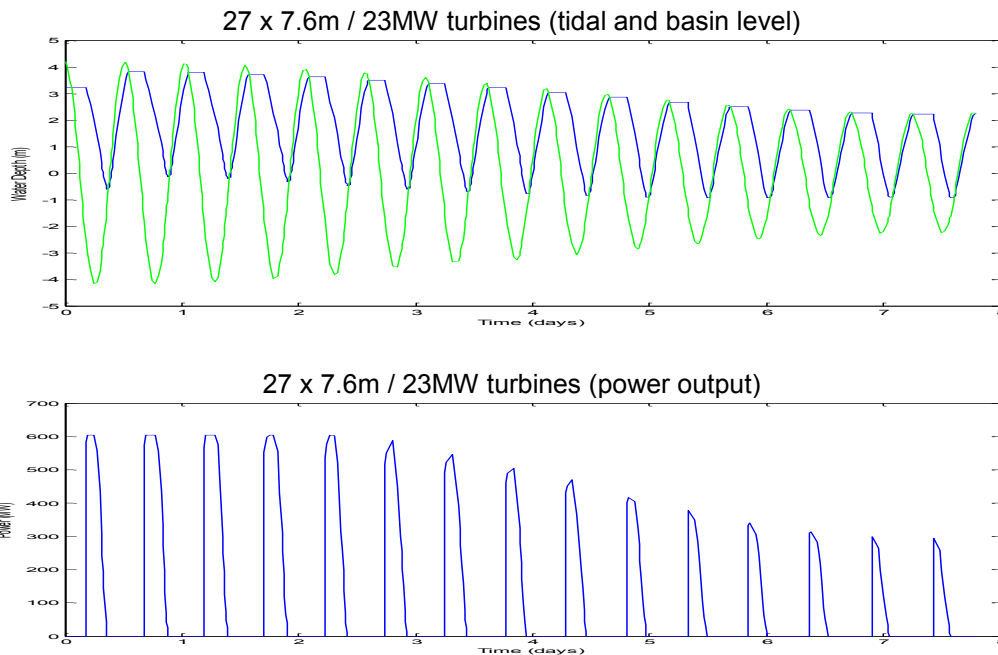


Figure 3.3.3.1.1: Mersey Barrage water levels and power output for 7.6m diameter 23MW turbines; ebb mode.

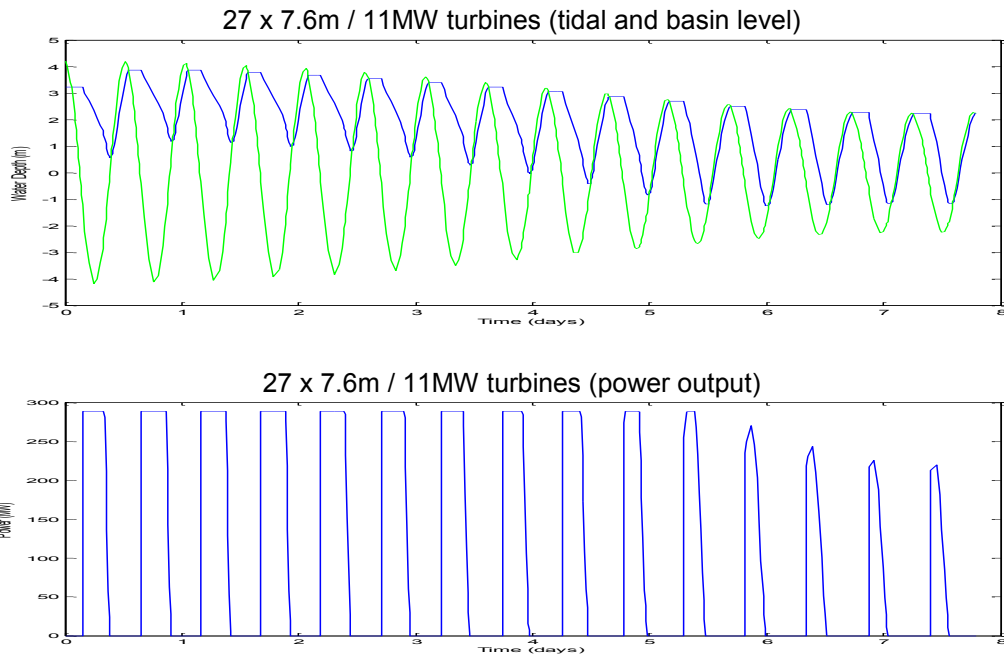


Figure 3.3.3.1.2: Mersey Barrage water levels and power output for 7.6m diameter 11MW turbines; ebb mode.

It is of interest to explore the effect that the smaller generator would have on the unit cost of electricity, and the results are shown in Tables 3.3.3.1.3 and 3.3.3.1.4.

Table 3.3.3.1.3: Annual energy output and cost of energy from Mersey Barrage for 7.6m 23MW turbines; 12m x 12m sluices.

Mode	Turbines	Sluices	Energy (TWh)	Cost (p/kWh)	Peak Power (MW) Spring / Neap	Installed Capacity (MW)
Ebb	27	18	1.07	4.28	600 / 300	621
Dual	27	18	0.98	5.16	440 / 180	621
Ebb	54	18	1.33	5.46	1200 / 800	1242
Dual	54	18	1.46	5.64	1200 / 600	1242
Ebb	81	0	1.25	7.77	1800 / 1200	1863
Dual	81	0	1.72	6.49	1800 / 1000	1863

Table 3.3.3.1.4: Annual energy output and cost of energy from Mersey Barrage for 7.6m 11MW turbines; 12m x 12m sluices.

Mode	Turbines	Sluices	Energy (TWh)	Cost (p/kWh)	Peak Power (MW) Spring / Neap	Installed Capacity (GW)
Ebb	27	18	0.87	5.05	297 / 220	297
Dual	27	18	0.93	5.12	297 / 140	297
Ebb	54	18	1.23	5.62	594 / 594	594
Dual	54	18	1.44	5.31	594 / 530	594
Ebb	81	0	1.23	7.43	891 / 891	891
Dual	81	0	1.66	6.16	891 / 891	891

As can be seen from the tables, the smaller generator is effective in lowering the cost of energy in dual mode operation for all the schemes considered. The energy output drops only slightly, and this is outweighed by the reduction in generator and transmission costs. It is also noted that, with the 11MW generator, the turbines are generating at more or less full capacity throughout the spring-neap cycle.

For ebb mode, the reductions in energy yields are much larger (the output is clipped for much of the time) and this outweighs the cost savings, driving up the cost of energy. Interestingly, for the 81 turbine scheme, the energy yield for the 11MW generator more or less matches the 23MW one, and hence the relative cost of electricity is smaller.

### 3.3.4 Increasing installed turbine capacity and cost implications arising

The calculations for the Dee essentially established how annual energy output and cost of energy varied as the number of turbines changed. For the Mersey, the calculations have been limited to showing these variations for ebb mode only, employing up to a 3xDoEn configuration of 81 turbines. The 81 turbine configuration should be treated with caution as it is at the absolute limit of physically fitting in the estuary, with no space for separate sluices. All calculations used 7.6m 23MW turbines (with 18 12m x 12m sluices).

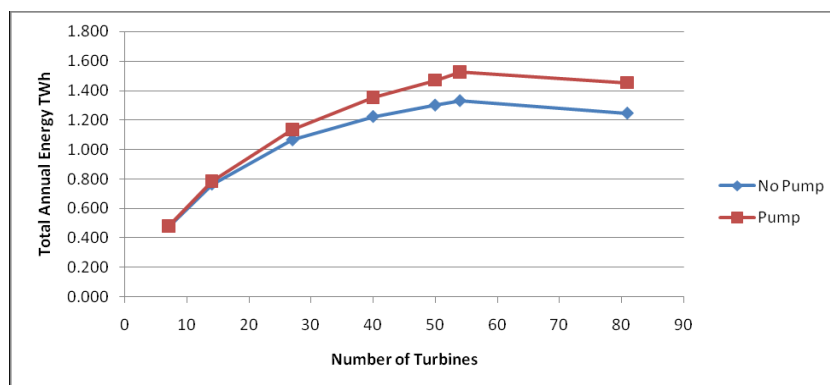


Figure 3.3.4.1: Annual energy output from Mersey Barrage operating in ebb mode, both with and without pumping, as a function of number of turbines.

Figure 3.3.4.1 illustrates the sensitivity of ebb mode operation to sluicing, as the 81 turbine calculations show lower energy outputs than the 54 turbine configuration due to there being insufficient sluicing capacity.

In addition to the energy runs, indicative costs were calculated by scaling the 1984 DoEn costs, and were used to derive the unit cost of the electricity produced in terms of 2007 prices (see Appendix A.3.2). The results are presented in Figure 3.3.4.2.

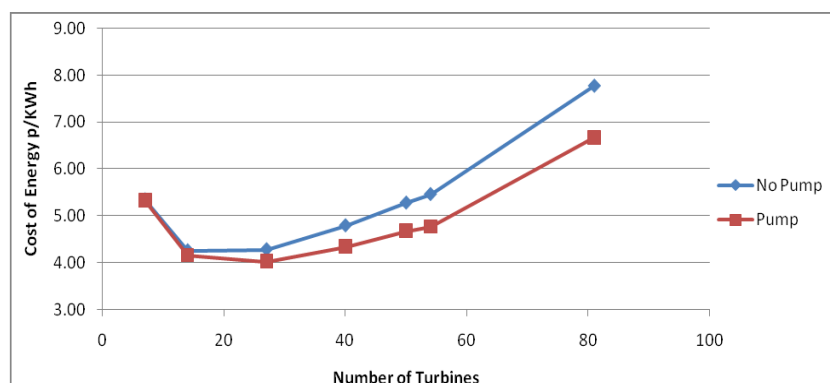


Figure 3.3.4.2: Unit cost of energy from Mersey Barrage as a function of number of turbines; ebb mode.

The figures show that the DoEn configuration of 27 23MW turbines gave the lowest cost of energy for that turbine size. Pumping is seen to give an energy gain of around 15% at higher turbine numbers.

The results for the 2xDoEn (54 turbines) and 3xDoEn (81 turbines) runs are presented in Tables 3.3.4.1 and 3.3.4.2.

Table 3.3.4.1: 2xDoEn scheme - annual energy output and cost of energy from Mersey Barrage for 54 7.6m 23MW turbines; 18 12m x 12m sluices.

Mode	Annual Energy (TWh)	Energy with Pumping (TWh)	Cost of Energy, No Pumping (p/kWh)	Cost of Energy with Pumping (p/kWh)
Ebb	1.33	1.52	4.70	4.10
Dual	1.46	1.60	4.85	4.44

Table 3.3.4.2: 3xDoEn scheme - annual energy output and cost of energy from Mersey Barrage for 81 7.6m 23MW turbines; no separate sluices.

Mode	Annual Energy (TWh)	Energy with Pumping (TWh)	Cost of Energy, No Pumping (p/kWh)	Cost of Energy with Pumping (p/kWh)
Ebb	1.25	1.45	6.69	5.75
Dual	1.72	1.87	5.59	5.15

Dual mode operation once again captures more of the available energy in both 2xDoEn (54 turbines) and 3xDoEn (81 turbines) schemes. The ebb 3xDoEn scheme is seen to suffer from a lack of sluicing capacity, whereas the dual scheme is not affected in the same way, as most of the flow is through the turbines anyway. In all instances, the cost of energy is higher than the base (1xDoEn) 27 turbine ebb scheme.

The final point to notice is that even though the schemes with higher installed capacity give higher costs of energy than the base 27 turbine scheme, the costs themselves are competitive with the other estuaries considered. This is a reflection of the low cost of the Mersey scheme, as the barrage is comparatively short at 1.75km. The Dee, by contrast, has a barrage length of 9.5km for comparable energy output, and the scheme economics reflect these factors in a higher cost of energy. In addition, a 2xDoEn (1242MW) or 3xDoEn (1863MW) scheme is likely to present less of an issue in terms of power pulses into the grid compared to larger schemes such as the Severn, Solway Firth or Morecambe Bay.

3.3.4.1 Effect on generation window

This study of the Mersey scheme also explored the effect on the generation window (the time that the barrage is generating electricity) of changing the number of turbines. This issue is of interest for estimating the base load capability from tidal power and for establishing the likely impact on the National Grid.

All calculations were performed using the 7.6m 23MW turbines (with a 13m minimum water depth at the turbines), and the results are shown in Figure 3.3.4.1.1, and relate to the use of optimal delay for maximum energy generation in each case. As the diagram shows, dual mode operation provides electricity for a longer total generation period during a tidal cycle (of 12 hours 25 minutes duration) than ebb mode operation. This is to be expected, as generation takes place on both the ebb and flood tides, and these two generation periods taken together might be expected to be longer than a single ebb period. It is also clear that the ebb part of the dual cycle is generally shorter than a comparable ebb-only generation, as the basin does not fill up as much during dual mode generation. Note that the convergence of the generation times at 81 turbines reflects the lack of independent sluicing capacity. Also of interest is the relatively long flood generation period of dual mode operation, a reflection of the reduced flows that are expected when the turbines are operated in reverse. The final

point of interest is how the overall generation period reduces with an increase in the number of turbines, leading to the sharp power pulses already discussed.

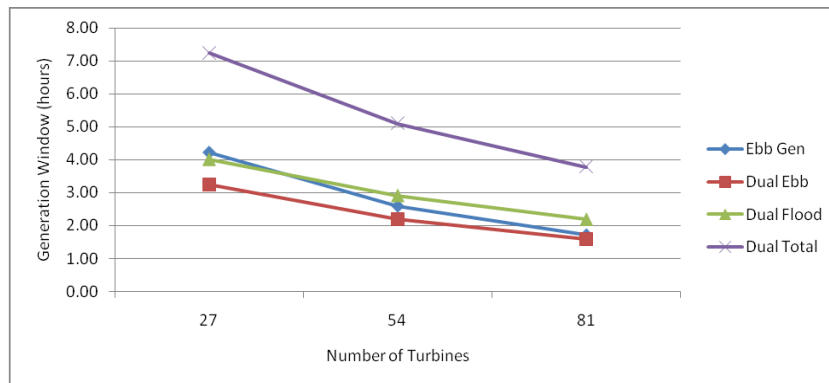


Figure 3.3.4.1.1: Average generation window per tide for Mersey Barrage as a function of operating mode and number of turbines.

### 3.3.5 Increasing installed sluice capacity and cost implications arising

Calculations were performed similar to those for the changes in the number of turbines, once again using the 7.6m diameter 23MW machine (with a 13m minimum water depth at the turbines), but this time varying the sluicing area. The number of sluices was varied from the baseline of 18 for the DoEn 27 turbine barrage configuration in ebb mode only. The results are shown in Figures 3.3.5.1 and 3.3.5.2.

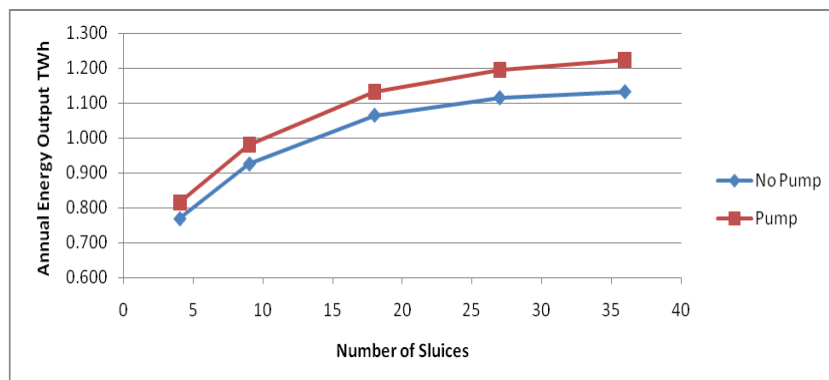


Figure 3.3.5.1: Annual energy output from Mersey Barrage operating in ebb mode as a function of number of sluices.

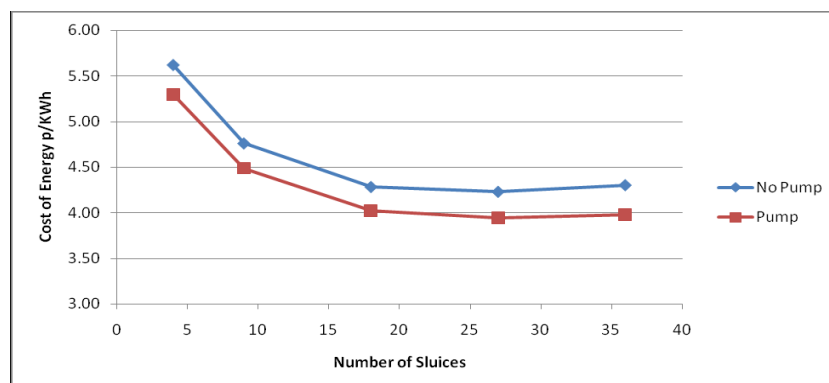


Figure 3.3.5.2: Unit cost of energy from Mersey Barrage with 27 turbines as a function of number of sluices.

The results suggest that the DoEn configuration could be slightly improved by increasing from 18 to 27 sluices. The sensitivity of ebb mode operation to sluicing has again been demonstrated.

### 3.3.6 Intertidal area

There has rightly been concern from the Royal Society for the Protection of Birds (RSPB) and other conservation interest groups about the impacts that barrages are likely to have on tidal estuaries, many of which are protected habitats. One way of gauging the potential impact is by evaluating the intertidal area of sediment exposed between low and high tide, as this provides a crude measure of the possible impact on the food source for birds.

Indicative calculations have been performed for 1xDoEn (27 turbines) and 2xDoEn (54 turbines) schemes, showing the effect of varying delays and operating modes on the intertidal area retained. It must be stressed that these results are indicative only, as environmental impact is a very complex issue which would require further detailed work including, but not limited to, full hydrodynamic and sedimentation studies. Section 5 of this report discusses the environmental implications in more detail, and it is expected that this crucial aspect will be given a thorough appraisal in the current Strategic Environmental Assessment (SEA) being undertaken for the Severn.

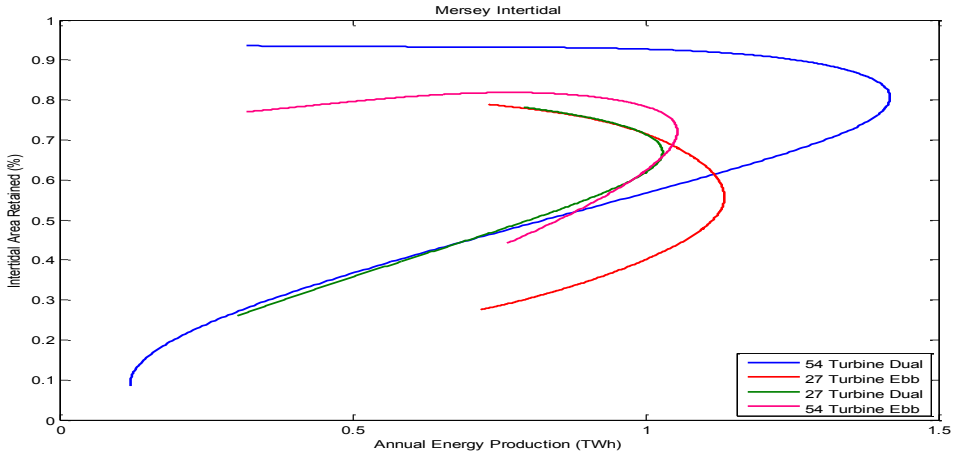


Figure 3.3.6.1: Intertidal area retained in the Mersey for 1xDoEn and 2xDoEn schemes in ebb and dual modes with varying time delays for an average ( $M_2$ ) tide.

The curves in Figure 3.3.6.1 encompass varying delays, with a 0 hour delay defining the lower limit and a 4 hour delay defining the upper limit of each curve, and with the maximum annual energy production corresponding to the optimum delay somewhere in between. The plot illustrates the sensitivity of the intertidal area to the chosen delay before which generation starts and to the operational mode.

With 27 turbines, the ebb and dual schemes are broadly comparable in terms of the intertidal area retained (at best 80%), and this is reflective of the water level modification seen during the discussion of operating mode in Section 3.3.2. For a 2xDoEn (54 turbines) scheme, the difference between ebb and dual modes is more pronounced, with dual mode generally conserving more of the intertidal area, though both are better than the 1xDoEn scheme. That dual mode conserves more of the intertidal area is to be expected: it has already been seen that such schemes preserve more of the tidal regime. In an ebb scheme, the water level will not drop as low.

The effect of delays and operating mode is now explored in more detail. The figures that follow show the intertidal area retained for a particular time delay, operating mode, and state of the tide, as the tide moves from spring to neap and back again. To be clear, the proportion of the intertidal area retained is, for each tide, the difference in areas exposed at low water and at high water in the barrage basin compared to conditions for the unmodified tide at low and high waters.

The unmodified tides are shown in Figure 3.3.6.2 to illustrate the time axis used. Figure 3.3.6.3 shows the basin wet area and estimated area of exposed sediment as a function of water level.

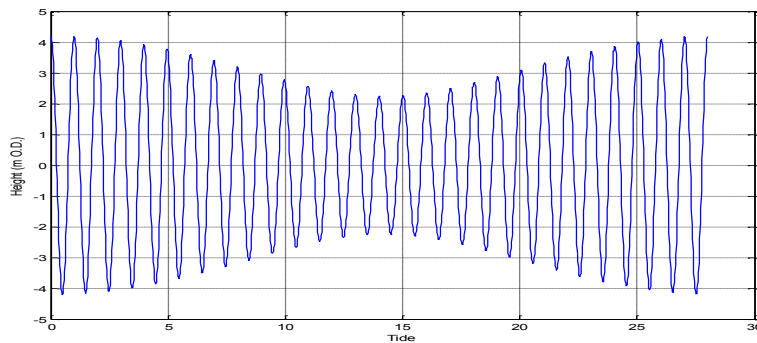


Figure 3.3.6.2: Unmodified tides in the Mersey during the spring to neap to spring cycle.

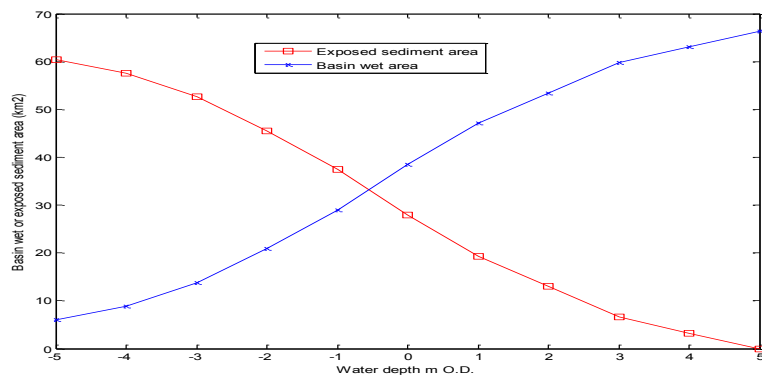


Figure 3.3.6.3: Mersey basin wet area ( $\text{km}^2$ , blue) and exposed sediment area ( $\text{km}^2$ , red) as a function of water level (mAOD).

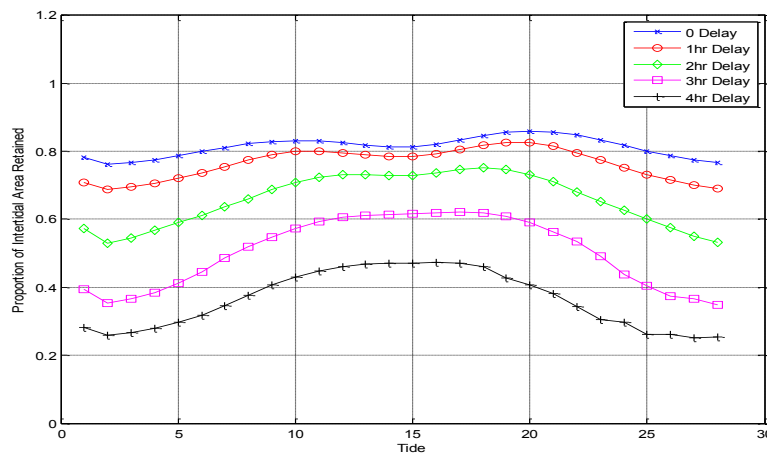


Figure 3.3.6.4: Intertidal area retained in the Mersey basin by tide with varying time delays; ebb mode, 27 turbines.

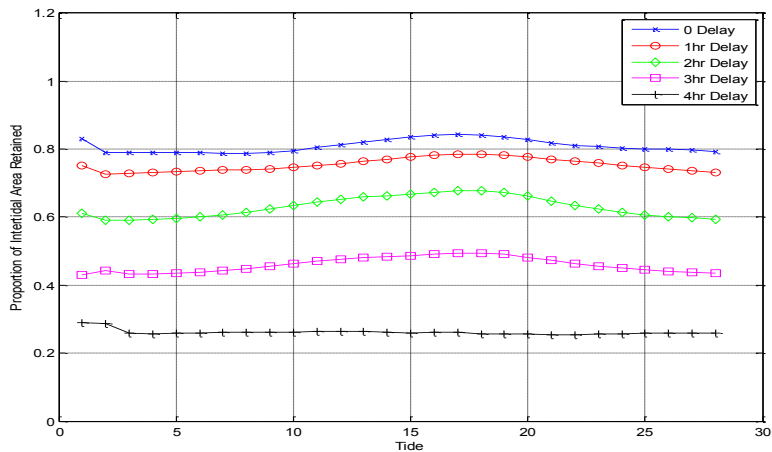


Figure 3.3.6.5: Intertidal area retained in the Mersey basin by tide with varying time delays; dual mode, 27 turbines.

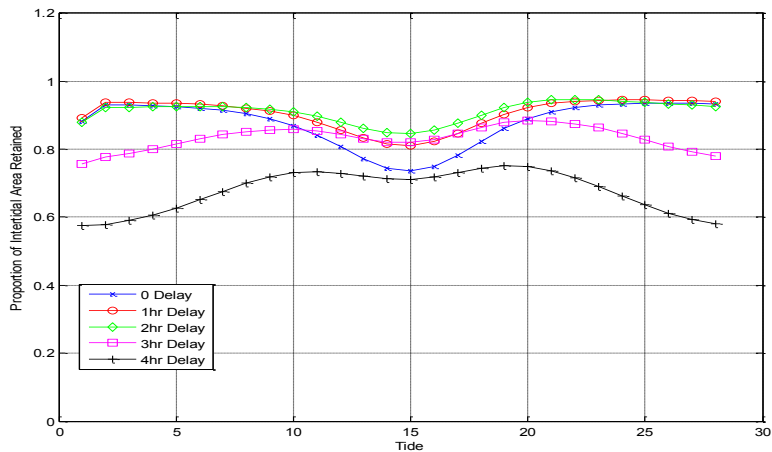


Figure 3.3.6.6: Intertidal area retained in the Mersey basin by tide with varying time delays; ebb mode, 54 turbines.

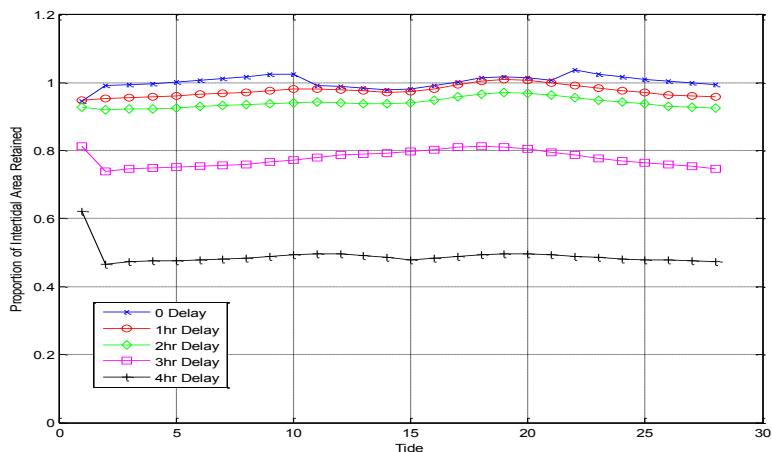


Figure 3.3.6.7: Intertidal area retained in the Mersey basin by tide with varying time delays; dual mode, 54 turbines.

(Values over one are due to numerical overshoot of the computer routines used to solve the equations. The anomalous values for tide one are due to starting conditions).

As Figures 3.3.6.4 to 3.3.6.7 show, both the ebb and dual mode results are sensitive to the time delay before the start of turbinning. They also show that, for dual mode, the intertidal area

retained is relatively constant throughout the spring – neap cycle (for a particular delay), as the presence of the barrage attenuates both the high and low water marks. It is also clear from the figures that the larger 2xDoEn scheme (54 turbines) leads to more of the intertidal area being retained: around 90% (at best) in ebb mode, and virtually 100% in dual mode.

The pattern of retention of intertidal area is more complicated for ebb mode than for dual mode operation. For the 27 turbine scheme, a higher proportion of the intertidal area is retained at neap tides than at spring tides. The reason is made clear in Figure 3.3.6.8. Obviously, more sediment is exposed at low water than at high water, and as the basin low water level more closely approaches the unrestricted tidal low water level, the intertidal area retained increases, with high water in the basin and for the unrestricted tide being closely matched.

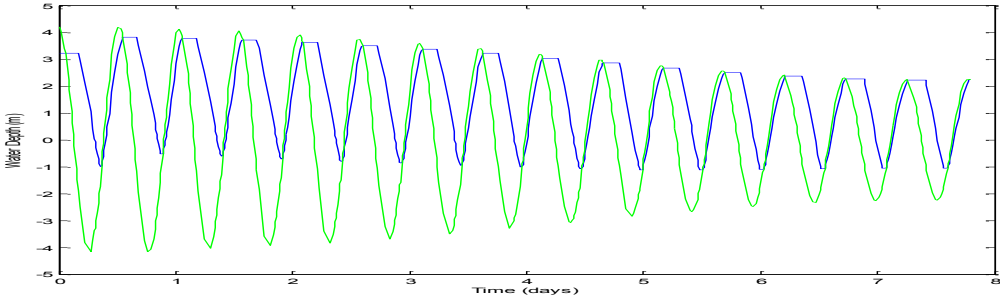


Figure 3.3.6.8: Tide and basin water levels in the Mersey for a 27 turbine ebb scheme, 2 hour delay.

For the 54 ebb turbine scheme, the situation is reversed, except for the 4 hour delay, with more intertidal area retained at spring tides than at neaps. See Figures 3.3.6.9 and 3.3.6.10.

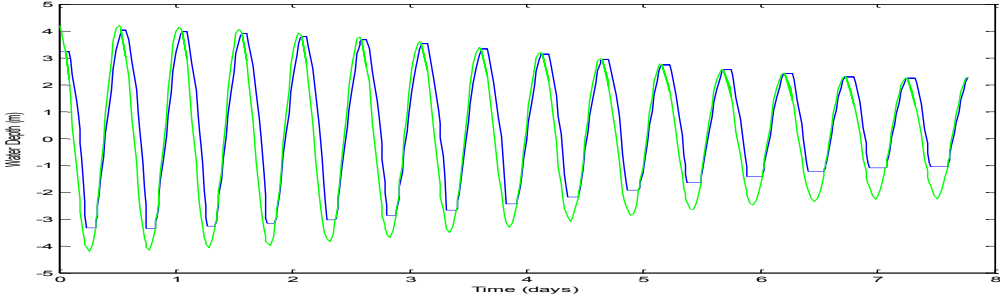


Figure 3.3.6.9: Tide and basin water levels in the Mersey for a 54 turbine ebb scheme, 0 hour delay.

Figure 3.3.6.9, for a 0 hour delay, shows that the low water level in the basin increases from spring to neap conditions, which also means that the low water sediment area at low water decreases. Given that high water levels in the basin and for the unrestricted tide are the same, this means that the intertidal area retained decreases from spring to neap conditions.

The basin and unrestricted tidal levels for a 4 hour delay with 54 turbines are shown in Figure 3.3.6.10. This displays the same pattern seen for 27 turbines, where the basin low water level at neap conditions more closely approaches the unrestricted tidal low water level. Hence, more intertidal area is retained.

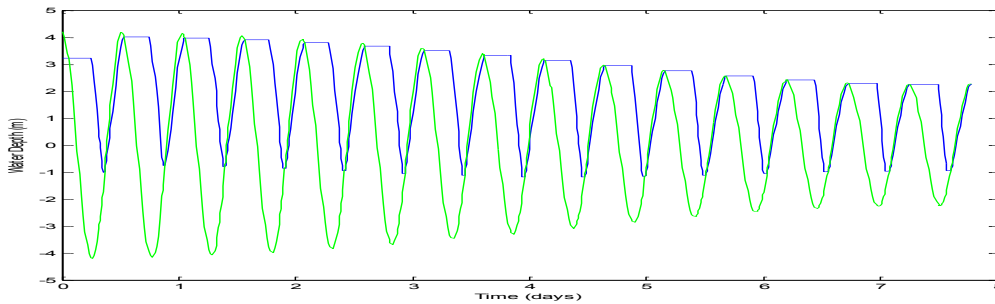


Figure 3.3.6.10: Tide and basin water levels in the Mersey for a 54 turbine ebb scheme; 4 hour delay.

### 3.4 Ribble Estuary

A possible alignment for a barrage on the Ribble Estuary is shown in Figure 3.4.1. This estuary was not considered in detail in the DoEn studies (UKAEA, 1984; DoEn, 1989) and so relevant barrage parameters have been estimated.

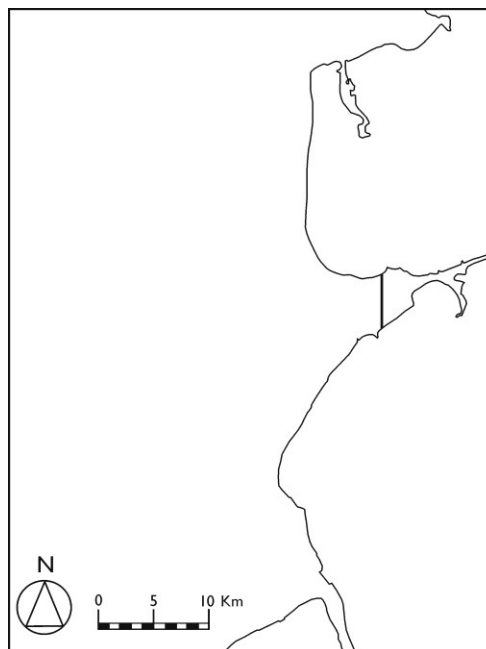


Figure 3.4.1: Sketch showing a possible location for a Ribble Barrage.

For the Ribble, the  $M_2$  and  $S_2$  tidal constituents were taken as the average of those for the Dee, Mersey and Morecambe Bay, which gave 3.092m and 0.928m. Water depths were taken from Admiralty charts, which gave a depth of about 7m in the deepest channel at low water of spring tides.

Other barrage parameters were estimated from LIDAR bathymetric data (see Figure 3.4.2) and by interpolating Baker's (1986) cost and energy functions. This analysis suggested a barrage configuration of 11 6.5MW turbines. The turbine diameter was taken to be 4m from a comparison with the smaller estuary schemes in the 1984 DoEn study, which would imply dredging of around 2m, given a minimum existing water depth of only 7m at the turbine location. The area of the sluices was taken to be 3.5 times the turbine sluicing area (the area of the turbine ducts less the area occupied by the turbine hubs) from comparison with other schemes. The energy outputs from this configuration, by barrage operating mode, are given in Table 3.4.1.

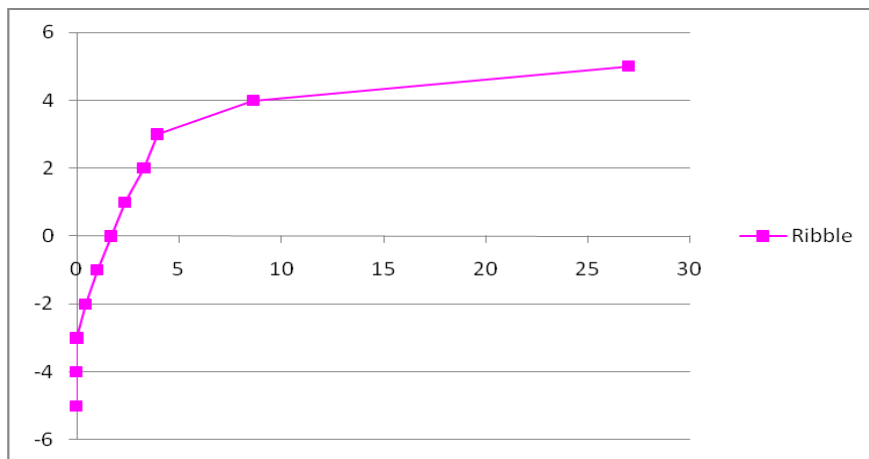


Figure 3.4.2: Ribble basin area (km<sup>2</sup>) as a function of water level (mAOD).

Table 3.4.1: Annual energy output from Ribble Barrage as a function of operating mode (11 4m diameter 6.5MW turbines).

Operating Mode	Energy Output (TWh) LIDAR Baythmetry	Energy Output % of ebb figure
Ebb	0.076	
Dual	0.059	77.4
Flood	0.024	32.1

Costs of energy for ebb generation were estimated from both Baker's cost and energy functions, and by modelling the costs of the comparable Dovey Barrage, using the energy outputs derived in this study. Figures are presented in Table 3.4.2.

Table 3.4.2: Cost of energy from Ribble Barrage operating in ebb mode.

Mode	Energy (TWh)	Cost of Energy (p/kWh – Baker)	Cost of Energy (p/kWh – based on Dovey)
No Pumping	0.076	7.45	8.04
Pumping	0.089	N/A	6.83

The figures show that the Ribble produces a unit cost of electricity of around 7.75p/kWh, which is comparable with the other estuaries examined. These figures should be taken to be indicative only, given the coarse nature of the estimating process. In particular, it is likely that relatively more dredging would be required than in the other estuaries already examined, which would increase scheme costs. Nevertheless, these calculations indicate that the Ribble is worth more detailed study, as a barrage could provide commercially viable electricity whilst also offering flood protection to significant areas of low-lying land.

### 3.5 Morecambe Bay

The alignment for a barrage in Morecambe Bay is that proposed in the DoEn study (UKAEA, 1980). It is depicted in Figure 3.5.1. Appendix A.3.1 contains extracts from the 1980 document showing both the alignment and a cross-section of the estuary.

For Morecambe Bay, the tidal conditions for the 0-D analysis were defined by the M<sub>2</sub> and S<sub>2</sub> tidal constituents, 3.07m and 0.93m, respectively. Water depths in the deep channel location for the turbines adopted in the earlier study were approximately 26m at low water of spring tides. This water depth was used for turbine selection and the energy calculations that follow.

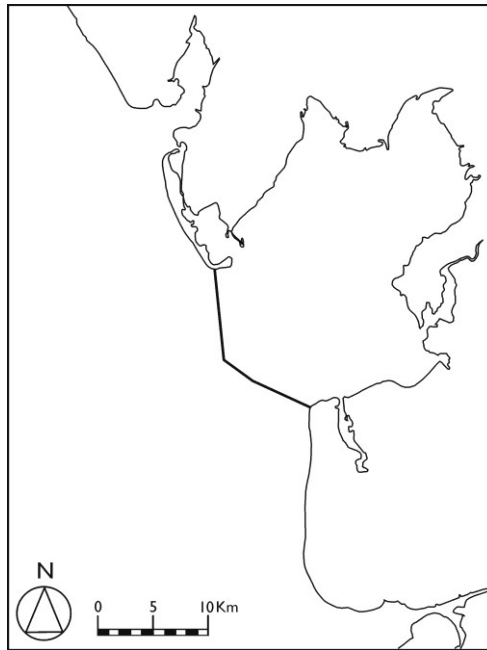


Figure 3.5.1: Sketch showing the location of the Morecambe Bay Outer Barrage.

The bathymetry within the impounded area of the barrage was taken as that given in the DoEn (UKAEA, 1980) report. Also considered were data from the British Oceanographic Data Centre (at the Proudman Oceanographic Laboratory), although this data set was known to have shortcomings in precision within the estuaries, which are beyond the region of normal interest for oceanographic modelling. The resulting surface area relationships with water level are presented in Figure 3.5.2. Tabulated values are given in Appendix A.3.1.

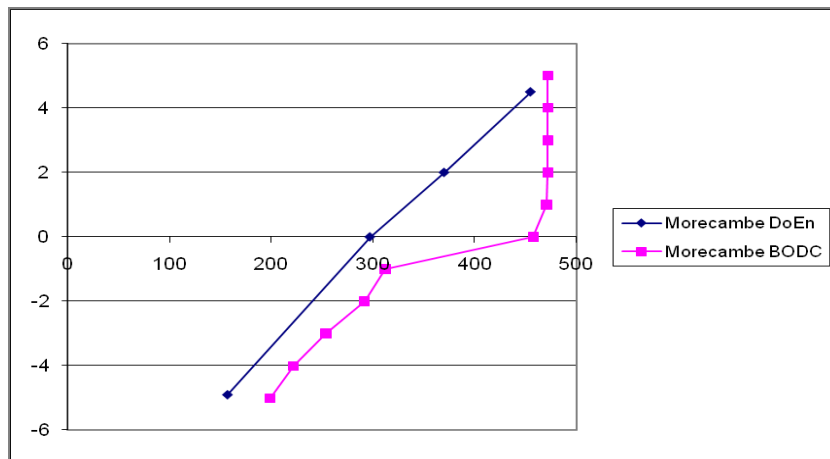


Figure 3.5.2: Morecambe Bay basin area ( $\text{km}^2$ ) as a function of water level (mAOD).

As the figure illustrates, the BODC derived bathymetry implies a very steep-sided estuary. This is thought to be due to incomplete coverage of the data within wetted areas. In view of the disparity, both relationships were considered in most of the calculations, though judgement places most credence on the original DoEn values. High quality LIDAR coverage is called for, and enquiries suggest that this is within the future work plan of the Environment Agency.

### 3.5.1 Initial appraisal (ebb generation only)

The aim here was to corroborate the findings of the 1980 Department of Energy Study (UKAEA, 1980) for the Morecambe Bay Outer Barrage. This was for a scheme of 120 9m diameter 50MW turbines and 140 12m x 12m sluices. The double-regulated turbine considered here has a rated head of 7.66m and a rotation speed of 63.2rpm. Since both the head and speed are higher than is preferred, a better conditioned configuration employing 16MW turbines has also been considered in Section 3.5.3.

As in Section 3.2, a figure of 80% was taken as the maximum turbine efficiency, with no subsequent losses. Calculations were undertaken both with the BODC bathymetry and with that used in the DoEn study. Table 3.5.1.1 presents the maximum energy predictions achieved by assuming a 1.0m minimum generating head ( $H_{min}$ ) together with the 'best' delay.

Table 3.5.1.1: Results of the corroboration calculations for Morecambe Bay Barrage in ebb mode using 9m diameter 50MW turbines with 140 12m x 12m sluices; minimum water depth at turbines = 26m.

Number of Turbines	DoEn Annual Energy (TWh)	BODC Bathymetry			DoEn Bathymetry		
		Energy (TWh)	% of DoEn*	Delay (hrs)	Energy (TWh)	% of DoEn*	Delay (hrs)
120	6.96	6.45	92.7	2.2	5.83	83.7	2.6

\* Percentage figures are a percentage of the figure reported in the 1980 DoEn study.

The DoEn bathymetry gives lower energy, which is what would be expected from Figure 3.5.2. Ebb mode typically operates between high water and mean water, and the DoEn bathymetry shows a smaller basin area than the BODC bathymetry over this range of water levels.

### 3.5.2 Investigating different operating modes

The figures derived in this section relate to a scheme of 120 9m diameter turbines of 50MW generator capacity (with a 26m minimum water depth) and 140 12m x 12m sluices consistent with the DoEn 1980 scheme specification.

Table 3.5.2.1: Annual energy output from Morecambe Bay Barrage as a function of operating mode.

Operating Mode	BODC Bathymetry		DoEn Bathymetry	
	Energy Output (TWh)	Energy Output % of ebb figure	Energy Output (TWh)	Energy Output % of ebb figure
Ebb	6.45		5.83	
Dual	5.41	83.8	5.24	89.9
Flood	5.24	81.2	4.49	77.1

Ebb mode produces the highest total energy output, with flood mode being hindered by the bathymetry of the estuary. The DoEn bathymetry gives significantly lower outputs, and this is reflective of the difference in bathymetries. As Figure 3.5.2 shows, the DoEn bathymetry implies a smaller water volume mobilised for both flood and ebb modes (and hence for dual mode), giving lower energy figures, and this is what is seen in the table. Figure 3.5.2.1 shows the basin level variations under the different operational modes.

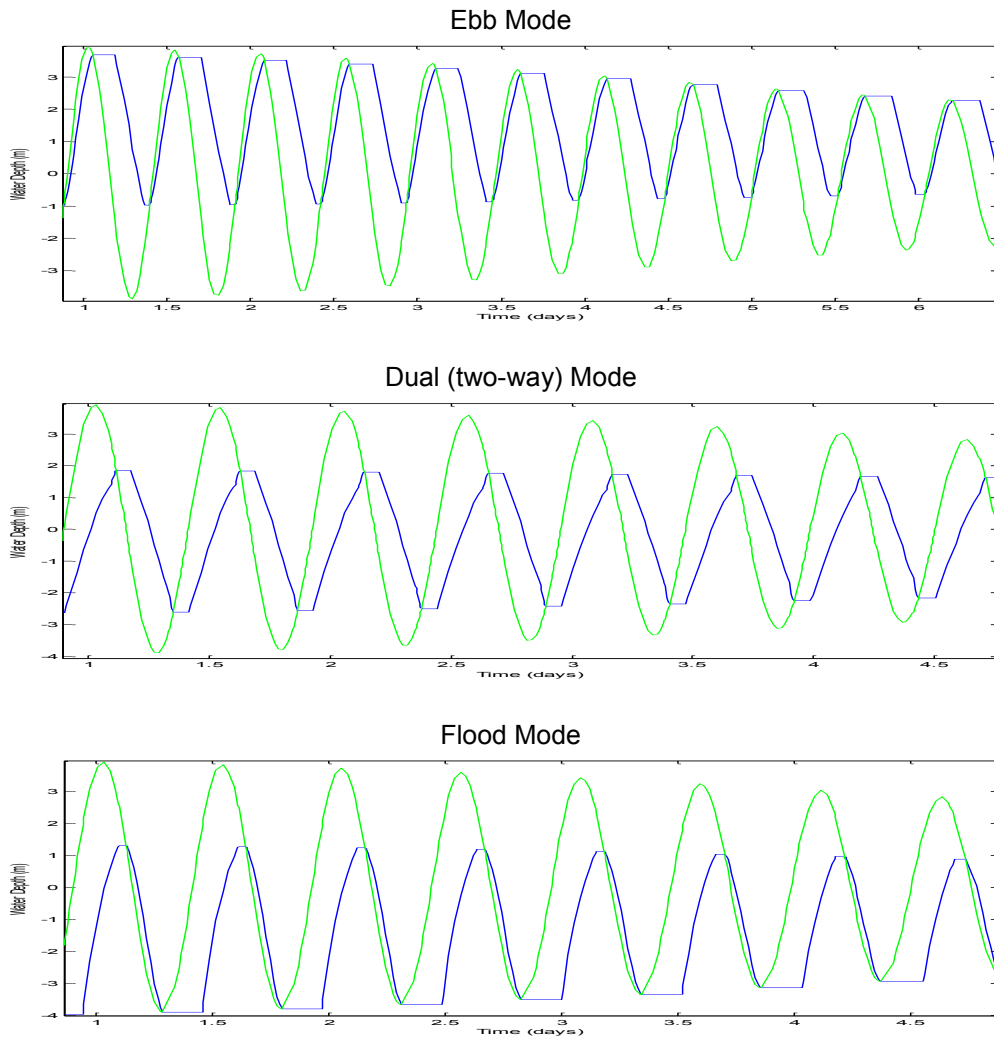


Figure 3.5.2.1: Morecambe Bay Barrage water levels for different operating modes (samples from the spring tidal phase; external tide level in green, basin water level in blue).

### 3.5.2.1 Effect of pumping

The calculations above were repeated with the addition of positive head pumping (before turbinng) to ascertain its effect. Pumping used the simple linear model described previously, with a minimum head of 1m. Table 3.5.2.1.1 shows that pumping is generally beneficial (especially for flood mode), and that operating mode and bathymetry are both factors which influence whether this will be so. The effects of pumping on different station configurations are considered in more detail later in Section 3.5.4.

Table 3.5.2.1.1: Annual energy output from Morecambe Bay Barrage as a function of operating mode, with positive head pumping and optimum delays.

Mode	BODC Bathymetry		DoEn Bathymetry	
	No Pumping (TWh)	Pumping (TWh)	No Pumping (TWh)	Pumping (TWh)
Ebb	6.45	6.77 (+4.88%)	5.83	6.26 (+7.39%)
Dual	5.41	5.37 (-0.77%)	5.24	5.31 (+1.25%)
Flood	5.24	5.74 (+9.45%)	4.49	5.08 (+13.1%)

### 3.5.3 Turbine conditioning

#### 3.5.3.1 Changing generator capacity

As previously, an attempt was made to condition the turbines by reducing the generator capacity and hence its rated head, with a target of around the average tidal amplitude (approximately 3m). This was considered especially important for dual mode operation where driving head is expected to be lower. The operating mode calculations were repeated for both the BODC and DoEn bathymetries using this smaller generator capacity (Table 3.5.3.1.1) and the results are summarised in Table 3.5.3.1.2. Once again, the better conditioning of the machine has a significant effect for dual mode operation.

Table 3.5.3.1.1: Morecambe Bay Barrage turbine characteristics as a function of generator capacity.

Generator (MW)	Rated Head (m)	Speed (rpm)
16	3.61	49.59

Table 3.5.3.1.2: Annual energy output from Morecambe Bay Barrage as a function of operating mode with conditioned turbine.

Mode	BODC Bathymetry			DoEn Bathymetry		
	50MW (TWh)	16 MW (TWh)	% change relative to 50MW	50MW (TWh)	16MW (TWh)	% change relative to 50MW
Ebb	6.45	6.04	-6.40	5.83	5.51	-5.36
Dual	5.41	6.06	+12.0	5.24	5.75	+9.66
Flood	5.24	5.22	-0.49	4.49	4.66	+3.83

It is of interest to explore the effect that the smaller generator has on the unit cost of electricity, and the results are shown in Tables 3.5.3.1.3 and 3.5.3.1.4 for the DoEn bathymetry.

Table 3.5.3.1.3: Annual energy output and cost of energy from Morecambe Bay Barrage for 9m 50MW turbines; 140 12m x 12m sluices.

Mode	Turbines	Sluices	Energy (TWh)	Cost (p/kWh)	Peak Power (GW) Spring / Neap	Installed Capacity (GW)
Ebb	120	140	5.83	6.41	4.3 / 1.6	6.0
Dual	120	140	5.24	7.91	2.1 / 0.8	6.0
Ebb	360	140	7.55	11.3	17.0 / 7.0	18.0
Dual	360	140	10.0	9.76	12.5 / 5.0	18.0

Table 3.5.3.1.4: Annual energy output and cost of energy from Morecambe Bay Barrage for 9m 16MW turbines; 140 12m x 12m sluices.

Mode	Turbines	Sluices	Energy (TWh)	Cost (p/kWh)	Peak Power (GW) Spring / Neap	Installed Capacity (GW)
Ebb	120	140	5.51	6.04	1.9 / 1.3	1.92
Dual	120	140	5.75	6.46	1.9 / 0.75	1.92
Ebb	360	140	8.61	8.50	5.7 / 5.7	5.76
Dual	360	140	11.5	7.39	5.7 / 5.0	5.76

The smaller generator decreases the cost of energy for both the 120 and 360 turbine installations, in both ebb and dual operating modes. Calculations presented in Appendix A.3.3 show that for the base (120 turbine) scheme, in ebb mode, the energy output drops 5.4%, whilst the cost drops 10.8%, giving a 5.8% reduction in the cost of energy. The energy yields are increased by using smaller generators and the scheme costs are also reduced for

all of the other cases considered, with a knock-on effect on the cost of energy. The final point worth noting from the tables is that the 50MW turbines rarely exploit their full capacity, whereas this is something that is frequently achieved using the smaller 16MW machines. Figures 3.5.3.1.1 and 3.5.3.1.2 show the power output and water levels for the two generators, with the base 120 turbine configuration operating in ebb mode. Given the degree of clipping shown in Figure 3.5.3.1.2, the 16MW generator is probably a little undersized, and an even lower unit cost of energy should be possible with a slightly larger generator (perhaps ~25MW).

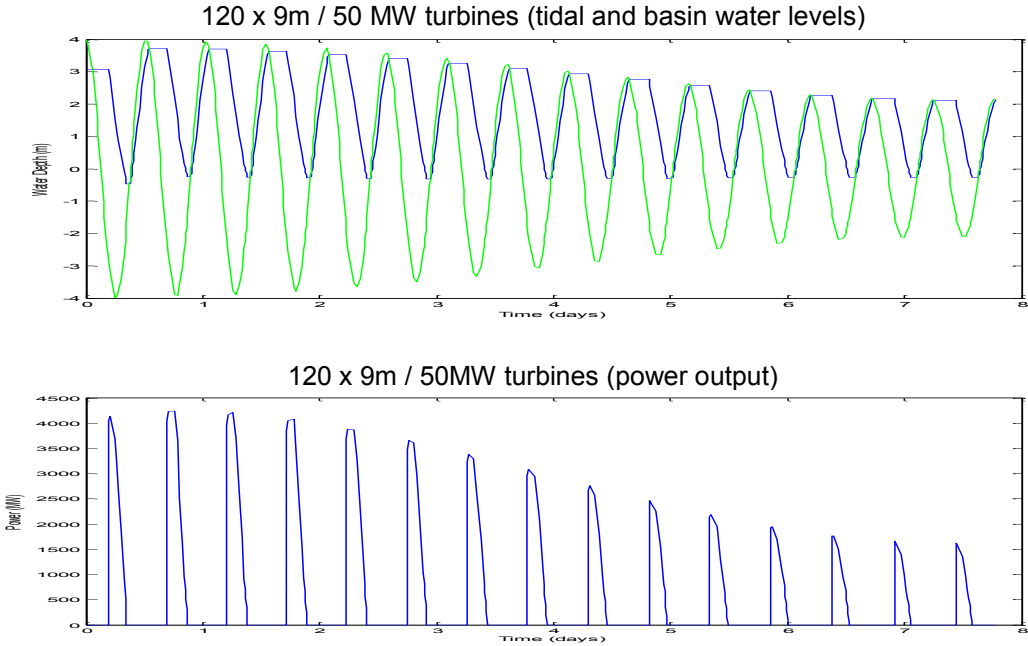


Figure 3.5.3.1.1: Morecambe Bay Barrage water levels and power output for 9m diameter 50MW turbines; ebb mode.

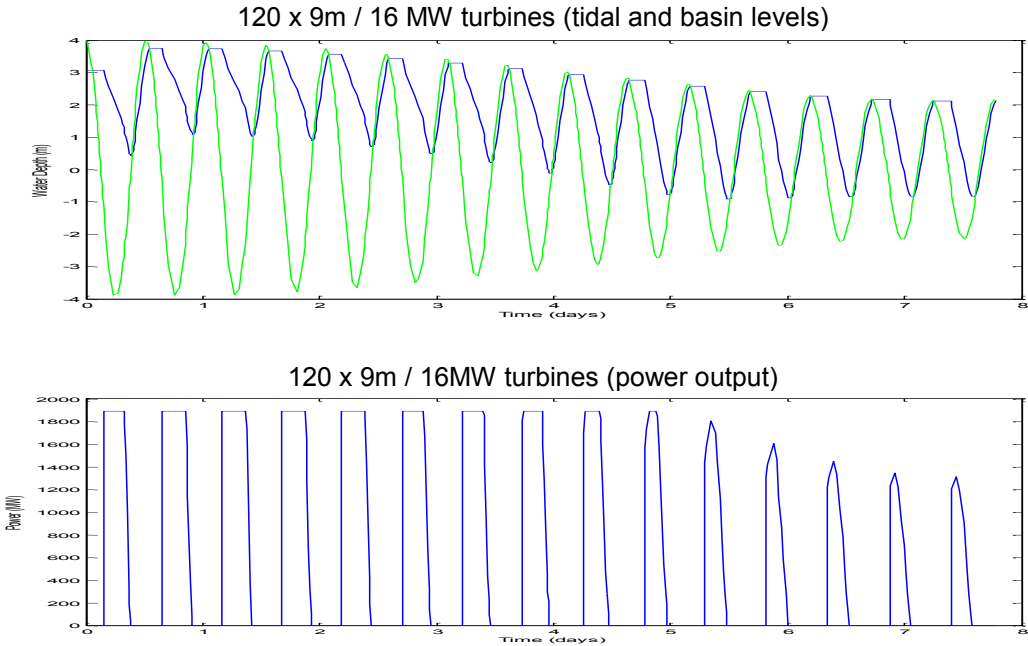


Figure 3.5.3.1.2: Morecambe Bay Barrage water levels and power output for 9m diameter 16MW turbines; ebb mode.

### 3.5.4 Increasing installed turbine capacity and cost implications arising

The calculations for the Dee have established essentially how annual energy output and the unit cost of energy vary as the number of turbines is changed. For Morecambe Bay, the calculations have been limited to showing these variations for ebb mode only, and up to a 3xDoEn configuration of 360 turbines (see Figure 3.5.4.1). Calculations used 9m diameter 50MW turbines with 140 12m x 12m sluices and the DoEn bathymetry.

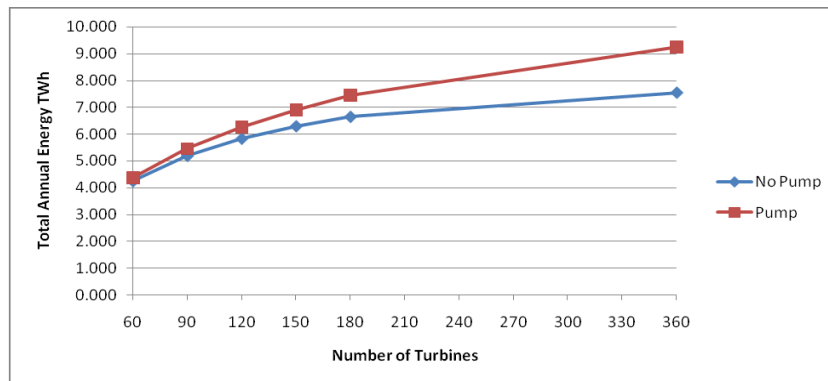


Figure 3.5.4.1: Annual energy output from Morecambe Bay Barrage operating in ebb mode, with and without pumping, as a function of number of turbines.

In addition to the energy runs, indicative costs were calculated by scaling the 1980 DoEn costs. They were used to derive the unit cost of the electricity produced (see Appendix A.3.2). The results are presented in Figure 3.5.4.2.

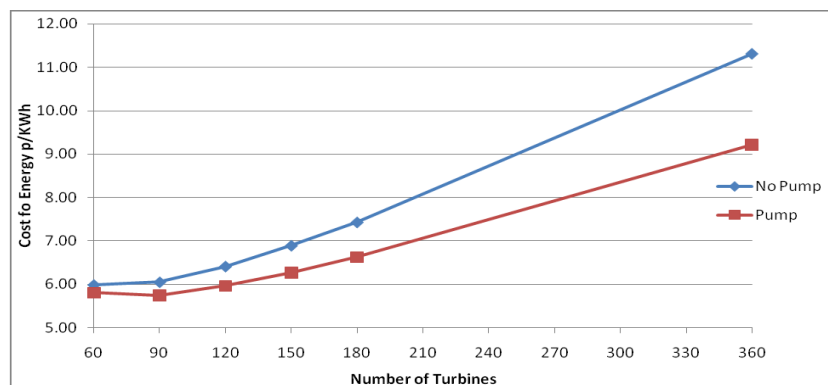


Figure 3.5.4.2: Unit cost of energy from Morecambe Bay Barrage as a function of number of turbines; ebb mode.

The graph indicates that the configuration giving the lowest costs of energy would have 60-90 turbines, and this is broadly in line with that found in the DoEn study. Pumping is seen to give an energy gain of around 23% at higher turbine numbers. The results for the 3xDoEn runs (360 50MW turbines) are presented in Table 3.5.4.1.

Dual mode operation again captures more of the available energy, but the cost of this energy, at 9.76p/kWh, is 52% more than the cost of 6.41p/kWh (seen in Table 3.5.3.1.3) for 120 9m 50MW turbines operating in ebb mode.

Table 3.5.4.1: Annual energy output and cost of energy from Morecambe Bay Barrage for 360 9m 50MW turbines; 140 12m x 12m sluices (DoEn bathymetry).

Mode	Annual Energy (TWh)	Energy with Pumping (TWh)	Cost of Energy, No Pumping (p/kWh)	Cost of Energy with Pumping (p/kWh)
Ebb	7.55	9.25	11.30	9.22
Dual	10.00	11.10	9.76	8.76

### 3.5.5 Increasing installed sluice capacity and cost implications arising

Calculations similar to the above were performed, once again using 9m diameter 50MW turbines (with a 26m minimum water depth at the turbines), but this time varying the sluicing area. The numbers of sluices were varied for the 120 turbine barrage configuration operating in ebb mode only. The results are shown in Figures 3.5.5.1 and 3.5.5.2.

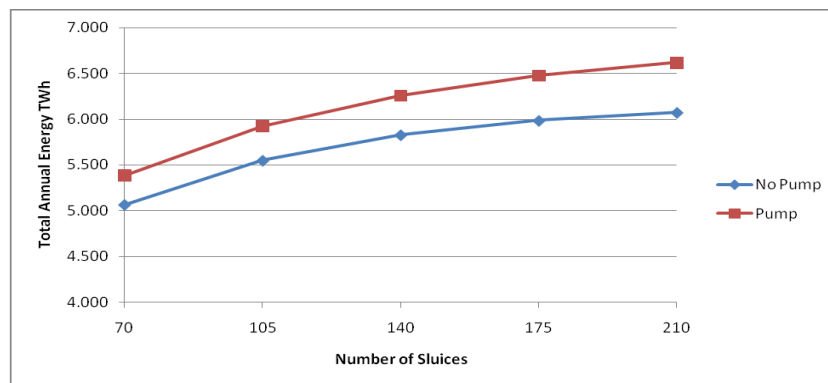


Figure 3.5.5.1: Annual energy output from Morecambe Bay Barrage operating in ebb mode as a function of number of sluices.

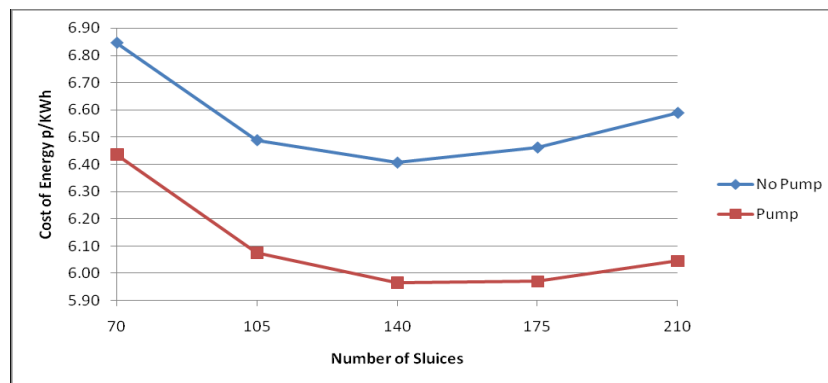


Figure 3.5.5.2: Unit cost of energy from Morecambe Bay Barrage with 120 turbines as a function of number of sluices.

The results suggest that the DoEn configuration of 140 sluices is the most cost effective configuration for 120 turbines, though installations with smaller numbers of turbines have a unit cost of electricity which is lower still.

## 3.6 Solway Firth

The alignment of a barrage on the Solway Firth is that proposed in the DoEn study (UKAEA, 1980). It is depicted in Figure 3.6.1. Appendix A.3.1 contains extracts from the 1980 document showing both the alignment and the cross-section of the estuary.

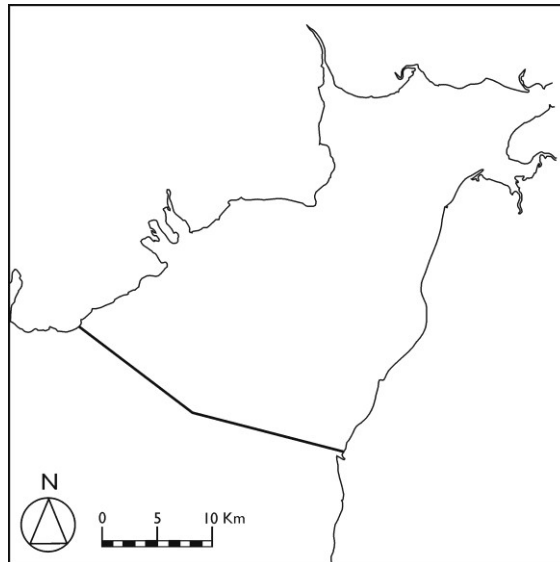


Figure 3.6.1: Sketch showing the location of a Solway Barrage.

For the Solway, the tidal conditions for the 0-D analysis were defined by the  $M_2$  and  $S_2$  tidal constituents, 2.82m and 0.88m, respectively. These values have been reduced by 3% and 2% respectively, to 2.74m and 0.86m, to account for the change in the tidal regime cause by the presence of the barrage, as suggested in the 1980 DoEn study. Water depths in the deep channel location for the turbines adopted in the earlier study are approximately 23m at low water spring tide level. This water depth was used for turbine selection and the energy calculations that follow.

The bathymetry within the impounded area of the barrage was taken as that given in the DoEn (UKAEA, 1980) report. Also considered were data from the British Oceanographic Data Centre (at the Proudman Oceanographic Laboratory), although this was known to have shortcomings in precision within the estuaries, which are beyond the region of normal interest for oceanographic modelling. The resulting surface area relationship with water level is presented in Figure 3.6.2. Tabulated values are given in Appendix A.3.1.

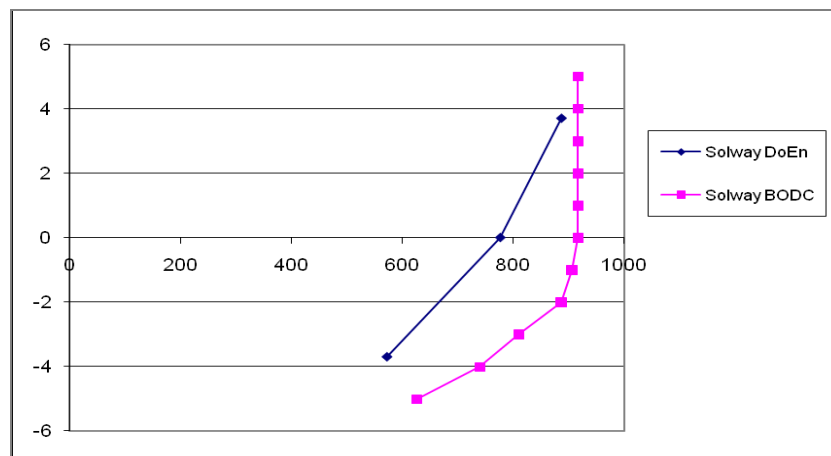


Figure 3.6.2: Solway Firth basin area ( $\text{km}^2$ ) as a function of water level (mAOD).

As the figure illustrates, the BODC derived bathymetry implies a very steep-sided estuary. This is thought to be due to incomplete coverage of the data within wetted areas. In view of the disparity, both relationships were considered in most of the calculations, though judgement places most credence on the original DoEn values. High quality LIDAR coverage

is called for, and enquiries suggest that this is in the future work plan of the Environment Agency.

### 3.6.1 Initial appraisal (ebb generation only)

The aim here was to corroborate the Department of Energy findings (UKAEA, 1980) for the Solway Firth. This was for a scheme of 180 9m diameter 40MW turbines, and 200 12m x 12m sluices. The double-regulated turbine considered here has a rated head of 6.6m and a rotation speed of 60.6rpm. Since both the head and speed are higher than is preferred, a better conditioned configuration employing 16MW turbines has also been considered in Section 3.6.3.

As in Section 3.2, a figure of 80% was taken as the maximum turbine efficiency, with no subsequent losses. Calculations were undertaken both with the BODC bathymetry and with that used in the DoEn study. Table 3.6.1.1 presents the maximum energy predictions achieved by assuming a 1.0m minimum generating head ( $H_{min}$ ) together with the 'best' delay.

Table 3.6.1.1: Results of the corroboration calculations for Solway Firth Barrage in ebb mode using 9m diameter 40MW turbines with 200 12m x 12m sluices; minimum water depth at turbines = 23m.

Number of Turbines	DoEn Annual Energy (TWh)	BODC Bathymetry			DoEn Bathymetry		
		Energy (TWh)	% of DoEn*	Delay (hrs)	Energy (TWh)	% of DoEn*	Delay (hrs)
180	10.25	8.61	84.0	1.9	8.44	82.4	2.0

\* Percentage figures are a percentage of the figure reported in the 1980 DoEn study.

Consistent with findings for the previous cases, the figures obtained are around 15% less than those reported in the 1980 study. The DoEn bathymetry gives lower energy, which is what would be expected from Figure 3.6.2. Ebb mode typically operates between high water and mean water, and the DoEn bathymetry shows a smaller basin area than the BODC bathymetry over this range of water levels.

### 3.6.2 Investigating different operating modes

The figures derived in this section relate to a scheme of 180 9m diameter turbines of 40MW generator capacity (with 23m minimum water depth) and 200 12m x 12m sluices consistent with the DoEn 1980 scheme specification.

Table 3.6.2.1: Annual energy output from Solway Firth Barrage as a function of operating mode.

Operating Mode	BODC Bathymetry		DoEn Bathymetry	
	Energy Output (TWh)	Energy Output % of ebb figure	Energy Output (TWh)	Energy Output % of ebb figure
Ebb	8.61		8.44	
Dual	7.02	81.5	6.97	82.6
Flood	8.51	98.9	7.94	94.1

Ebb mode produces the highest total energy output, but is closely followed by flood mode which is not greatly hindered by the bathymetry of this estuary. The lower DoEn figures are reflective of the inappropriately near-vertical-sided estuary implied by the BODC bathymetry. Figure 3.6.2.1 shows the basin level variations under the different operational modes.

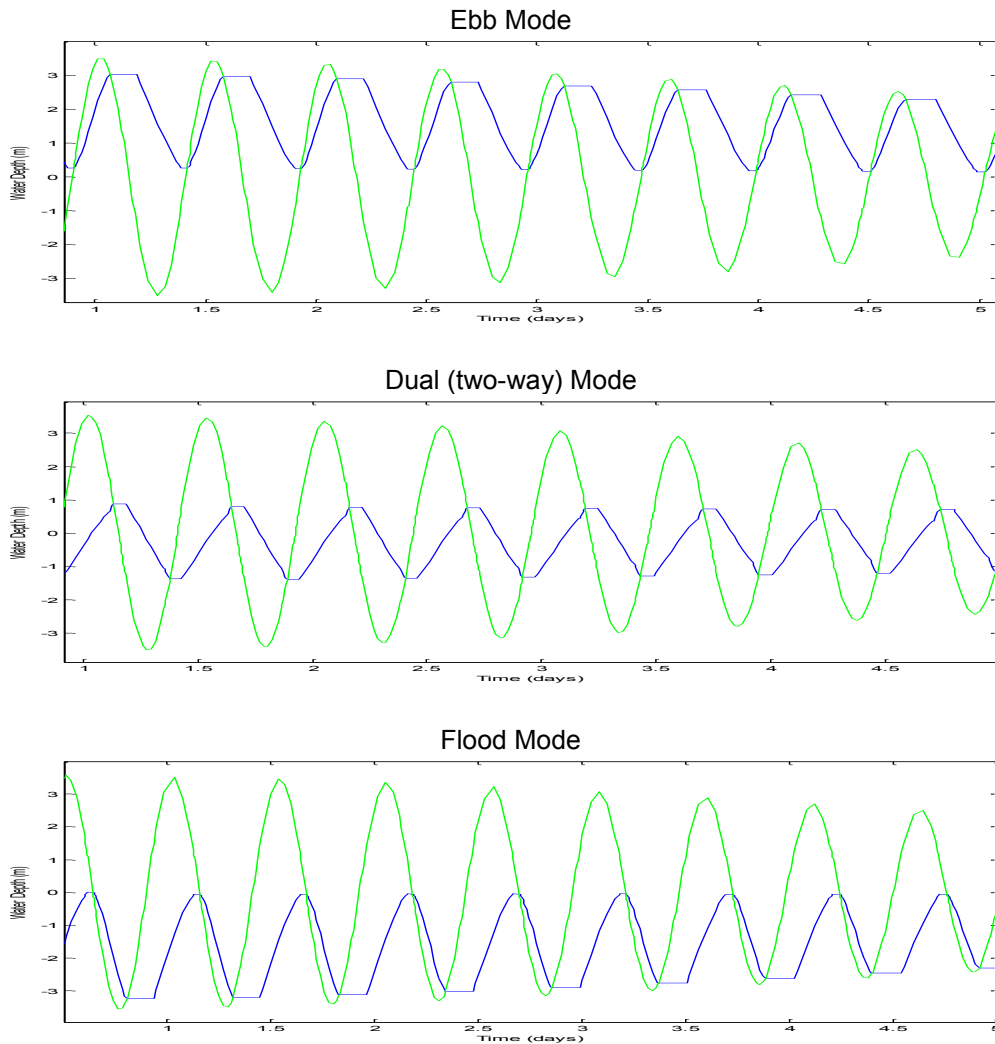


Figure 3.6.2.1: Solway Firth Barrage water levels for different operating modes (samples from the spring tidal phase; external tide level in green, basin water level in blue).

### 3.6.2.1 Effect of pumping

The calculations above were repeated with the addition of positive head pumping (before turbinng) to ascertain its effect. Pumping used the simple linear model described previously (Section 3.2), with a minimum head of 1m. Table 3.6.2.1.1 shows that pumping is generally beneficial, apart from dual mode where the smaller generation window and lower average head mean that, in this case, there is no gain from pumping. The effects of pumping on different station configurations are considered in more detail later in Section 3.6.4.

Table 3.6.2.1.1: Annual energy output from Solway Firth Barrage as a function of operating mode, with positive head pumping and optimum delays.

Mode	BODC Bathymetry		DoEn Bathymetry	
	No Pumping (TWh)	Pumping (TWh)	No Pumping (TWh)	Pumping (TWh)
Ebb	8.61	8.92 (+ 3.65%)	8.44	8.79 (+ 4.06%)
Dual	7.02	6.75 (- 3.89%)	6.97	6.77 (- 2.97%)
Flood	8.51	8.84 (+ 3.84%)	7.94	8.40 (+ 5.72%)

### 3.6.3 Turbine conditioning

#### 3.6.3.1 Changing generator capacity

As previously, an attempt was made to condition the turbines by reducing the generator capacity and hence its rated head, with a target of around the average tidal amplitude (approximately 3m). This was considered especially important for dual mode operation where driving head is expected to be lower. The operating mode calculations were repeated for both the BODC and DoEn bathymetries using this smaller generator capacity (Table 3.6.3.1.1) and the results are summarised in Table 3.6.3.1.2. The better conditioning of the machine has a positive effect only for dual mode operation.

Table 3.6.3.1.1: Solway Firth Barrage turbine characteristics as a function of generator capacity.

Generator (MW)	Rated Head (m)	Speed (rpm)
16	3.61	49.6

Table 3.6.3.1.2: Annual energy output from Solway Firth Barrage as a function of operating mode with conditioned turbine.

Mode	BODC Bathymetry			DoEn Bathymetry		
	40MW (TWh)	16 MW (TWh)	% change relative to 40MW	40MW (TWh)	16MW (TWh)	% change relative to 40MW
Ebb	8.61	8.36	-2.88	8.44	8.19	-3.02
Dual	7.02	7.83	+11.6	6.97	7.78	+11.5
Flood	8.51	8.30	-2.50	7.94	7.85	-1.21

Whilst the energy output was only increased for dual mode, it is interesting to note that the outputs for flood and ebb modes were only slightly reduced (by less than 3%) with a 16MW generator, which implies lower costs both for transmission and for the generator itself. Tables 3.6.3.1.3 and 3.6.3.1.4 show the resulting cost of energy (using the DoEn bathymetry) taking into account these reduced costs.

Table 3.6.3.1.3: Annual energy output and cost of energy from Solway Firth Barrage for 9m 40MW turbines; 200 12 x 12m sluices.

Mode	Turbines	Sluices	Energy (TWh)	Cost (p/kWh)	Peak Power (GW) Spring / Neap	Installed Capacity (GW)
Ebb	180	200	8.44	6.17	5.2 / 1.8	7.2
Dual	180	200	6.97	8.16	2.4 / 0.8	7.2
Ebb	540	200	12.90	8.09	20.0 / 8.0	21.6
Dual	540	200	16.17	7.33	11.0 / 4.5	21.6

Table 3.6.3.1.4: Annual energy output and cost of energy from Solway Firth Barrage for 9m 16MW turbines; 200 12 x 12m sluices.

Mode	Turbines	Sluices	Energy (TWh)	Cost (p/kWh)	Peak Power (GW) Spring / Neap	Installed Capacity (GW)
Ebb	180	200	8.19	5.83	2.8 / 1.6	2.88
Dual	180	200	7.78	6.71	2.8 / 0.9	2.88
Ebb	540	200	12.23	6.41	8.6 / 7.3	8.64
Dual	540	200	17.84	5.86	8.6 / 4.8	8.64

It can be seen from the tables that the 16MW turbines lower the cost of energy for both the 180 (1xDoEn) and 540 (3xDoEn) schemes, in both dual and ebb modes. For the 1xDoEn scheme (180 ebb turbines), the cost of energy is reduced by 5.5%: the 3% reduction in

energy yield is outweighed by an 8.5% cost reduction (see Appendix A.3.3). With a 3xDoE dual mode scheme, energy yield is increased alongside the cost reduction, giving a 20% fall in the cost of electricity, one which is nearly as low as for the base scheme. It is also worth noting that this scheme would give a similar annual energy output to that from a Cardiff-Weston Barrage (SDC, 2007). The final point worth noting from the tables is that the 40MW turbines rarely exploit their full capacity, whereas this is something that is achieved using the smaller 16MW machines. Figures 3.6.3.1.1 and 3.6.3.1.2 show the power output and water levels for the two generators in ebb mode, with the base 180 turbine configuration.

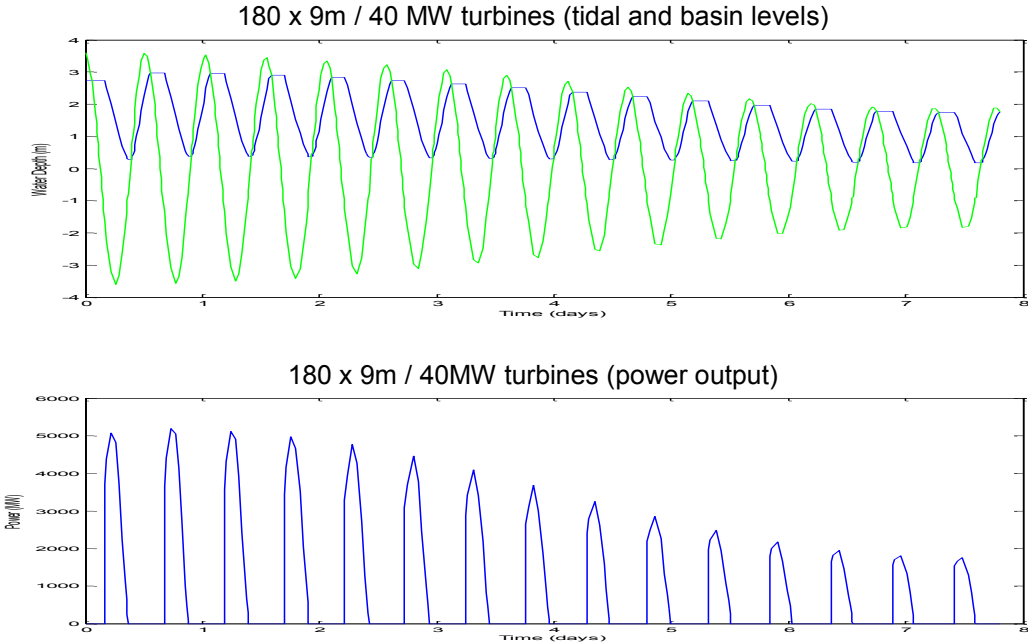


Figure 3.6.3.1.1: Solway Firth Barrage water levels and power output for 9m diameter 40MW turbines; ebb mode.

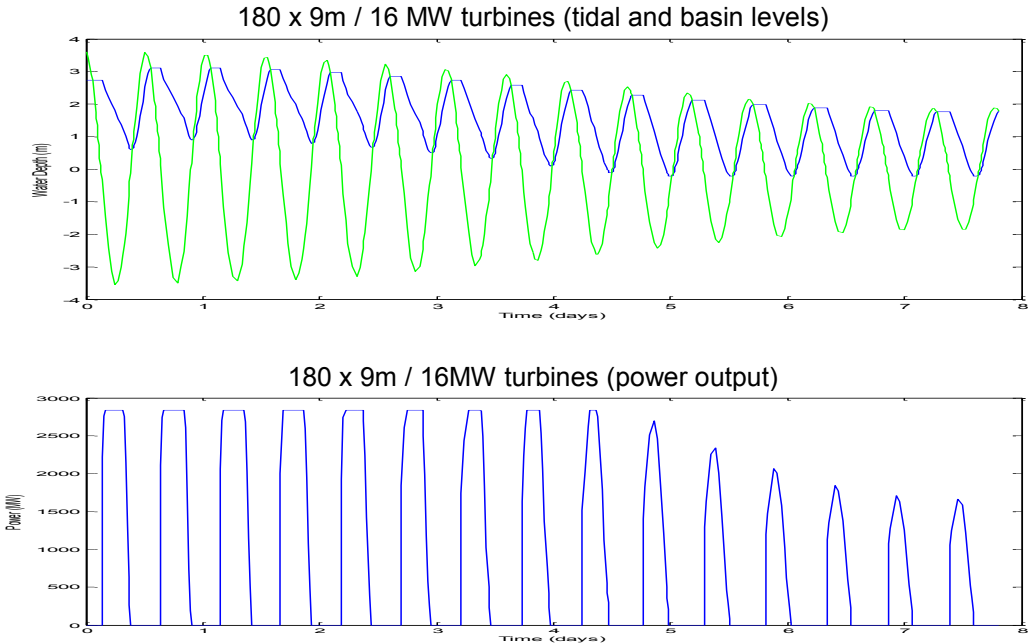


Figure 3.6.3.1.2: Solway Firth Barrage water levels and power output for 9m diameter 16MW turbines; ebb mode.

### 3.6.4 Increasing installed turbine capacity and cost implications arising

The calculations for the Dee have established in essence how the annual energy output and cost of energy vary as the number of turbines is changed. For the Solway Firth, the calculations have been limited to showing these variations for ebb mode only, and up to a 3xDoEn configuration of 540 turbines. Calculations used the 9m diameter 40MW turbines with 200 12m x 12m sluices and were for both bathymetries.

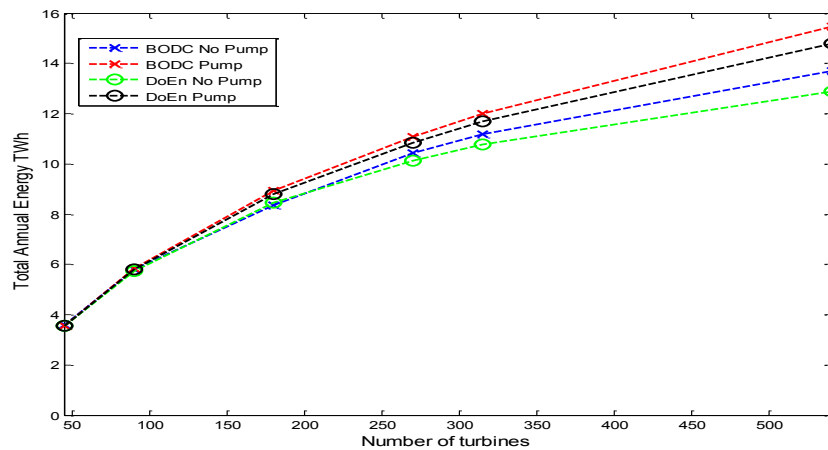


Figure 3.6.4.1: Annual energy output from Solway Firth Barrage operating in ebb mode, both with and without pumping, as a function of the number of turbines.

In addition to the energy runs, indicative costs were calculated by scaling the 1980 DoEn costs, and were used to derive the unit cost of the electricity produced (see Appendix A.3.2). The results are presented in Figure 3.6.4.2.

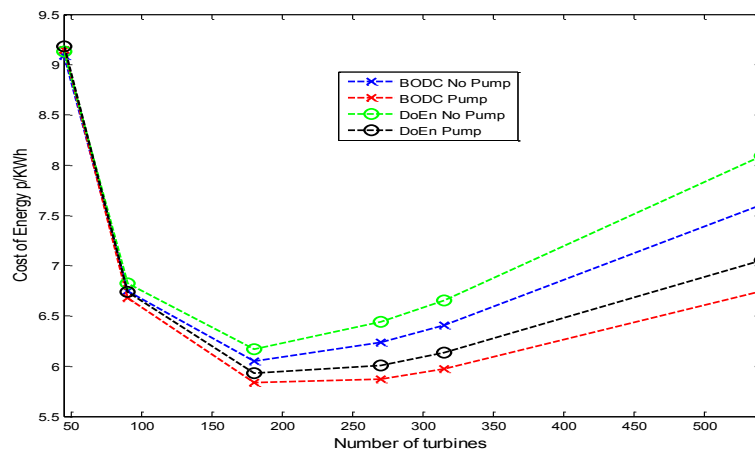


Figure 3.6.4.2: Unit cost of energy from Solway Firth Barrage as a function of number of turbines; ebb mode.

The figures again confirm that the DoEn configuration of 180 9m diameter 40MW turbines gave the lowest cost of energy (with no pumping) for that turbine size. The different bathymetries are also seen to give similar results. Pumping is seen to give an energy gain of around 15% at higher turbine numbers.

The results for the 3xDoEn runs are presented in Table 3.6.4.1.

Table 3.6.4.1: Annual energy output and cost of energy from Solway Firth Barrage for 540 9m 40MW turbines; 200 12m x 12m sluices (DoEn bathymetry).

Mode	Annual Energy (TWh)	Energy with Pumping (TWh)	Cost of Energy, No Pumping (p/kWh)	Cost of Energy with Pumping (p/kWh)
Ebb	12.90	14.80	8.09	7.05
Dual	16.17	17.01	7.33	6.97

Dual mode again captures more of the available energy, and gives an energy output comparable to that from the Cardiff-Weston Barrage. The price of energy, 7.33p/kWh, is 19% more than that calculated for the DoEn base scheme (see Table 3.6.3.1.3). Less tidal modification would be expected, but with the need to manage larger energy pulses. Such an installed capacity would certainly fit within the estuary, but is not necessarily cost effective due to the additional dredging that would be required.

### 3.6.5 Increasing installed sluice capacity and cost implications arising

Calculations similar to the above were performed, once again using the 9m diameter 40MW turbines (with a 23m minimum water depth at the turbines), but this time varying the sluicing area. The numbers of sluices were varied for the DoEn 180 turbine barrage configuration in ebb mode only. The results are shown in Figures 3.6.5.1 and 3.6.5.2.

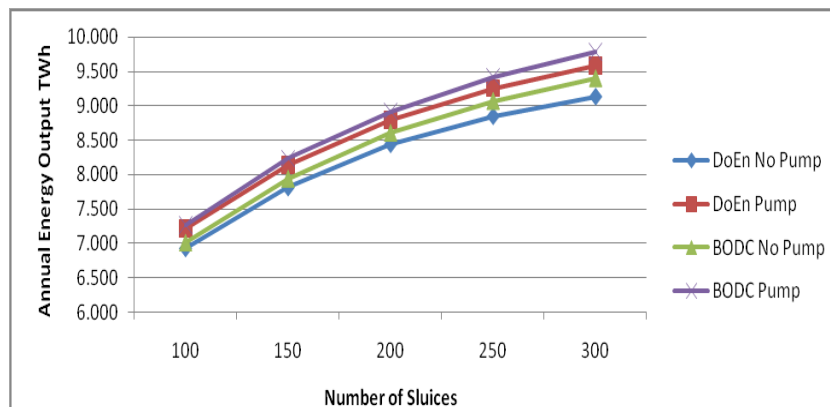


Figure 3.6.5.1: Annual energy output from Solway Firth Barrage operating in ebb mode as a function of number of sluices (BODC and DoEn bathymetries).

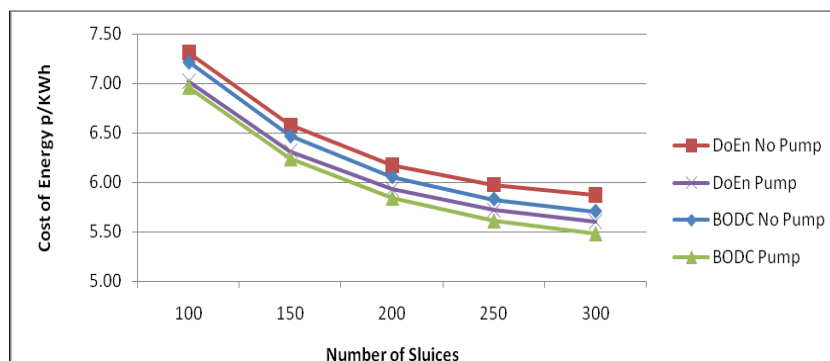


Figure 3.6.5.2: Unit cost of energy from Solway Firth Barrage for 180 turbines as a function of number of sluices.

The results suggest that the DoEn configuration could be further optimised by increasing the number of sluices. This again demonstrates how ebb mode generation is sensitive to the level of sluicing.

### 3.6.6 Conclusion

Calculations from this study of the Solway Firth suggest that for a double-regulated turbine, a 40MW generator is ill-conditioned, and a 16MW machine would give gains both in the unit cost of energy and in the energy output in dual mode. For ebb mode operation, the unit cost of energy could also be reduced, by around 5%, by an increase in the sluicing capacity compared to the DoEn base scheme (see Figure 3.6.5.2). Finally, it is worth noting that, from the 0-D modelling study, over 17TWh could theoretically be generated in dual mode operation for a 3xDoEn scheme (540 turbines), at a cost of energy comparable to the best 1xDoEn ebb scheme if 16MW turbines were used. However, assimilation of the power pulses into the grid system is likely to represent a considerable challenge.

## 4. CONJUNCTIVE (MULTI-SCHEME) ENERGY CAPTURE (2-D MODELLING)

### 4.1 Introduction

The operation, energy production, and impacts, of barrages when operated in conjunction, throughout the Irish Sea and the Severn Estuary, have been examined through the use of the ADCIRC 2-D depth-integrated shallow water model. This model permits the simulation of the entire region of interest and, therefore, allows for the investigation of the impacts of any tidal devices placed within it. Of particular interest is the impact of the conjunctive operation of 5 major barrages in the Solway Firth, Morecambe Bay, Dee, Mersey and Severn estuaries upon the hydrodynamic regime throughout the region, and the ramifications both for energy production at each barrage and environmental modification. The model accurately represents the movement of water at this scale, introducing extra physics not present in the 0-D modelling. These extra physics tend to reduce the tidal range at the barrage sites and may produce other local phenomena that alter the energy predictions associated with each barrage when compared to the 0-D predictions given in Section 3. For a more detailed description of the ADCIRC model used to perform the simulations, see Appendix 4.

The model grid used for the simulations of the barrages is shown in Figure 4.1.1. The ocean boundary is placed in deep water for a number of reasons. The main reason is that it is relatively simple to obtain suitable boundary conditions in deep water due to the regular sinusoidal nature of the tidal wave. When the tidal wave enters shallow water, it becomes less sinusoidal and, therefore, more accuracy is required in modelling the tidal wave. Hence, any error may be magnified and transmitted into the model through the boundary conditions. The second reason is to allow ADCIRC to model the progress of the tidal wave across the shelf edge and thus permit the development of the resonant modes as a result of the distance between the shelf edge and the estuaries, such as the Severn. These resonant effects would be visible in the boundary conditions if they were on the shelf, and any change to the resonant conditions due to the inclusion of a barrage would not be modelled properly.

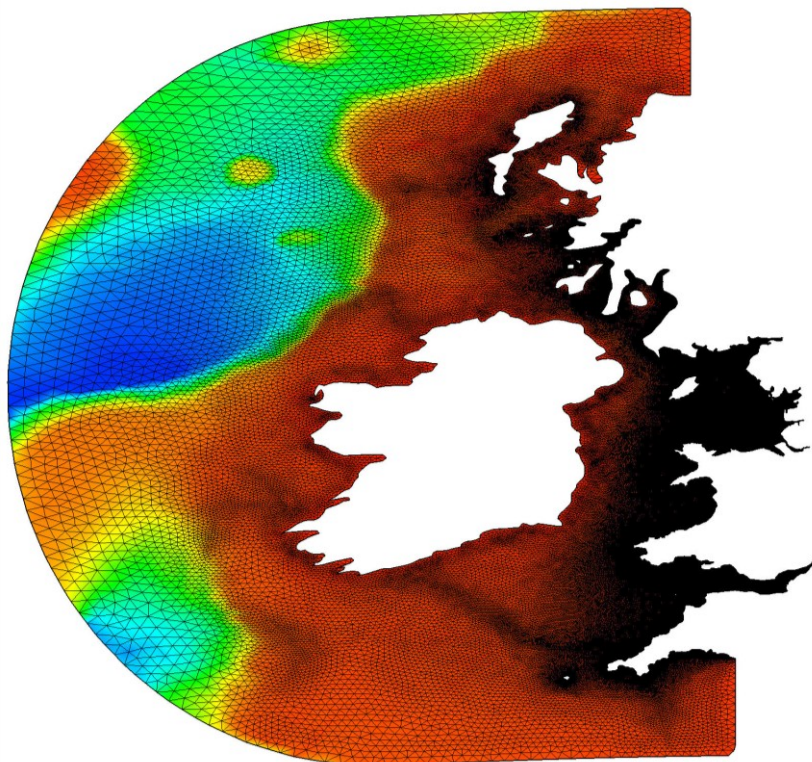


Figure 4.1.1: Total grid used to model the tides in the Irish Sea.

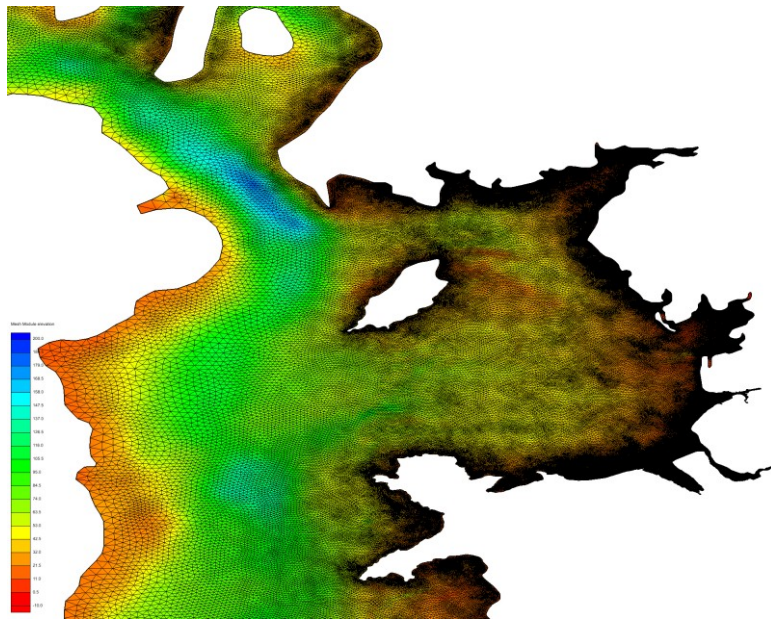


Figure 4.1.2: Model grid representation of the Irish Sea.

A closer view of the grid in the Irish Sea is shown in Figure 4.1.2. In this region, the resolution is of the order of 4-5km and is more refined as the coast is approached. Within the estuaries, particularly those for which LIDAR bathymetric information is available, the resolution becomes very fine, down to about 50m, which permits the modelling of wetting and drying due to the tidal motions. The fine resolution within each estuary permits accurate representation of the bathymetry within the basin and outflow regions around the barrage. Therefore, it should provide insights into any potential restrictions on barrage operations due to hydrodynamic effects from the bathymetry. A close-up of the Dee Estuary is shown in Figure 4.1.3. The main channels are clearly visible in the plot and the fine resolution is evident in the areas in which there is regular wetting and drying.

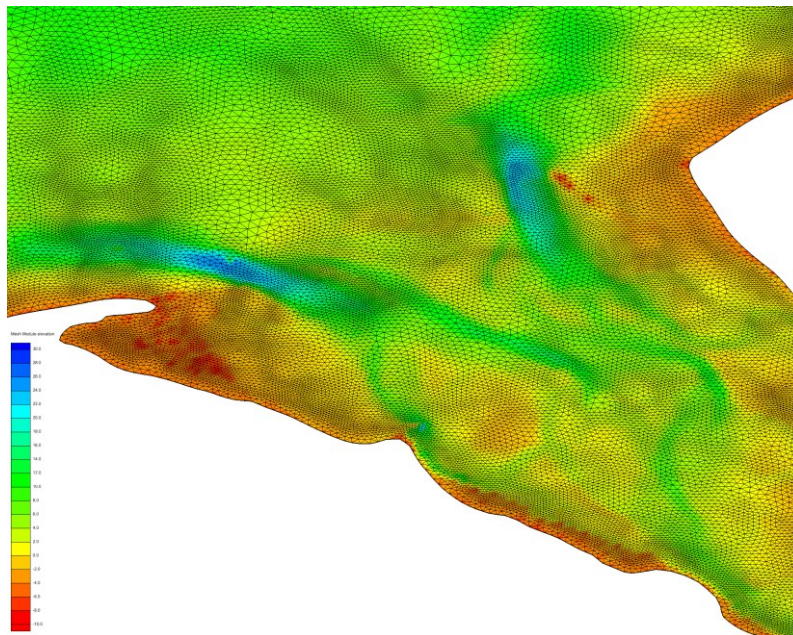


Figure 4.1.3: Model grid in the Dee Estuary.

The present tidal amplitudes at the 5 barrage locations are shown in Table 4.1.1. These values were obtained by averaging the amplitudes across the areas where the sluice gates and turbines were located in the standard barrage runs. Using these tidal amplitudes, the maximum potential annual energy available at each barrage line is shown in Table 4.1.2.

Table 4.1.1: Present tidal component amplitudes at each barrage location.

Barrage	M <sub>2</sub> (m) Amplitude	S <sub>2</sub> (m) Amplitude
Solway Firth	2.64	0.82
Morecambe Bay	2.99	0.95
Mersey	3.16	0.99
Dee	2.88	0.89
Severn	3.90	1.37

Table 4.1.2: Maximum annual energy available at each barrage line using undisturbed tidal amplitudes, as predicted by the 0-D model.

Barrage	Maximum Potential Energy (TWh)
Solway Firth	52.90
Morecambe Bay	27.38
Mersey	3.14
Dee	3.59
Severn	77.58
Total	164.59

## 4.2 Present climate scenario

### 4.2.1 Base configuration (1xDoEn)

The grid used in the base run calculations, shown in Figure 4.1.1, was modified to include barrages across 5 estuary locations: the Solway Firth, Morecambe Bay, Mersey, Dee and Severn. The number of turbines and the sluice gate area used for each barrage are listed in Table 4.2.1.1. These have been drawn from earlier 1980s Department of Energy (DoEn) studies of these barrages and were considered, at the time, to be the optimum for economic energy production in ebb mode operation.

Table 4.2.1.1: Number of turbines, total installed capacity and sluice gate area for each modelled barrage (1xDoEn).

Barrage	Number of Turbines	Total Capacity (MW)	Sluice Gate Area (m <sup>2</sup> )
Solway Firth	180	7200	28800
Morecambe Bay	80	4000	14400
Mersey	27	648	3888
Dee	50	1050	3960
Severn	216	8640	24048

#### 4.2.1.1 One-way (ebb) mode operation

The modelled barrages were operated in ebb mode using the turbine characteristics generated for use in the 0-D modelling of Section 3; and all of the barrages functioned using a 1m minimum start and end generation head with a delay of 2 hours. The bathymetry, 2-3 nodes from the barrage sluices and turbines, was artificially lowered to 30m below mean sea level. Some lowering of the bathymetry at the barrage sites is inevitable in their construction. However, the main reason for increasing the depths was to provide additional stability to the model. The large fluxes through the barrage turbines and sluices produced considerable restrictions on the stable time step in the model. This was eased when the water depth was increased.

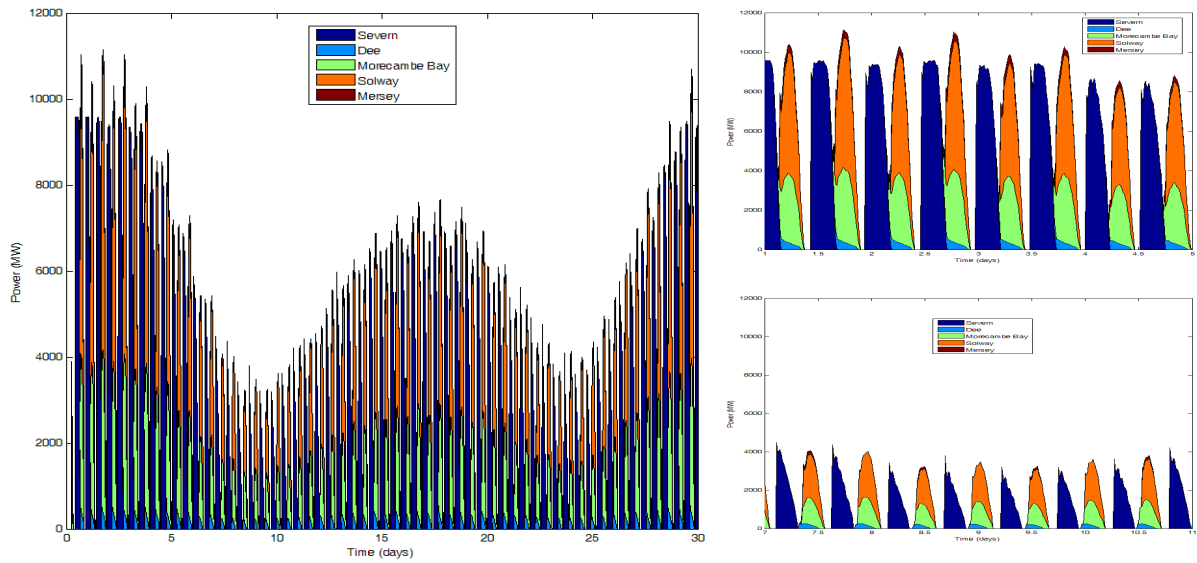


Figure 4.2.1.1.1: Power output from barrages with 1xDoEn capacity operated in ebb mode (typical spring and neap tidal power outputs are shown in the upper and lower right panels, respectively).

Figure 4.2.1.1.1 shows the power output from all the barrages throughout the entire 30 days of the simulation. The most obvious features are the variation in the twice-daily total power output throughout this period and the variation in the spring peak outputs due to the interaction of the 5 tidal constituents being used to force the model boundaries, as discussed in Appendix 4. The complementary nature of the power produced from the North West estuaries and the power produced from the Severn Barrage should also be noted. However, the two systems do not provide complete 24-hour coverage: a gap exists after the pulses from the North West estuaries subside and before the next Severn power pulse arrives. These results are in keeping with those presented earlier using the 0-D modelling approach. The main difference is in the total energy production available from the barrages. The annual energy output from each barrage is shown in Table 4.2.1.1.1, together with the total annual production. The theoretical approximate maximum potential energy for each barrage location, derived from only the  $M_2$  and  $S_2$  tidal components, is listed, together with the percentage of energy extraction of this maximum at each site. The Severn Estuary is seen to be performing very well, whereas the Mersey and Solway estuaries do relatively poorly. In general, ebb mode operation would expect to provide an extraction efficiency of about 25% for the installed capacities considered, as discussed in Section 2.1.

Table 4.2.1.1.1: Annual energy outputs from barrages operating in ebb mode (1xDoEn).

Barrage	Annual Energy (TWh)	Maximum Potential Energy (TWh)	Energy Extracted (%)
Solway Firth	9.66	47.94	20
Morecambe Bay	5.98	24.88	24
Mersey	0.57	2.54	22
Dee	0.89	2.35	38
Severn	15.81	50.05	32
Total	32.91	127.76	26

The changes in tidal component amplitudes at each barrage location are shown in Table 4.2.1.1.2. The reduction in tidal amplitude at the barrage sites, associated with the presence of each barrage, is the main reason for the reduction in annual energy generation when compared with 0-D model predictions. The tidal amplitudes are not constant along the length of the barrages and so the values listed here are average values along the length of the barrage where turbines and sluices are located.

Table 4.2.1.1.2: Changes in  $M_2$  and  $S_2$  tidal amplitudes at the barrages operating in ebb mode (1xDoEn).

Barrage	$M_2$ (m)		$S_2$ (m)	
	Amplitude	Difference	Amplitude	Difference
Solway Firth	2.50	-0.14	0.80	-0.02
Morecambe Bay	2.84	-0.15	0.92	-0.03
Mersey	2.82	-0.34	0.86	-0.13
Dee	2.32	-0.56	0.68	-0.21
Severn	3.10	-0.80	1.18	-0.19

The final table in this section, Table 4.2.1.1.3, compares the energy predictions from the 0-D model and the ADCIRC model, whilst using the values of the new tidal components predicted by ADCIRC. The differences may be largely attributed to the additional components included within the ADCIRC model. However, in itself, this reveals the necessity of accurately modelling the tidal regimes at the barrage sites, even for 0-D models, which has not been done previously. The only barrage site which produces less energy in the 2-D model is the Mersey.

Table 4.2.1.1.3: Predicted annual energy outputs of barrages operating in ebb mode (1xDoEn) from 0-D and ADCIRC models using ADCIRC predictions for tidal regime.

Barrage	0-D Model (TWh)	ADCIRC (TWh)	Difference (TWh)
Solway Firth	8.29	9.66	1.37
Morecambe Bay	4.40	5.98	1.58
Mersey	0.88	0.57	-0.31
Dee	0.80	0.89	0.09
Severn	11.33	15.81	4.48
Total	25.70	32.91	7.21

#### 4.2.1.2 Two-way (dual) mode operation

The same grid and boundary conditions were used to simulate dual mode operation as those used for the ebb mode simulation. However, in dual mode, the barrages were operated with a 1 hour delay throughout, on both the ebb and flood phases of the tide, and with a reduced efficiency of 79% for the turbines when operating on the flood. The power output from the barrages when operated in dual mode is shown in Figure 4.2.1.2.1.

As in the ebb mode simulation, the power output does not provide continuous 24-hour coverage for any of the tides. In dual mode, the power coverage is actually reduced compared to the ebb-only situation. The peak power output for each power pulse is also increased when operated in dual mode. This is due to the phasing of the Severn Barrage compared to the North West barrages and means that, when the latter are operating on the ebb tide, the Severn Barrage is producing power on the flood tide. Thus, in dual mode, instead of the Severn and the North West estuaries providing complementary power output, they now coincide and produce large power spikes.

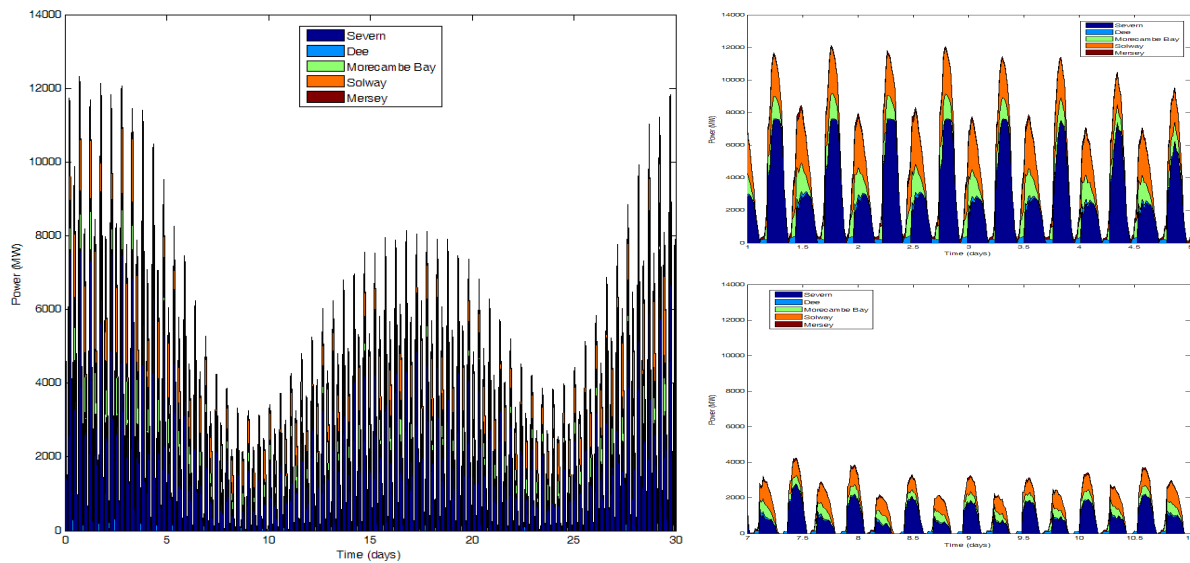


Figure 4.2.1.2.1: Power output from barrages with 1xDoEn capacity operated in dual mode (typical spring and neap tidal power outputs are shown in the upper and lower right panels, respectively).

The annual energy output for each barrage is shown in Table 4.2.1.2.1. Consistent with previous studies, as also noted in the 0-D study, the dual mode energy output from the DoEn scheme is about 80% of the ebb mode value. The only anomaly is the Mersey Barrage, where the annual energy output has increased from 0.57TWh to 0.74TWh when changing from ebb mode to dual mode operation. This increase in energy output is difficult to explain and requires further study.

Table 4.2.1.2.1: Annual energy outputs from barrages operating in dual mode (1xDoEn).

Barrage	Annual Energy (TWh)	Maximum Potential Energy (TWh)	Energy Extracted (%)
Solway Firth	6.82	48.73	14
Morecambe Bay	3.99	25.31	16
Mersey	0.74	2.70	27
Dee	0.80	2.58	31
Severn	14.01	49.17	28
Total	26.35	128.49	21

In Table 4.2.1.2.2, the changes to the tidal component amplitudes at the barrage locations are shown. In general, there is a smaller reduction in amplitude, of both the  $M_2$  and  $S_2$  tidal components, when barrages are operated in dual mode instead of ebb mode. The one exception to this trend occurs in the  $M_2$  tidal component at the Severn Barrage.

Table 4.2.1.2.2: Changes in  $M_2$  and  $S_2$  tidal amplitudes at the barrages operating in dual mode (1xDoEn).

Barrage	$M_2$ (m)		$S_2$ (m)	
	Amplitude	Difference	Amplitude	Difference
Solway Firth	2.52	-0.12	0.81	-0.01
Morecambe Bay	2.86	-0.13	0.94	-0.01
Mersey	2.88	-0.28	0.96	-0.03
Dee	2.43	-0.45	0.73	-0.16
Severn	3.06	-0.84	1.20	-0.17

As seen in Table 4.2.1.2.3, and in contrast to the ebb mode case, only the Morecambe Bay and Severn barrages show an increase in energy output from modelling with ADCIRC over the 0-D result (notwithstanding the larger number of tidal constituents). The underlying reason for this outcome remains to be determined.

Table 4.2.1.2.3: Predicted annual energy outputs of barrages operating in dual mode (1xDoEn) from 0-D and ADCIRC models using ADCIRC predictions for tidal regime.

Barrage	0-D Model (TWh)	ADCIRC (TWh)	Difference (TWh)
Solway Firth	6.97	6.82	-0.15
Morecambe Bay	3.22	3.99	0.77
Mersey	0.85	0.74	-0.11
Dee	0.81	0.80	-0.01
Severn	13.22	14.01	0.79
Total	25.07	26.36	1.29

#### 4.2.2 Tidal stream turbine farm energy capture

Given that there are other tidal energy production methods, a number of tidal stream farms have been investigated using the ADCIRC model. The four farms that were modelled (Figure 4.2.2.1) are all at locations suggested in other studies or are under active consideration by energy companies.

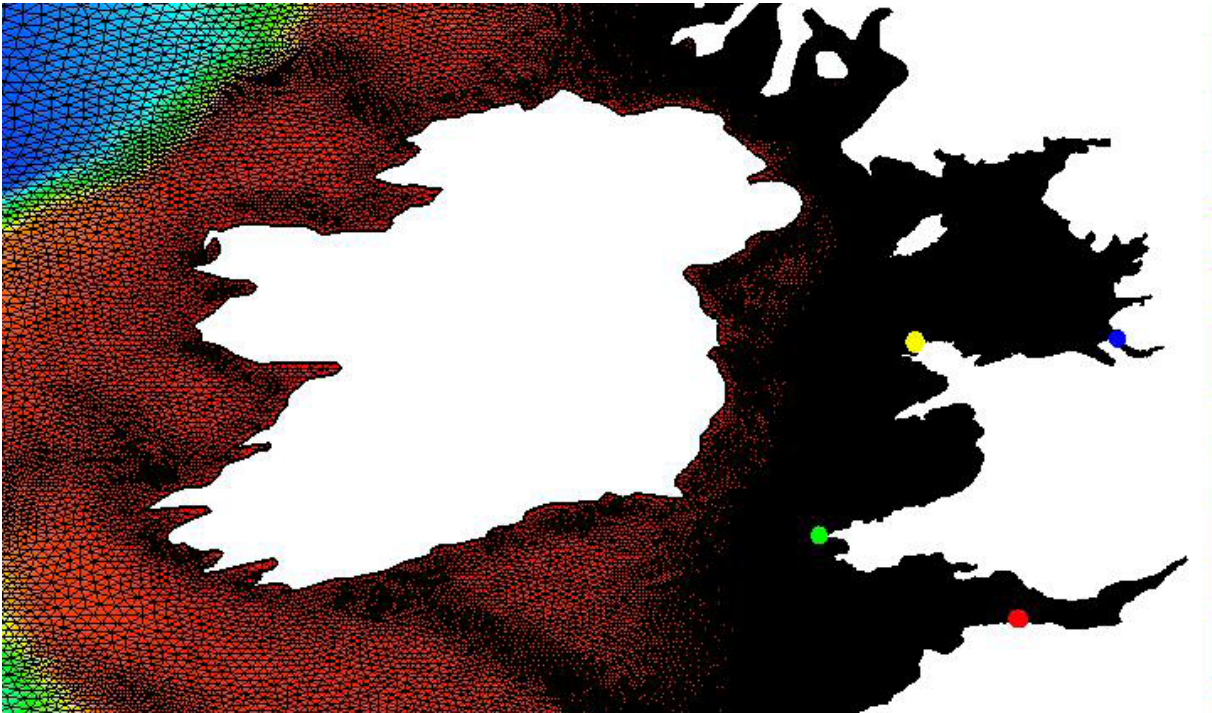


Figure 4.2.2.1: The locations of the four simulated tidal stream farms: Mersey (blue); Skerries (yellow); West Wales (green); Lynmouth (red).

The first site is located within the Mersey channel and is an unconstrained estuary farm suggested in the Mersey Tidal Power Study (<http://www.merseytidalpower.co.uk>). The second site is also an unconstrained farm and is located off Lynmouth in the Severn Estuary. It was examined within the SDC (2007) report. The third and fourth farms are under active consideration by Npower and Eon for commercial use. These farms are located off the north west coast of Anglesey by the Skerries and off the west coast of Pembrokeshire. The exact location of the tidal stream farms is not guaranteed within these simulations.

The installed capacity of each tidal stream farm is shown in Table 4.2.2.1, together with the rated speed of each device used within the farm. The exact values of the rated speed were not possible to obtain for each farm and, where necessary, ‘best guesses’ were adopted from published information. Therefore, the power output obtained should only be considered as indicative of the magnitude of the power expected from the farms. Another consideration when viewing the power output calculations is that the predictions are based upon a somewhat unrealistic assumption of a 0% maintenance downtime for each farm.

Table 4.2.2.1: The installed capacity and rated speed of each tidal stream farm.

Farm	Installed Capacity (MW)	Rated Speed (m/s)
Mersey	20	2.4
Lynmouth	30	2.0
Skerries	10.5	2.4
West Wales	8	2.0

The anticipated power production of the tidal stream farms over a 30 day period is shown in Figure 4.2.2.2. The most noticeable feature of the plot is the two bands of dark and light blue, which are the power outputs from the two offshore farms. These farm locations both reach their maximum power production at peak tide flows and, for the West Wales location, even during peak neap flow. The two estuarine farm locations do not have this feature, although this is probably due to the two offshore farms being commercial and having been rated accordingly, whereas the estuarine farms have not undergone such a rigorous level of study.

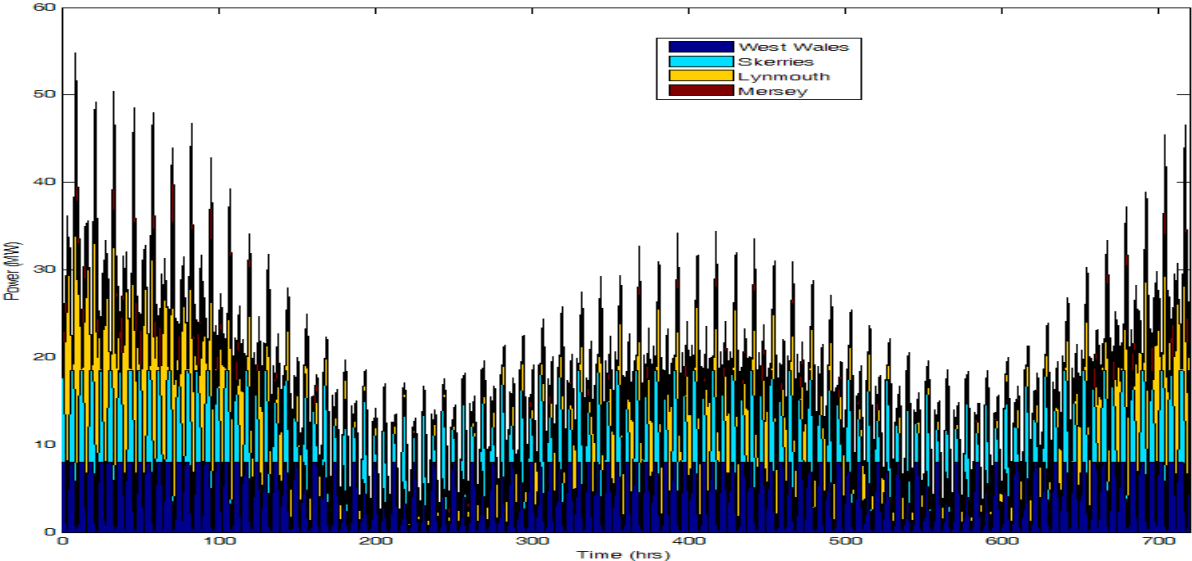


Figure 4.2.2.2: Power output from tidal stream farms.

The total annual energy production is shown in Table 4.2.2.2, together with the utilisation rates for each farm. A marked difference in utilisation rates between the offshore and estuarine tidal stream farms is clearly visible, with a much higher rate seen in the offshore farms. The higher utilisation rates seen in the Lynmouth and West Wales sites when compared to the Mersey and Skerries locations, respectively, may be due to the reduced rated speed associated with the former sites. If the higher speeds of the latter sites had been used then it would be expected that the utilisation rates might drop accordingly.

Table 4.2.2.2: Annual energy production and utilisation rate for the tidal stream farms.

Farm	Annual Energy Output (GWh)	Utilisation (%)
Mersey	18.55	11
Lynmouth	52.74	20
Skerries	44.95	49
West Wales	45.21	65
Total	161.45	27

With the additional consideration that power generation will not occur below a specific speed, which is what occurs in reality, then the annual energy production figures, for a 1m/s start velocity, are as shown in Table 4.2.2.3. Energy production at the open-sea site at the Skerries experiences only a slight drop, whereas the other sites lose about 2% of their utilisation.

Table 4.2.2.3: Annual energy production and utilisation rates for the tidal stream farms with an initial generation velocity of 1m/s.

Farm	Annual Energy Output (GWh)	Utilisation (%)
Mersey	16.12	9
Lynmouth	47.30	18
Skerries	44.51	48
West Wales	44.30	63
Total	152.22	25

#### 4.2.3 Enhanced energy capture from tripling turbine capacity (3xDoEn)

The barrage boundary conditions were modified so that there was an increase in the number of turbines associated with each barrage, and a removal of sluice gates (sluicing then being provided exclusively through the turbine ducts); see Table 4.2.3.1. This set-up corresponds to the 3xDoEn schemes outlined in the 0-D modelling, with a smaller increase in turbine numbers in the Mersey Barrage due to space restrictions.

Table 4.2.3.1: Number of turbines, total installed capacity and sluice gate area for each modelled barrage (3xDoEn).

Barrage	Number of Turbines	Total Capacity (MW)	Sluice Gate Area (m <sup>2</sup> )
Solway Firth	540	21600	0
Morecambe Bay	240	12000	0
Mersey	56	1344	0
Dee	150	3150	0
Severn	648	25920	0

##### 4.2.3.1 One-way (ebb) mode operation

The total power output associated with operating the barrages with increased capacity in ebb mode is shown in Figure 4.2.3.1.1.

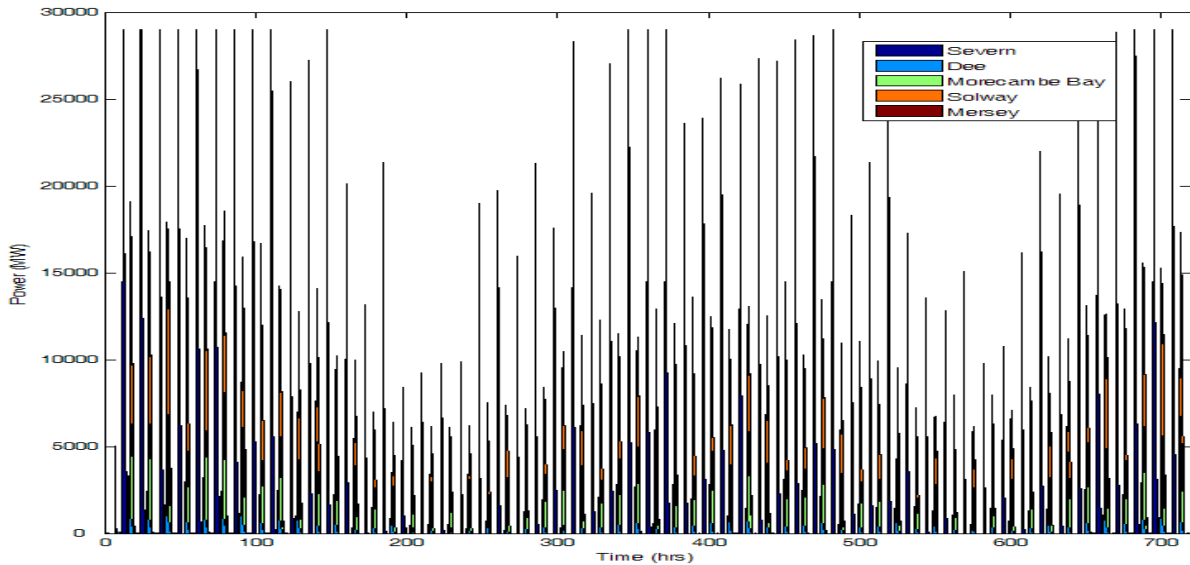


Figure 4.2.3.1.1: Power output from barrages with 3xDoEn capacity operated in ebb mode.

Again, the power generation is complementary between the North West estuaries and the Severn. However, unlike the original schemes, the power produced in this configuration has a shorter generation window throughout the spring-neap cycle. Furthermore, as shown in Table 4.2.3.1.1, the annual energy output from all the barrages, except the Dee, actually decreases. Note that the delays required to achieve maximum power output are longer for the increased-capacity barrages, but this maximum has not been achieved here, the 2-hour ebb mode delay and the 1-hour dual mode delay again being employed.

Table 4.2.3.1.1: Annual energy outputs from barrages operating in ebb mode (3xDoEn).

Barrage	Annual Energy (TWh)	Maximum Potential Energy (TWh)	Energy Extracted (%)
Solway Firth	7.88	47.15	17
Morecambe Bay	3.34	24.88	13
Mersey	0.55	2.16	25
Dee	1.17	2.37	49
Severn	11.72	44.92	26
Total	24.67	121.48	20

The changes in tidal component amplitudes at the barrage lines are shown in Table 4.2.3.1.2. The changes seen in this operating mode are greater for all the barrage locations, when compared to the standard configuration, other than for the Dee.

Table 4.2.3.1.2: Changes in  $M_2$  and  $S_2$  tidal amplitudes at the barrages operating in ebb mode (3xDoEn).

Barrage	$M_2$ (m)		$S_2$ (m)	
	Amplitude	Difference	Amplitude	Difference
Solway Firth	2.48	-0.16	0.79	-0.03
Morecambe Bay	2.83	-0.16	0.91	-0.04
Mersey	2.58	-0.58	0.78	-0.21
Dee	2.33	-0.55	0.68	-0.21
Severn	2.94	-0.96	1.11	-0.26

The differences in predicted energy outputs between the 0-D and ADCIRC models are shown in Table 4.2.3.1.3. Unlike in the runs for the standard barrage configuration, the 0-D model now predicts, in general, more energy output than the 2-D model. This suggests that the high flow rates associated with the increased turbine capacity encounter major hydrodynamic restraints, which means that the energy production is adversely affected. The problem cannot be modelled within the 0-D context as the requisite physics are not present.

Table 4.2.3.1.3: Predicted annual energy outputs of barrages operating in ebb mode (3xDoEn) from 0-D and ADCIRC models using ADCIRC predictions for tidal regime.

Barrage	0-D Model (TWh)	ADCIRC (TWh)	Difference (TWh)
Solway Firth	9.57	7.88	-1.69
Morecambe Bay	5.06	3.34	-1.72
Mersey	0.79	0.55	-0.24
Dee	0.99	1.17	0.18
Severn	12.98	11.72	-1.26
Total	29.39	24.66	-4.73

4.2.3.2 Two-way (dual) mode operation

In this run, the 3xDoEn scheme was operated in dual mode. The power output from the barrages in this mode of operation is shown in Figure 4.2.3.2.1. The power is produced in very short time windows and, thus, the increased power output is at the cost of very high power peaks to the grid which may be up to around 35GW. This figure represents over half the national instantaneous electricity requirements. It would produce difficulties in the assimilation of the power from the barrages, an issue which would need to be overcome.

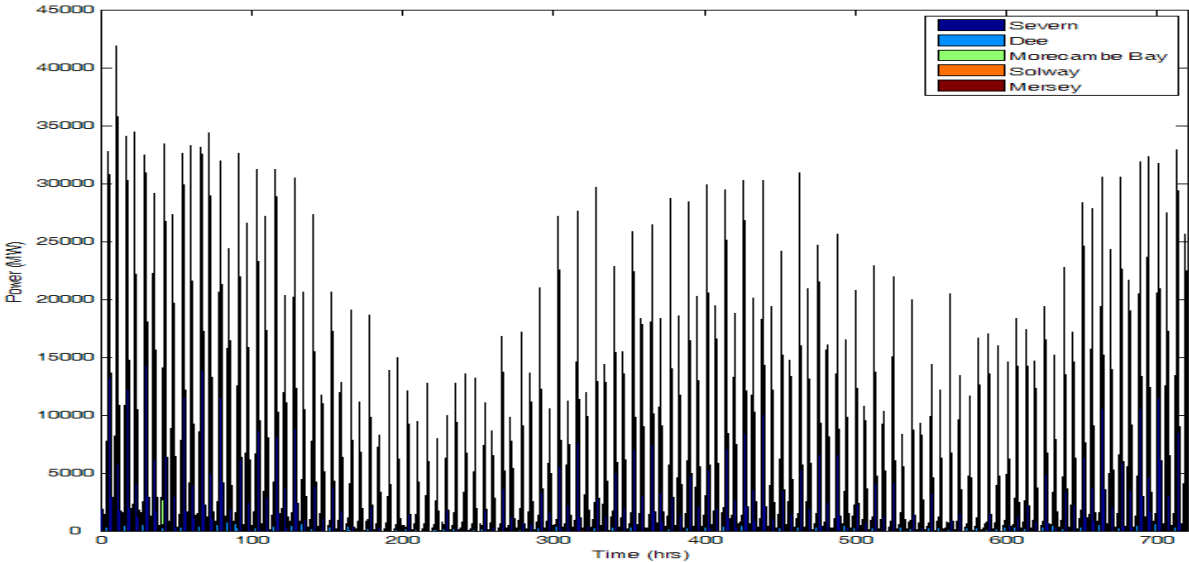


Figure 4.2.3.2.1: Power output from barrages with 3xDoEn capacity operated in dual mode.

The annual energy production from each barrage is shown in Table 4.2.3.2.1. The energy output from the barrages is increased when operating in dual mode in a 3xDoEn scheme when compared to all the other operating schemes examined, except for the Mersey where the 1xDoEn scheme in dual mode performs better. The Severn and Dee barrages in particular perform very well in extracting large fractions of the maximum potentially available energy at 46% and 58%, respectively. The Solway Barrage performs least well of all the barrages, in terms of utilisation of potential energy. The cause needs to be established, but it may be due to the large size of the estuary and some internal flow circulation which is

reducing energy production. This issue needs careful examination. It may be that a better choice of location for the turbines along the barrage would produce greater energy returns.

Table 4.2.3.2.1: Annual energy outputs from barrages operating in dual mode (3xDoEn).

Barrage	Annual Energy (TWh)	Maximum Potential Energy (TWh)	Energy Extracted (%)
Solway Firth	9.78	48.73	20
Morecambe Bay	7.02	24.37	29
Mersey	0.72	2.50	29
Dee	1.46	2.50	58
Severn	19.53	42.72	46
Total	38.51	120.82	32

The changes in the amplitudes of the  $M_2$  and  $S_2$  tidal components at the barrage lines are shown in Table 4.2.3.2.2. They may be compared with the changes in amplitudes under ebb mode operation shown in Table 4.2.3.1.2. There is no consistent pattern to the changes.

Table 4.2.3.2.2: Changes in  $M_2$  and  $S_2$  tidal amplitudes at the barrages operating in dual mode (3xDoEn).

Barrage	$M_2$ (m)		$S_2$ (m)	
	Amplitude	Difference	Amplitude	Difference
Solway Firth	2.52	-0.12	0.81	-0.01
Morecambe Bay	2.81	-0.18	0.91	-0.04
Mersey	2.78	-0.38	0.88	-0.11
Dee	2.39	-0.49	0.72	-0.17
Severn	2.86	-1.04	1.10	-0.27

Table 4.2.3.2.3 compares the energy predictions of the 0-D and ADCIRC models. The ADCIRC model predicts a larger return of energy than the 0-D model for the Dee and Severn. This suggests that the hydrodynamic restraints perceived in the ebb mode operation of the Dee Barrage are not so prevalent in the 3xDoEn simulation. The result could possibly be due to the shorter delays employed in the dual mode scheme, which means that the initial generating heads are smaller and, thus, the corresponding flow rates are reduced. In contrast, for the Solway and Morecambe Bay barrages, the 0-D model predicts a higher energy output. The exact cause of this inconsistent behaviour is not known, but it may be due to the detailed layouts of the barrages in terms of the placement of the turbines. It suggests that the placement of turbines in large barrages must be carefully considered and that there may be sub-optimal locations for turbines which should be avoided. The lack of consistency gives cause for concern and further investigation of the water motions within the estuaries will be conducted in follow-up studies, as will issues of computational stability.

Table 4.2.3.2.3: Predicted annual energy outputs of barrages operating in dual mode (3xDoEn) from 0-D and ADCIRC models using ADCIRC predictions for tidal regime.

Barrage	0-D Model (TWh)	ADCIRC (TWh)	Difference (TWh)
Solway Firth	15.13	9.78	-5.35
Morecambe Bay	7.70	7.02	-0.68
Mersey	0.72	0.72	0.00
Dee	1.15	1.46	0.31
Severn	16.20	19.53	3.33
Total	40.90	38.51	-2.39

#### 4.2.4 Combined tidal range (1xDoEn barrages, ebb mode) and tidal stream extraction

A combination of tidal stream farms and barrages of 1xDoEn capacity generating in ebb mode were simulated to examine the total energy output and the associated impacts when operating in conjunction. It should be noted, however, that the farms considered here are not representative of the full potential for tidal stream extraction within the model domain.

##### 4.2.4.1 Tidal range

The power output over the simulated period from the barrages in the combined simulation is shown in Figure 4.2.4.1.1. As in the barrage-only ebb mode simulation (Figure 4.2.1.1.1), the complementary generation times between the North West estuaries and the Severn Estuary are visible and provide a large time window of power generation.

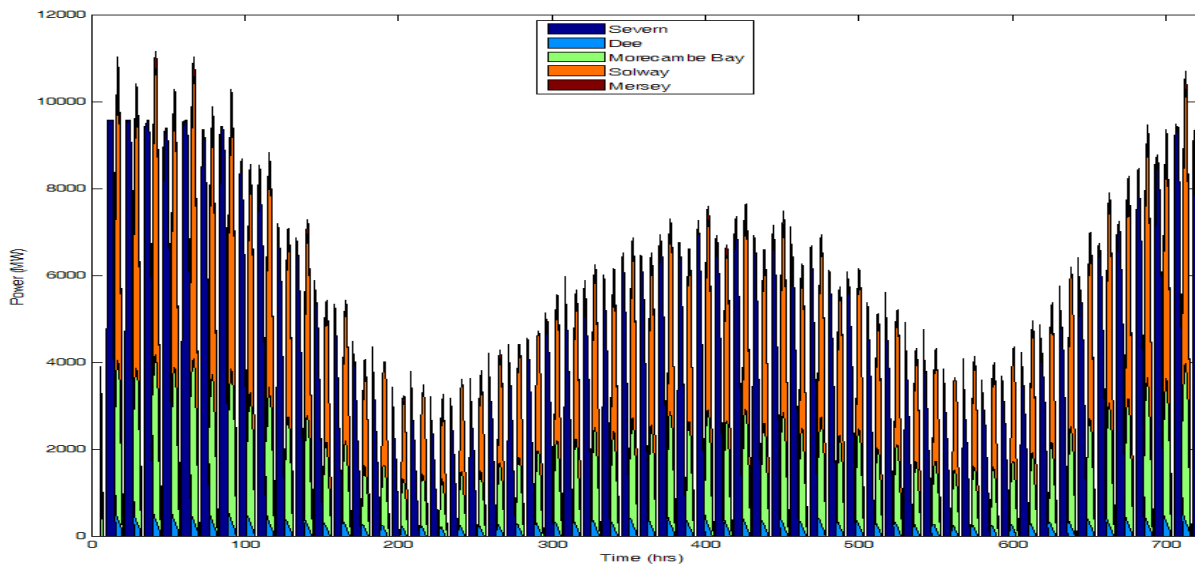


Figure 4.2.4.1.1: Power output from barrages with 1xDoEn capacity operated in ebb mode in conjunction with tidal stream farms.

Table 4.2.4.1.1 shows the annual energy production for each barrage and the percentage of the maximum energy extracted. The Severn and Dee barrages again extract more than might be expected of the total energy. If, however, the original undisturbed maximum potential energy is used (Table 4.1.2), then the Severn extracts about 20%, which is more in line with expectations. The Dee Estuary has a non-sinusoidal external tide at the turbines due to the restricted channel in which these have been sited, which may also help to explain the relatively high percentage energy extraction.

Table 4.2.4.1.1: Annual energy outputs from barrages operating in ebb mode (1xDoEn) in conjunction with tidal stream farms.

Barrage	Annual Energy (TWh)	Maximum Potential Energy (TWh)	Energy Extracted (%)
Solway Firth	9.68	47.94	20
Morecambe Bay	5.99	25.24	24
Mersey	0.65	2.51	26
Dee	0.89	2.17	41
Severn	15.89	49.77	32
Total	33.11	127.63	26

The changes in tidal component amplitudes at the barrage lines are shown in Table 4.2.4.1.2. A similar pattern is again seen, with the Severn, Dee and Mersey having large amplitude reductions and the Solway Firth and Morecambe Bay having only small decreases. The changes in amplitudes seen in the Severn, Dee and Mersey are larger when compared to the simulation without including the tidal stream farms (Table 4.2.1.1.2).

Table 4.2.4.1.2: Changes in  $M_2$  and  $S_2$  tidal amplitudes at the barrages operating in ebb mode (1xDoEn) in conjunction with tidal stream farms.

Barrage	$M_2$ (m)		$S_2$ (m)	
	Amplitude	Difference	Amplitude	Difference
Solway Firth	2.50	-0.14	0.80	-0.02
Morecambe Bay	2.86	-0.13	0.93	-0.02
Mersey	2.79	-0.37	0.87	-0.12
Dee	2.23	-0.65	0.64	-0.25
Severn	3.09	-0.81	1.18	-0.19

Except for the Mersey, the annual energy production predicted by the 0-D model is, again, smaller than that obtained from the 2-D model, as seen in Table 4.2.4.1.3.

Table 4.2.4.1.3: Predicted annual energy outputs of barrages operating in ebb mode (1xDoEn) in conjunction with tidal stream farms from 0-D and ADCIRC models.

Barrage	0-D Model (TWh)	ADCIRC (TWh)	Difference (TWh)
Solway Firth	8.29	9.68	1.39
Morecambe Bay	4.46	5.99	1.53
Mersey	0.87	0.65	-0.22
Dee	0.74	0.89	0.15
Severn	11.26	15.89	4.63
Total	25.62	33.10	7.48

The difference in annual energy production from each barrage, when simulated concurrently with the tidal stream farms and independently, is shown in Table 4.2.4.1.4. The barrages apparently produce slightly more energy throughout the year with the inclusion of the tidal stream farms. The increase may be at least partially attributable to computational imprecision, and further investigation is called for. Although it can be seen that the farms' presence has been slight, surprisingly the Mersey Barrage shows more than a 10% increase with the small tidal stream array downriver.

Table 4.2.4.1.4: Differences in annual energy production of barrages operating in ebb mode (1xDoEn) without and with tidal stream farms.

Barrage	Without Tidal Stream (TWh)	With Tidal Stream (TWh)	Difference (TWh)
Solway Firth	9.66	9.68	0.02
Morecambe Bay	5.98	5.99	0.01
Mersey	0.57	0.65	0.08
Dee	0.89	0.89	0.00
Severn	15.81	15.89	0.08

#### 4.2.4.2 Tidal stream

The power production over the simulation period for each tidal stream farm is shown in Figure 4.2.4.2.1. The power output is again dominated by the two open-sea farms at the Skerries and off the West Wales coast, as shown by the light and dark blue portions.

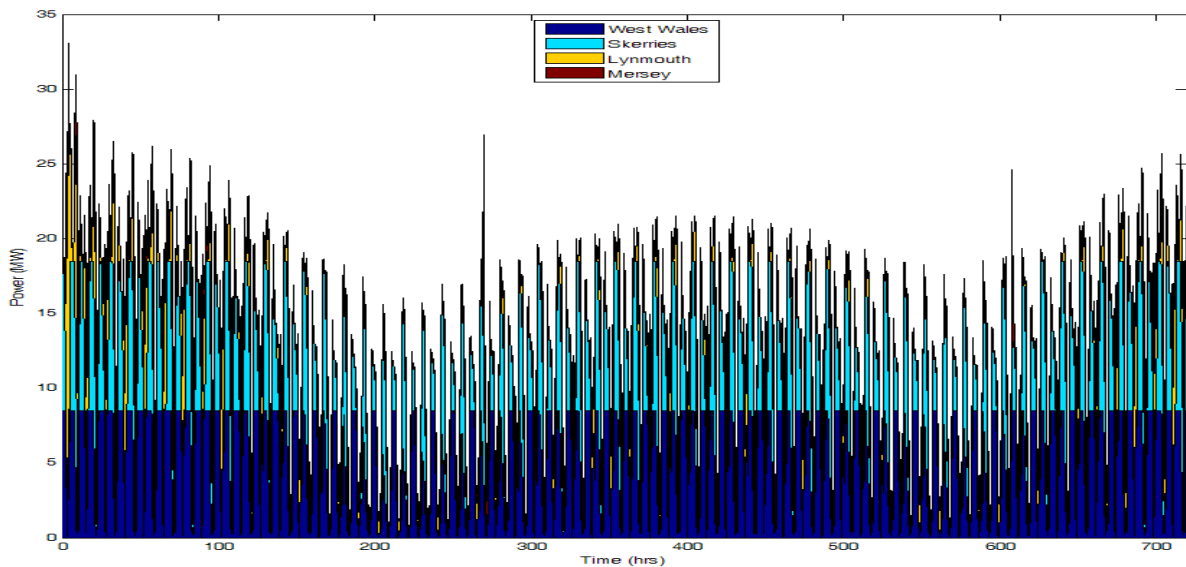


Figure 4.2.4.2.1: Power output from tidal stream farms operated in conjunction with barrages with 1xDoEn capacity in ebb mode.

The total annual energy output from the tidal stream farms decreases by about 30% through the inclusion of the barrages, as shown in Table 4.2.4.2.1. The majority of the losses in energy come from the estuary-based farms, as might be expected. However, the total decrease of nearly 50GWh is only about a quarter of the apparent 190GWh of additional energy generated by the barrages due to the inclusion of the tidal stream farms (Table 4.2.4.1.4).

Table 4.2.4.2.1: Annual energy outputs from tidal stream farms when operating in ebb mode (1xDoEn) in conjunction with barrages; and the changes from operating alone.

Farm	Annual Energy Output (GWh)	Utilisation (%)	Change from simulation without barrages (GWh)
Mersey	5.31	3	-13.24
Lynmouth	19.83	8	-32.91
Skerries	41.35	47	-3.60
West Wales	45.20	61	-0.01
Total	111.69	20	-49.76

#### 4.2.5 Summary

Table 4.2.5.1 summarises the total predicted annual energy for each barrage, installed turbine capacity and operating mode which has been simulated.

Table 4.2.5.1: Annual energy production for each barrage, installed turbine capacity and operating mode.

Barrage	1xDoEn (TWh)		3xDoEn (TWh)		1xDoEn and Tidal Stream (TWh)
	Ebb	Dual	Ebb	Dual	Ebb
Solway Firth	9.66	6.82	7.88	9.78	9.68
Morecambe Bay	5.98	3.99	3.34	7.02	5.99
Mersey	0.57	0.74	0.55	0.72	0.65
Dee	0.89	0.80	1.17	1.46	0.89
Severn	15.81	14.01	11.72	19.53	15.89
Total	32.91	26.35	24.67	38.51	33.11

The 1xDoEn scheme performs better in ebb mode than dual mode for all the barrages except the Mersey. The total annual energy output from this arrangement of the North West barrages in combination with the Severn Barrage represents 8.7% of the present UK annual electricity demand.

Dual mode operation is better than ebb mode operation in all cases when the installed capacity is increased to 3xDoEn. Indeed, the 3xDoEn ebb mode arrangement produces less energy than the 1xDoEn ebb mode scheme for all of the barrages except the Dee. However, the Dee Barrage in the 3xDoEn simulation has had the advantage of the new turbines being placed outside the restrictive channel of the original design. This suggests that if dredging was undertaken to remove this constraint on the original Dee Barrage configuration, it would perform better than currently suggested. It might also have less of an impact on the local tidal amplitude.

If the North West barrages together with the Severn Barrage had the 3xDoEn configuration and operated in dual mode, then the total energy produced would represent 10% of the present UK annual electricity demand.

When the tidal stream farms are operated in conjunction with the barrages (in 1xDoEn ebb mode), there is a slight increase in barrage output. This increase more than offsets the corresponding loss in energy from the tidal stream farms. However, whilst it is unlikely that a tidal stream farm would be built in close proximity to a barrage in the same estuary, the study has not investigated the full potential for tidal stream energy capture across the whole modelling domain.

**4.3 Future climate scenario**

The grid used for the original runs was also employed in a climate scenario with increased sea level. The number of runs was reduced and focused only on the most economical generation mode, 1xDoEn in ebb mode, and for the 3xDoEn capacity in dual mode, which produces the greatest energy output. The sea level was increased throughout the domain by 80cm, which is a reasonably large increase in sea-level but one which is consistent with recently published estimates.

The changes in tidal amplitudes are generally small throughout the domain (Table 4.3.1). The Severn Estuary has a small decrease in average tidal amplitude but the Dee Estuary sees a larger increase in average tidal amplitude and an increase in mean spring tides of up to 9cm. With the addition of the 80cm rise in mean sea level, the Dee Estuary at spring tides would experience a high water level increase of nearly 90cm from the current situation.

Table 4.3.1: Changes in M<sub>2</sub> and S<sub>2</sub> tidal amplitudes at the barrages due to the increase in sea level.

Barrage	M <sub>2</sub> (m)		S <sub>2</sub> (m)	
	Amplitude	Difference	Amplitude	Difference
Solway Firth	2.65	0.01	0.83	0.01
Morecambe Bay	2.99	0.00	0.95	0.00
Mersey	3.16	0.00	1.01	0.02
Dee	2.93	0.05	0.93	0.04
Severn	3.86	-0.04	1.37	0.00

The maximum annual energy potential is shown in Table 4.3.2 for both the present and future climate scenarios. The changes in annual energy potential are due not only to the changes in tidal amplitudes at the barrage sites but also to the uplifting of the water levels in the basins behind the barrages, meaning that, in general, there is a larger volume of water

that can be mobilized than in the present situation. Thus, the lack of good intertidal bathymetric data for some of the barrage locations becomes more problematic in the future climate scenario.

Table 4.3.2: Maximum annual energy available at each barrage line in present and future climate scenarios, as predicted from 0-D model.

Barrage	Present Climate (TWh)	Changed Climate (TWh)	Difference (TWh)
Solway Firth	52.90	56.00	3.10
Morecambe Bay	27.38	28.04	0.66
Mersey	3.14	3.79	0.65
Dee	3.59	4.54	0.95
Severn	77.58	76.20	-1.38

4.3.1 Tidal range

4.3.1.1 One-way (ebb) mode operation (1xDoEn)

A simulation was run for the future climate scenario with barrages operating in ebb mode with the 1xDoEn base configuration (see Table 4.2.1.1). The power output from this simulation is shown in Figure 4.3.1.1.1. A delay of 2 hours was applied at all of the barrages. Power output is qualitatively the same as for the present climate 1xDoEn ebb scheme, with complementary power output from the Severn and the North West barrages.

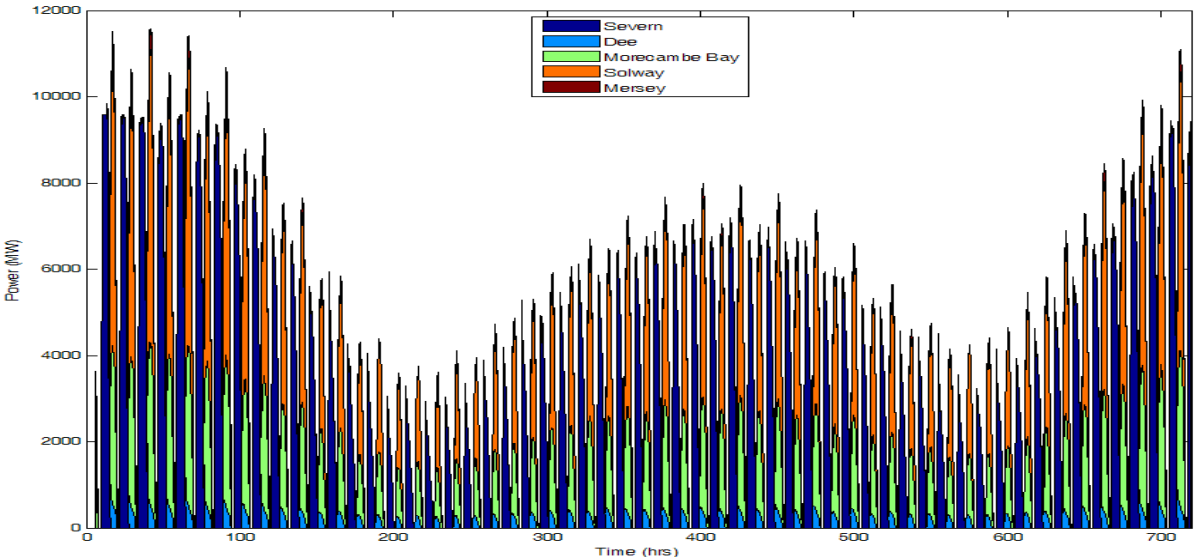


Figure 4.3.1.1.1: Power output from barrages with 1xDoEn capacity operated in ebb mode in future climate scenario.

Table 4.3.1.1.1 shows the annual energy output from each barrage under the future climate scenario. The annual energy output increases for all the North West barrages due to the increase in the  $M_2$  tidal amplitude at the barrage lines and the increased basin volume due to the uplifted water levels. In contrast, there is a slight decrease in the annual energy output predicted for the Severn Estuary, associated with the decrease in the  $M_2$  amplitude at the barrage line. The total increase in annual energy production is about 0.6TWh in the future climate scenario when compared with the present situation.

Table 4.3.1.1.1: Annual energy output, maximum potential energy and percentage of energy extracted at each barrage operating in ebb mode (1xDoEn) in future climate scenario.

Barrage	Annual Energy (TWh)	Maximum Potential Energy (TWh)	Energy Extracted (%)
Solway Firth	9.99	51.83	19
Morecambe Bay	6.12	26.32	23
Mersey	0.79	3.19	25
Dee	1.19	3.33	36
Severn	15.43	47.51	32
Total	33.52	132.18	25

The tidal amplitudes, shown in Table 4.3.1.1.2, are again reduced through the introduction of the barrages, as in the present climate scenario. The Solway Firth and Morecambe Bay have relatively small changes; the other three estuaries have larger differences.

Table 4.3.1.1.2: Changes in  $M_2$  and  $S_2$  tidal amplitudes at the barrages operating in ebb mode (1xDoEn) in future climate scenario.

Barrage	$M_2$ (m)		$S_2$ (m)	
	Amplitude	Difference	Amplitude	Difference
Solway Firth	2.54	-0.11	0.81	-0.02
Morecambe Bay	2.89	-0.10	0.94	-0.01
Mersey	2.87	-0.29	0.91	-0.10
Dee	2.51	-0.42	0.74	-0.19
Severn	3.02	-0.84	1.15	-0.22

The predicted annual energy output for each barrage, except on the Mersey, is again higher from the ADCIRC model than from the 0-D model, as seen in Table 4.3.1.1.3.

Table 4.3.1.1.3: Predicted annual energy outputs of barrages operating in ebb mode (1xDoEn) from 0-D and ADCIRC models in future climate scenario.

Barrage	0-D Model (TWh)	ADCIRC (TWh)	Difference (TWh)
Solway Firth	8.61	9.99	1.38
Morecambe Bay	4.68	6.12	1.44
Mersey	1.00	0.79	-0.21
Dee	1.09	1.19	0.10
Severn	10.72	15.43	4.71
Total	26.10	33.52	7.42

#### 4.3.1.2. Two-way (dual) mode operation (3xDoEn)

The model set up of Section 4.2.3.2 was again used, but within the context of sea-level rise due to climate change. The power output from this simulation is shown in Figure 4.3.1.2.1. The dual mode operation again produces a series of narrow spikes of energy which reach to more than 35GW.

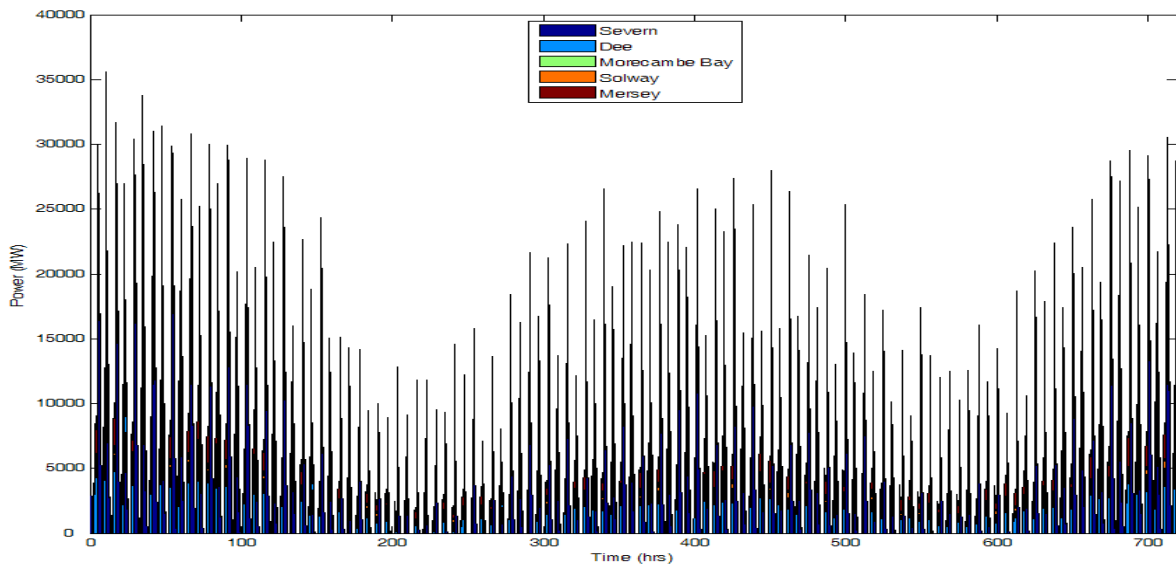


Figure 4.3.1.2.1: Power output from barrages in 3xDoEn configuration operated in dual mode in future climate scenario.

The annual energy production from each barrage shows an increase when compared to the present climate simulations, as seen in Table 4.3.1.2.1, with the total annual energy production increasing by 3.07TWh (from the figure in Table 4.2.3.2.1).

Table 4.3.1.2.1: Annual energy output, maximum potential energy and percentage of energy extracted at each barrage operating in dual mode (3xDoEn) in future climate scenario.

Barrage	Annual Energy (TWh)	Maximum Potential Energy (TWh)	Energy Extracted (%)
Solway Firth	10.88	50.94	21
Morecambe Bay	7.62	25.39	30
Mersey	1.10	2.82	39
Dee	1.63	3.58	46
Severn	20.34	41.38	49
Total	41.57	124.11	34

The changes in tidal amplitudes at the barrage lines in this climate change simulation are shown in Table 4.3.1.2.2. The changes are qualitatively similar to the present climate simulation of the 3xDoEn scheme operating in dual mode.

Table 4.3.1.2.2: Changes in  $M_2$  and  $S_2$  tidal amplitudes at the barrages operating in dual mode (3xDoEn) in future climate scenario.

Barrage	$M_2$ (m)		$S_2$ (m)	
	Amplitude	Difference	Amplitude	Difference
Solway Firth	2.52	-0.13	0.80	-0.03
Morecambe Bay	2.84	-0.15	0.92	-0.03
Mersey	2.68	-0.48	0.85	-0.16
Dee	2.60	-0.33	0.79	-0.14
Severn	2.82	-1.04	1.07	-0.30

As in the present climate simulation, the ADCIRC model no longer predicts a significantly greater total annual energy return from the barrages than that obtained through the 0-D model, as seen in Table 4.3.1.2.3. Again, inconsistent behaviour is experienced across the different estuaries, similar to that found in the present climate scenario.

Table 4.3.1.2.3: Predicted annual energy outputs of barrages operating in dual mode (3xDoEn) from 0-D and ADCIRC models in future climate scenario.

Barrage	0-D Model (TWh)	ADCIRC (TWh)	Difference (TWh)
Solway Firth	15.65	10.88	-4.77
Morecambe Bay	6.55	7.62	1.07
Mersey	1.15	1.10	-0.05
Dee	1.68	1.63	-0.05
Severn	15.67	20.34	4.67
Total	40.70	41.57	0.87

### 4.3.2 Tidal stream

Power output from the tidal stream farms under a future climate scenario is shown in Figure 4.3.2.1. The tidal stream farms were set at the same locations and in the same configurations used in the current climate scenario (see Table 4.2.2.1). As in the present climate runs, the Skerries and West Wales schemes run at peak loads for some time throughout most tidal cycles; those at Lynmouth and the Mersey never produce their peak power potential, even under spring tides.

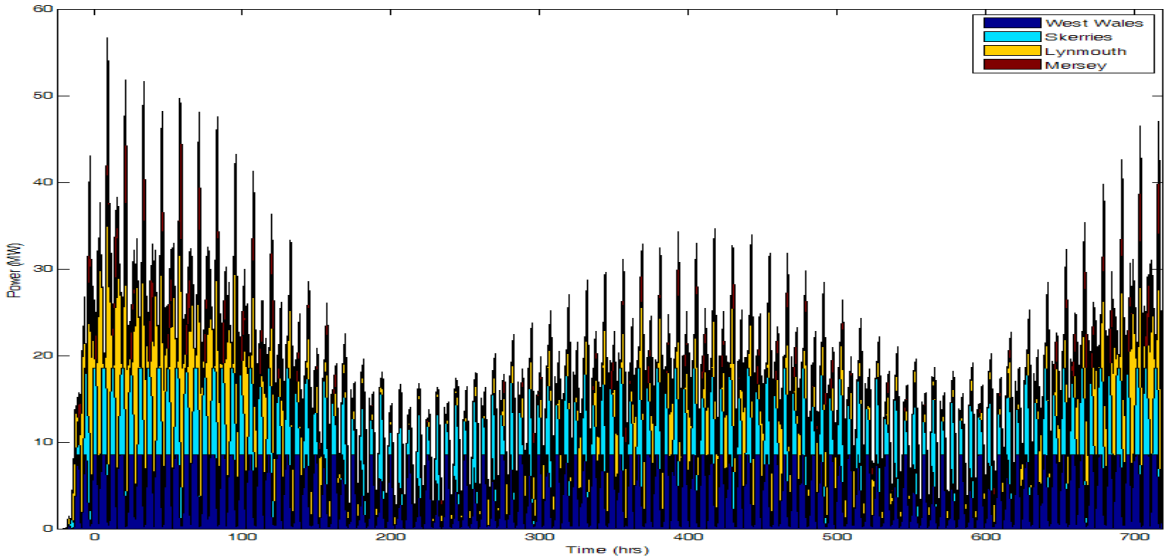


Figure 4.3.2.1: Power output from tidal stream farms operated in conjunction with barrages with 3xDoEn capacity in dual mode in future climate scenario.

The annual energy output is shown in Table 4.3.2.1. Comparing with Table 4.2.2.2, it is seen that there is little change in the total annual energy output in this climate scenario. As in the present climate runs, the inclusion of a lower bound of 1m/s on the initial velocity before the generation of power causes a reduction of about 2% in the utilisation rate of each farm.

Table 4.3.2.1: Annual energy production and utilisation rate for the tidal stream farms in future climate scenario.

Farm	Annual Energy Output (GWh)	Utilisation (%)
Mersey	22.18	13
Lynmouth	49.72	19
Skerries	45.08	49
West Wales	45.67	65
Total	162.65	27

#### 4.3.3 Combined tidal range (3xDoEn barrages, dual mode) and tidal stream extraction

A combined barrage and tidal stream simulation was run, similar to the simulation for the present climate. However, in this case, barrages were set up with a 3xDoEn installation and operated in dual mode, in the way described in Section 4.2.3.2, and as simulated without the inclusion of tidal stream farms in Section 4.3.1.2.

##### 4.3.3.1 Tidal range

In this simulation, the presence of the tidal stream farms was found to have no discernible effect on the tidal regime at each barrage location or on the power and annual energy outputs, figures remaining the same as those in Tables 4.3.1.2.1 to 4.3.1.2.3.

##### 4.3.3.2 Tidal stream

Figure 4.3.3.2.1 shows the power production from the tidal stream farms over the simulation period when the farms are run in conjunction with the 5 barrages with 3xDoEn installed capacity operated in dual mode. The power output is dominated, again, by the two open-sea tidal stream farms which, at their locations, would experience less impact upon the current speeds due to the presence of the barrages.

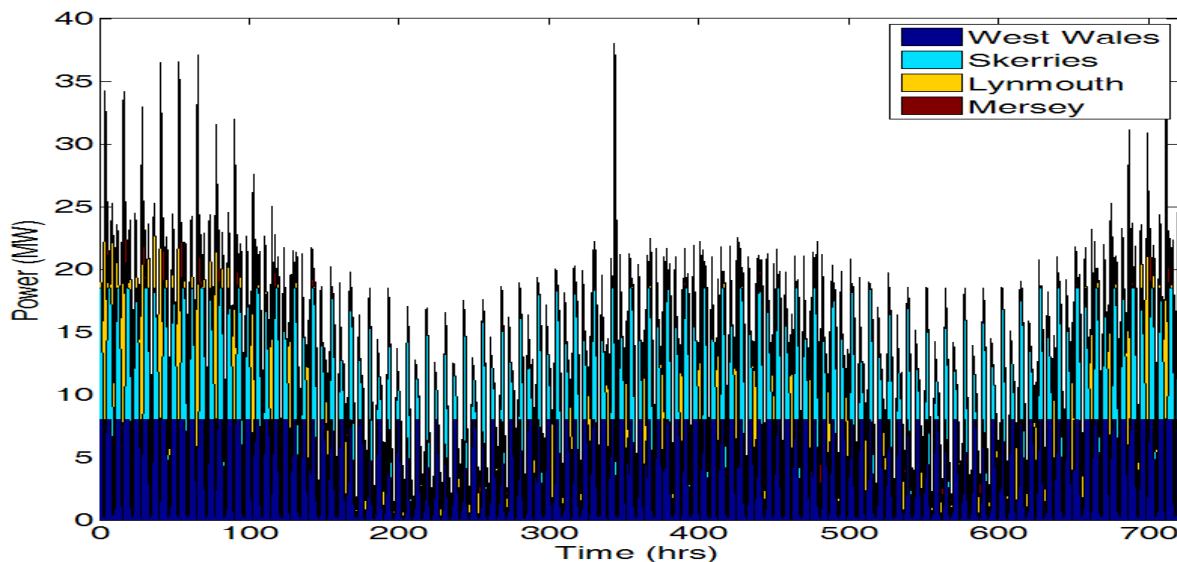


Figure 4.3.3.2.1: Power output from tidal stream farms operated in conjunction with barrages with 3xDoEn capacity in dual mode in future climate scenario.

The annual energy output from the tidal stream farms is shown in Table 4.3.3.2.1, together with the impact on energy production due to the inclusion of the barrages. Again, as would be expected, the inclusion of the barrages has a major impact upon the energy production of those farms within estuaries. The impact of the barrages on the open-sea farms is consistent with that seen in Section 4.2.4.2, with small decreases in annual energy output. However, unlike in the 1xDoEn combined simulation, there is now no energy production increase from the barrages to offset the loss from the tidal stream farms. Thus, there is an overall decrease in annual energy production of just under 45GWh.

Table 4.3.3.2.1: Annual energy outputs from tidal stream farms when operating in dual mode (3xDoEn) in conjunction with barrages; and the changes from operating alone in future climate scenario.

Farm	Annual Energy Output (GWh)	Utilisation (%)	Change from simulation without barrages (GWh)
Mersey	7.39	4	-14.79
Lynmouth	25.20	10	-24.52
Skerries	43.50	47	-1.58
West Wales	43.31	62	-2.36
Total	119.40	20	-43.25

#### 4.3.4 Summary

Table 4.3.4.1 gives the annual energy production from each barrage for each future climate simulation. The increase in sea level produces larger annual energy production for each barrage, associated with the increased water volume available in the enclosed basins and, in most cases, an increased tidal amplitude.

Table 4.3.4.1: Annual energy output from each barrage in future climate scenario.

Barrage	1xDoEn Ebb (TWh)	3xDoEn Dual (TWh)
Solway Firth	9.99	10.88
Morecambe Bay	6.12	7.62
Mersey	0.79	1.10
Dee	1.19	1.63
Severn	15.43	20.34
Total	33.52	41.58

The total annual energy production from the tidal stream farms under the future climate scenario is 162.7GWh (Table 4.3.2.1) in comparison with 161.5GWh (Table 4.2.2.2) in the present climate. The figure would reduce to 119.4GWh (Table 4.3.3.2.1) under their conjunctive operation with the 5 barrages operating in 3xDoEn dual mode.

## 5. ENVIRONMENTAL IMPLICATIONS

### 5.1 Introduction

Any planned tidal barrage (or other coastal and offshore engineering) scheme should be (Elliott et al, 2006):

- environmentally sustainable;
- technologically feasible;
- economically viable;
- socially desirable/tolerable;
- legally permissible;
- administratively achievable; and
- politically expedient.

While many of these issues are socio-economic/political and will require public debate and value judgements, here we wish to elucidate the technological and environmental facts related to various options. It has already been demonstrated (Baker, 1991) that the locations for the largest procurement of renewable marine energy, whilst still remaining cost-effective, are estuaries with a high tidal range, utilising barrages. Tidal barrage solutions use established low-head hydropower technology. The tidal power scheme at La Rance in France has now passed its 40th year of operation (Frau, 1993). Thus, tidal barrages are technologically feasible. In other areas with large tidal currents (e.g. straits and headlands), there is potential for power generation using free-standing tidal stream turbines, and other schemes using tidal lagoons have been proposed. The economic viability is assessed in the Sustainable Development Commission report on tidal power (SDC, 2007).

Here, we review the potential environmental impacts of tidal power schemes in the near-field and also at a distance, mainly with respect to tidal barrages. The impacts of the currently proposed tidal current schemes will be minimal and very local to the scheme due to their small power ratings. Impacts may be beneficial as well as harmful to the environment and some mitigation of potential harmful effects is possible. However, in planning any construction, notice must be taken of conservation issues and existing legislation. The European Habitats, Birds and Water Framework Directives are particularly relevant. Many estuaries have some protected status.

From this study of the potential tidal power of the Eastern Irish Sea, some quantitative results have been shown for the combined effects of barrages on North West estuaries acting in combination with a barrage on the Severn. The first approach, see Section 3, used a 0-D model in which turbine characteristics and tidal range were considered but not the detailed hydrodynamics. In the second phase of the modelling, Section 4, a 2-D depth-averaged model (ADCIRC) was employed. This used an unstructured finite-element grid to model the details of the tidal propagation around the West Coast of the UK, with and without tidal barrages. It has high resolution (down to 50m) around the barrage locations. The predicted physical changes in tidal range, residuals, energy budget, bottom stress and mixing have been used to assess the likely environmental and ecological consequences.

### 5.1.1 Generic impacts of tidal power schemes

It has long been recognised that there will be environmental implications in building a tidal barrage; e.g. Hodd (1977) discussed impacts for the Bay of Fundy scheme. Baker (1991) and Matthews and Young (1992) reviewed generic environmental impacts for tidal power schemes. Many studies have been carried out in the UK for the Severn Estuary, including estimation of impacts on the sediment regime and water quality (Shaw, 1980; Miles, 1982; Odd, 1982; Parker and Kirby, 1982; Radford, 1982; Kirby, 1987; Shaw, 1990) with a recent resurgence of interest (Kirby and Shaw, 2005). BERR (2008) has identified the need for a strategic environmental assessment for the Severn Tidal Power Feasibility Study which is addressing the environmental impacts of any chosen scheme on biodiversity and wildlife, flood management, geomorphology, water quality and other issues. This study is now (2009) being coordinated through the UK Government Department of Energy and Climate Change (DECC).

In order to assess the present state of the environment and potential impacts, it is desirable to have some quantitative indicators. Aubry and Elliott (2006) describe potential indicators of nearshore seabed disturbance which have been grouped into three broad indices (Coastline Morphological Change, Resource Use Change, and Environmental Quality and its Perception) and have applied them to the Humber Estuary. Further work is still needed to refine these methods (Boesch and Paul, 2001). Some information may be obtained from the experience of the existing tidal barrage at La Rance (Kirby and Retiere, 2007). For completeness, we here list the main local issues which may be of concern with respect to tidal barrages. Later, we also explore potential far-field impacts.

#### 5.1.1.1 Physical changes

By impounding the water for part of the tide, there will inevitably be some changes in the estuary basin and channels. The tidal and residual flows will be modified, possibly leading to some local scouring around the structure, specifically in the outflow regions of the turbines and sluices, together with siltation in the basin. The amount of vertical mixing will be reduced where the tidal flows are reduced and, with less re-suspension, the levels of suspended particulate matter will drop, leading to increased light penetration. There will be reduced saline penetration within the basin leading to freshening, i.e. more brackish water. There may be a build-up of contaminants, both physical and chemical, due to reduced flushing rates. In areas of increased flows, there may be potential re-suspension of contaminated sediments. This may result in a net reduction in water quality. An abundance of nitrates may lead to increased primary production, leading to eutrophication. An increase in average water level behind the basin would lead to a decrease in ground water runoff, which may have impacts on fluvial flooding. All these effects are to a large degree dependent upon the mode of operation of the barrage and are site specific. Of course, various mitigation works, including dredging and more stringent controls on discharges, may be undertaken.

#### 5.1.1.2 Environmental and ecological impacts

It must not be overlooked that a benefit of building tidal power plants is to reduce carbon emissions and, hence, benefit the environment both locally and globally. However, the most publicised impact of tidal barrages is the potential loss of certain habitats, especially intertidal mudflats and saltmarshes. These are particularly important for some species of birds and can be nationally and internationally protected areas. Benthic habitats may change in that the bottom stress due to waves and currents may be modified. Salinity and water quality may also change. Migratory fish may be impeded, although fish passes can be constructed. Fish and marine mammals may suffer damage from the turbines. Some estuaries may provide nurseries for breeding fish and conditions for these may no longer be suitable.

### 5.1.1.3 Human, economic, aesthetic and amenity impacts

The character of an area and the landscape may be drastically changed if a tidal barrage is constructed but, in this case, there may be pros and cons. Some people may find the visual intrusion objectionable but others may find it adds interest. There may be increased noise, especially during construction but also during operation. There may be a loss of historic sites in intertidal areas. However, there may also be an increase in tourism and the recreational potential of the area. During construction, there will be increased demand for resources and potential disruption, e.g. road transport may increase, but there will be economic benefits in terms of local jobs.

Fisheries, e.g. cockles and mussels, could be affected, although, if submerged for longer, it could be advantageous in giving them more time to filter nutrients from the water. There will be a change in access for the activities of cockle-pickers. Some coastal land used for agricultural grazing or crops may be lost or more gained. Other activities such as marine transport and navigation may be disrupted, but a barrage also gives potential for road and rail crossings.

The National Grid is not currently adapted to receive large pulses of electricity, and so some costly re-development and innovative solutions may be necessary.

### 5.1.2 Modelling studies: far-field effects

The ADCIRC model has been used to examine large-scale changes in bed stress, stratification/mixing and residual flows and, hence, their implications for sediment transport, fisheries and other environmental change. The direction of bed stress is an indicator of sediment movement, as bed load and various regions of convergence and divergence are often in good agreement with locations of sediment deposition. The bedload sediment transport rate is expected to be related to some power of the bed stress. 2-D models have been used to examine the spatial distributions of sediments on the North West European shelf (Pingree and Griffiths, 1979), or in more limited regions (Aldridge, 1997). The success of these models in relating sediment transport pathways to the direction of maximum tidal bed stress, without involving the complexity of using a sediment-transport model, has been demonstrated by Aldridge (1997), using a detailed comparison with observations in the Morecambe Bay region.

The mixing (due to the tidal stirring) and stratification (due to solar heating) of the water column are in balance at the shelf sea tidal mixing fronts, the position of which can be described by the ratio of the total water depth to the cube of a measure of the tidal current strength (e.g. Simpson and Hunter, 1974). Convergence and upwelling associated with tidal fronts can be important for the feeding of fish larvae (e.g. Hao et al, 2003). There may be some implications of the movement of the tidal mixing front for Nephrops in the Irish Sea (Nephrops is also known as scampi, Dublin Bay Prawn, or Langoustine.) The Irish Sea Nephrops fishery is the second largest Nephrops fishery for the UK outside the North Sea, with reported international landings of 9,120 tonnes in 2007. The majority of the catch is from the Western Irish Sea (<http://www.cefas.co.uk/media/63515/nephropsirishsea.pdf>), in an area centred on the location of the tidal mixing front. Nephrops distribution is limited by the extent of suitable muddy sediment in which they construct burrows. Burrow emergence is known to depend on biological and environmental factors such as ambient light level and tides.

Spring-neap frontal migration can be a few kilometres (Sharples, 2008). Sharples (2008) also shows that inter-annual changes in the timing of the spring-neap cycle can have a large impact on the primary productivity associated with fronts. The strongest impacts are predicted within 15–50km of the tidal mixing fronts, with increases in sub-surface primary production and carbon export. At the fronts, there is substantial extra primary production driven by the spring-neap cycle, contributing an extra 70% annually compared to fronts forced by the  $M_2$  tide only.

Local changes near headlands, where proposed tidal stream turbines would harness the energy of tidal streams, may have effects on the location of offshore sand-banks. Sand-banks are of considerable economic and ecological importance. They may occur on the open shelf, in estuaries and associated with headlands (Dyer and Huntley, 1999). Theories of sand-bar dynamics due to tidal currents have been presented, e.g. by Pingree and Maddock (1979) and Huthnance (1982). Those close to the shore may be linked to beaches in a dynamic exchange of sediment. They may act to dissipate wave energy and, thus, provide some coastal protection from erosion and wave overtopping. They can be hazards to shipping. Finally, they can provide exploitable reserves of sand and gravel (marine aggregates). Sand-banks are also areas of great importance to the health of the fishing industry, as the banks are important nursery and feeding grounds for many fish species.

## 5.2 Present hydrodynamics in the Irish Sea (base run)

The runs to provide the baseline from which to observe the influence of the inclusion of tidal power devices was simulated in a 2-D ADCIRC model using the grid shown in Section 4. The boundary conditions were obtained using an inverse model and tidal elevation data obtained from the TOPEX satellite. The bottom friction used within the model varied spatially. Generally, a bottom friction coefficient,  $c_D$ , of 0.002 was adopted. However, this was increased to 0.003 in the Severn Estuary. For a more detailed description of the model setup and the model grid validation, see Appendix 4.

Figure 5.2.1 shows the co-tidal charts for the  $M_2$  and  $S_2$  tidal components. The two amphidromic points, one north of Ireland and one off the eastern coast of Ireland within the modelled region, are clearly visible. The amplitude contours are 20cm apart for the  $M_2$  chart and are 10cm apart on the  $S_2$  chart, and the phase contours are 20 degrees for both co-tidal charts.



Figure 5.2.1:  $M_2$  and  $S_2$  co-tidal charts (amplitudes are plotted in green, with contour steps of 20cm and 10cm in left and right charts, respectively, and the phase is plotted in red, with contour steps of 20° in both charts).

The stratification parameter,  $\log_{10}(h/|u|^3)$ , in which  $h$  is the local water depth and  $u$  is the depth-averaged current velocity, gives an indication of the amount of stratification present when using a 2-D depth-integrated model. The critical value of  $2.7 \pm 0.3$  defines the tidal mixing fronts where the water column changes from stratified to fully mixed. Larger values indicate stratified conditions and lower values more well-mixed conditions. The major fronts in the Celtic Sea and the Western Irish Sea are clearly visible in Figure 5.2.2(a), running from the Southern Irish Coast to the North Coast of Cornwall and from the Eastern Coast of Ireland across to the Isle of Man.

Figure 5.2.2(b) shows the magnitude of the bottom stress,  $c_D|u|$  (where  $c_D$  is the bed friction coefficient), which reveals the location of the major areas of energy dissipation. The position of the step change in the coefficient is clearly visible in the plot. The high bottom stress in the Bristol Channel largely explains the substantial amount of suspended sediment in the waters in this area. The large stresses seen off the coasts of West Wales and Northern Anglesey reveal strong currents in areas proposed for tidal stream farms.

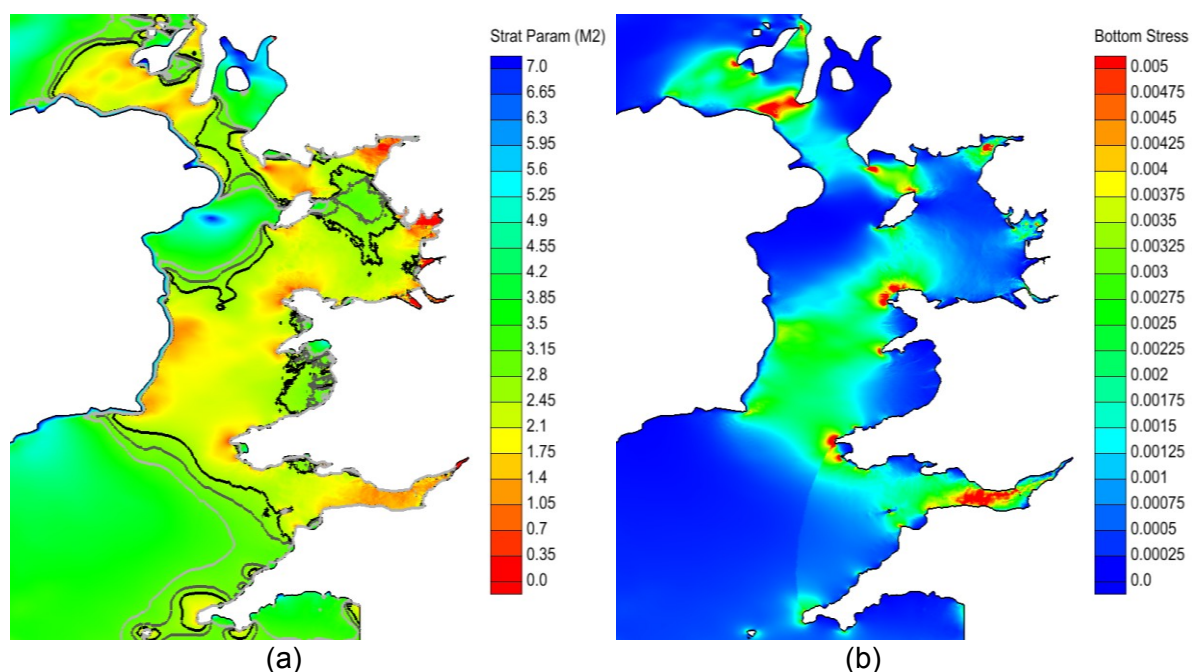


Figure 5.2.2: Plots of (a) stratification parameter and (b) bottom stress magnitude (the contours shown in plot (a) are the stratification parameter values of 2.4, 2.7 and 3.0 moving from black to light grey).

The residual currents in the Irish Sea generated by the model are shown in Figure 5.2.3. A number of features stand out in this plot. There is a broad southward current between the Isle of Man and the north west coast of England, which feeds into a clockwise gyre off the north coast of Anglesey. A similar clockwise gyre can be seen off the north east coast of the Isle of Man and a smaller anticlockwise gyre is visible south of the island. All of these features have been observed previously in a number of models of the Irish Sea (see Jones and Davies, 2007b). An interesting feature of the residual currents is an offshore 'jet' associated with headlands, as can be seen travelling westward from Holyhead towards Ireland.

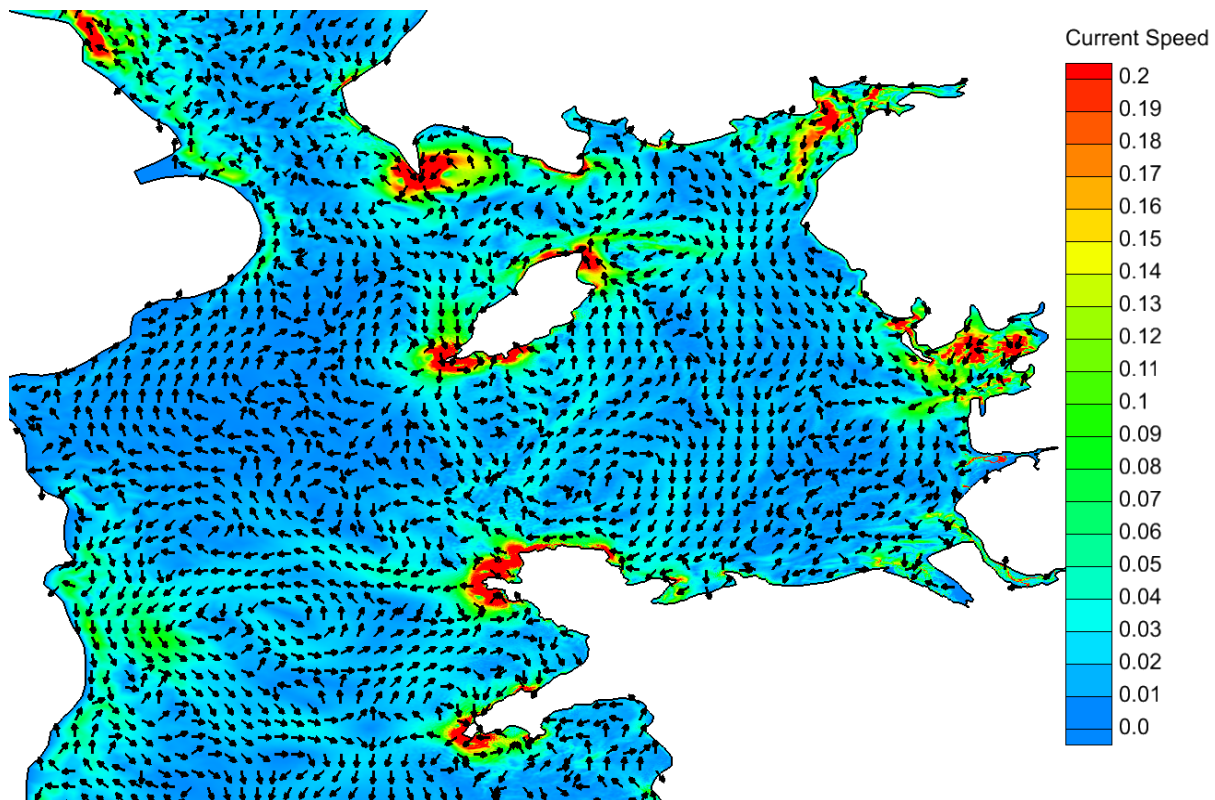


Figure 5.2.3: Present residual currents (m/s) in the Irish Sea.

### 5.3 Impact of changes in tide-induced circulation

#### 5.3.1 One-way (ebb) mode operation (1xDoEn)

The addition of 5 barrages within the Solway Firth, Morecambe Bay, Mersey, Dee and Severn estuaries has been simulated when the optimal economic cost of energy production is used to determine the number of turbines and sluice gates and the mode of operation within each barrage. This scheme is called the 1xDoEn scheme and is comparable to the schemes determined by the Department of Energy in their 1980s studies of these estuaries for best economic viability (Baker, 1991).

The first far-field impact to consider is the change in the  $M_2$  tidal amplitude shown in Figure 5.3.1.1(a). The amplitude is obviously decreased considerably behind the barrages but the amphidromic point off the east coast of Ireland is also shifted slightly. There is a decrease in tidal amplitude seen to the south of the amphidromic point, across St George's Channel and up the Bristol Channel, where the barrage has removed some of the resonance and, thus, markedly lowered the tidal amplitude. North of the amphidromic point, the tidal amplitude increases. In this simulation, the increase along the Irish coastline is about 10-15cm, but this varies depending upon the mode of operation of the barrages.

The change in bottom stress is shown in Figure 5.3.1.1(b). It is clear that there is a decrease in bottom stress throughout the Severn Estuary and within the basins of the Solway Firth and Morecambe Bay barrages. A decrease is also noted north of the Isle of Man. These decreases are associated with a drop in water speed at these sites, which will tend to allow a larger amount of sediment settlement. It will also generally decrease bed scour and re-suspension in these regions.

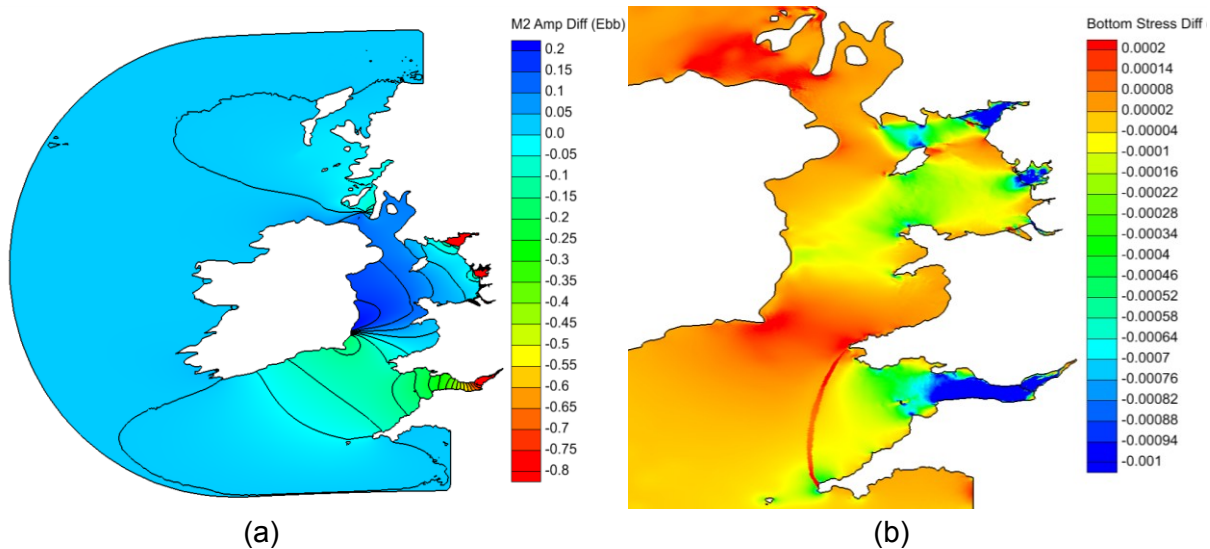


Figure 5.3.1.1: Changes induced by barrages installed with 1xDoEn capacity operating in ebb mode to (a)  $M_2$  tidal amplitude and (b) bottom stress.

Figure 5.3.1.2(a) shows the changes in stratification parameter due to the inclusion of the tidal barrages operated in ebb mode with a 1xDoEn installed scheme. There is an increase in stratification parameter associated with all the barrages, which suggests a more stratified and stable water column. The changes in the locations of the tidal mixing fronts are shown in Figure 5.3.1.2(b). The exact locations of the fronts are affected by the barrages, but they remain within the natural variability of the present frontal locations.

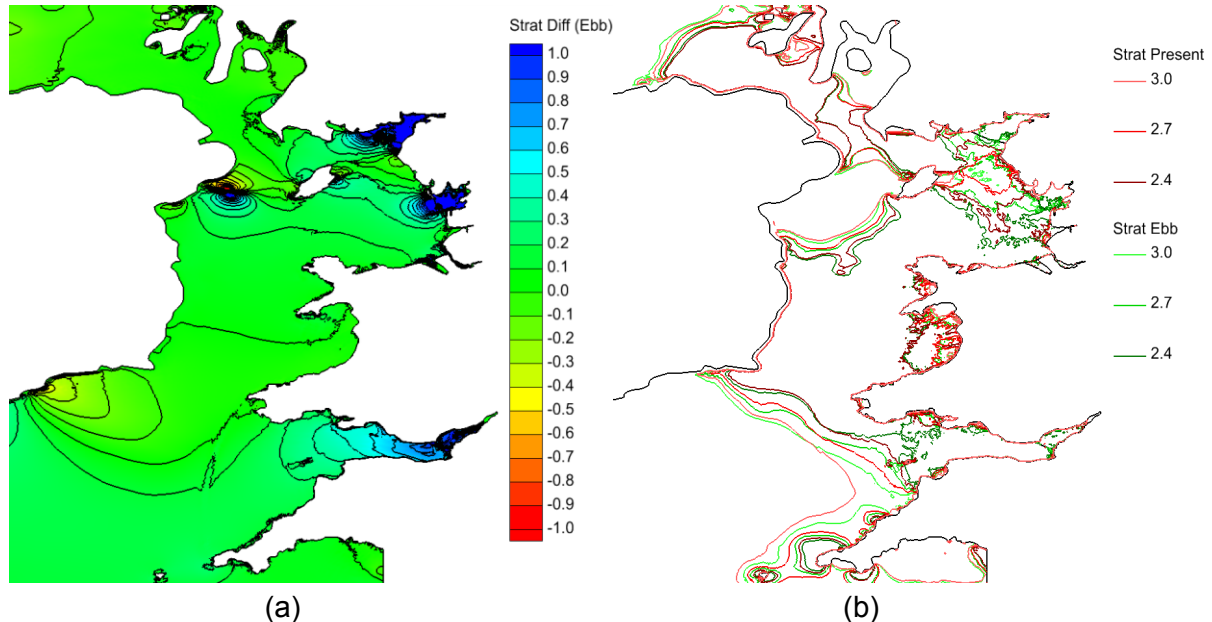


Figure 5.3.1.2: Changes due to barrages installed with 1xDoEn capacity operating in ebb mode to (a) stratification parameter and (b) tidal mixing frontal locations.

The residual currents in the Irish Sea, for the 1xDoEn scheme operating in ebb mode, are shown in Figure 5.3.1.3. Through comparison with Figure 5.2.3, it is clear that the major changes occur within the immediate vicinity of the barrages. The residual currents are determined mainly by the operational mode and the location of the sluice gates and turbines in the barrages. The inflow through the sluice gates and outflow through the turbines is

clearly seen in both the Solway Firth and Morecambe Bay, together with the resultant gyres. Although not obvious from the figures, the Mersey is affected to a much greater extent seaward of its barrage than the other estuaries are affected, due to the up-river location of the Mersey Barrage.

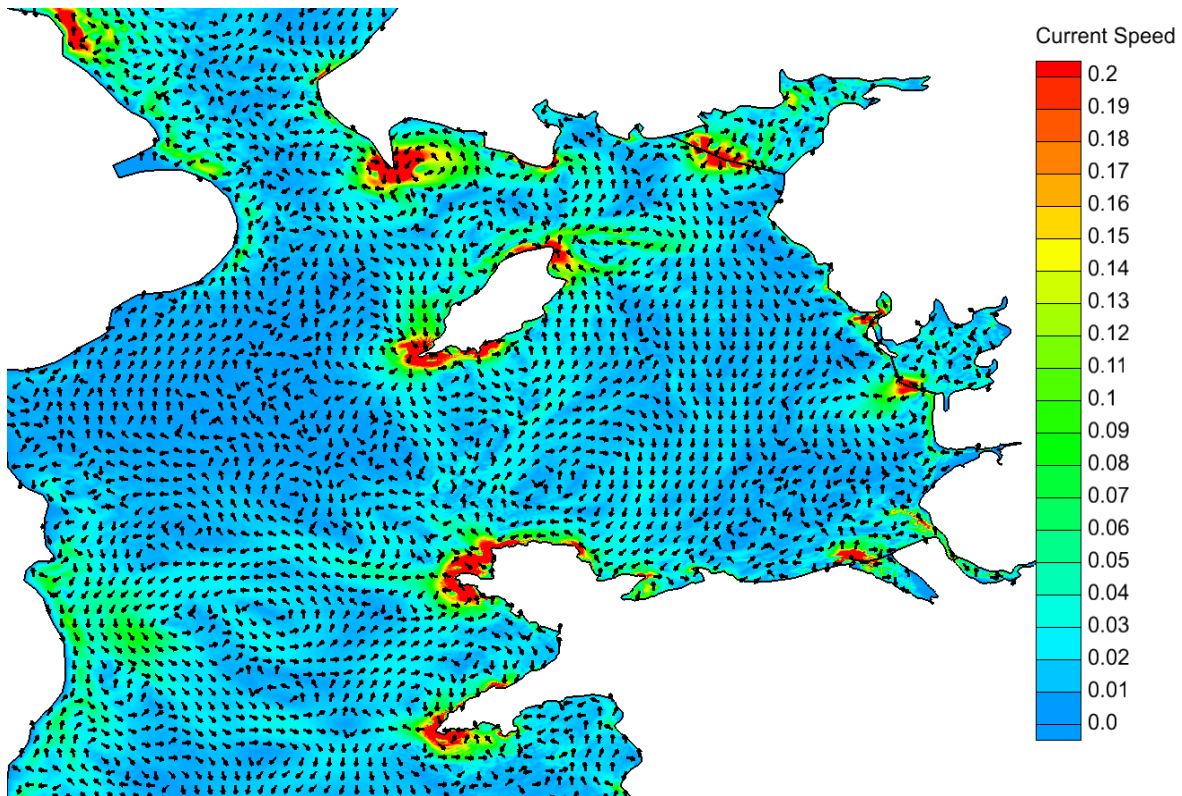


Figure 5.3.1.3: Residual currents (m/s) with 1xDoEn ebb mode operation.

### 5.3.2 Two-way (dual) mode operation (3xDoEn)

The 3xDoEn scheme is an enhanced turbine scheme whereby three times as many turbines are used than are prescribed in the best economic case of the original Department of Energy studies. This arrangement results in a larger volume of water passing through the barrages and, when operated in dual (ebb and flood generation) mode, preserves a larger portion of the tidal range within the enclosed basins behind the barrages. This outcome may be considered, rightly or wrongly, to be the best environmental solution, although the economics of energy production deteriorate, as shown in Section 3.

The changes to the  $M_2$  tidal amplitude are shown in Figure 5.3.2.1(a). The same qualitative pattern is seen as for the 1xDoEn schemes operating in ebb mode, shown in Figure 5.3.1.1(a). However, in the 3xDoEn configuration, the impacts are larger throughout the Irish Sea, with an increase along the Irish coast of 15-20cm in tidal amplitude.

The changes in bottom stress are shown in Figure 5.3.2.1(b). Again, the changes are qualitatively similar to the 1xDoEn scheme, but are larger. There is up to a 30% decrease in bottom stress in the Bristol Channel in this operational mode than in the ebb scheme considered previously.

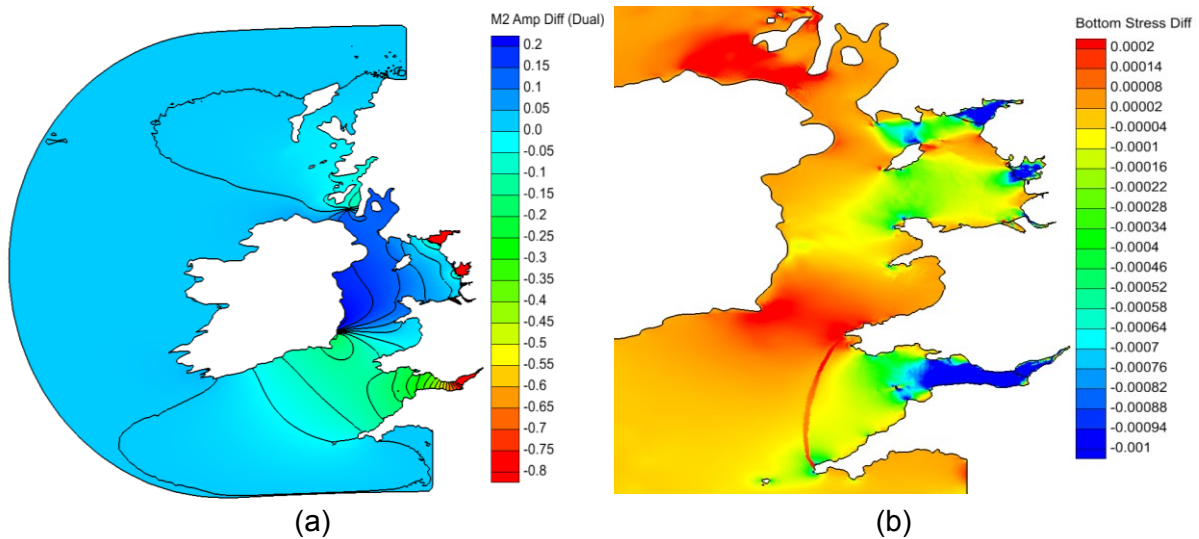


Figure 5.3.2.1: Changes due to barrages installed with 3xDoEn capacity operating in dual mode to (a)  $M_2$  tidal amplitude and (b) bottom stress.

The changes in the stratification parameter, as shown in Figure 5.3.2.2(a), reveal a similar pattern to the 1xDoEn scheme. There is an increase in stratification within the Bristol Channel and within each basin. The tidal mixing fronts, seen in Figure 5.3.2.2(b), again do not move very far, and remain within the natural variability of the present situation, but the range of variability of the Celtic Sea front is quite different from that seen in the 1xDoEn case and the present situation.

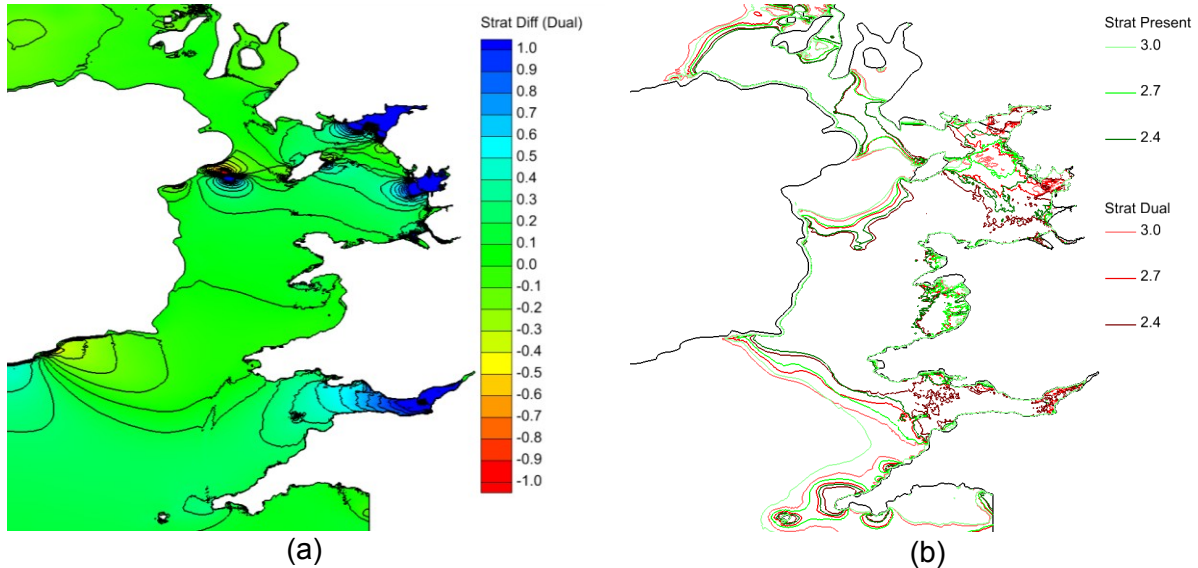


Figure 5.3.2.2: Changes due to barrages installed with 3xDoEn capacity operating in dual mode to (a) stratification parameter and (b) tidal mixing front locations.

The residual currents in the Irish Sea are shown in Figure 5.3.2.3. The residual currents in the 3xDoEn dual mode simulation closely match the residual currents in present conditions. The gyre circulation patterns associated with the 1xDoEn ebb mode scheme are not present here. As the turbines are generally situated in the deep water channels, through which the majority of the natural water fluxes occur, the currents associated with the restricted flow regime through the turbines in this dual mode case match well with the present conditions.

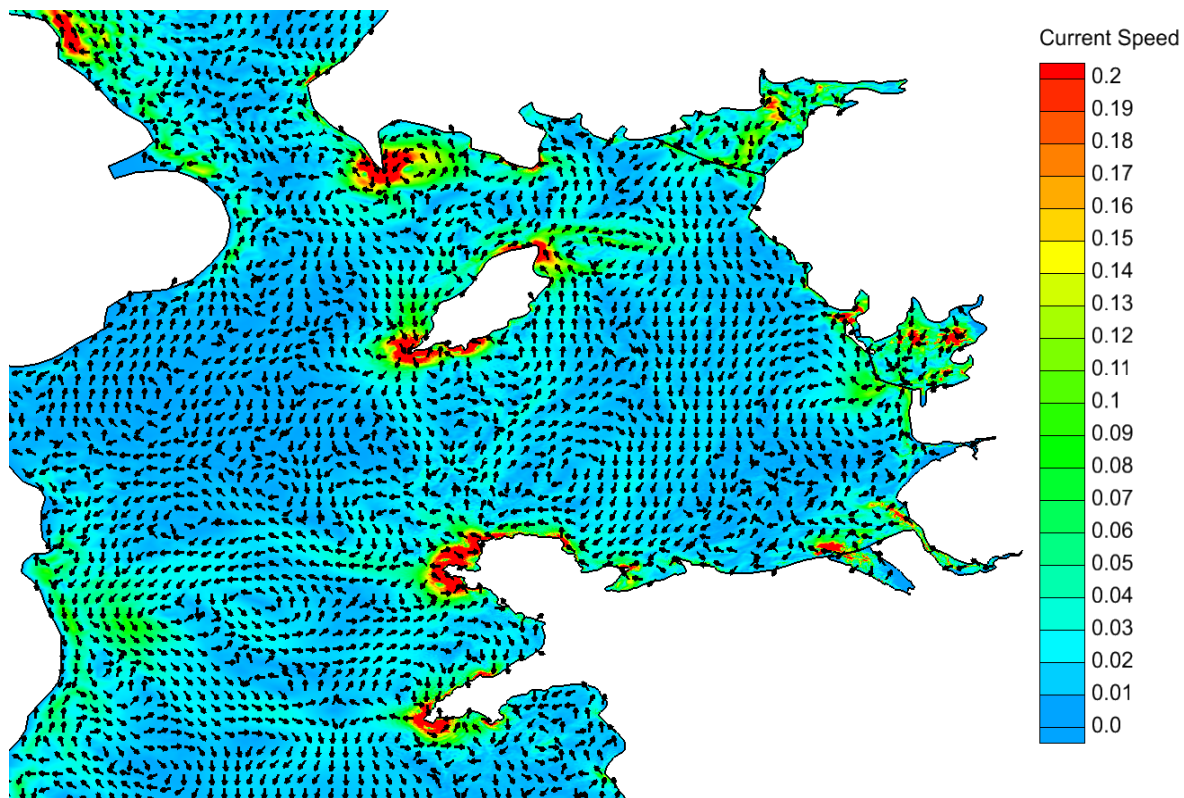


Figure 5.3.2.3: Residual currents (m/s) with 3xDoEn dual mode operation.

### 5.3.3 Environmental implications

The far-field environmental implications of the installation of the five barrages are qualitatively similar, whichever scheme and mode of operation are chosen. However, the quantitative values of the changes are dependent upon both the scheme and mode of operation chosen for each barrage.

The primary impact of the barrages is the increased flooding risk, due to the increase in tidal amplitude of 15-20cm along the east coast of Ireland and Northern Ireland. This is the greatest far-field effect and has environmental, social and political implications. The tides in the Bristol Channel are reduced in amplitude and this may help reduce storm surge flooding risks in this area. The impact on the tides in the Irish Sea as a whole is small, with a slight increase in amplitude being seen of about 5cm on average across the region under the 1xDoEn ebb mode scheme and 10cm for the 3xDoEn scheme in dual mode.

The reduction in bottom stress seen in the Bristol Channel has implications for the sediment regime in this area. The reduced bottom stress and associated velocities mean that the water column will become less turbid, allowing more light penetration. The changes will also permit a greater bio-diversity in the benthic habitat as the velocities at the sea bed reduce (Kirby and Retiere, 2008).

The stratification of the Irish and Celtic seas remains largely unchanged by the inclusion of the barrages, which means that the regions of high primary production will remain in the same locations.

The residual currents within the region are only significantly affected in the immediate locality of the barrages. The largest effect away from a barrage is seen in the Mersey Estuary, due to its position upriver of the estuary mouth.

## 5.4 Impacts on the estuarial waters and intertidal regime

### 5.4.1 Introduction

The main impacts of barrages, identified by many conservation groups, are the changes in intertidal area from the undisturbed situation and the impact upon the fish, invertebrate and bird populations within the estuaries. It is clear that there will be a reduction in the intertidal mudflats due to the construction of estuarine barrages; and mudflats provide important habitats for many species and feeding grounds for birds. The 0-D model results identified the potential for amelioration of this effect by use of dual-mode operation and increased turbine capacity, which would act to increase the tidal range within the basin relative to ebb mode operation (although this would generally increase the cost of the electricity generated).

A barrage will largely block the entry of longer period swell waves, but local generation of waves within an estuary can still impact on intertidal areas (Wolf, 2003 and 2004, Moller and Spencer, 2002 and 2003). Raised low water levels can increase the effective time-averaged fetch within an estuary (Gray, 1992) and, thereby, increase the impact of the waves generated within a barraged area compared to the present situation.

The 2-D ADCIRC model has been used to calculate the change in intertidal area, but the numbers are highly dependent upon the available bathymetry. The Mersey and Dee estuaries have excellent high resolution LIDAR data, whilst data for the other estuaries is coarse, with little vertical resolution above mean water level. Thus, the quantitative results shown should be interpreted with this in mind. Examples of the intertidal areas for different installation and operation scenarios are shown in Figures 5.4.1.1 to 5.4.1.3 for the Severn, Mersey and Dee estuaries, respectively. The relative changes in intertidal area are seen to alter from spring to neap tides and from site to site, depending upon the underlying bathymetry. What is consistent throughout the simulations is the phase shift in the intertidal dynamics. This is due to the barrage operation requiring the tides to be held back to generate a head difference for energy production.

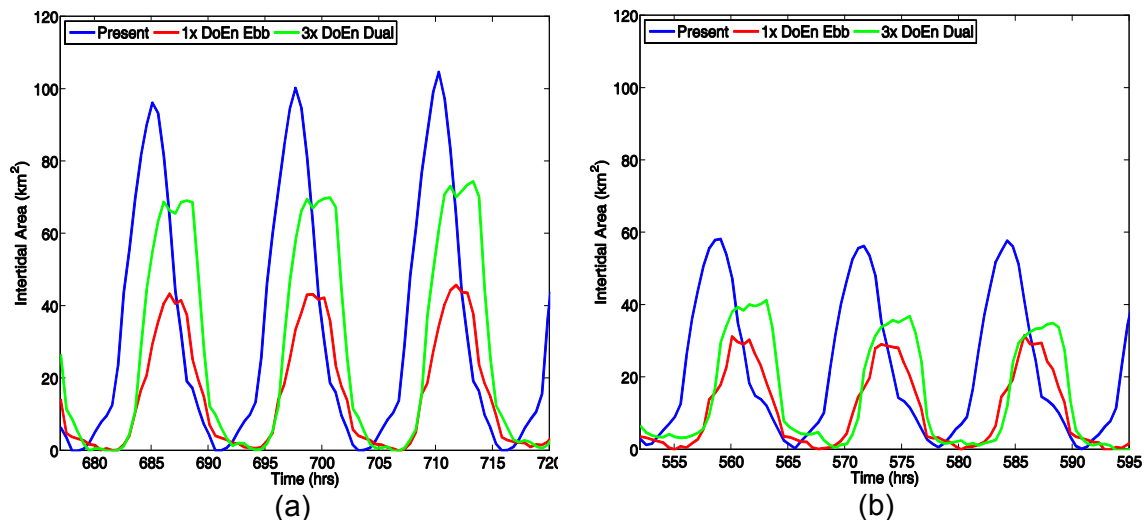


Figure 5.4.1.1: Variation in intertidal area exposed through several tidal cycles in the Severn Barrage basin for: (a) spring tide; (b) neap tide.

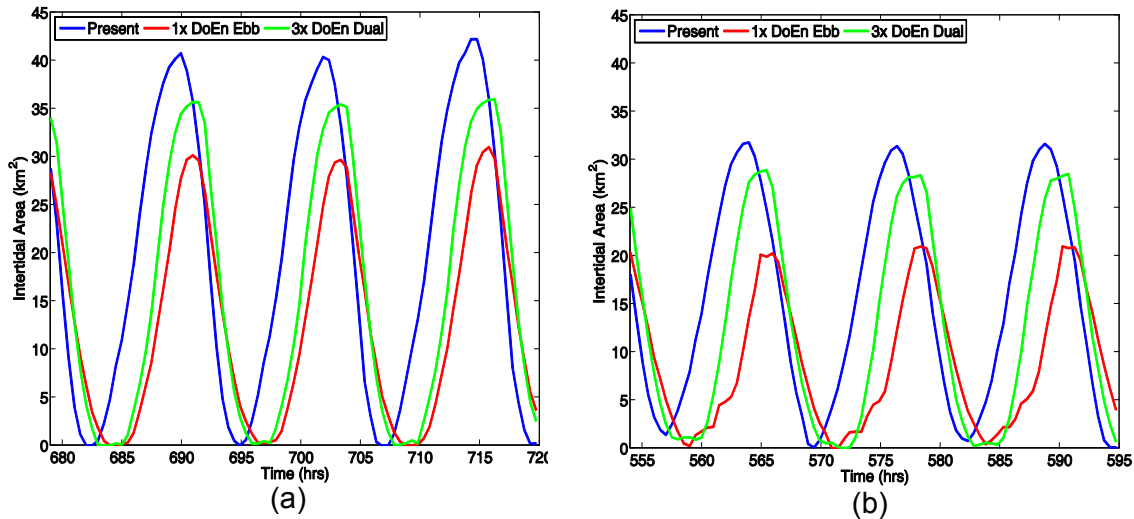


Figure 5.4.1.2: Variation in intertidal area exposed through several tidal cycles in the Mersey Barrage basin for: (a) spring tide; (b) neap tide.

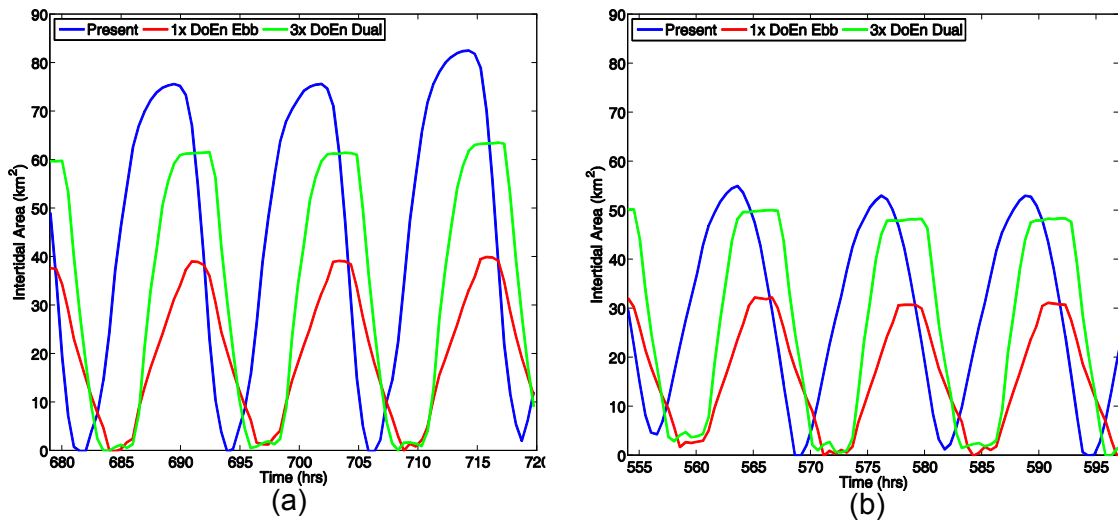


Figure 5.4.1.3: Variation in intertidal area exposed through several tidal cycles in the Dee Barrage basin for: (a) spring tide; (b) neap tide.

The averages of the maximum intertidal areas exposed over each tide in the 30-day sequence are shown in Table 5.4.1.1. It reveals that increasing the installed turbine capacity in dual mode results in a marked increase in the maximum intertidal area retained within the basin. As noted earlier, the actual maximum area retained by any given scheme is highly dependent upon the bathymetry of the enclosed basin.

Table 5.4.1.1: Tidal-averaged maximum intertidal area within each basin.

	Present area (km <sup>2</sup> )	1xDoEn ebb mode		3xDoEn dual mode	
		Area (km <sup>2</sup> )	Percentage of base	Area (km <sup>2</sup> )	Percentage of base
Solway Firth	74	20	27	30	41
Morecambe Bay	102	77	75	83	81
Mersey	37	26	70	32	86
Dee	67	36	54	56	84
Severn	80	38	48	55	69

The values in Table 5.4.1.1 are for areas within the enclosed basins. They do not include the effects on the maximum intertidal area outside the basin. For three of the barrage schemes, the latter effect is negligible; but for the Severn and Mersey barrages there is a marked impact on tidal amplitudes for some distance seaward of each barrage.

It is also instructive to consider the average area of mudflats available. By integrating the area over time and dividing by the length of the simulation, an average area of exposed mudflats may be determined, as shown above in Table 5.4.1.2. The average areas are also shown in Figure 5.4.1.4(b). The anomalous results for the Solway Firth and Morecambe Bay barrages may suggest the necessity for better bathymetry within these regions.

Table 5.4.1.2: Average intertidal area within each basin.

	Present average area (km <sup>2</sup> )	1xDoEn ebb mode		3xDoEn dual mode	
		Mean area (km <sup>2</sup> )	Percentage of base	Mean area (km <sup>2</sup> )	Percentage of base
Solway Firth	21.6	6.8	31	10.1	47
Morecambe Bay	37.3	31.9	86	28.8	77
Mersey	18.2	11.0	60	14.2	78
Dee	38.5	18.2	47	29.5	77
Severn	29.5	14.2	48	23.1	78

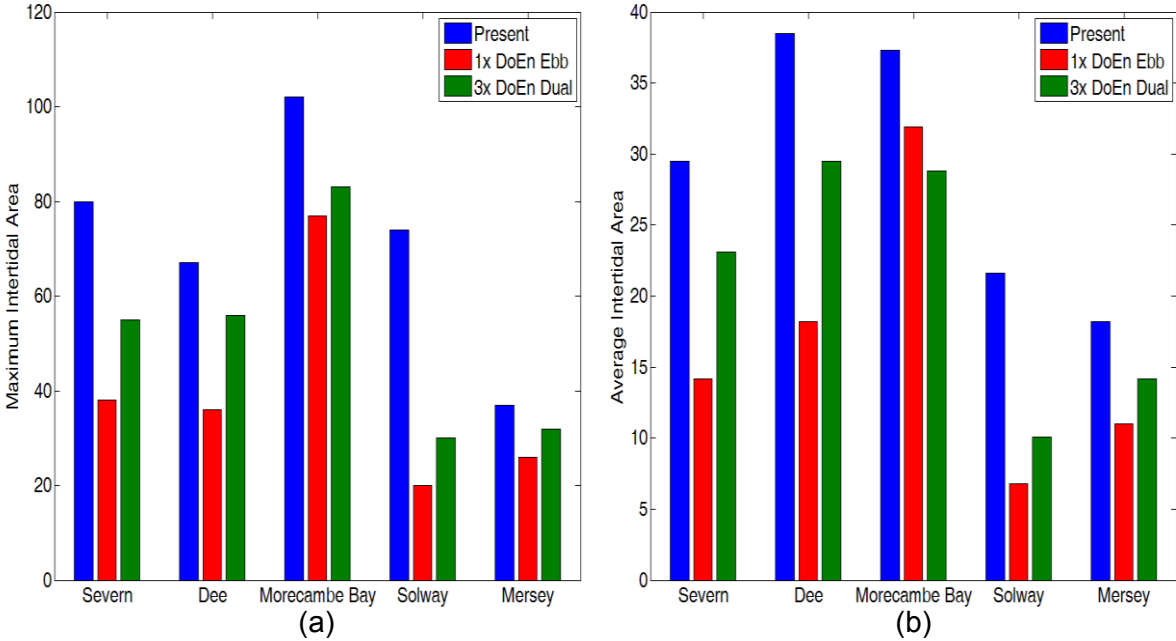


Figure 5.4.1.4: Intertidal area in each basin: (a) tidal-averaged maximum extent; (b) average available. (Note the difference in vertical scales.)

5.4.2 Case study for the Mersey Estuary

The Mersey Estuary is a macrotidal coastal plain estuary (see the Estuary Guide <http://www.estuary-guide.net/search/estuaries/details.asp?fileid=35>). The River Mersey catchment covers an area of about 5000km<sup>2</sup>. Modal river flow is about 3.26 x 10<sup>6</sup> m<sup>3</sup>/day. The maximum spring tidal range is about 10.4m; the neap tidal range is around 4m. The high spring tide volume of the estuary is 6.5 x 10<sup>2</sup> Mm<sup>3</sup>.

Habitats in the outer estuary are mainly dune. The inner estuary includes intertidal and sub-tidal environments with mud, saltmarsh and rocky shoreline. Species include overwintering birds, natterjack toads, benthic invertebrates and fish (sole, trout, dace, river lamprey and salmon). The Mersey is an internationally important site for 3 species of ducks: shelduck, teal and pintail, and 4 species of wading birds: dunlin, black-tailed godwit, redshank and turnstone. It is also a site of national importance to the widgeon, golden plover, grey plover, lapwing and curlew. Parts of the Mersey are designated as a Special Protected Area (SPA) under the EU Birds Directive (79/409/EEC). There are also an internationally important Ramsar wetland site and a European marine site. In addition, much of the Mersey Estuary has been included in one of the four Sites of Special Scientific Interest (SSSIs): New Ferry, Mersey Estuary, the Mersey Narrows and the North Wirral Foreshore (RSK, 2007).

Previous studies of the Mersey have identified various environmental issues (Towner, 1990); and renewed interest in Mersey tidal power has led to new studies, e.g. RSK (2007). However, use of the 0-D and ADCIRC models for the Mersey now permits a more quantitative assessment of the likely impacts. A parallel study using the Telemac/Tomawac/Sisyphe suite of models for the Mersey, to investigate changes in sediment transport and estuarine morphology, is in progress (Carroll et al, 2008). This has shown that the presence of a barrage may increase scouring in the Narrows and reverse the direction of the tidal residual from seawards to landwards, resulting in further importation of fine sediment and increased siltation behind the barrage.

Tidal residuals are only one part of the residual (time-averaged) flow. There are also density and wind-driven residuals which may have different directions to the tidal residual. They also have a significant vertical structure, whereby the surface and bottom flows are in opposite directions. For example, surface wind-driven transport in the Irish Sea is predominantly from the west due to the prevailing wind. Continuity requires a return flow at the bottom. For these reasons, it is difficult to fully assess the likely net sediment transport in a 2-D homogeneous model.

#### 5.4.2.1 2-D modelling

The present residual currents within the Mersey Estuary are shown in Figure 5.4.2.1.1. The main features are the generally outward flow at the mouth of the river and a clockwise circulation between the mouth and the Narrows. Within the broader portion of the estuary, the flow is downstream and is concentrated mainly in the relatively deep channels. At the proposed line of the barrage, there is an anticlockwise circulation with a weak upstream flow in the deep channel, which would be the location of choice for the turbines in the barrage.

The 1xDoEn ebb mode scheme has the turbines located in the deep channel and the sluices in the northern section. The general flow then would be upstream through the sluices and downstream through the turbines. This is in opposition to the natural residual currents, where an anti-clockwise circulation takes place. The residual currents associated with the 1xDoEn ebb mode scheme are shown in Figure 5.4.2.1.2. The change in the residual currents at the turbines and sluice gates are as expected. Beyond the close proximity to the barrage, the residual currents remain similar to the present situation. A slight decrease in downstream flow speed is noted in the broader inner estuary within the barrage basin.

Figure 5.4.2.1.3 shows the residual currents when the 3xDoEn dual mode scheme is employed. The flow structure away from the barrage is again, as in the 1xDoEn case, similar to the present state, although the outward flux at the mouth is increased once more, whilst the speed in the broader basin region is reduced.

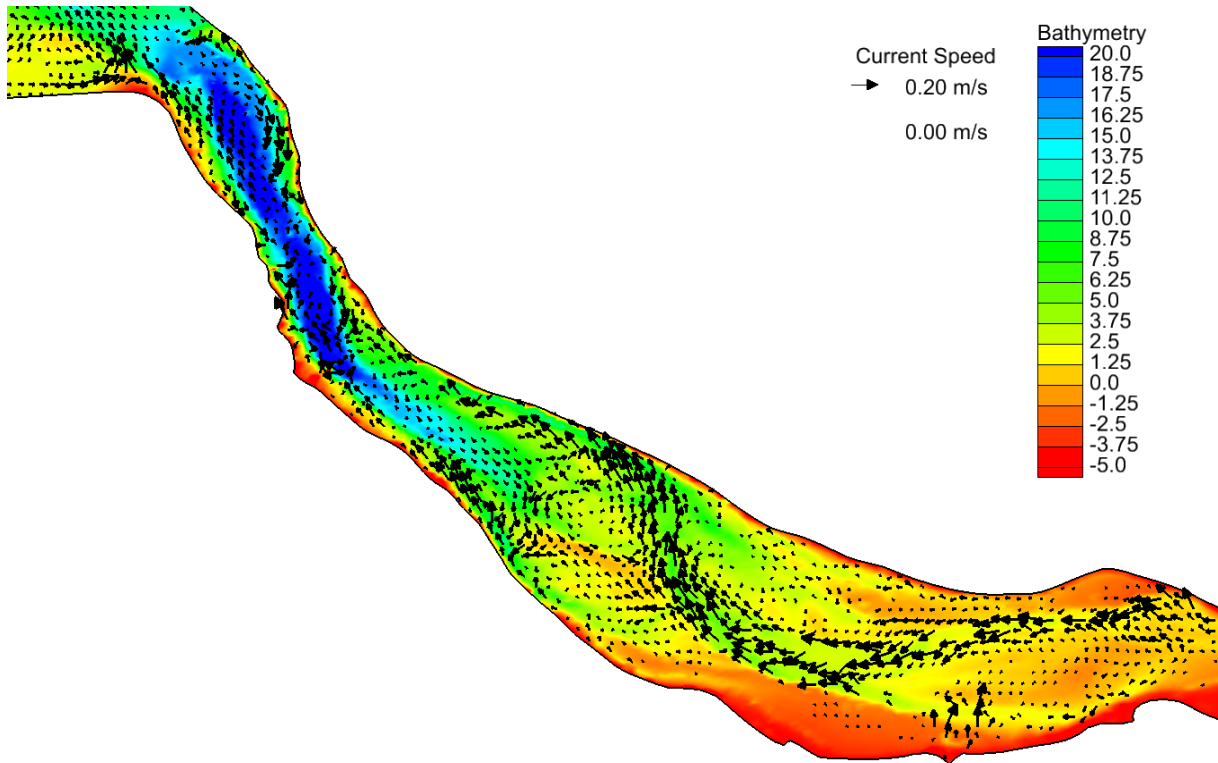


Figure 5.4.2.1.1: Present residual currents and bathymetry (m below mean sea level) in the Mersey.

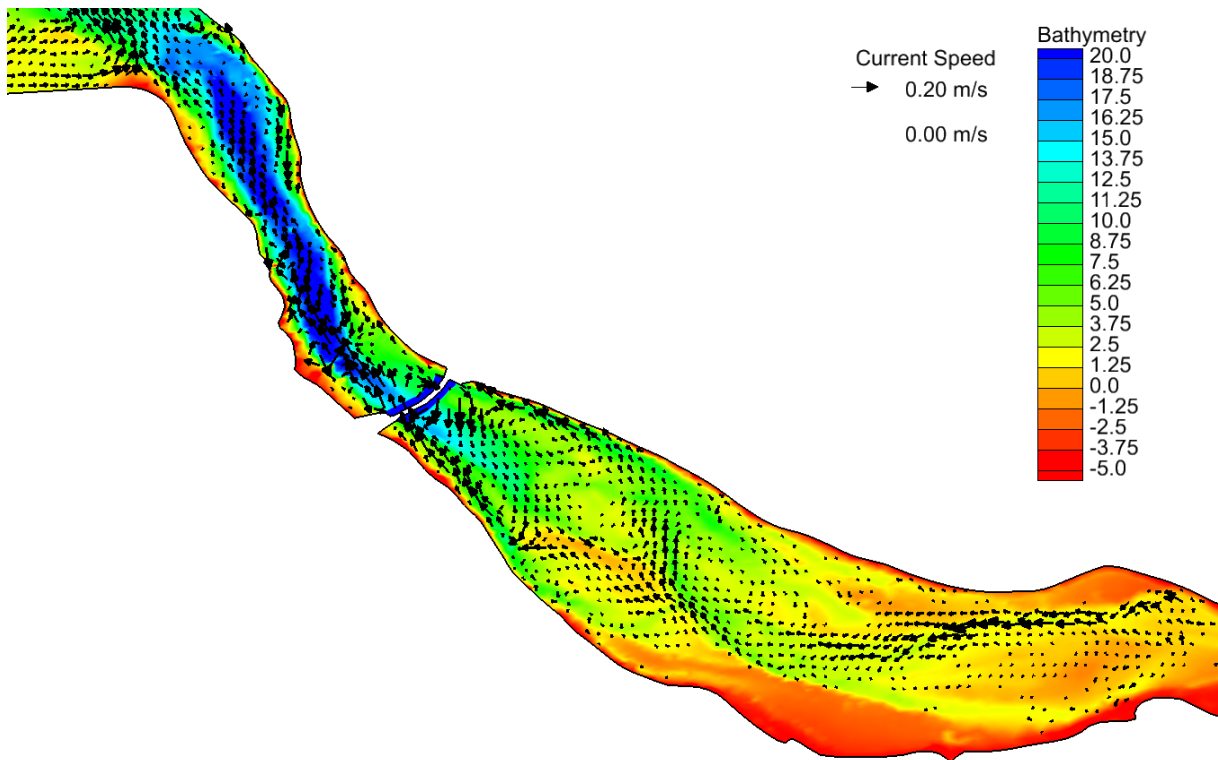


Figure 5.4.2.1.2: Residual currents in the Mersey with barrage in 1xDoEn ebb mode operation.

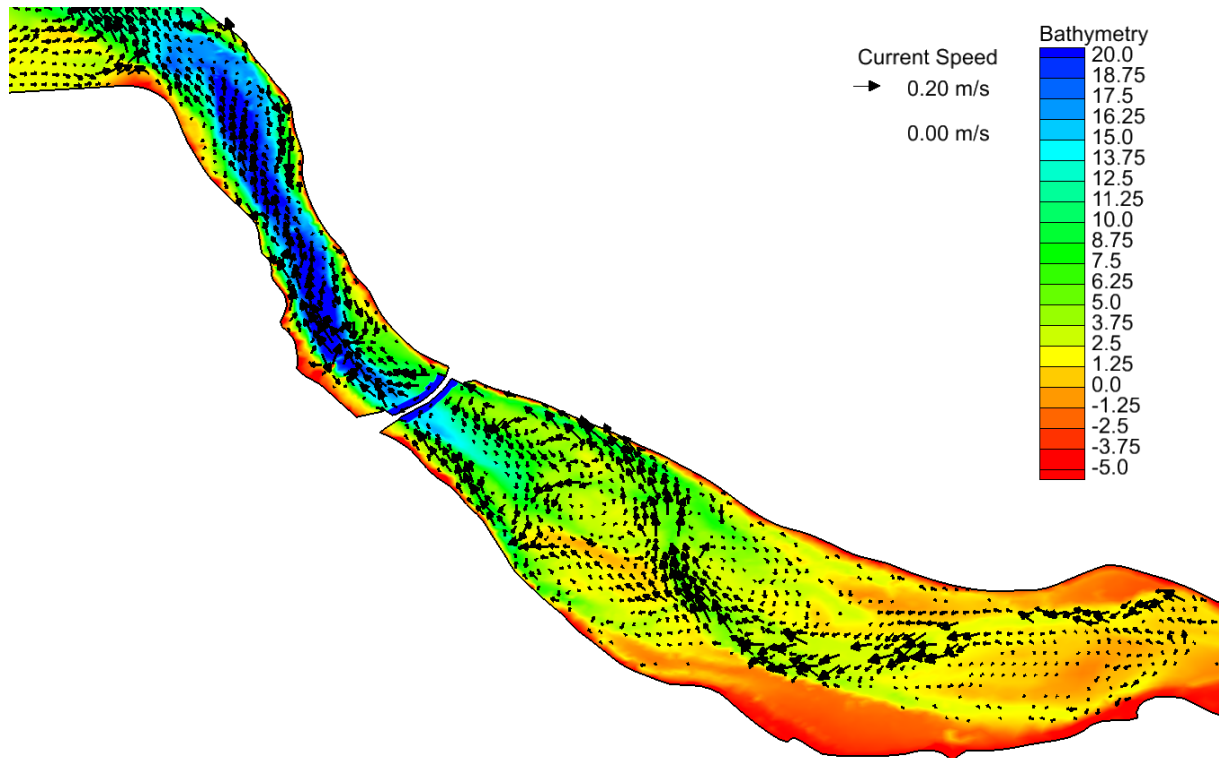


Figure 5.4.2.1.3: Residual currents in the Mersey with barrage in 3xDoEn dual mode operation.

#### 5.4.2.2 Environmental implications

The change in intertidal extent within the Mersey Barrage basin (see Tables 5.4.1.1 and 5.4.1.2) will have an impact upon the wildlife that depends upon this habitat. The mudflats, as defined by the Natural England GIS Digital Boundary dataset ([http://www.english-nature.org.uk/pubs/gis/gis\\_register.asp](http://www.english-nature.org.uk/pubs/gis/gis_register.asp)) within the basin, are highlighted in green in Figure 5.4.2.2.1, with the present low water and high water conditions shown in (a) and (b), respectively. Figures 5.4.2.2.2 and 5.4.2.2.3 show the changes in intertidal regime and the resultant impacts upon the mudflats for the 1xDoEn ebb mode scheme and the 3xDoEn dual mode scheme, respectively.

There is a reduction in mudflat area for both schemes at low water of about the same amount; and at high water there is a reduction in the mudflat area covered by the water, although this effect is smaller in the 3xDoEn scheme. The reduced coverage at high water levels and the reduced exposed area at low water will both lead to a reduction in the mudflat habitat. The use of pumping, especially in the dual mode scheme, could act to lower the low water levels and heighten the high water levels and, thus, lead to an increase in the intertidal extent within the basin, thereby reducing the loss of habitat in the basin.

The local high velocities at the barrage turbines and sluices would lead to a short-term scouring of new channels, causing some re-suspension of the bottom sediments which, due to the past history of the Mersey, contain a large quantity of contaminants. Thus, in the short term, the water quality of the Mersey may be reduced until the scoured channel formation ends and a new equilibrium is reached within the estuary.

The general reduction in water velocities within the barrage basin is likely to increase sedimentation. This process might lead, in the long-term, to some loss in tidal prism and energy generation capacity, but it could also increase the intertidal habitat available within the estuary as a new equilibrium is reached.

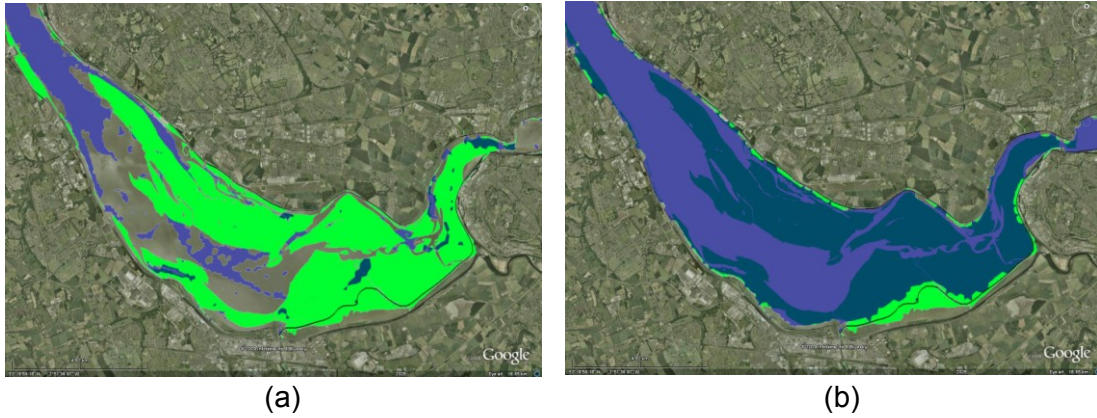


Figure 5.4.2.2.1: Mudflats in the Mersey Estuary (in green) with present spring tide simulation at (a) low water and (b) high water.

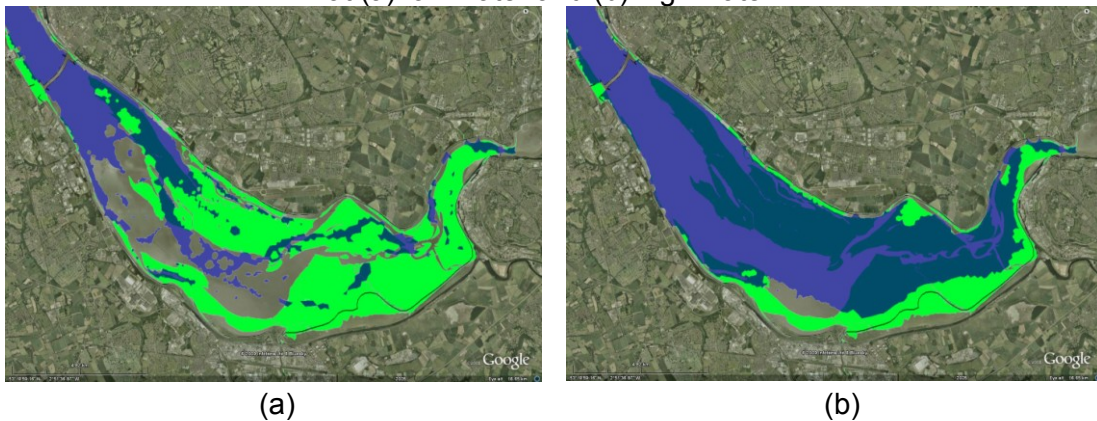


Figure 5.4.2.2.2: Mudflats in the Mersey estuary (in green) with 1xDoEn ebb mode, spring tide simulation at (a) low water and (b) high water.

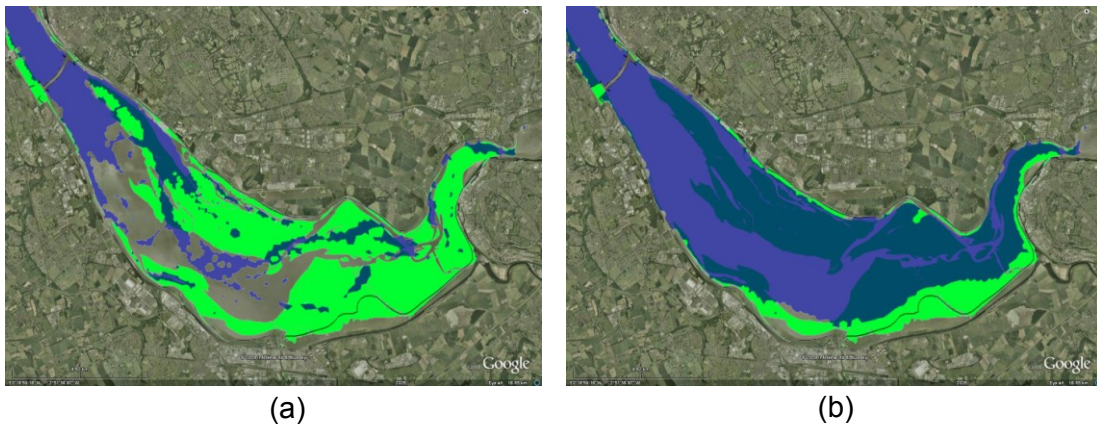


Figure 5.4.2.2.3: Mudflats in the Mersey Estuary (in green) with 3xDoEn dual mode, spring tide simulation at (a) low water and (b) high water.

## 5.5 Impact on sediment regime and induced morphological changes

The impact on the sediment regime and the resulting changes in morphology around barrages are addressed here by considering the case of the Mersey Estuary. It draws from an ongoing PhD study in the Department of Engineering being undertaken by Ben Carroll, with support from the EPSRC-DTA fund (Carroll et al, 2008).

Over the last century, there have been many significant changes in the bathymetry of the Mersey Estuary. These changes are particularly noticeable for the period between 1906 and 1977. Surveys suggest a loss of tidal volume in the estuary of approximately 10% between 1936 and 1956: some 80Mm<sup>3</sup> of estuary water volume has been lost since the turn of the last century, despite the removal of over 400Mm<sup>3</sup> by dredging (O'Connor, 1987). However, recently the tidal volume of the estuary has become more stable, with even signs of a small increase in the volume capacity of 10Mm<sup>3</sup> (Lane, 2004).

The adjustments to the bathymetry have been attributed to changes in the sediment transport process due to the construction of the training walls in Liverpool Bay at the beginning of 20<sup>th</sup> century; see Blott et al (2006), Price and Kendrick (1963), Thomas et al (2002) and Lane (2004). A tidal barrage is likely also to cause a change in the tidal volume before the estuary settles to a new equilibrium. To quantify the possible changes in sediment transport and, hence, in the morphology, both in the short term (~ 1 year) and in the long term (~ 10 years), computer modelling work is being carried out, based on the TELEMAC suite (Hervouet and Bates, 2000).

The TELEMAC model system includes a wave module (Tomawac), a hydrodynamic module (Telemac-2d) and a morphodynamic module (Sisyphe). Tomawac is a third generation spectral wave model that includes wave breaking, energy dissipation by bottom friction, wind-induced wave generation, directional spreading and wave-current interaction. The computed radiation stress from Tomawac is fed into Telemac-2d, coupling with tidal forces, to predict combined waves and currents. Based on the wave and current information, the sediment transport module, Sisyphe, is then used to compute the total or the bed-load transport for non-cohesive sediments and the subsequent morphological evolutions under the effects of currents and waves. Instantaneous sand transport rates are calculated using the Soulsby (1997) formula.

Due to the depth-averaging nature of the model, the density-driven circulation is not considered in the present study. The fact that the river input into the Mersey Estuary is small compared to the average tidal discharge suggests that the contribution from gravitational circulation may be insignificant. However, several previous studies (Price and Kendrick, 1963, Thomas et al, 2002) maintain its importance in moving sediment from Liverpool Bay into the upper estuary. Experiments are still being undertaken, both with and without considering the density current factor, to test this hypothesis.

The computational domain used in the present studies covers both the Mersey and Dee estuaries and the majority of Liverpool Bay. An unstructured triangular mesh, similar to that employed in the ADCIRC 2-D model described in Section 4, is used to discretise the domain with approximately 14,200 elements and 7,500 nodes. It is employed for both an open estuary and one with a barrage, with inter-node spacing ranging from 50m in the Narrows of the Mersey Estuary to 1km in outer Liverpool Bay. The typical time step adopted in the calculations is 10s to ensure stability and convergence.

Initial model testing on wave propagation under mean spring tides (range 8.4m) suggests insignificant effects from the barrage operation for the upper estuary. Outside the estuary, within Liverpool Bay, there are certain differences in wave heights and directions for the barrage and non-barrage cases, although small for the simulated conditions. Further simulation with different wave conditions is underway to confirm these findings.

Based on mean spring and mean neap tides, the hydrodynamic module and sediment module have been calibrated using data from an early Mersey Barrage Company (1993) study, see Figure 5.5.1.

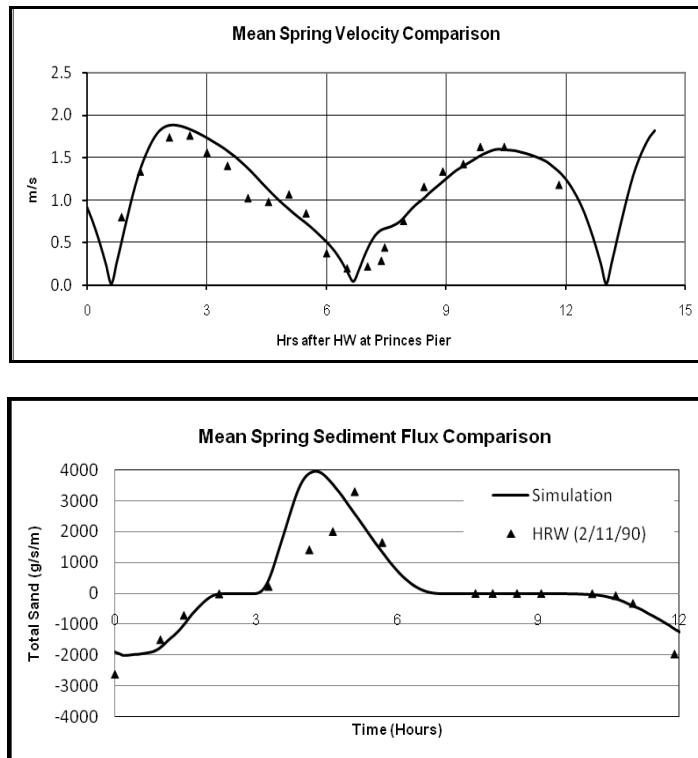


Figure 5.5.1: Comparison of observed (HRW) and predicted velocity and sediment flux at the Narrows for mean spring tide.

Assuming an ebb-mode energy generation strategy, the model results indicate, as expected, that a barrage across the entrance to the estuary will hinder the natural movement of the tidal flow, effectively reducing the tidal range by as much as 60% and increasing the low water level upstream of the structure by approximately 4.0m (Figure 5.5.2).

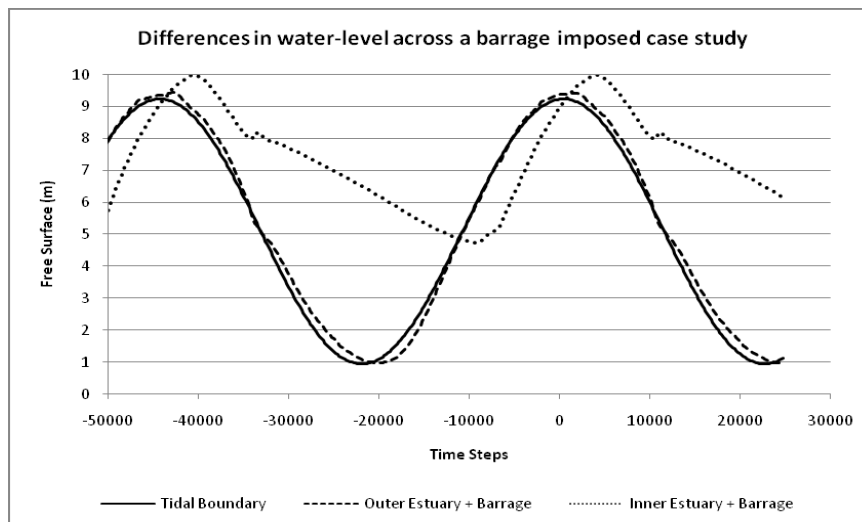


Figure 5.5.2: Variations in water level downstream and upstream of Mersey Barrage.

The tidal-averaged residual flow around the structure, shown in Figure 5.5.3, shows a net upstream flow through the sluices and a seaward flow through the turbines, as expected, with seaward flow into the outer estuary consistent with Figure 5.4.2.1.2. The strong channel-following transport pattern upstream of the barrage is diminished and accretion within the estuary occurs, particularly in the reach where the river is wide; see Figure 5.5.4. In the

immediate vicinity of the barrage, however, both erosion and deposition can be seen around the turbine structure and sluice gates. The barrage operation seems to lead to a reduction in sediment transport across the entrance to the estuary.

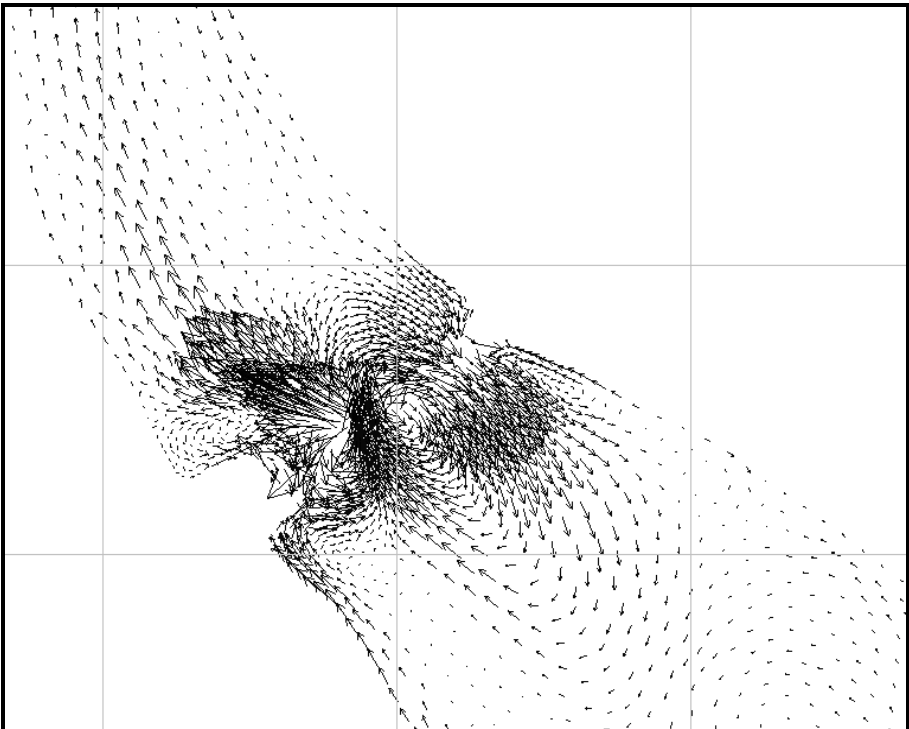


Figure 5.5.3: Velocity residuals near the barrage location.

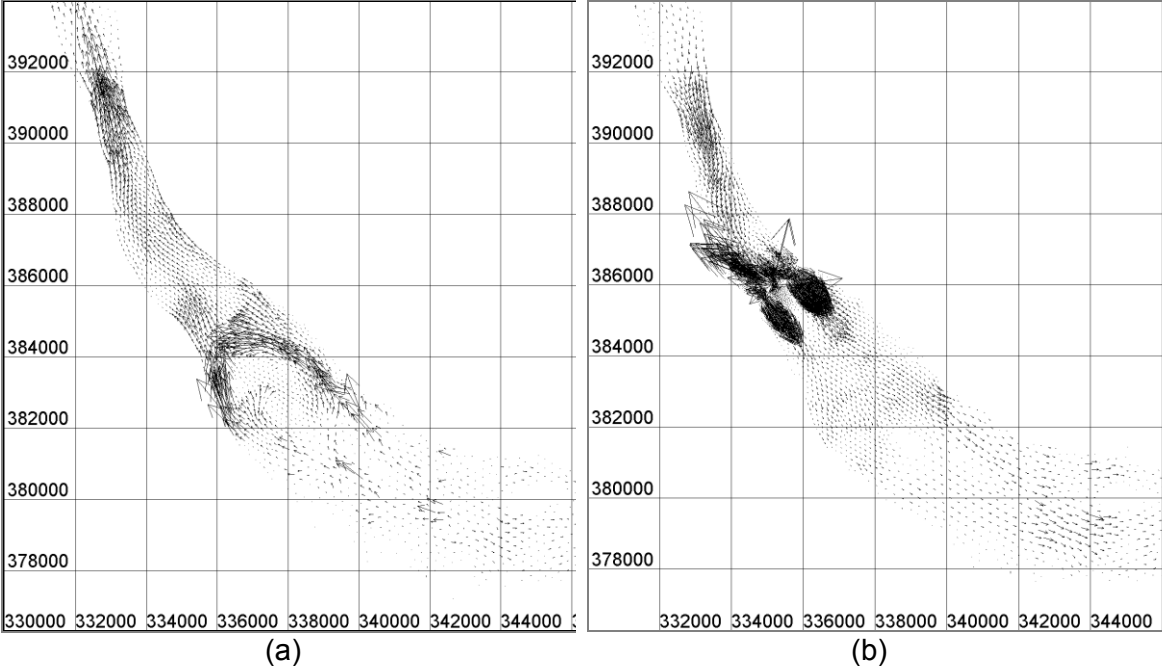


Figure 5.5.4: Comparison of bed-load residuals (a) in an open river and (b) with a barrage.

These features are also reflected in the net sediment transport through the Narrows, as shown in Table 5.5.1, in which the transport flux for open river conditions and with a barrage are compared. The reversed transport (the negative value under ‘Barrage’) suggests a change in the sediment regime as a result of barrage operation. However, the magnitude is

smaller than for the open estuary case. Given the uncertainty in estimating the instantaneous transport rates, the results should be considered with caution and require further substantiation. Indeed, many other factors are likely to complicate matters. For example, preliminary model tests also suggest that strong spatial sediment size variation can lead to reversed net transport across the entrance to the estuary; inclusion of offshore wave-induced littoral drift into the mouth of the estuary may also enhance the upstream transport (see Figure 5.5.5). These factors are expected to be particularly important to long-term changes in the morphology of the estuary. Therefore, further study is needed to develop understanding to a point where robust guidance can be provided on the matter of sedimentation associated with tidal barrage installations.

Table 5.5.1: Sediment transport rate in the Narrows integrated over a spring tide (range = 8.4m) and a neap tide (range = 4.6m) in both open estuary and barrage scenarios. The values are from the Port Advisory Service (1990) Mersey Barrage feasibility study and the present work.

Sediment	Tide	Open estuary		Barrage
		PAS (m <sup>3</sup> )	Modelled (m <sup>3</sup> )	Modelled (m <sup>3</sup> )
Sand	Spring	11627	8538	-2197
	Neap	930	957	431

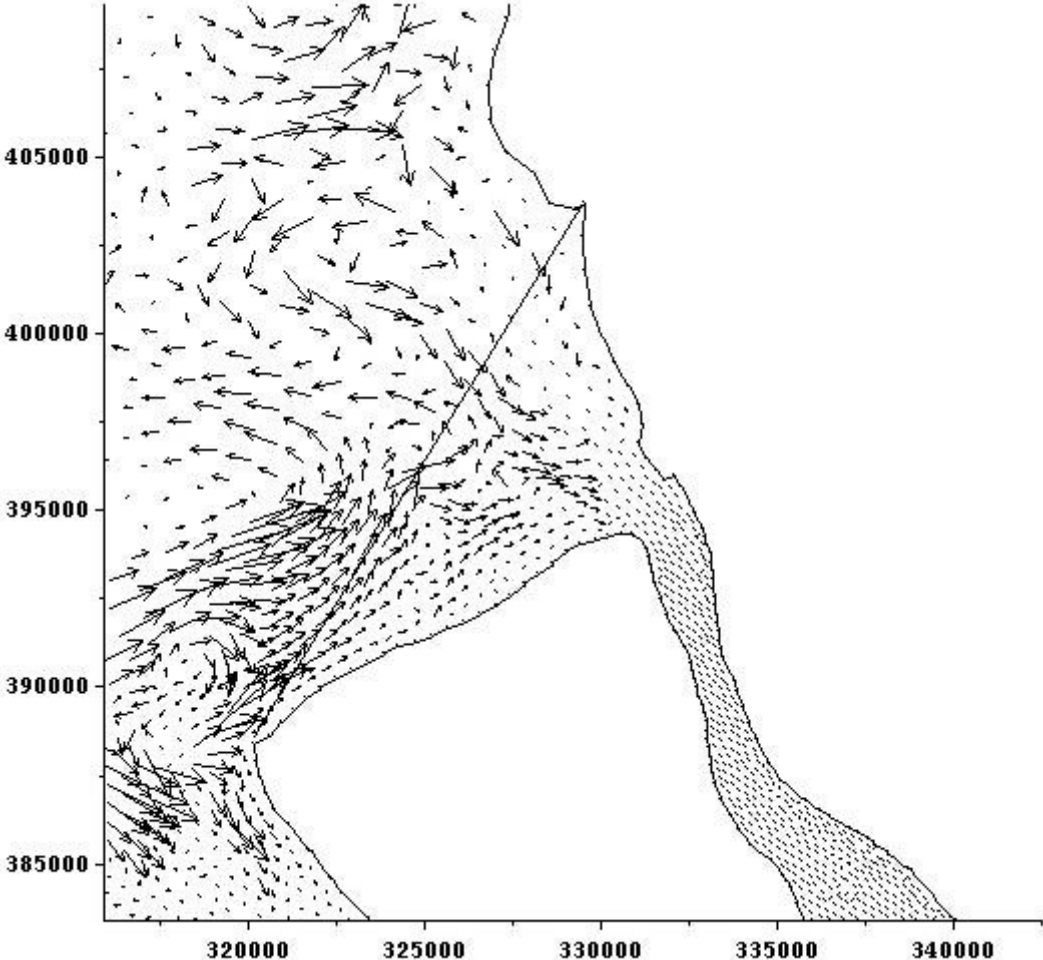


Figure 5.5.5: Bedload transport at the mouth of the Mersey Estuary due to waves with a significant height of 5m and from a dominant north-westly direction in Liverpool Bay.

## 5.6 Water quality issues from reduced exchange and sediment disturbance

### 5.6.1 Surface water quality

UK estuaries had been polluted to various degrees since the Industrial Revolution. Among them, the Mersey probably represented the worst case. It is instructive, therefore, to focus on the Mersey in considering the impacts of barrages.

The Mersey was much polluted, from the end of the 18th century until recently, both from industrial effluent and household sewage. A cleanup of the estuary started after the 1960s; and the Mersey Basin Campaign was established in 1985. Major wastewater collection and treatment schemes have now improved the water quality in the Mersey, as indicated by the dissolved oxygen distributions of Figure 5.6.1.1. Fish have now returned to the river (Jones, 2006). Nevertheless, there is still much industry and pressure from population. Harland et al (2000) found the upper estuary to be class D, which denotes bad water quality; the inner estuary and the Narrows were class C; and, due to tidal flushing, the outer estuary was class B (fair). Recent reports have discussed the effects of various pollutants on water quality (Hartnett et al, 2006, Huang, 2007; Johnson, 2008). This brief description of the history of the river highlights the problem of assessing changes due to a tidal barrage, as the present-day baseline has to be established and this is changing rapidly.

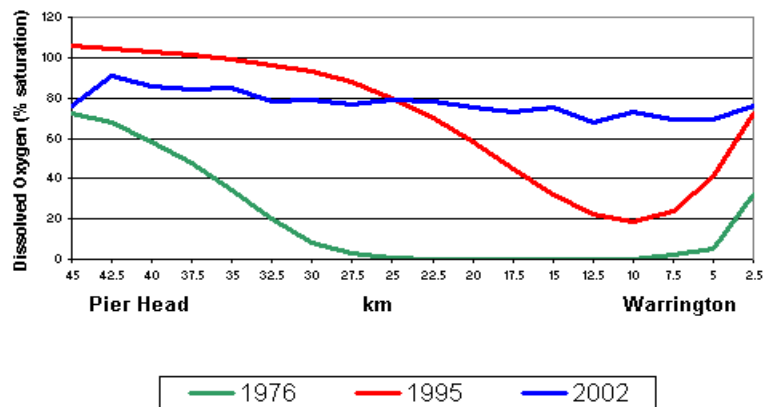


Figure 5.6.1.1: Typical dissolved oxygen levels in the Mersey Estuary (Source: North West Environment Agency Website).

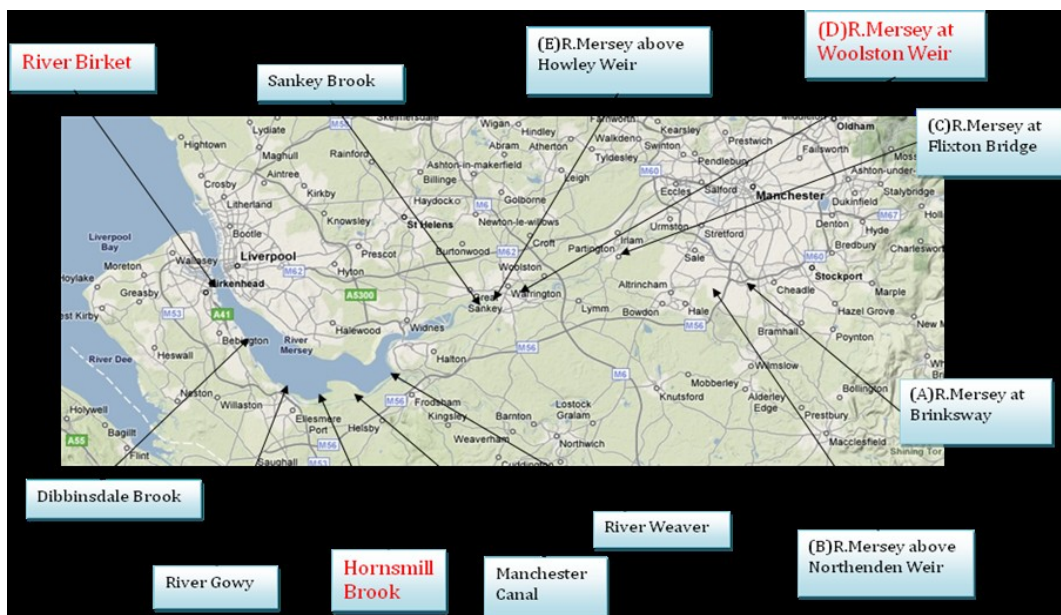


Figure 5.6.1.2: Sites around the Mersey for water quality data collection.

To gain further insight into the more recent surface water quality (WQ) status, investigations have been conducted to collect water quality data from the EA for various tributaries around the Mersey, as indicated in Figure 5.6.1.2. WQ parameters considered include pH, temperature, BOD, nitrogen (oxidized nitrogen – nitrites and nitrates, ammonia), suspended solids, hardness (calcium and magnesium), chloride ion, phosphate (organic and inorganic), copper, zinc, dissolved oxygen, etc. The EA's ecosystem classification scheme was then applied to the data and water quality ranged from RE3 to RE5, as shown in Table 5.6.1.1. The two sites with poor quality (RE5) are located outside of the areas influenced by the tide.

Table 5.6.1.1: The River Ecosystem Classification for 2007.

River/Location	Class
Mersey_A River Mersey at Brinksway	(2006) Re3 (fairly good quality)
Mersey_B River Mersey above Northenden Weir	Re4 (fair quality)
Mersey_C River Mersey at Flixton Road Bridge	Re4 (fair quality)
Mersey_D River Mersey at Woolston Weir	Re5 (poor quality)
Mersey_E River Mersey Above Howley Weir	Re3 (fairly good quality)
Sankey Brook at Dallam Bridge	Re4 (fair quality)
River Weaver above Sutton Weir	Re4 (fair quality)
River Weaver at Frodsham Road Bridge	Re4 (fair quality)
Hornsmill Brook D/S Works	(2006) Re5 (poor quality)
River Gowy above Folly Gates	Re3 (fairly good quality)
Dibbinsdale Brook below Railway Viaduct	Re4 (fair quality)
River Birket at Bidston Bridge	Re5 (poor quality)

As noted in Section 5.4.2, the Mersey Estuary is a macrotidal estuary with an industrialised catchment of about 5000km<sup>2</sup> and with a modal river flow of around 3.26 x 10<sup>6</sup> m<sup>3</sup>/day. The maximum spring tidal range is about 10.4m, giving the estuary a high spring tide volume of 6.5 x 10<sup>2</sup> Mm<sup>3</sup>. The neap tidal range is around 4m. As the daily river flow is only about 0.5% of the tidal volume, the tidal regime determines the flushing time of the estuary.

At present the total residence time for pollutants is about 32.4 days from Warrington to the estuary mouth (NRA, 1995). With a tidal barrage, the exchange will be reduced significantly and residence times will inevitably increase. The consequential change in water quality parameters will need to be investigated in detail. If there are any local problems, they might need to be resolved by enhancement to wastewater collection and treatment.

### 5.6.2 Contaminated sediments

Sediment contamination is a widespread environmental problem that can potentially pose threats to a variety of aquatic ecosystems. Sediment functions as a reservoir for common chemicals such as pesticides, herbicides, polychlorinated biphenyls (PCBs), polycyclic aromatic hydrocarbons (PAHs), and metals such as lead, mercury, and arsenic. Contaminated sediments may be directly toxic to aquatic life (organisms found in the water column and in or near the sediment) or can be a source of contaminants for bioaccumulation (where a substance is taken up by an organism) in the food chain.

In the past, fish had deserted the Mersey because of bad water quality. They have now started to return as a result of the improvement in water quality, evidenced by the sighting of salmon for the first time in many years in November 2001 and, subsequently, in an upper reach near Stockport in 2005. Nevertheless, health risks via bioaccumulation through the food chain are likely to increase. Therefore, the possible transport of the pollutants from contaminated sediments to human beings has become a real threat. The recent national consortium

EMPHASYS programme (EMPHASYS Consortium, 2000; Pye and Allen, 2000) has identified the contaminants locked-up in estuarine sediment and the effects on water quality if released back into the water column as major challenges for the next phase of UK estuary research.

The British Geological Survey (BGS) collected sediment samples from the Mersey between 2000 and 2002 and tested them for PAHs and PCBs (polychlorinated biphenyls). Some PAHs are toxic or carcinogenic. Sources include anode baking, vehicles and the general products of incomplete combustion. PAHs are also associated with petrogenic sources e.g. crude oil and coal deposits. Most common are fluoranthene, pyrene and benzo(a)pyrene (one of the products from smoking, known to be carcinogenic). They fall into the category of Persistent Organic Compounds (POPs) which cannot be degraded by chemical, biological or photolytic processes in the environment. They tend to accumulate in organic compounds, being of low solubility in water but high solubility in lipids (fatty acids and related substances).

In the environment, most PAHs are found in soil and sediment. The concentrations of PAHs in the Mersey range from 626 $\mu\text{g}/\text{kg}$  to 3766 $\mu\text{g}/\text{kg}$ , which is now better than some other industrialized UK estuaries (e.g. the Tyne, Wear and Tees in North East England) but worse than non-industrialised estuaries (e.g. the Solway Firth). The Rivers Orwell and Ouse are similar to the Mersey. The Mersey has higher concentrations than the Pearl River Estuary (one of the largest and most industrialized in China). This may be explained by the fact that the Mersey has experienced a longer history of pollution, and PAHs are associated with sediment deposits.

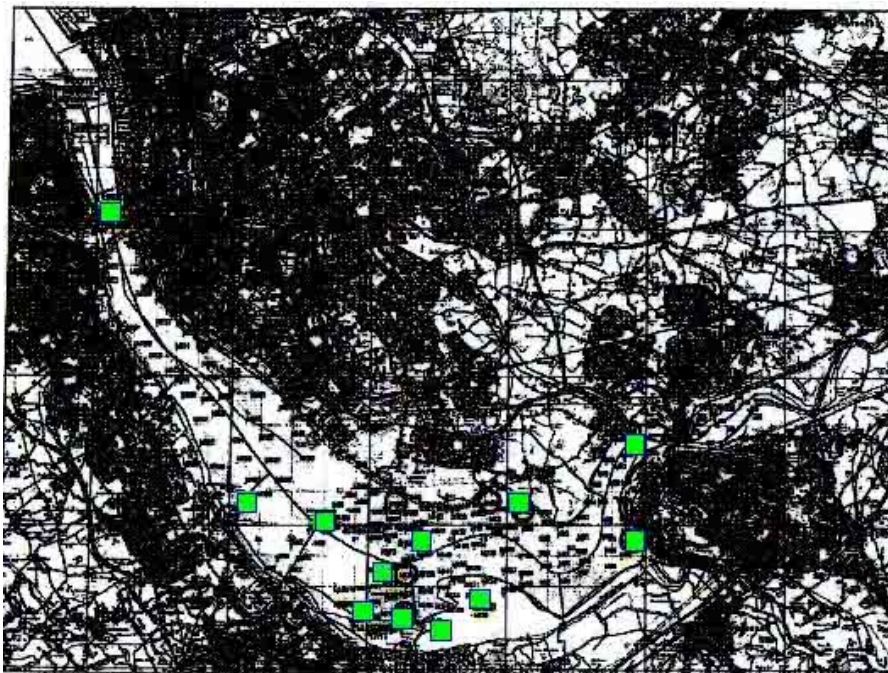


Figure 5.6.2.1: Sampling sites for sediment quality (indicated by green squares); British Geological Survey.

The highest concentration of PAHs in the Mersey is found near Ellesmere Port and the Manchester Ship Canal (Figure 5.6.2.1), with its high density of industry, including refineries. Other areas of high concentration are Birkenhead, Liverpool Airport and Widnes-Runcorn. Emissions are declining due to environmental legislation, but concentration in sediment persists from historic emissions. Through time (from sediment cores), PAH figures increased with industrialization until about 1968, especially during 1957-1968 (an increase possibly related to the Empress of Canada fire in Gladstone Dock in 1953). Values then dropped abruptly between 1968-1977, due to the economic recession and the introduction of

environmental legislation, which reduced the industrial pollution level by 30%. Total PAH concentration was found to exceed the sediment quality guidelines at 7% of the sample sites in the BGS survey of 2000-2002.

In the National Monitoring Programme Survey of the Quality of UK Coastal Waters (MPMMG, 1998), the highest fish liver PCB concentrations around UK coastal waters were found near Liverpool Bay, with a median value over 100µg/kg. In some of sediment quality assessments, concentrations ranged from 36 to 1,400µg/kg, compared to typical threshold-effect concentrations of between 30 and 200µg/kg, and typical probable-effect concentrations of between 240 and 5300µg/kg (MacDonald et al, 2000). Furthermore, Wright and Mason (1999) found that saltmarshes accumulated higher concentrations of most metals than general sediments; and remobilization of these previously consolidated sediments was considered responsible for significant perturbations in the overall reduction of the contamination level in the Mersey Estuary (Harland et al, 2000).

Tidal barrages, or other large scale tidal energy extraction systems, will inevitably cause significant morphological changes in an estuary. As a consequence, any contaminated sediments may be disturbed, with potential impacts to human health and the ecosystem.

## **5.7 Flood defence**

### **5.7.1 Flood risk in the estuaries and protection offered by barrages**

According to the National Appraisal of Assets at Risk from Flooding and Coastal Erosion (Halcrow, 2001), the total number of properties potentially at risk of sea/tidal flooding in the North West is around 125,000 (119,000 residential plus 6,000 commercial). In addition, there are 47,000 hectares of agricultural land potentially at risk. The capital value of these assets at the time of Halcrow's report in 2001 was £8.0 billion. Updating to 2008 by applying an escalation factor of  $4.13/3.41 = 1.21$  (Appendix A.2.5), the assets are now worth around £9.7 billion. The potential annual average damage from sea/tidal flooding in the North West, if nothing were done to prevent it, was estimated to be about £137 million in 2001 (£166 million in 2008). Note that much of the property at risk falls within the North West estuaries (see Figures 5.7.1.1 and 5.7.1.2).

A more recent report to the Environment Agency, North West Region, on tidal areas benefiting from defences in the Central Area (JBA Consulting, 2008) covered the coastline from Silverdale in the north to Crosby in the south. It included the rivers Keer, Lune, Conder, Wyre, Ribble, Darwen, Lostock, Yarrow, Douglas and Alt, together with a number of major urban settlements. The report aimed to map areas at risk of tidal flooding during a 0.5% (1 in 200) Annual Exceedance Probability (AEP) event and a 0.1% (1 in 1000) AEP event. The report identified approximately 22,360 properties within the 0.5% outline, whilst 34,000 properties lay within the 0.1% outline. Only about 18,700 of these properties fell within areas currently benefiting from coastal flood defences. Thus, it is clear that barrages across the major estuaries of the Eastern Irish Sea would reduce the threat to a large proportion of the properties and agricultural land at risk of tidal flooding in the North West.

Climate change, in raising sea levels and increasing the levels of storminess, is already having significant economic consequences with regard to flooding. Tidal flooding is particularly affected because it is sensitive both to changes in sea level and to wave conditions. As a result, the frequency of flooding along coasts and within estuaries is expected to increase significantly and the potential for breaching of defences will be raised (see Global Warming and Coastal Vulnerability, below).

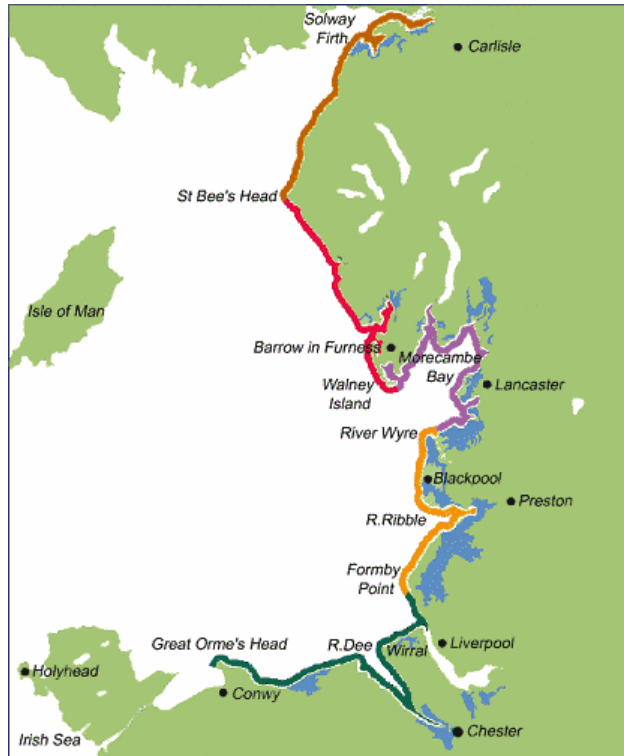
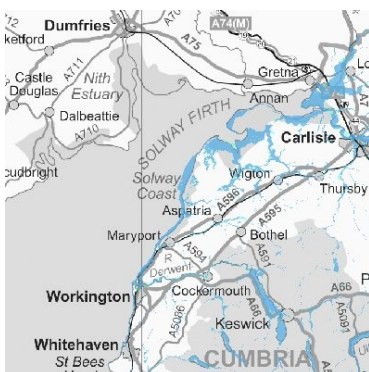


Figure 5.7.1.1: Areas (in blue) in North West England below highest recorded tide level.



(a)



(b)



(c)

There are two different kinds of area shown on the Flood Maps. They can be described as follows. Dark blue ■ shows the area that could be affected by flooding, either from rivers or the sea, if there were no flood defences. This area could be flooded:

from the sea by a flood that has a 0.5% (1 in 200) or greater chance of happening each year; or

from a river by a flood that has a 1% (1 in 100) or greater chance of happening each year.

Light blue □ shows the additional extent of an extreme flood from rivers or the sea. These outlying areas are likely to be affected by a major flood, with up to a 0.1% (1 in 1000) chance of occurring each year.

These two colours show the extent of the natural floodplain if there were no flood defences or certain other manmade structures and channel improvements.

Figure 5.7.1.2.: Environment Agency flood maps for (a) Solway Firth; (b) Morecambe Bay; and (c) Liverpool Bay.

Besides the properties at risk from sea/tidal flooding, Halcrow (2001) reports that there are 40,000 properties and 34,000 hectares of agricultural land in the North West potentially at risk from fluvial flooding, with a capital value in 2001 of £3.1 billion (£3.8 billion at 2008). In addition to reducing sea/tidal flooding, barrages might also be used to lessen fluvial flooding by managing water levels within barrage basins. However, the exact extent of the likely benefit cannot be established without detailed modelling of extreme river flow conditions.

Flood defences are expensive and, according to Halcrow (2001), they need to be replaced about once every 60 years. The average annual equivalent replacement costs (both at 2001 values and updated to 2008) are approximately as given in Table 5.7.1.1. In addition, flood defences attract maintenance costs. The construction of tidal barrages across estuaries would obviate the need to construct and to maintain many kilometres of flood defences in the North West. Figure 5.7.1.3 shows the current Shoreline Management Plans for the North West, indicating where the intention is to 'hold the line'.

Table 5.7.1.1: Average annual equivalent replacement costs of tidal and coastal flood defences.

Type	Cost in 2001 (£/km/yr)	Cost in 2008 (£/km/yr)
Fluvial flood defences	8,400	10,175
Tidal flood defences	10,300	12,475
Coastal flood defences	32,300	39,120

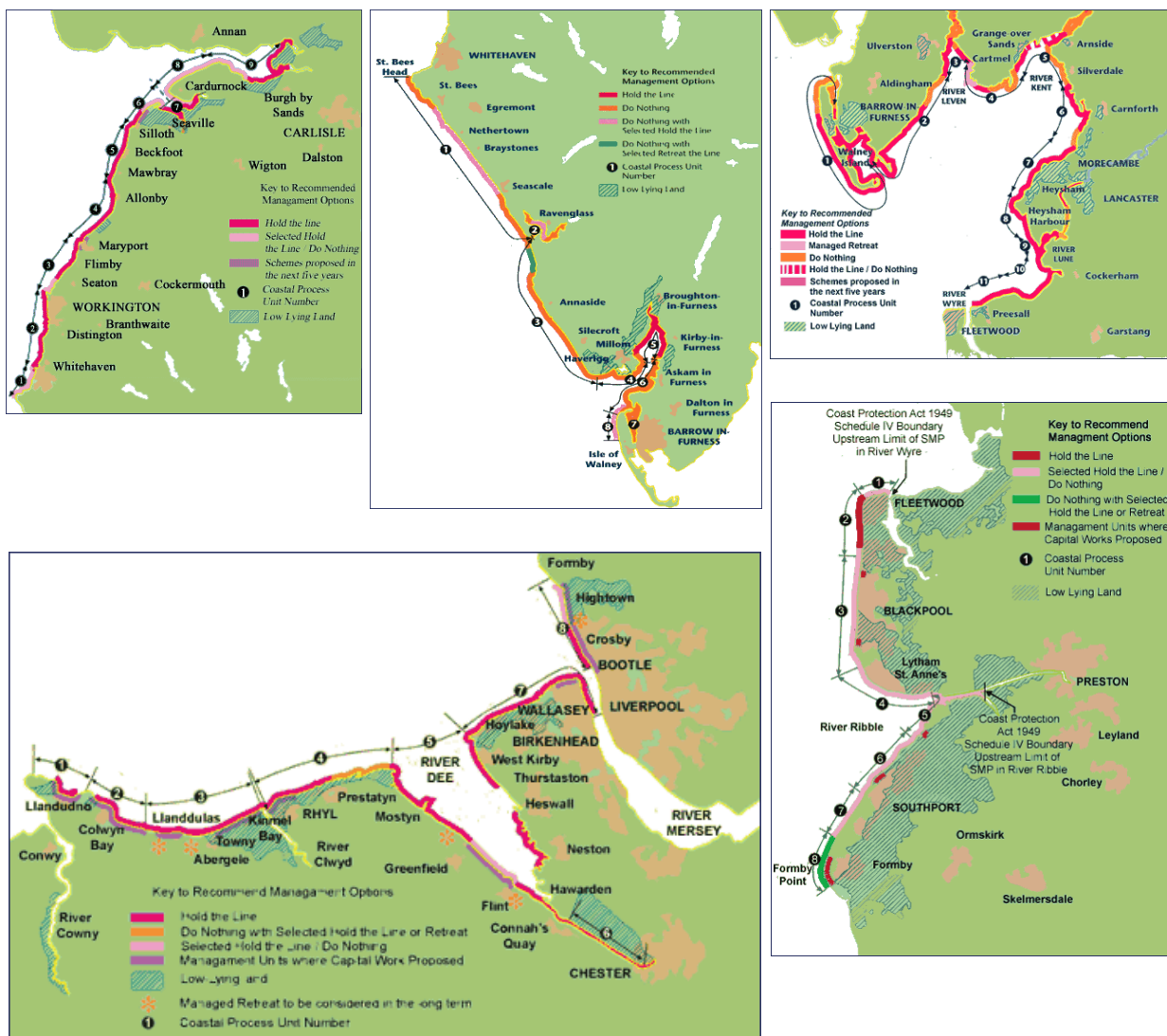


Figure 5.7.1.3: Current Shoreline Management Plans for the North West. (Note that maps are not all at the same scale. Source: <http://mycoastline.org>)

### 5.7.2: Global warming and coastal vulnerability

People who suffer from flooding are clearly subject to physical danger during the event. Many victims also describe the stress, disruption and unhappiness which they feel long afterwards. The storm of 31st January 1953, with an associated tidal surge of 3m in the North Sea, caused extensive flooding down the coast of Eastern England and was probably the UK's worst peace-time disaster. It resulted in the deaths of more than 300 people and about 30,000 were evacuated from their homes. Thousands of animals also drowned. Unfortunately, changes in our climate are resulting in rising sea levels and more severe storms, increasing the probability of coastal flooding of this severity (Lane et al, 2009).

Predicted future increases in global surface temperature and sea level are subject to considerable uncertainty. They are even greater at a regional level. Furthermore, whilst more confidence can be attached to changes in the mean values of climate parameters than to changes in extremes, it is the extreme conditions which are of greatest significance when assessing coastal vulnerability. To add to the difficulties, overtopping of flood defences may result from extreme water levels combined with moderate wave conditions or more normal water levels combined with extreme waves. Thus, the doubts associated with each parameter are magnified when considering the probability of occurrence of particular combinations. For these and other reasons, any predictions must be treated with caution.

Sutherland and Wolf (2002) assess the possible changes in coastal defence vulnerability to wave overtopping or beach erosion caused by global climate change to the year 2075. The results are not site specific but generic: simplified bathymetries and typical structure types were used to provide results broadly representative of stretches of coastline, rather than for specific locations. Changes in wave climate around the UK are predicted to be small (generally less than 5% for wave height) and the predicted increase in future extreme water levels is generally within 20% of the increase in mean sea level.

The report suggests that a sea level rise of 0.35m would cause average increases in wave overtopping volumes, if present day defences are unchanged by 2075, of between about 50% and 150%, depending on structure type. A continuation of the observed coastal steepening would add about a further 15%. In addition, there would be implications for damage to the flood defences themselves and to coastal sediment movements in both long-shore and cross-shore directions. In most cases, the simulated future mean annual long-shore transport rates are slightly greater than the present day rates by an average of around 15%.

JBA Consulting (2008) also report on the impact of climate change on the potential extent of flooding in the North West, in this case for the Central Area. The 'climate change outlines', corresponding to a 0.5% AEP tidal flood event in 2115 are considerably more extensive than the 'present day' outlines. The largest increases are in the flat, low-lying agricultural areas, but there are also significant increases in urban areas, most notably in North Morecambe and Cleveleys. Significant increases are also indicated for Lancaster, Fleetwood and Southport.

### 5.7.3 Conclusion

Barrages across the North West estuaries would eliminate the threat from tidal flooding for a large proportion of the 125,000 properties and 47,000 hectares of agricultural land at risk at present. In addition to reducing sea/tidal flooding, barrages might also be used to lessen fluvial flooding by managing water levels within barrage basins. Furthermore, coasts are vulnerable to the impacts of global warming. Barrages across estuaries and bays would shorten considerably the lengths of exposed coastline to be protected. In addition, a reduction in wave activity in the lees of barrages could lead to environmental improvements, for example in the growth and stability of saltmarshes, which are also valuable for the purposes of coastal defence.

## 6. CONCLUSIONS AND RECOMMENDATIONS

### 6.1 Conclusions

1. Barrages on the Solway Firth, Morecambe Bay, Mersey and Dee, operating in ebb-only generation with 1xDoEn turbine provision could meet about 5% of UK demand. With further scheme optimisations and refined representation of pumping efficiencies, a figure close to 6% might be achieved. Based on the scale of the North West's economy at approximately 12% of the UK total, this energy capture should supply about half the North West's present electricity needs.
2. In economic terms, this study has shown that the North West schemes should be no more than 70% more expensive in unit cost of energy produced when compared to that achievable from the Severn with, in each case, lowest costs arising from installations consistent with the Department of Energy's 1980s studies (1xDoEn turbine installations).
3. Increasing turbine provision substantially (to up to 3 times the default provision) would increase energy capture and enable retention of more of the intertidal area in the estuarial basin, so alleviating some of the environmental concerns, but at extra cost of electricity produced.
4. 2-D modelling significantly alters the energy predictions from the 0-D modelling, so demonstrating the necessity of the more rigorous approach.
5. As a consequence of 4 above, further investigation is required to determine how much of the substantial energy increases predicted from 0-D modelling of 3xDoEn installations can be realised in the 2-D modelling. Presently, only about a 20% enhancement has been achieved, in part because of the reduction of tidal amplitudes at the barrage locations.
6. Whilst power production between the North West estuaries and the Severn is fully complementary in ebb-mode operation, dual-mode (two-way) operation would give rise to synchronised and higher peak power pulses for the electricity grid to handle.
7. Earlier studies (DoEn/CEGB/STPG, 1989) reported the potential for an outer line for the Severn barrage producing an additional 6.80TWh/year and barrages on the Wash, Humber and Thames capable of yielding 3.75, 1.65 and 1.37TWh/year, respectively (UKAEA, 1980). Combining these with the 33TWh/year obtained herein for the North West barrages and the Cardiff-Weston Severn barrage scheme (for similar 1xDoEn ebb-mode operation) would achieve a total of about 46.5TWh/year. This should be capable of uplift to around 50TWh/year by addition of positive head pumping, representing 13% of the UK (2005) electricity consumption of 387TWh/year.
8. Further energy capture from other small barrage schemes in estuaries or embayments (DoEn, 1989, Anderson, 2008) should enable tidal range energy extraction to meet 15% of UK electricity consumption.
9. Adding an extractable UK tidal stream resource of about 5% (SDC, 2007), would uplift the potential for tidal energy to meet up to 20% of the nation's (present) electricity consumption.
10. Outline studies have been conducted to investigate modest tidal stream generator array deployments, as a demonstration of this capability, within the domain of the 2-D ADCIRC model developed in this project.

## 6.2 Recommendations

1. Further optimisations of the barrage configurations and operational controls (i.e. chosen time delays and the use of pumping) are called for in the 2-D modelling studies, to obtain robust estimates of potential maximum energy capture, under both ebb-only and dual-mode generation and for up to 3xDoEn turbine installations.
2. Barrage schemes should be introduced individually in the 2-D modelling to identify the influence of each on changes to the tidal regime in the Irish Sea.
3. Further refinement of the ADCIRC modelling routines is required to better explain the tendency for occasional instability and to suppress occasional aberration in its outputs.
4. Sediment transport should be incorporated into the ADCIRC modelling routines to enable a better understanding of the likely morphological changes, both in the near vicinity of the barrage installations and in the far field.
5. Further study on barrages is called for in respect of proactive management of extreme fluvial flows to reduce flood risk in the lower river reaches.
6. The full potential of tidal-stream farm resources in the domain of the Irish Sea warrants more extensive investigation.
7. The operation of the electricity grid under the injection of large power pulses (~ 10GW) from these potential tidal resources requires urgent consideration.
8. Alternative turbine technologies, including single-regulated bulb units and possible 'fence' or 'reef' systems, could be incorporated in both the 0-D and 2-D ADCIRC modelling systems to investigate their behaviour.

## 7. REFERENCES AND BIBLIOGRAPHY

- AEA Technology, 2006. Tidal Lagoon Power Generation Scheme in Swansea Bay: a report on behalf of the Department of Trade and Industry and the Welsh Development Agency, <<http://www.berr.gov.uk/files/file30617.pdf>>.
- Aldridge JN, 1997. 'Hydrodynamic model predictions of tidal asymmetry and observed sediment transport paths in Morecambe Bay', *Estuarine, Coastal and Shelf Science*, 44, 39–56.
- Anderson S, 2008. The Resurgam Project: feasibility study brief for a pilot commercial offshore tidal energy storage and release (TESAR) scheme and exhibition centre on the North Wales coast, e-mail: <[clr.dr.stuart.anderson@conwy.gov.uk](mailto:clr.dr.stuart.anderson@conwy.gov.uk)>.
- Aubry A and Elliott M, 2006. 'The use of environmental integrative indicators to assess seabed disturbance in estuaries and coasts: application to the Humber Estuary, UK', *Marine Pollution Bulletin*, 53(1-4), 175-185.
- Baker AC, 1986. 'The development of functions relating cost and performance of tidal power schemes and their application to small-scale sites', in *Tidal Power*, Thomas Telford Ltd, London, 331-344.
- Baker AC, 1991. *Tidal Power*, Institution of Electrical Engineers Energy Series 5, Peter Peregrinus Ltd, London.
- Blott SJ, Pye K, van der Wal D and Neal A, 2006. 'Long-term morphological change and its causes in the Mersey Estuary, NW England', *Geomorphology*, 81(1-2), 185-206.
- Boesch DF and Paul JF, 2001. 'An overview of coastal environmental health indicators', *Human and Ecological Risk Assessment*, 7, 1409-1417.
- Burrows R, Walkington IA, Yates NC, Hedges TS, Li M, Zhou JG, Chen DY, Wolf J, Holt J and Proctor R, 2009. 'Tidal energy potential in UK waters', *Proceedings of the Institution of Civil Engineers, Maritime Engineering* (in press).
- Burrows R, Walkington IA, Yates NC, Hedges TS, Li M, Zhou JG, Wolf J, Holt J, Proctor R and Prandle D, 2009. 'Tidal power from the estuaries of NW England', *Proceedings of Conference on Coasts, Marine Structures and Breakwaters 2009*, Edinburgh, Institution of Civil Engineers, Thomas Telford Ltd, London (in press).
- Burrows R, Walkington IA, Yates NC, Hedges TS, Wolf J and Holt J, 2009. 'The tidal range energy potential of the west coast of the United Kingdom', *Applied Ocean Research* (in press).
- Carroll B, Li M, Pan S, Wolf J and Burrows R, 2008. 'Morphodynamic impacts of a tidal barrage in the Mersey Estuary', *Proceedings of 31st International Conference on Coastal Engineering*, Hamburg, World Scientific Publishing Company, 2743-2755.
- Cottillon J, 1978. 'La Rance tidal power station – review and comments', *Proceedings of Colston Symposium on Tidal Energy*, Bristol, Sciencetchnia, 46-66.
- Department for Business, Enterprise and Regulatory Reform (BERR), 2008. *Severn Tidal Power Feasibility Study: Strategic Environmental Assessment*, April, <[www.berr.gov.uk/files/file46064.pdf](http://www.berr.gov.uk/files/file46064.pdf)>.
- Department of Energy (DoEn), 1981. *Tidal Power From the Severn Estuary*, Energy Paper No. 46, HMSO, London.
- Department of Energy (DoEn), 1989. *The UK Potential for Tidal Energy from Small Estuaries*, ETSU TID 4048-P1, Binnie & Partners, London.

- Department of Energy (DoEn), Central Electricity Generating Board (CEGB) and Severn Tidal Power Group (STPG), 1989. The Severn Barrage Project: General Report, Energy Paper Number 57 (EP57), HMSO, London.
- Department of Trade and Industry (DTI), 2004. Atlas of Marine Renewable Energy Resources: Technical Report, Report No. R1106, ABP Marine Environmental Research Ltd, Southampton.
- Dyer KR and Huntley DA, 1999. 'The origin, classification and modelling of sand banks and ridges', *Continental Shelf Research*, 19, 1285-1330.
- Elliott M, Boyes SJ and Burdon D, 2006. 'Integrated marine management and administration for an island state—the case for a new Marine Agency for the UK', *Marine Pollution Bulletin*, 52, 469-474.
- EMPHASYS Consortium, 2000. A Guide to Prediction of Morphological Change within Estuarine Systems: Version 1B, Report TR 114, Ministry of Agriculture, Fisheries and Food, Environment Agency and English Nature <[http://www.estuary-guide.net/pdfs/emphasys\\_guide.pdf](http://www.estuary-guide.net/pdfs/emphasys_guide.pdf)>.
- Fells Associates, 2008. A Pragmatic Energy Policy for the UK, <[www.fellsassociates.com](http://www.fellsassociates.com)>.
- Fong SW and Heaps NS, 1978. Note on Quarter-Wave Tidal Resonance in the Bristol Channel, Report No. 63, Institute of Oceanographic Sciences, Wormley.
- Frau JP, 1993. 'Tidal energy: promising projects - La Rance – a successful industrial scale experiment', *Institute of Electrical and Electronics Engineers, IEEE Transactions on Energy Conversion*, 8(3), 552-558.
- Gordon DC, 1994. 'Intertidal ecology and potential power impacts, Bay of Fundy, Canada', *Biological Journal of the Linnean Society*, 51, 17-23.
- Gray A (ed.), 1992. The Ecological Impact of Estuarine Barrages, *Ecological Issues*, No. 3, British Ecological Society, Field Studies Council, Shrewsbury.
- Halcrow, 2001. National Appraisal of Assets at Risk from Flooding and Coastal Erosion, Including the Potential Impact of Climate Change, Department for Environment, Food and Rural Affairs.
- Hammons TJ, 1993. Tidal Power, *Proceedings of the Institute of Electrical and Electronics Engineers*, 81(3), 419-433.
- Hao W, Jian S, Ruijing W, Lei W and Yi'an L, 2003. 'Tidal front and the convergence of anchovy (*Engraulis japonicus*) eggs in the Yellow Sea', *Fisheries Oceanography*, 12(4-5), 434-442.
- Harland BJ, Taylor D and Wither A, 2000. 'The distribution of mercury and other trace metals in the sediments of the Mersey over 25 years: 1974-1998', *The Science of the Total Environment*, 253, 45-62.
- Hartnett M, Lin B, Jones PD and Berry A, 2006. 'Modelling the fate and transport of nickel in the Mersey Estuary', *Journal of Environmental Science and Health, Part A*, 41, 825-847.
- Hench JL and Luettich RA, 2003. 'Transient tidal circulation and momentum balances at a shallow inlet', *Journal of Physical Oceanography*, 33, 913-932.
- Hervouet J-M and Bates P, 2000. 'The Telemac modelling system', *Special Issue of Hydrological Processes*. 14(13): 2207-2364.
- Hillairet P and Weisrock G, 1986. 'Optimizing production from the Rance tidal power station', *Proceedings 3rd International Symposium on Wave, Tidal, OTEC, and Small Scale Hydropower*, Brighton, 165-177.

- Hodd SL, 1977. 'Environmental considerations of a Fundy tidal power project', in *Fundy Tidal Power and the Environment*, Proceedings of a Workshop on the Environmental Implications of Fundy Tidal Power, Wolfville, Nova Scotia, 71-81.
- Holt JT, Allen JI, Proctor R and Gilbert F, 2005. 'Error quantification of a high-resolution coupled hydrodynamic-ecosystem coastal-ocean model: Part 1 model overview and assessment of the hydrodynamics', *Journal of Marine Systems*, 57, 167-188.
- House of Commons, 2008. *Renewable Electricity-Generation Technologies*. Innovation, Universities, Science and Skills Committee Report, Volume II, HC 216-II, Memorandum 4, Ev 86-91, The Stationery Office, London.
- Huang H, 2007. 'Sources and distribution of polycyclic aromatic hydrocarbons (PAHs) in sediments from the Mersey Estuary', University of Liverpool, Department of Engineering, MRes thesis.
- Huthnance JM, 1982. 'On one mechanism forming linear sandbanks', *Estuarine and Coastal Marine Science* 14, 79-99.
- JBA Consulting, 2008. *Central Area Tidal Areas Benefiting from Defences: Main Assessment Report*, Environment Agency, North West Region.
- Johnson S, 2008. 'Investigating of the Environmental Impact for a Tidal Barrage in the Mersey Estuary: Water Quality', Final Year Project Thesis, Department of Engineering, University of Liverpool.
- Jones JE and Davies AM, 2007a. 'A high-resolution finite element model of the  $M_2$ ,  $M_4$ ,  $M_6$ ,  $S_2$ ,  $N_2$ ,  $K_1$  and  $O_1$  tides off the west coast of Britain', *Ocean Modelling*, 19(1-2), 70-100.
- Jones JE and Davies AM, 2007b. 'On the sensitivity of tidal residuals off the west coast of Britain to mesh resolution', *Continental Shelf Research*, 27(1), 64-81.
- Jones JE, Hall P and Davies AM, 2008. 'An intercomparison of tidal solutions computed with a range of unstructured grid models of the Irish and Celtic Sea regions', *Ocean Dynamics* (in press).
- Jones PD, 2006. 'Water quality and fisheries in the Mersey Estuary, England: a historical perspective', *Marine Pollution Bulletin*, 53, 144-154.
- Kirby R and Retiere C, 2007. 'Comparisons between environmental and water quality issues at the tidal power scheme at La Rance, France and those expected in the Severn Estuary, UK', Unpublished Manuscript.
- Kirby R and Retiere C, 2008. 'Comparing environmental effects of Rance and Severn barrages', *Proceedings of the Institution of Civil Engineers, Maritime Engineering*, 162, MA1, 11-26.
- Kirby R and Shaw TL, 2005. 'Severn Barrage, UK – environmental reappraisal', *Proceedings of the Institution of Civil Engineers, Engineering Sustainability*, 158, ES1, 31-39.
- Kirby R, 1987. 'Changes to the fine sediment regime in the Severn Estuary arising from two current barrage schemes', in *Tidal Power*, Proceedings of Symposium, Institution of Civil Engineers, Thomas Telford Ltd, London, 221-234.
- Lane A, 2004. 'Bathymetric evolution of the Mersey Estuary, UK, 1906–1997: causes and effects', *Estuarine, Coastal and Shelf Science*, 59(2), 249-263.
- Lane A, Hu K, Hedges TS and Reis MT, 2009. *New north east of England tidal flood forecasting system*, Proceedings of the European Conference on Flood Risk Management Research into Practice (FLOODrisk 2008), Oxford, CRC Press, 1377-1387.

- Leuttich RA and Westerink JJ, 1995. 'Continental shelf scale convergence studies with a barotropic tidal model', in Quantitative Skill Assessment for Coastal Ocean Models (Lynch DR and Davies AM, eds.), American Geophysical Union, 349-411.
- MacDonald DD, Ingersoll CG and Berger TA, 2000. 'Development and evaluation of consensus-based sediment quality guidelines for freshwater ecosystems', Archives of Environmental Contamination and Toxicology, 39, 20-31.
- Marine Pollution Monitoring Management Group (MPMMG), 1998. First Report of the Marine Pollution Monitoring Management Group, UK National Marine Monitoring Programme, Defra.
- Matthews ME and Young RM, 1992. 'Environmental impacts of small tidal power schemes', in Tidal Power: Trends and Developments, Proceedings of the 4th Conference on Tidal Power, Institution of Civil Engineers, Thomas Telford Ltd, London, 197-214.
- Mersey Barrage Company, 1992. Tidal Power from the River Mersey: A Feasibility Study Stage III, MBC.
- Mersey Barrage Company, 1993. Tidal Power from the River Mersey: A Feasibility Study Stage IIIa, MBC.
- Miles GV, 1982. 'Impact on currents and transport processes'. in Severn Barrage, Proceedings of Symposium, Institution of Civil Engineers, Thomas Telford Ltd, London, 59-64.
- Ministry of Agriculture, Fisheries and Food (MAFF), 2000. Flood and Coastal Defence Project Appraisal Guidelines: Environmental Appraisal, MAFF Publications, <[www.maff.gov.uk](http://www.maff.gov.uk)>.
- Möller I and Spencer T, 2002. 'Wave dissipation over macro-tidal saltmarshes: effect of marsh edge typology and vegetation change', Journal of Coastal Research, Special Issue 36, 506-521.
- Möller I and Spencer T, 2003. 'Wave transformations over mudflat and saltmarsh surfaces on the UK East coast - implications for marsh evolution', Proceedings of the International Conference on Coastal Sediments '03, Florida, CD-ROM.
- National Rivers Authority (NRA), 1995. The Mersey Estuary: A Report on Environmental Quality, Almondsbury.
- O'Connor BA, 1987. 'Short and long term changes in estuary capacity', Journal of the Geological Society, 144(1), 187-195.
- Odd NVM, 1982. 'The feasibility of using mathematical models to predict sediment transport in the Severn Estuary', in Severn Barrage, Proceedings of Symposium, Institution of Civil Engineers, London, Thomas Telford Ltd, London, 195-202.
- Parker WR and Kirby R, 1982. 'Sources and transport of sediment in the inner Bristol Channel and Severn Estuary' in Severn Barrage, Proceedings of Symposium, Institution of Civil Engineers, London, Thomas Telford Ltd, London, 181-194.
- Pingree RD and Griffiths DK, 1979. 'Sand transport paths around the British Isles resulting from M2 and M4 tidal interactions', Journal of Marine Biological Association of the United Kingdom, 59(2), 497-513.
- Pingree RD and Maddock L, 1979. 'The tidal physics of headland flows and offshore tidal bank formation', Marine Geology, 32, 269-289.
- Pingree RD, Holligan PM, Mardell GT and Head RN, 1976. 'Influence of physical stability on spring, summer and autumn phytoplankton blooms in Celtic Sea', Journal of the Marine Biological Association of the United Kingdom, 56(4), 845-873.

- Port Advisory Services, 1990. Review Feasibility Study: Mersey Barrage, Port Advisory Services B.V., Delft.
- Prandle D, 1984. 'Simple theory for designing tidal power schemes', *Advances in Water Resources*, CML Publications, 7, 21-27.
- Price WA and Kendrick MP, 1963. 'Field and model investigation into the reasons for siltation in the Mersey Estuary', *Proceedings of the Institution of Civil Engineers*, 24, 473-517.
- Proctor R, 1981. 'Mathematical modelling of tidal power schemes in the Bristol Channel', *Proceedings 2nd BHRA International Symposium on Wave and Tidal Energy*, Cambridge, England, 33-51.
- Pye K and Allen JRL, 2000. 'Past, present and future interactions, management challenges and research needs in coastal and estuarine environments', *Coastal and Estuarine Environments: Sedimentology, Geomorphology and Geoarchaeology*, Geological Society, Special Publications, 175, 1-4.
- Radford PJ, 1982. 'The effects of a barrage on water quality', in *Severn Barrage, Proceedings of Symposium*, Institution of Civil Engineers, Thomas Telford Ltd, London, 203-208.
- RSK Environmental Ltd, 2007. Mersey Tidal Power Study: an Exploration of the Potential for Renewable Energy, Full report, <[www.merseytidalpower.co.uk](http://www.merseytidalpower.co.uk)>.
- Sharples J, 2008. 'Potential impacts of the spring-neap tidal cycle on shelf sea primary production', *Journal of Plankton Research*, 30(2), 183-197.
- Shaw TL and Watson MJ, 2003. 'The effects of pumping on the energy potential of a tidal power barrage', *Proceedings of the Institution of Civil Engineers, Engineering Sustainability*, 156, ES2, 111-117.
- Shaw TL, 1980. *An Environmental Appraisal of Tidal Power Stations: with Particular Reference to the Severn Barrage*, Pitman Advanced Publishing Program, London.
- Shaw TL, 1990. 'Ecological aspects of the Severn barrage', in *Developments in Tidal Energy, Proceedings of the 3rd Conference on Tidal Power*, Institution of Civil Engineers, Thomas Telford Ltd, London, 245-262.
- Simpson JH and Hunter JR, 1974. 'Fronts in the Irish Sea', *Nature*, 250, 404-406.
- Soulsby R, 1997. *Dynamics of Marine Sands*, Thomas Telford Ltd, London.
- Sustainable Development Commission (SDC), 2007. *Turning the Tide: Tidal Power in the UK*, Sustainable Development Commission, London, <[www.sd-commission.org.uk](http://www.sd-commission.org.uk)>.
- Sutherland J and Wolf J, 2002. *Coastal Defence Vulnerability 2075*, Report SR 590, HR Wallingford.
- Thomas CG, Spearman JR and Turnbull MJ. 2002. 'Historical morphological change in the Mersey Estuary', *Continental Shelf Research*, 22, 1775-1794.
- Towner JV, 1990. 'Environmental impacts of a Mersey tidal project', in *Developments in Tidal Energy, Proceedings of the 3rd Conference on Tidal Power*, Institution of Civil Engineers, Thomas Telford Ltd, London, 263-274.
- United Kingdom Atomic Energy Authority (UKAEA), 1980. *Preliminary Survey of Tidal Energy of UK Estuaries*, Severn Tidal Power Report STP-102, Binnie & Partners, London.
- United Kingdom Atomic Energy Authority (UKAEA), 1984. *Preliminary Survey of Small Scale Tidal Energy*, Severn Tidal Power Report STP-4035 C, Binnie & Partners, London.
- Walkington I and Burrows R, 2009. 'Modelling tidal stream power potential', *Applied Ocean Research* (in press).

- Watson MJ and Shaw TL, 2007. 'Energy generation from a Severn barrage prior to full commissioning', Proceedings of Institution of Civil Engineers, Engineering Sustainability, 160, ES1, 35-39.
- Wolf J, 2003. Parametric Modelling of Waves in Liverpool Bay and Dee Estuary, Internal Document No. 162, Proudman Oceanographic Laboratory, Liverpool.
- Wolf J, 2004. Wave Modelling for the Blackwater Estuary, Internal Document No. 167, Proudman Oceanographic Laboratory, Liverpool.
- Wolf J, Walkington IA, Holt J and Burrows R, 2009. 'Environmental impacts of tidal power schemes', Proceedings of the Institution of Civil Engineers, Maritime Engineering (in press).
- Wright P and Mason CF, 1999. 'Spatial and seasonal variation in heavy metals in the sediments and biota of two adjacent estuaries, the Orwell and the Stour, in eastern England', The Science of the Total Environment, 226(2-3), 139-156.

# **Tapping the Tidal Power Potential of the Eastern Irish Sea**

## **APPENDIX 1**

comprising three separate documents:

- A.1.1 The research team
- A.1.2 House of Commons evidence
- A.1.3 Tidal stream energy extraction from estuaries

**March 2009**

**[www.liv.ac.uk/engdept/tidalpower](http://www.liv.ac.uk/engdept/tidalpower)**

### **A.1.1 The research team**

The Maritime Engineering and Water Systems Research Group at the University of Liverpool has for many years been involved in national and international research projects, studying coastal hydrodynamics and morphodynamics and using both large-scale laboratory facilities and advanced process-based numerical models.

The Proudman Oceanographic Laboratory has world-class expertise and is internationally known for research on tides, coastal oceanography and numerical modelling. It hosts the British Oceanographic Data Centre (BODC) and the Permanent Service for Mean Sea Level (PSMSL).

## A.1.2 House of Commons evidence



Science and Technology Committee  
Committee Office  
House of Commons  
7 Millbank  
London SW1P 3JA

### INQUIRY INTO RENEWABLE ENERGY GENERATION TECHNOLOGIES

Submitting Organisation: The University of Liverpool, Department of Engineering,  
Brownlow Street, Liverpool L69 3GQ

Contact person:

Professor Richard Burrows,

Maritime Environmental and Water Systems Research Group

tel/fax: 0151-794-5235/5218; e-mail: r.burrows@liv.ac.uk

**Executive Summary:** This submission aims to bring back to full attention the substantial potential role of tidal barrage solutions for renewable energy generation in the UK. It is demonstrated here that installations on as few as 8 major estuaries should be capable of meeting 10-12% of present electricity demand (possibly over 15% with a more ambitious scheme on the Severn) this employing fully proven technology. This far exceeds the potential of tidal 'stream' turbine or practicable 'lagoon' systems much vaunted by funding agencies over recent times. It also brings attention to an ongoing study investigating the tidal power potential in the North West of England.

#### ***Tapping the UK Tidal Power Potential***

1. The medium to long-term procurement of energy and the related issue of climate change is set to remain at the top of government and public agendas, both nationally and internationally, for some time to come. No clear vision has yet emerged for a sustainable global energy future and the combination of rapid growth in both economies and populations in the developing world are set to place extreme pressure on fossil fuel reserves. It seems inevitable, therefore, that as the 21<sup>st</sup> century evolves, ever greater utilisation of renewable energy resources must be made if the means for modern living are to be preserved. From the perspective of the global community, it is argued that it will ultimately become an obligation for all societies to properly and fully exploit the natural energy resources at their disposal for the common good.

2. The geographical location of the United Kingdom and the seas that surround it provide internationally enviable renewable resources. Technologies for wind power extraction are now mature and an increasing role for the opportunistic capture of this intermittent energy source for the electricity grid is firmly established. Marine wave energy offers even greater scope for the future with a somewhat lower degree of unpredictability but with necessary technological advances still outstanding at present. Even more exclusive, however, is the potential for tidal energy extraction from around the UK coastline. The most attractive locations for harnessing tidal power are estuaries with a high tidal range for barrages and other areas with large tidal currents (e.g. straits and headlands) for free-standing tidal stream turbines. Pertinent here is the fact that tidal barrage solutions, drawing on established low-head hydropower technology, are fully proven. The La Rance scheme in France is now in its 39<sup>th</sup> year of operation (Cottillon, 1978; Pierre, 1993).
3. Of about 500-1000TWh/year of energy potentially available worldwide (Baker 1991), Hammons (1993) estimated the UK to hold 50TWh/year, representing 48% of the European resource, and few sites worldwide are as close to electricity users and the transmission grid as those in the UK. Following from a series of government funded studies commissioned by UKAEA in the 1980s, Rufford (1986) identified 16 UK estuaries where tidal barrages would be capable of procuring 44TWh/year and Baker (1986) identified further sites suitable for small-scale installations. In fact the bulk of this energy yield would accrue from 8 major estuaries, in rank order of scale, the Severn, Solway Firth, Morecambe Bay, Wash, Humber, Thames, Mersey and Dee (see also Baker, 1991).
4. In the context of the future UK energy mix, it is worth noting that the earlier estimates of UK tidal barrage potential amounted to approximately 20% of UK electricity need in the late 1980s and today could offer in the region of 15% (DTI, 2005), with the added benefit (over wind and wave based renewables) of predictable availability. In addition to barrage solutions to tidal energy capture, there is also more modest scope for tidal-stream energy generation using submerged rotors, either free standing or as part of a 'tidal fence', these extracting from the kinetic energy of the tidal flows. With attention inevitably to be placed upon reduced energy consumption and demand management, a future tidal power contribution at 20%+ of UK electricity demand would appear realistic.
5. Although all tidal energy generation is intermittent locally, covering about 10-11 hours per day, normally in two pulses synchronised with the approximately 12½ hour tidal cycle, tidal phase lag around the coastline provides an opportunity for the grid input window to be extended to closer to 24 hours. With its complete predictability, and operating in a mix with thermal, hydropower and nuclear production as well as thermal renewables, an effective base-load role should be attainable.
6. The case for a tidal barrage in the Severn estuary, with the highest tidal range in Europe, has and is being actively promoted by the Severn Tidal Power Group with increasing influential support. This scheme alone, (the smaller 'inner' of two earlier options [Baker, 1991]), would be capable of meeting about 5-6% of current UK electricity need (Watson & Shaw, 2007).
7. The estuaries of the North West of England offer fully complementary potential to the Severn by virtue of the tidal phase lag, as will be illustrated below. The Dee, Mersey, Ribble and Wyre estuaries, Morecambe Bay and the Solway Firth all have a macro-tidal range. Based on the earlier studies (Baker, 1991) a total installed capacity of 12GW was estimated (Ribble excluded), with a potential energy yield of at least 17.5TWh/year, approximately 6% of UK national need and by inference a sizeable proportion of the North West's electricity demand. Of all potential UK sites, the Mersey with a very narrow mouth, and therefore needing a relatively short barrage length (MBC 1992), could offer power production at the lowest unit cost of all UK sites (Baker 1991).

8. In this region of the Eastern Irish Sea, exploitable tidal stream resources have also been identified to the north of Anglesey and to the north of the Isle of Man, with more localised resources in the approaches to Morecambe Bay and the Solway Firth (DTI, 2004). In the estuarial situation, however, it is unlikely that tidal stream options can come close to the energy yield of barrage alternatives. Recent assessments for the Mersey <[www.merseytidalpower.co.uk](http://www.merseytidalpower.co.uk)> offer estimates of 40-100GWh for tidal stream arrays, contrasting with 1200GWh estimated for a barrage, at an equivalent location. In a similar vein, whilst tidal lagoons are often mooted as a viable alternative to estuary barrages, offering a similar operational function, it is highly unlikely that they could be realised at a comparable scale and remain competitive on cost against the major barrage schemes cited above.
9. It should be noted that a barrage solution attempts merely to delay the natural motion of the tidal flux as sea level changes: holding back the release of water as tide level subsides under 'ebb generation' so that 'head' (water level) difference is sufficient for turbine operation; deferring the entry of rising tidal flow into the inner estuary basin for 'flood generation'; or 'dual mode', a combination of both. Each mode has some restricting effect, so reducing the range of tidal variation within the basin, ebb generation solutions generally uplifting mean water levels, 'flood' reducing mean levels and dual mode resulting in little change. A degree of environmental modification is, therefore, inevitable, but this does not necessarily imply serious degradation from a physical or ecological perspective, though issues related to protection of habitats would inevitably need to be confronted.
10. Barrage schemes are unique amongst power installations, being inherently multi-functional infrastructure, offering flood protection, road and rail crossings and significant amenity/leisure opportunities, amongst other features. Thus, a fully holistic treatment of overall cost-benefit is imperative for robust decision-making. It is suggested that, to date, this position has been inadequately addressed in the formulation of energy strategy, especially in respect of barrages' potential strategic roles in flood defence and transportation planning. It follows, therefore, that apart from the direct appraisal of energy capture, other complementary investigations must be sufficiently advanced to enable proper input in decision-making in respect of these 'secondary' functions, as well as the various adverse issues, such as sediment regime change, impact on navigation and environmental modification.
11. It is important that robust estimates of the realisable UK tidal energy reserves be established so that they can properly be assimilated into future energy planning (accepting the 10-15 year time horizons necessary). Thereby, rational implementation might be initiated as and when concerns over energy price, security, or carbon emissions dictate. Furthermore, it is considered paramount that this energy potential be fully appreciated when planning application is received for alternative schemes, which might compromise maximum exploitation of the renewable resource. Such instances might arise, for example, should a tidal stream array or tidal fence installation be promoted where the barrage option remains viable and for which a substantially increased energy capture might be expected.
12. Following this line of argument, there now remains a need to re-appraise the earlier study estimates of potential barrage energy yield and to further this detailed technical scrutiny with assessment of the various operational mode options (ebb, flood or dual) and in conjunctive action, to firmly establish the scope for an extended (near 24 hour) generation window and a potential base-load role within the electricity grid.
13. This submission offers some new insight in this respect, and aims also to bring attention to an ongoing study 'Tapping the tidal power potential of the Eastern Irish Sea' being conducted jointly by the University of Liverpool and Proudman Oceanographic Laboratory. Project aims are summarised in the Appendix.

14. At this early phase of the project, it is possible to offer only preliminary findings on the potential for large scale energy procurement from estuary barrages. This draws on energy generation routines developed for the project (Figure 1) and applied to the base data on the estuary bathymetries, barrage lines and tidal regimes taken from the 1980s' literature (later phases will use more precise and updated inputs).

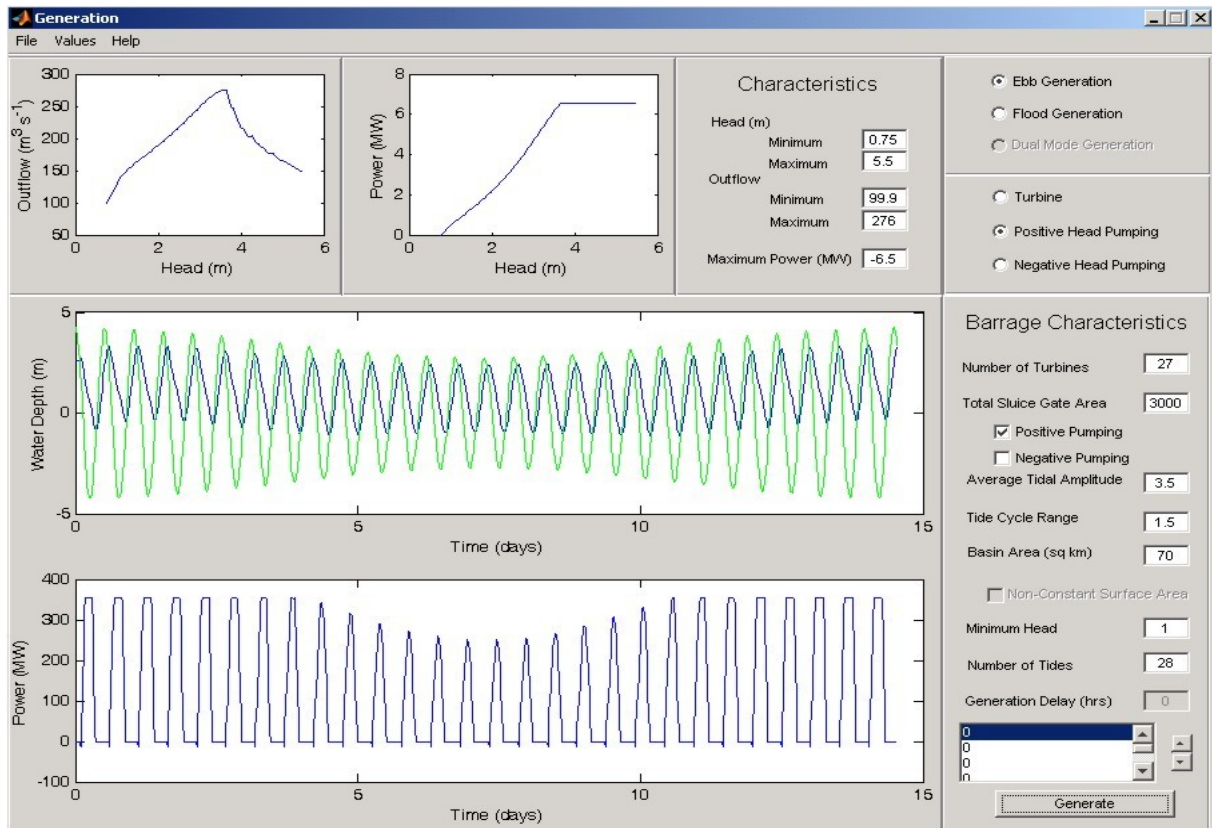
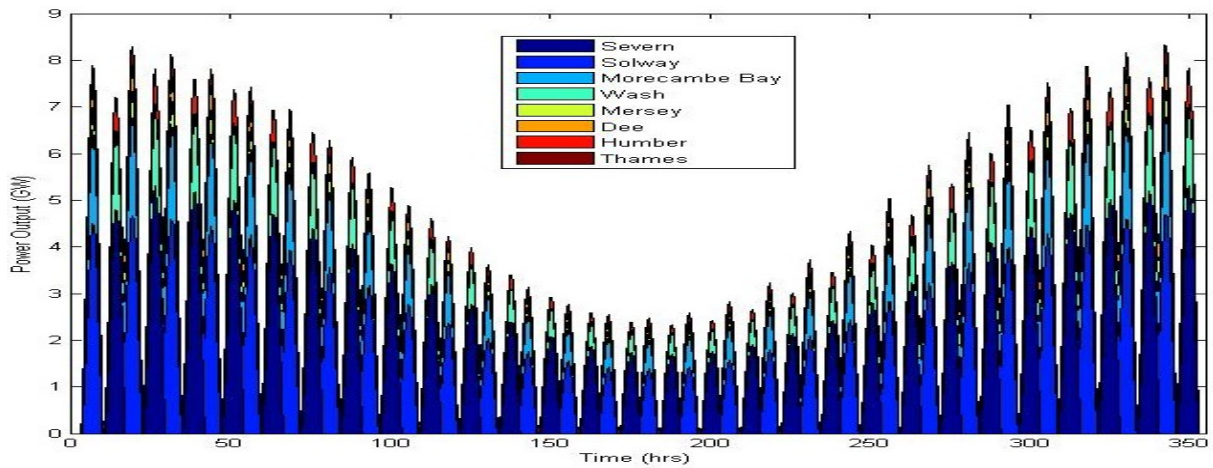
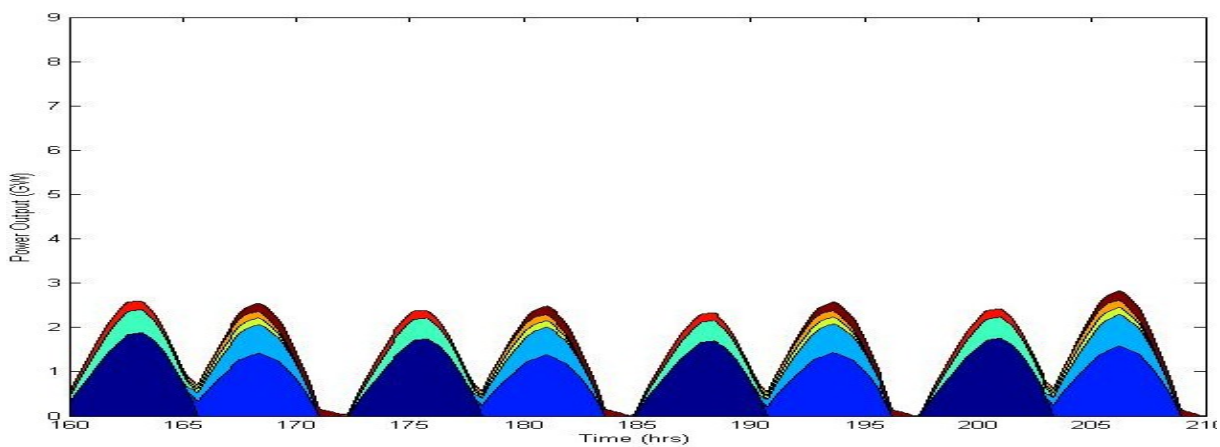


Figure 1: Screen image showing: top – turbine performance characteristics; middle – tidal (green) and basin (blue) level variations; and bottom – power outputs. [Unattributed example for illustration only.]

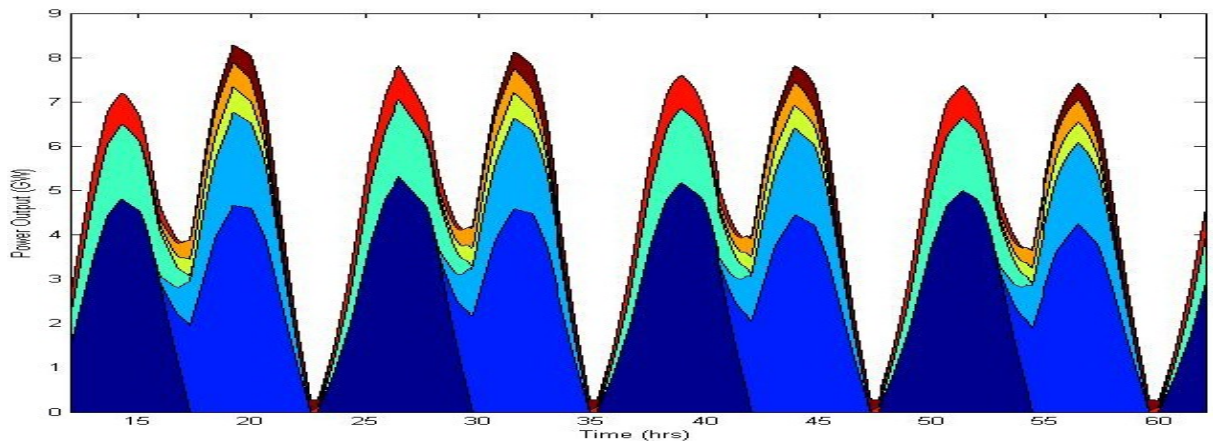
15. Figure 2, over the page, illustrates potential outcomes from the introduction of the 8 major barrage schemes considered earlier (Baker, 1991). These show the combined power outputs, from the favoured ebb-generation using double regulated axial flow turbines (after Baker, 1991), at each of the barrages. It is immediately apparent that they form essentially two distinct 'co-phase' focused groups, the Severn/Wash/Humber and the Solway/Morecambe/Mersey/Dee, with the Thames lying somewhere in between.
16. As far as possible an attempt has been made to consider equivalent barrage power schemes to those adopted in the earlier studies (ie similar number and size of turbines and sluices and generator capacities), though limitations in detail available in the literature led to the need for assumptions and compromises, the technical details of which are not given here, but which will be fully explained in future publications.
17. The operation strategy depicted in Figure 2 is that configured to provide the widest generation window on each barrage. The simulation has been undertaken for 28 tides representing a spring-neap-spring series, shown in part (a), whilst (b) and (c) show the power produced over two-day periods from the neap and spring phases respectively.



a) 28 tide spring-neap-spring series



b) 2-day segment from 'neaps'



c) 2-day segment from 'springs'

Figure 2: Summative plots of power outputs from multiple tidal barrages (provisional).

#### 18. Observations arising and implications:

- The North West group of estuary barrages would operate in a complementary fashion to the Severn (and 'phase-aligned' Wash and Humber). It should be noted that only approximate estimates of tidal phase have been used herein, based mostly on records from nearest ports and so slight adjustments to the synchronisation might be expected from a more refined analysis.

- By judicious use of pumping to enhance water capture around high tide (essentially short-term 'pumped storage') and optimal conjunctive operation of the individual schemes, it would seem possible that the power dip between the Severn group outputs and the following NW Group peaks might be smoothed out.
- It appears less likely that such action could eliminate the major daily trough, during which only the Thames makes a significant contribution. Other potential estuary barrage or 'lagoon' locations, for example around the East coast of Scotland, may be worthy of future consideration, or else different modes of operation may need consideration. 'Flood generation' or 'dual-mode' operation, whilst generally less efficient in energy conversion than 'ebb generation', may provide the added flexibility necessary to provide a significant 24-hr (continuous) output to the grid. The ongoing 'Tapping the tidal power potential of the Eastern Irish Sea' study should go some way towards appraisal of these possibilities.
- Whilst, therefore, the ability to offer a balanced daily supply remains unproven at this point, it is clear that substantial contributions to daily electricity demands could be made. From this preliminary analysis, it appears that for much of the day, tidal power contributions of close to 6GW could be provided during 'springs', falling to around 2GW during 'neaps'. These figures should be set against typical power demands in summer ranging, approximately, from 25-40GW and in winter from 30-50GW.
- The annual energy output from this 'maximum generation window' operation simulation is 29.4TWh; an alternative 'maximum power' operation yields 36.1TWh, these figures representing about 10% and 12 % of UK annual demand, respectively. The more ambitious outer Severn option (Baker, 1991) would be required to lift output above 15%.
- The practicability of rapid introduction of such large power inputs to the grid will need careful attention, though this has recently been broached by the proponents of the Severn barrage (Watson & Shaw, 2007).
- It is clear that a phased introduction of the schemes in pairs could enable an incremental increase in capacity whilst preserving a reasonable power balance across the generation window, ie pairing the Severn and Solway, Morecambe Bay and Wash, and Humber with Mersey/Dee.
- Whilst it is appreciated that the economics are likely to play a major part in any progression of these major tidal power proposals, it is reassuring to note that the unit cost estimates made in the 1980s varied by little more than a factor of 2, with the Severn and Mersey lowest and the Thames highest (Baker, 1991).

## **References**

- Baker AC, 1986. The development of functions relating cost and performance of tidal power schemes and their application to small-scale sites, in *Tidal Power*, Thomas Telford, London.
- Baker AC, 1991. *Tidal Power*, *Energy Policy*, 19(8), 792-797.
- Cottillon J, 1978. La Rance tidal power station—review and comments. *Proc Colston Symp on Tidal Energy*, Bristol, *Scientechnia*, 46-66.
- DTI, 2004. *Atlas of Marine Renewable Energy Resources: Technical Report*. Report no. R1106, ABP Marine Environmental Research Ltd.
- Hammons JH, 1993. *Tidal Power*, *Proc IEEE*, 81(3), 419-433.
- Mersey Barrage Company, 1992. *Tidal power from the River Mersey: A feasibility study Stage III*, MBC, 401

\*Pierre J, 1993 Tidal energy: promising projects - La Rance – a successful industrial scale experiment, Proc IEEE Trans Energy Conversion, 8(3), 552-558.

Rufford N, 1986. Tidal power still in the running, New Civil Engineer, 22 May 1986, 12.

Shaw, TL, 1980. An environmental appraisal of tidal power stations: with particular reference to the Severn barrage. Shaw (ed.), London: Pitman Advanced Publishing Program, 220pp.

Watson MJ & Shaw TL, 2007. Energy generation from a Severn barrage prior to full commissioning, Proc ICE Engineering Sustainability, 160, March, ES1, 35-39.

\* In the Final Report, this reference has been corrected to:

Frau JP, 1993. 'Tidal energy: promising projects - La Rance – a successful industrial scale experiment', Institute of Electrical and Electronics Engineers, IEEE Transactions on Energy Conversion, 8(3), 552-558.

### ***Appendix: 'Tapping the Tidal Power Potential of the Eastern Irish Sea'***

An ongoing research project is being conducted, over the period October 2006 - September 2008, jointly by the University of Liverpool and Proudman Oceanographic Laboratory for the Joule Centre, under financial support from the North West Development Agency.

Project Aims: to establish a generic regional modelling approach to study the interaction between the practicable exploitation of tidal energy and potential hydrological, morphological and environmental impacts in the Eastern Irish Sea. Its principal study objectives, each with distinctive deliverable outcomes, are:

1. To evaluate the realisable tidal energy potential of the coasts of the North West of England, stretching from the Dee estuary to the Solway, with regard to the installation of estuary barrages, tidal fence structures or tidal stream rotor arrays, or combinations thereof.
2. To establish the potential daily generation window from optimal conjunctive operation of such devices, taking account of the different possible modes of operation (ebb, flood or dual phase generation) in the case of barrages.
3. To evaluate any impact on the overall tidal dynamics of the Irish Sea as a consequence of this energy extraction and the associated modifications by time lag in estuary momentum exchange.
4. Arising from (3), to assess the implications, if any, of biophysical coupling in the marine ecosystem, manifesting water quality or ecological consequences.
5. To ascertain the scale of flood protection benefit likely to accrue from proactive operation of barrages, fully accounting for the worsening effects of sea level rise (SLR) and change in catchment rainfall regimes as a consequence of climate change, so affecting fluvial flood magnitudes and frequencies.

The study outcomes will place on a firm footing the potential of the North West to achieve contributions (in terms of generating capacity, daily generation window and predictability) towards renewable energy targets by exploitation of its substantial tidal resources.

### **A.1.3 Tidal stream energy extraction from estuaries**

See “Extracting ‘free-stream’ tidal current energy in estuaries” by David Prandle, PECS 2008: Physics of Estuaries and Coastal Seas, Liverpool, 25-29th August 2008 <<http://www.pecs-conference.org>>.

# **Tapping the Tidal Power Potential of the Eastern Irish Sea**

## **APPENDIX 2**

comprising five separate documents:

- A.2.1 Theoretical background to energy computations (0-D modelling)
- A.2.2 Implication of entry and exit losses in turbine conduits
- A.2.3 Validation of Turgency/Generation Matlab computational routines
- A.2.4 Preliminary studies – potential from barrages on major UK estuaries
- A.2.5 Constructional aspects

**March 2009**

**[www.liv.ac.uk/engdept/tidalpower](http://www.liv.ac.uk/engdept/tidalpower)**

**A.2.1 Theoretical background to energy computations (0-D modelling)**

**Introduction**

A number of barrage schemes have been suggested for various estuarial sites around the coast of the UK. These schemes vary from small scale sites such as the Dovey, which might produce about 50GWh per year (UKAEA, 1984), to very large power generation schemes such as the proposed outer line in the Severn Estuary, which could potentially produce up to 19.7TWh per year (UKAEA, 1980, 1984). Operation of the tidal barrages has, in general, only been considered in detail for the Severn site, although power output estimates have been produced for a number of other barrage proposals. The basis for all previous studies has been the optimal power generation for a given scheme; no consideration has been given to the conjunctive operation of the various potential schemes around the UK coast. The major benefit of multiple schemes is the possibility for a wider generation window to be maintained, rather than the single peak produced from a single power generation proposal. This increased generation window should provide easier integration within the national power grid and thus make tidal power a more attractive proposition.

To facilitate the study into conjunctive operation of tidal barrages, reported here, an approach analogous to that of the DoEn was developed independently. Two programs were written to investigate the impact of turbine characteristics and operational mode on power production. The first program, Turgency, produces the power and outflow against head characteristics of a given turbine. The second program, Generation, allows the integration of these turbine characteristics into a modelled barrage scheme. It determines the power output and the tide and basin levels over the modelled period for given barrage attributes, such as sluice gate area or number of turbines. Assuming that the barrage sites are independent of each other, the power outputs from each barrage scheme can then be linearly superimposed to estimate the overall combined power output.

**Turgency**

The Turgency program calculates the power output and outflow relationships through the use of a turbine hill chart. The version used in this study, shown in Figure 1, was for a double-regulated bulb turbine, as given by Baker (1991). The hill chart provides non-dimensional efficiencies as a function of specific discharge and unit speed to enable computation of power output. Marked on the hill chart is the maximum output curve, which is followed as closely as possible so as to extract the best performance from a turbine.

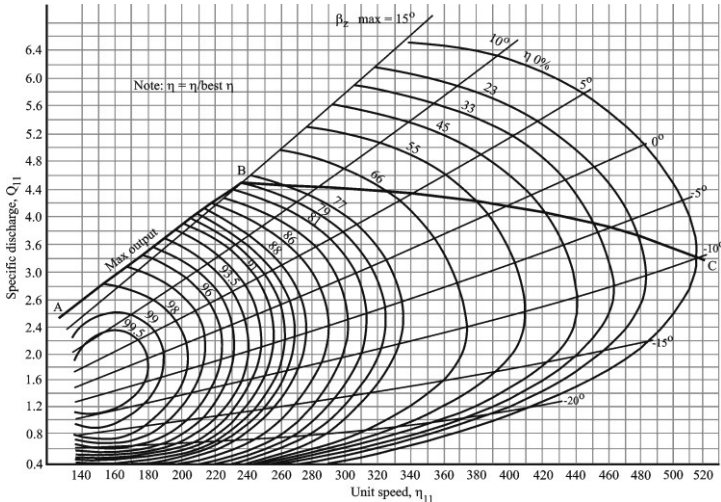


Figure 1: Hill chart for a double-regulated bulb turbine.

The program takes two main sets of attributes as input: river and turbine properties. The river properties determine information about the site within which the turbine will operate, the flow restrictions required to prevent cavitation occurring, and the limits between which the turbine characteristic relationships will be defined. The turbine properties are the physical attributes of the turbine, such as its diameter and generator power output. Figure 2 shows the main window of Turgency. The input data are entered in the two panels on the right and the power grid frequency set in the file menu. The turbine outflow and power output characteristics are generated and displayed in the two plots, with other information shown in the text boxes beneath. Here the rated head, maximum power output, turbine speed and number of generator poles are shown. As part of the process, a cavitation check is made for the root of the rotor vanes and, if insufficient submergence is provided, the maximum outflow is recalculated given the available water depth by moving down the maximum output curve on the hill chart (Baker, 1991).

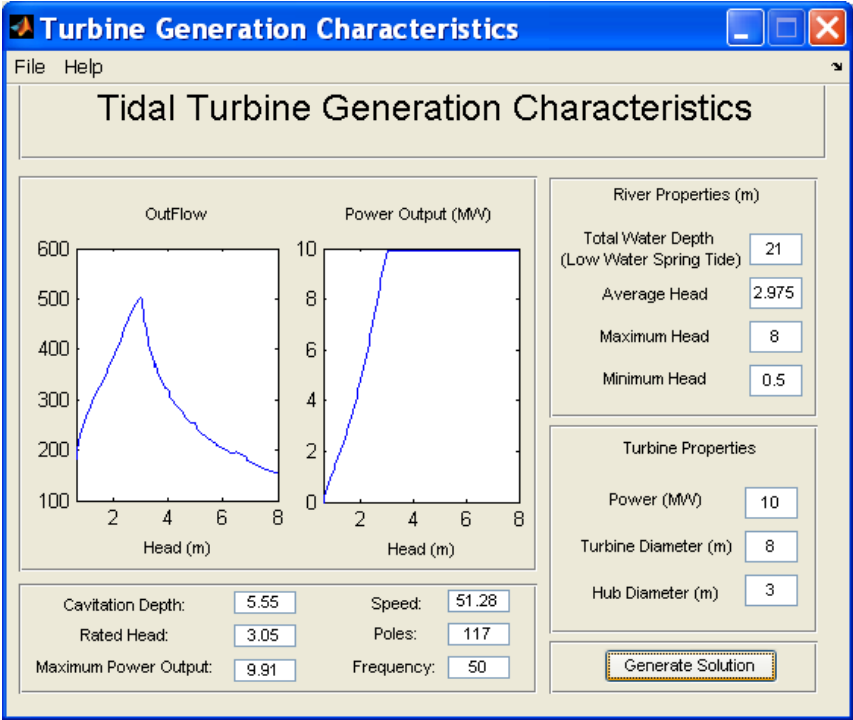


Figure 2: Turgency user interface.

Once the maximum outflow rate has been calculated, the speed of the turbine,  $n$ , can be obtained from:

$$n = \frac{2 \times 60 \times f}{N}$$

where  $f$  is the frequency of the electricity grid and  $N$  is the number of generator poles. It is then possible to obtain the power output for a given head and outflow and, thus, calculate the characteristic relationships of power and outflow against head. Varying the head is equivalent to changing the non-dimensional unit speed, as shown on the hill chart in Figure 1, as the two are linked by the equation:

$$n_{11} = \frac{nD}{\sqrt{H}}$$

in which  $n_{11}$  is the unit speed and  $D$  is the turbine diameter.

The power output,  $P$ , is obtained from:

$$P = \rho g Q H \eta$$

where  $Q$  is the discharge rate and  $\eta$  is the efficiency of the turbine. The turbine output can be split into two regions of the hill chart. The first is when the maximum available power is less than the generator output rating. In this region, the efficiency and specific discharge rate are obtained from the maximum output curve given in the hill chart. The actual turbine discharge is obtained from the specific discharge rate, through the equation:

$$Q = Q_{11} D^2 \sqrt{H}$$

where  $Q_{11}$  is the specific discharge as given by the hill chart. In the second region, the available maximum power is greater than the generator rating and so the actual discharge rate does not lie on the maximum output curve. Instead, the power equations must be solved as a transcendental equation in terms of specific discharge. This leads to the reduced flows necessary to maintain the rated power output seen in Figure 2.

### Generation

The Generation program (see Figure 3) aims to model the operation of a barrage through a range of tidal sequences and calculate the potential power output and water level within the basin throughout the modelled period. It requires a number of input parameters which determine the operational characteristics of any given barrage scheme. The turbine characteristics, extracted from Turgency, model the throughflow of water and power production as the head difference across the barrage varies. The program also needs information about the bathymetry within the basin (which may be entered as an area-depth relationship or as a constant value), the tide at the barrage line (which may be entered as a time series or as the two major UK tidal constituents, the  $M_2$ , lunar semidiurnal, and  $S_2$ , solar semidiurnal, components), the number of turbines, and the effective sluice gate area. The program permits all three operational modes, with the option included for the provision of pumping. For example, in ebb generation, pumping may be used to further raise the water level after tidal high water and, thus, increase the head before onset of power generation. It is also possible to specify a delay, after the minimum generation head has been reached, before generation will begin in order to explore optimal energy capture. The barrage is ultimately modelled by the continuity equation:

$$S(z) \frac{dz}{dt} = Q(H) + Q_{in}$$

Here,  $z$  is the basin water surface elevation above local mean sea level,  $t$  is the time,  $S(z)$  is the surface area as a function of elevation,  $Q(H)$  is the flow rate through the barrage as a function of head,  $H$ , and  $Q_{in}$  is the river inflow, which is assumed constant in this model.

The complexity in the modelling comes in determining the flow rate for different parts of each tidal cycle. When the barrage is generating, the flux function,  $Q(H)$ , through the turbines within the barrage is calculated through the use of the turbine characteristics. When the barrage is operating in sluice mode the standard orifice flow equation is used:

$$Q(H) = G_\varepsilon \sqrt{2gH}$$

in which  $G_\varepsilon$  is the effective gate area:

$$G_\varepsilon = \sum_n C_{Dn} G_n$$

where  $C_{Dn}$  is the contraction, or discharge, coefficient of the  $n$ th sluice or free-spinning turbine and  $G_n$  is the respective area.

The variation in the tide about mean sea level is described by:

$$Y(t) = M_2 \cos(\omega_M t) + S_2 \cos(\omega_S t)$$

where  $\omega_k$  is the frequency of the tide for the  $k = M, S$  component. The head difference is then:

$$H = Y(t) - z$$

Solving for the basin water level,  $z$ , then enables the power output from the turbines to be determined from the Turgency power-head characteristic.

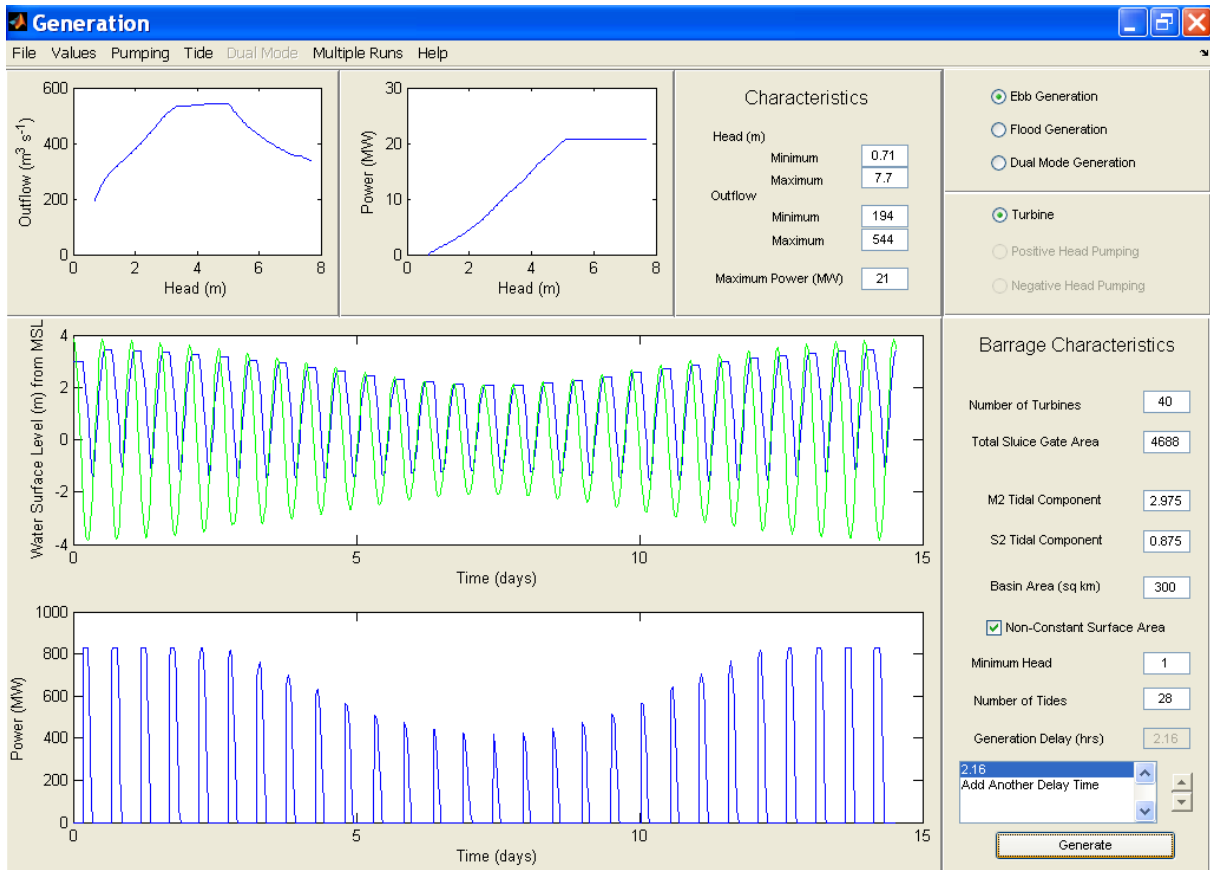
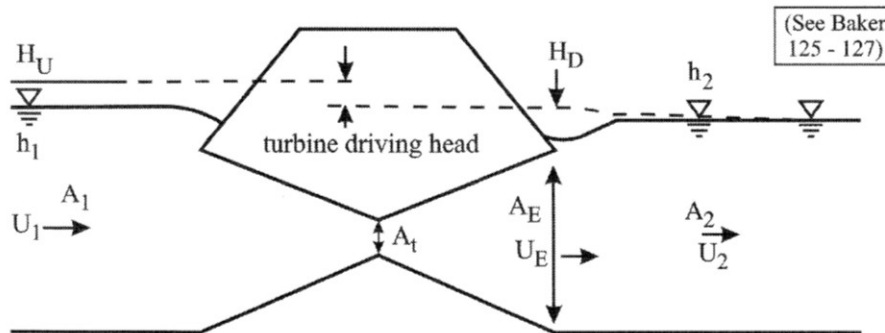


Figure 3: Generation program user interface.

## References

- Baker AC, 1991. Tidal Power, Institution of Electrical Engineers Energy Series 5, Peter Peregrinus Ltd, London.
- United Kingdom Atomic Energy Authority (UKAEA), 1980. Preliminary Survey of Tidal Energy of UK Estuaries, Severn Tidal Power Report STP-102, Binnie & Partners, London.
- United Kingdom Atomic Energy Authority (UKAEA), 1984. Preliminary Survey of Small Scale Tidal Energy, Severn Tidal Power Report STP-4035 C, Binnie & Partners, London.

## A.2.2 Implication of entry and exit losses in turbine conduits



$$H_U = h_1 + \frac{Q^2}{2gA_1^2} \quad H_D = h_2 + \frac{Q^2}{2gA_2^2} \left[ \left( \frac{A_2}{A_E} \right)^2 - \frac{2A_2}{A_E} + 2 \right]$$

Turbine driving head

$$= H_U - H_D = [h_1 - h_2] - \frac{Q^2}{2gA_2^2} \left[ \left( \frac{A_2}{A_E} \right)^2 - \frac{2A_2}{A_E} + 2 - \left( \frac{A_2}{A_1} \right)^2 \right]$$

(i) Based upon Severn design (Baker, 1991, Figure 3.10)

$$A_E \approx 4A_t.$$

(ii) Assume turbine velocity as orifice flow for head difference of 5m, i.e.

$$U_T = \sqrt{2gH} \approx 10\text{m/s}.$$

(iii) Assume Power  $\propto H^{3/2}$  [  $P = \rho g H Q \eta$ ;  $Q \propto \sqrt{H}$ ,  $\eta$  - const ]

$$\therefore \frac{dP}{P} = \frac{3}{2} \frac{dH}{H}.$$

(a) Worst Case  $A_1 \approx A_2 \gg A_E$

$$\frac{Q^2}{2gA_2^2} \left[ \left( \frac{A_2}{A_E} \right)^2 - 2 \left( \frac{A_2}{A_E} \right) + 2 - \left( \frac{A_2}{A_1} \right)^2 \right] \rightarrow \frac{Q^2}{2gA_E^2} = \frac{U_E^2}{2g}$$

and with

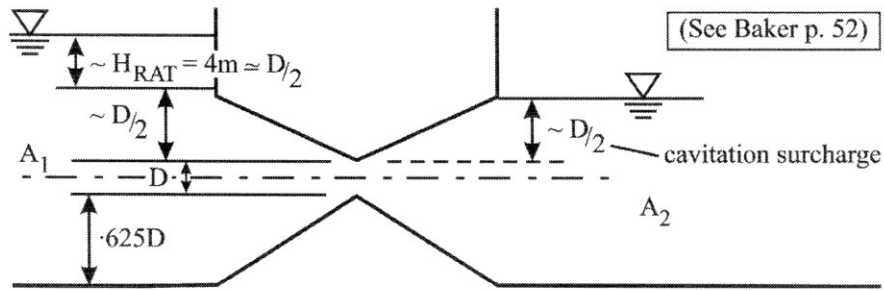
$$U_T \approx 10\text{m/s}, \quad U_E \approx 10 \times \left( \frac{A_t}{A_E} \right) = 2.5\text{m/s} \quad \therefore \frac{U_E^2}{2g} = 0.32\text{m}.$$

Consider  $(h_1 - h_2) \approx 4\text{m}$  (rated head,  $H_{rat}$ ) at maximum power production and flow rate.

$$\text{Reduction in turbine head} = \frac{U_E^2 / 2g}{4\text{m}} = \frac{0.32}{4} = 8\%.$$

$$\text{Reduction in power} = \frac{3}{2} \times 8 = \underline{\underline{12\%}}.$$

(b) More realistic case



Ignoring lateral variations,  $\frac{A_1}{A_2} \approx \frac{2.6D}{2.1D} \approx 1.25$ .

Assume  $A_2 = A_E$

$$\frac{Q^2}{2gA_2^2} \left[ \left( \frac{A_2}{A_E} \right)^2 - 2 \left( \frac{A_2}{A_E} \right) + 2 - \left( \frac{A_2}{A_1} \right)^2 \right] \Rightarrow \frac{Q^2}{2gA_2^2} \left[ 1 - \left( \frac{1}{1.25} \right)^2 \right]$$

$$\frac{Q^2}{2gA_E^2} [1 - 0.64] = \frac{0.36}{2g} U_E^2 = 0.11\text{m} \quad (\text{with } U_E \approx 2.5\text{m/s, see (a) above}).$$

Reduction in turbine head (again taking rated head,  $H_{\text{rat}} = 4\text{m}$ ) is:  $\frac{dH}{H} = \frac{0.11}{4.0} = 2.75\%$ .

Effect on power,  $\frac{dP}{P} = \left( \frac{0.11}{4.0} \right) \times \frac{3}{2} = \underline{\underline{4\%}}$ .

Finally, noting that when the driving head is greater than 0.11m (or 0.32m for worst case) during times when the power pulses are 'clipped' at maximum output, these exit head losses will not yield power reductions. So the power generation reduction figures above, in the range 4% to 12% are likely to be overly pessimistic, i.e. taking 20% of the generation to be above the rated head (say), the figures might be expected to reduce proportionately to say 3% to 10%. Therefore, the exit head losses, if applicable to hill chart calculations, would reduce energy generation by no more than 10% for a typical design situation.

**Reference**

Baker AC, 1991. Tidal Power, Institution of Electrical Engineers Energy Series 5, Peter Peregrinus Ltd, London.

## A.2.3 Validation of Turgency/Generation MATLAB computational routines

### Camel Estuary

#### 1. Introduction

- (a) Basin information: The Camel estuary is small estuary and the bathymetric data are given in Table 1.

Table 1: Basin area.

Level above OD (m)	Area (km <sup>2</sup> )
-4.08	0
-2.58	1
0.93	4
2.43	5.7
3.43	7.0

- (b) The tide in the open sea, expressed by the following equation, is assumed to be semi-diurnal governed by the M<sub>2</sub> and S<sub>2</sub> constituents shown in Table 2.

$$\eta = \sum_{i=1}^2 a_i \cos(\omega_i t)$$

Table 2: Tidal constituents.

Constituents	Tidal amplitude a <sub>i</sub> (m)	Frequency ω <sub>i</sub> (rad/hour)
M <sub>2</sub>	2.38	0.5059
S <sub>2</sub>	0.88	0.5236

- (c) Turbine parameters:

Table 3: Turbine parameters.

Diameter (m)	4
Speed (rpm)	88.2
Generator rating (MW)	4.7
Nominal head (m)	5.08

#### 2. Calculations and results

Table 4: Turbines and sluices.

Number of turbines	6
Number of sluices	6
Installed power (MW)	28.2

- (a) The total sluice area is estimated by the formula:

$$G_e = g_e \frac{S}{2T} \sqrt{\frac{R}{g}}$$

in which S is the basin area, g<sub>e</sub> = 7, g = 9.81m/s<sup>2</sup>, R is the tidal range and T = 12.42 hours.

(b) The tides in the open sea and basin are shown in Figure 1.

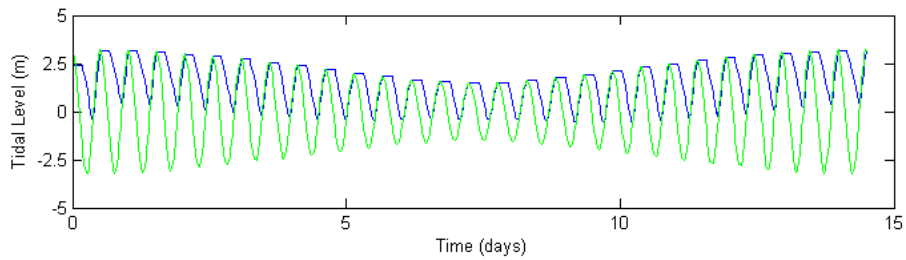


Figure 1: Tides in open sea and basin.

(c) The power generation over a 14-day period is shown in Figure 2.

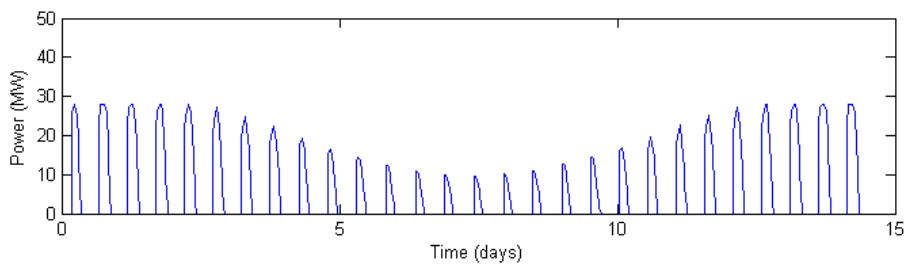
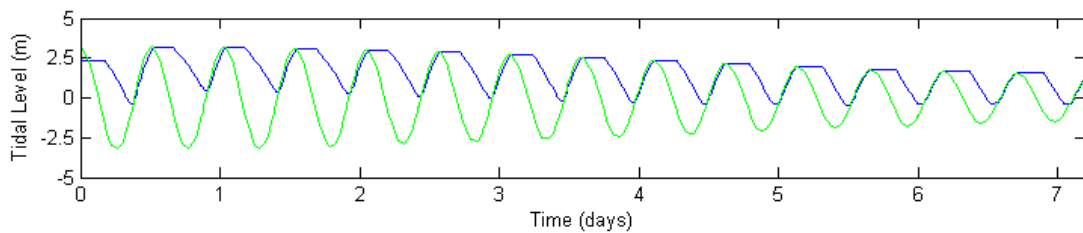


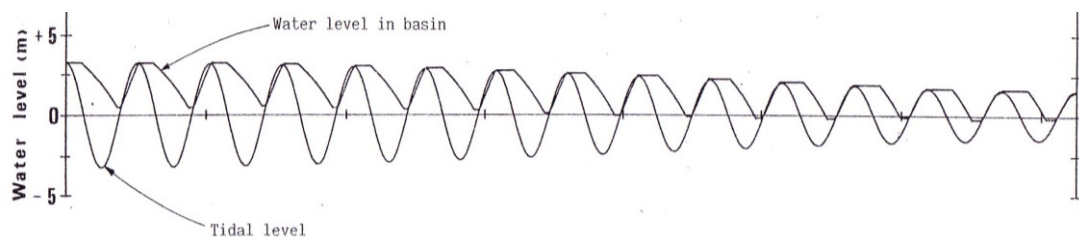
Figure 2: Power output over 14 days.

(d) Annual power output obtained is  $P = 0.0505\text{TWh/yr}$ .

3. Comparison with earlier study: The present predicted annual power output of  $0.0505\text{TWh/yr}$  is close to that reported by UKAEA (1984) of  $0.0551\text{TWh/yr}$ . The tidal and electricity generation patterns are also similar, as shown in Figures 3 and 4, respectively. Since many details are missing from the UKAEA report, the agreement can be regarded as acceptable.

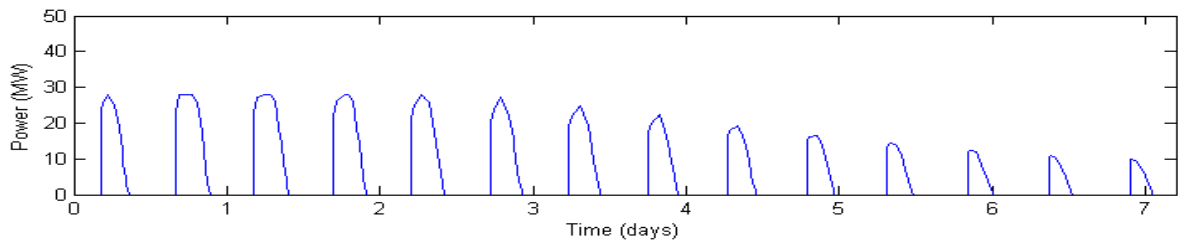


(a) From present model

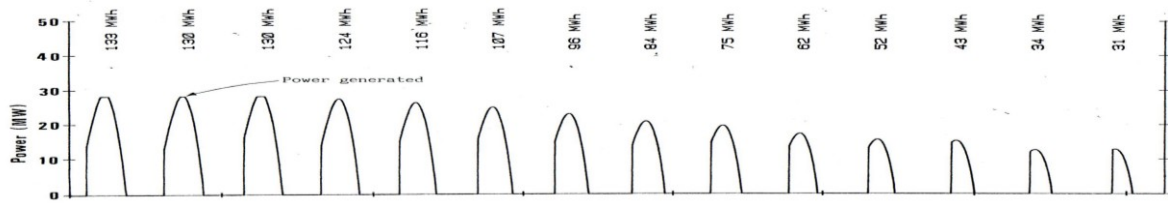


(b) From UKAEA report

Figure 3: Comparison with earlier study of tides.



(a) From present model



(b) From UKAEA report

Figure 4: Comparison with earlier study of annual power outputs.

## Hamford Estuary

### 1. Introduction

- (a) Basin information: The Hamford estuary is also a small estuary and the bathymetric data are given in Table 5.

Table 5: Basin area.

Level above OD (m)	Area (km <sup>2</sup> )
-2.52	0
-1.5	2.8
-0.02	6.8
1.5	10.9
2.04	12.4

- (b) The tide in the open sea, expressed by the following equation, is assumed to be semi-diurnal governed by the M<sub>2</sub> and S<sub>2</sub> constituents shown in Table 6.

$$\eta = \sum_{i=1}^2 a_i \cos(\omega_i t)$$

Table 6: Tidal constituents.

Constituents	Tidal amplitude a <sub>i</sub> (m)	Frequency ω <sub>i</sub> (rad/hour)
M <sub>2</sub>	1.5	0.5059
S <sub>2</sub>	0.35	0.5236

- (c) Turbine parameters

Table 7: Turbine parameters.

Diameter (m)	4
Speed (rpm)	81.08
Generator Rating (MW)	2.25
Nominal head (m)	2.78

### 2. Calculations and results

Table 8: Turbines and sluices.

Number of Turbines	9
Number of Sluices	8
Installed power (MW)	20.25

- (a) The total sluice area is estimated by the formula:

$$G_e = g_e \frac{S}{2T} \sqrt{\frac{R}{g}}$$

in which S is the basin area, g<sub>e</sub> = 7, g = 9.81m/s<sup>2</sup>, R is the tidal range and T = 12.42 hours.

- (b) The tides in the open sea and basin are shown in Figure 5.

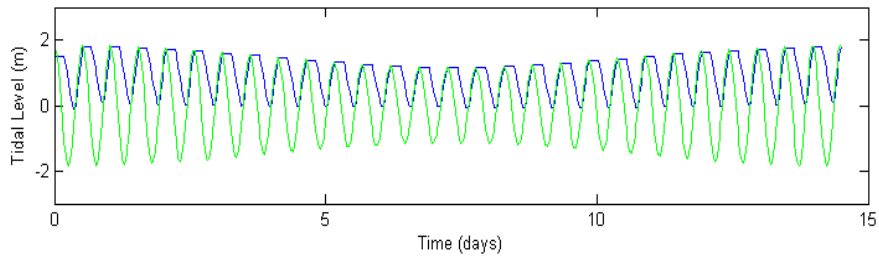


Figure 5: Tides in open sea and basin.

(c) The power generation over a 14-day period is shown in Figure 6.

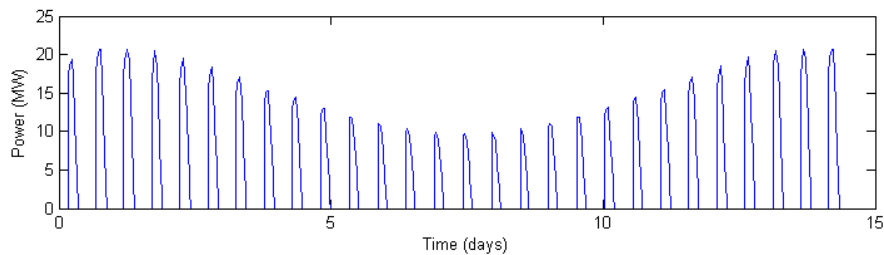
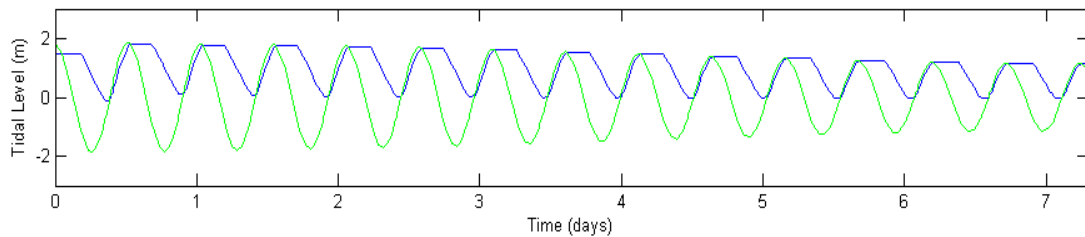


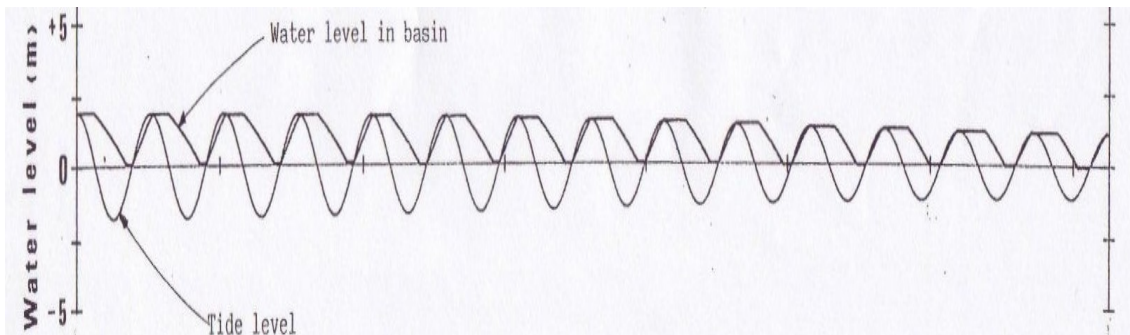
Figure 6: Power output over 14 days.

(d) Annual power output obtained is  $P = 0.0335\text{TWh/yr}$ .

- Comparison with earlier study: The present predicted annual power output of  $0.0335\text{TWh/yr}$  is close to that reported by UKAEA (1984) of  $0.038\text{TWh/yr}$ . The tidal and electricity generation patterns are also similar, as shown in Figures 7 and 8, respectively. Since many details are missing from the UKAEA report, the agreement can be regarded as acceptable.

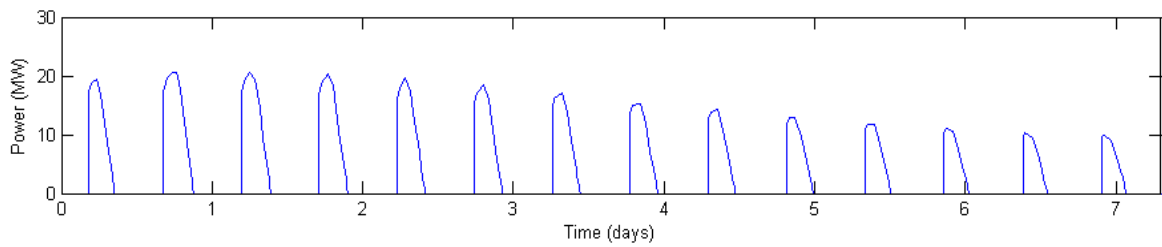


(a) From present model

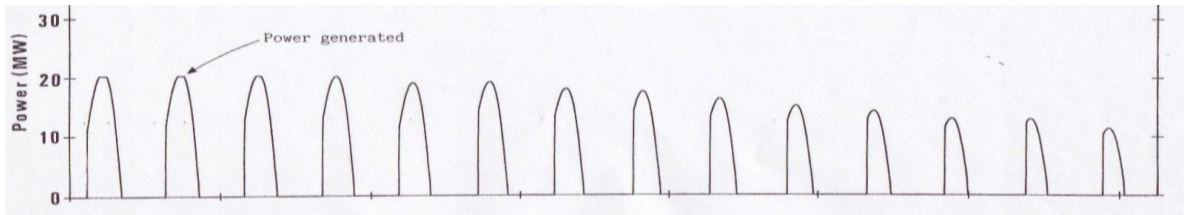


(b) From UKAEA report

Figure 7: Comparison with earlier study of tides.



(a) From present model



(b) From UKAEA report

Figure 8: Comparison with earlier study of annual power outputs.

**Reference**

United Kingdom Atomic Energy Authority (UKAEA), 1984. Preliminary Survey of Small Scale Tidal Energy, Severn Tidal Power Report STP-4035 C, Binnie & Partners, London.

## A.2.4 Preliminary studies – potential from barrages on major UK estuaries

### Severn Estuary

The Severn Estuary Barrage was modelled upon the inner (Cardiff-Weston) line and thus permits the addition of a bunded basin for out-of-phase generation. The basin was assumed to have a flat bottom and the constant surface area was assumed to be 480km<sup>2</sup>, consistent with previous studies. The tidal components had a 3% reduction applied to them, due to the impact of the barrage upon the tidal elevation:

$$M_2: 3.15\text{m};$$

$$S_2: 0.95\text{m}.$$

Information on the turbines used in the model is given in Table 1, and the outflow and power output against head relationships are shown in Figure 1.

Table 1: Severn Barrage turbine information.

Diameter (m)	Hub diameter (m)	Maximum power output (GW)	Maximum outflow rate (m <sup>3</sup> s <sup>-1</sup> )
9	3	40.9	891
Cavitation depth (m)	Speed (rpm)	Number of poles	Rated head (m)
21.1	63.83	94	5.98

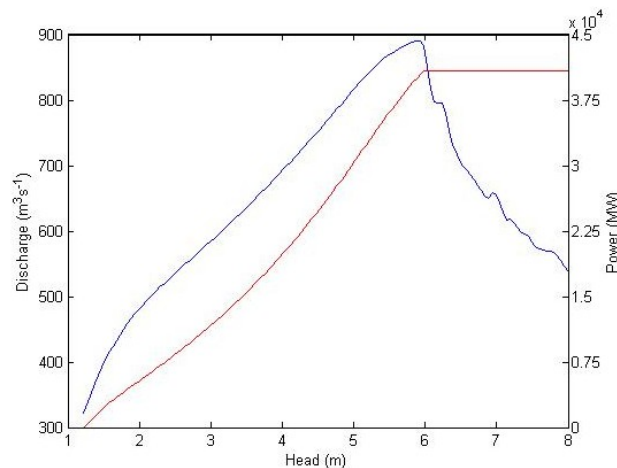


Figure 1: Characteristics of turbines used in the Severn Barrage.

Within the barrage, 216 turbines were used together with a total effective sluice gate area of 47000m<sup>2</sup>. The annual energy output was 11.12TWh. The energy output as a function of delay is shown in Figure 2. It attains a maximum when there is a delay of 2hrs 55mins after generation can first begin.

Figure 3 shows the levels of the tide and the water within the basin impoundment. The basin levels have been lifted, relative to the tidal average level, through operating in ebb generation mode. The minimum elevation is nearly always around mean water level, with little variation throughout the tidal cycle.

The power output changes significantly over the spring-neap tidal cycle, as shown in Figure 4. The maximum neap power output is about 48% of the spring value, with the total energy output for the neap tide being roughly 26% of that for the spring tide.

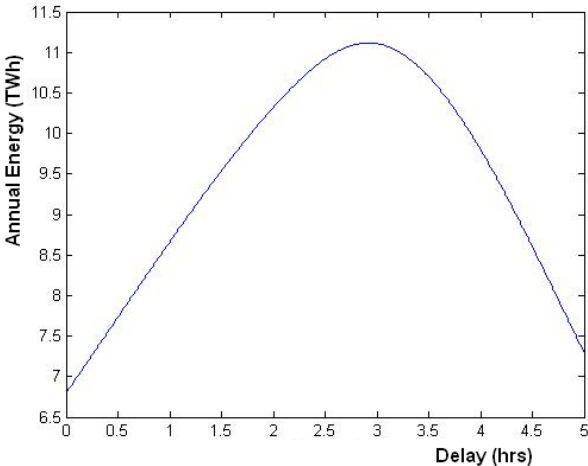


Figure 2: Annual energy output as a function of delay for the Severn Barrage.

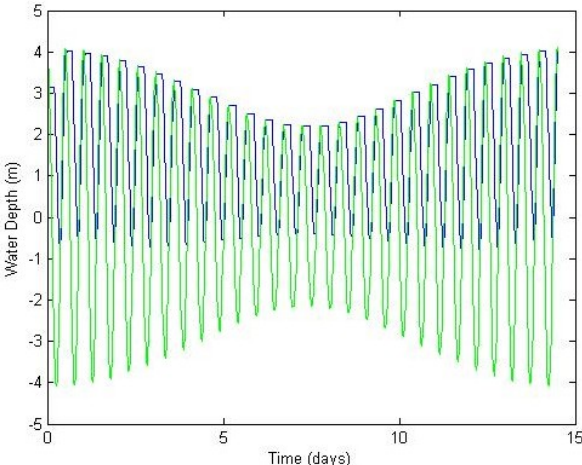


Figure 3: Basin (blue line) and tide (green line) levels for the Severn Barrage.

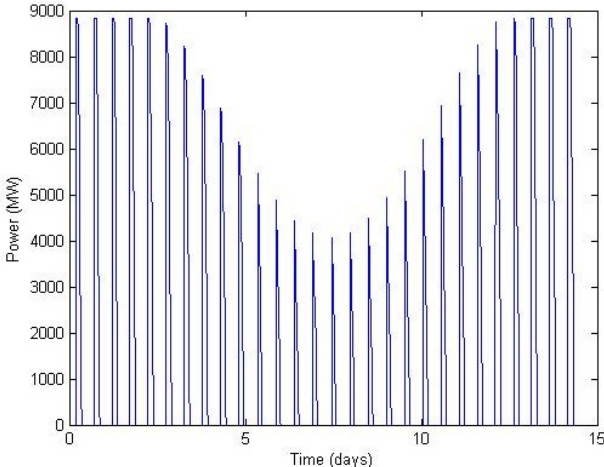


Figure 4: Power output from the Severn Barrage.

## The Wash

The Wash Barrage scheme has been modelled on the inner line. The bathymetry within the basin is summarized in Table 2. The tidal components had no reduction applied:

$M_2$ : 2.23m;

$S_2$ : 0.76m.

Table 2: Elevation-area relationship for the Wash basin.

Level above OD (m)	Area (km <sup>2</sup> )
-2	260
0	330
1	380
2	430
3	500

Information on the turbines used in the model is given in Table 3, and the outflow and power output against head relationships are shown in Figure 5.

Table 3: Wash Barrage turbine information.

Diameter (m) 9	Hub Diameter (m) 3	Maximum Power Output (GW) 30.7	Maximum Outflow Rate (m <sup>3</sup> s <sup>-1</sup> ) 734
Cavitation Depth (m) 10	Speed (rpm) 51.72	Number of Poles 116	Rated Head (m) 5.14

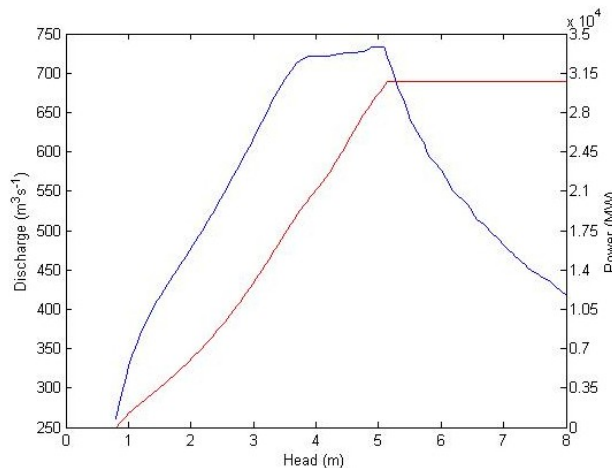


Figure 5: Characteristics of turbines used in the Wash Barrage.

Within the barrage, 80 turbines were used together with a total effective sluice gate area of 18500m<sup>2</sup>. The annual energy output was 3.24TWh. The energy output as a function of delay is shown in Figure 6. It attains a maximum when there is a delay of 1hr 55mins after generation can first begin.

Figure 7 shows the levels of the tide and the water within the basin impoundment. The basin level has been lifted, relative to the tidal average level, through operating in ebb generation mode. Again, the minimum elevation is nearly always around mean water level, with little variation throughout the tidal cycle.

The power output changes significantly over the spring-neap tidal cycle, as shown in Figure 8. The maximum neap power output is about 32% of the spring value, with the total energy output for the neap tide being roughly 25% of that for the spring tide.

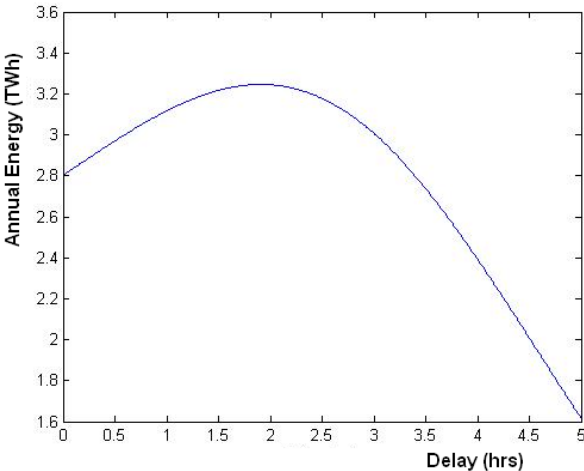


Figure 6: Annual energy output as a function of delay for the Wash Barrage.

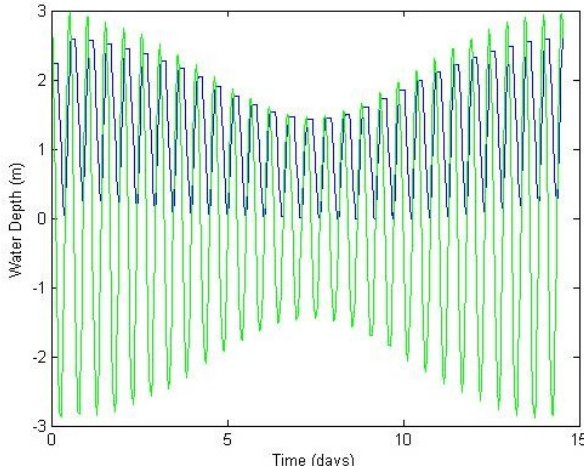


Figure 7: Basin (blue line) and tide (green line) level for the Wash Barrage.

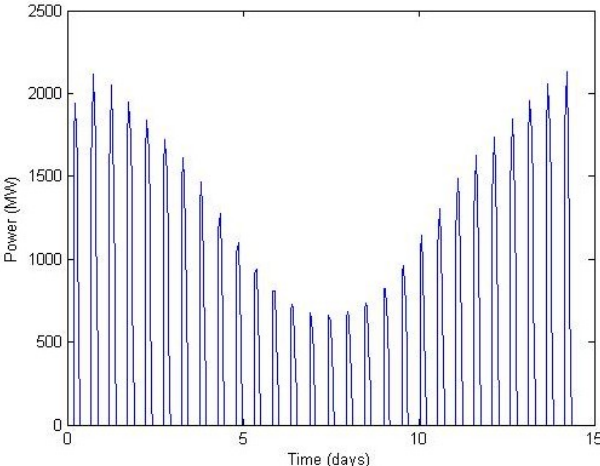


Figure 8: Power output from the Wash Barrage.

## Dee

The Dee Barrage scheme has been modelled on the standard line. The bathymetry within the basin is summarized in Table 4. The tidal components had no reduction applied:

$M_2$ : 2.975m;

$S_2$ : 0.875m.

Table 4: Elevation-area relationship for the Dee basin.

Level above OD (m)	Area (km <sup>2</sup> )
-2	27
0	50
2	76
4	109

Information on the turbines used in the model is given in Table 5, and the outflow and power output against head relationships are shown in Figure 9.

Table 5: Dee Barrage turbine information.

Diameter (m) 6	Hub Diameter (m) 2.2	Maximum Power Output (GW) 20.2	Maximum Outflow Rate (m <sup>3</sup> s <sup>-1</sup> ) 341
Cavitation Depth (m) 11.6	Speed (rpm) 81.08	Number of Poles 74	Rated Head (m) 6.9

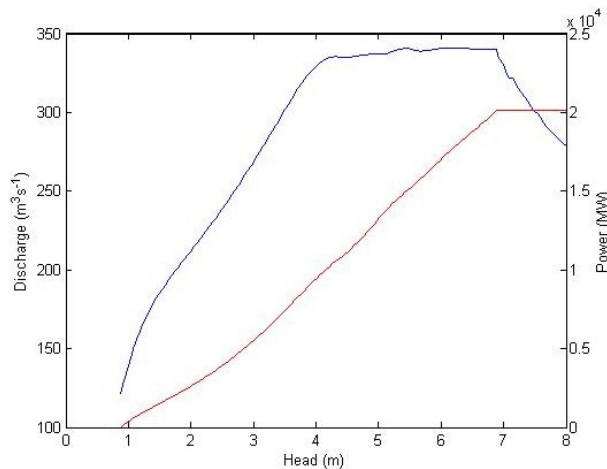


Figure 9: Characteristics of turbines used in the Dee Barrage.

Within the barrage, 50 turbines were used together with a total effective sluice gate area of 5000m<sup>2</sup>. The total annual power output was 1.29TWh. The energy output as a function of delay is shown in Figure 10. It attains a maximum when there is a delay of 2hrs 35mins after generation can first begin.

Figure 11 shows the levels of the tide and the water within the basin impoundment. The basin level has been lifted, relative to the tidal average level, through operating in ebb generation mode. As before, the minimum elevation is nearly always around mean water level, with little variation throughout the tidal cycle.

The power output changes significantly over the spring-neap tidal cycle, as shown in Figure 12. The maximum neap power output is about 35% of the spring value, with the total energy output for the neap tide being roughly 27% of that for the spring tide.

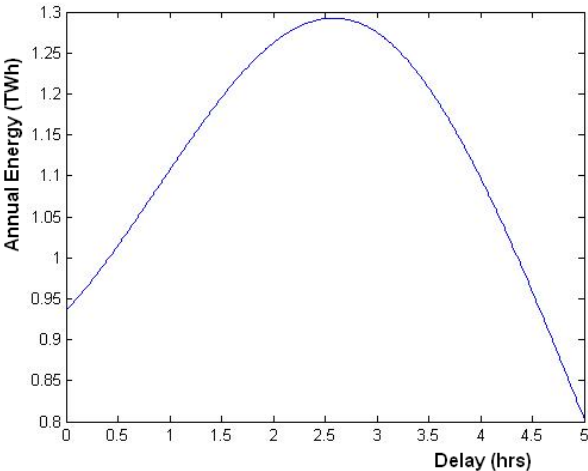


Figure 10: Annual energy output as a function of delay for the Dee Barrage.

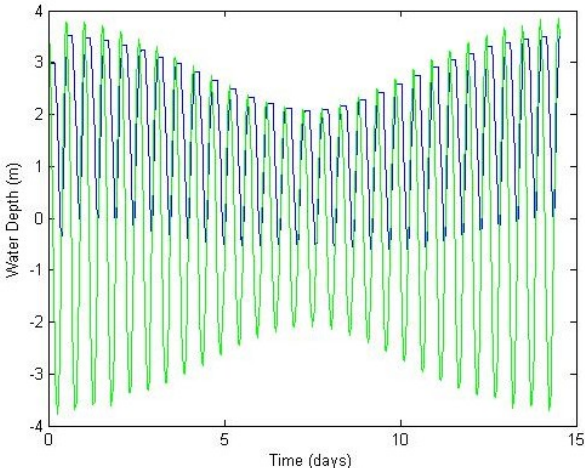


Figure 11: Basin (blue line) and tide (green line) level for the Dee Barrage.

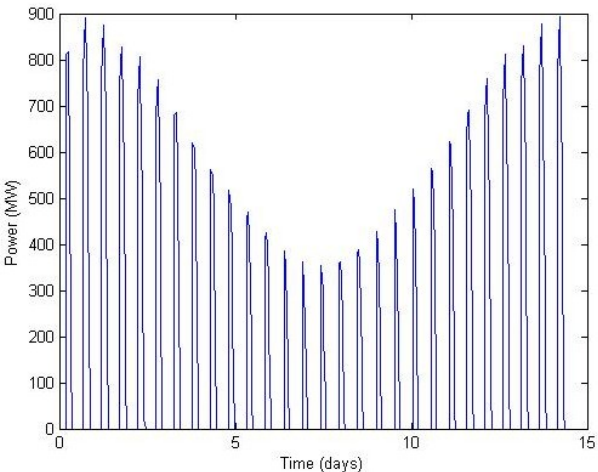


Figure 12: Power output from the Dee Barrage.

## Morecambe Bay

The Morecambe Bay Barrage scheme has been modelled on the inner line. The bathymetry within the basin is summarized in Table 6. The tidal components had no reduction applied:

$M_2$ : 3.15m;

$S_2$ : 0.95m.

Table 6: Elevation-area relationship for the Morecambe Bay basin.

Level above OD (m)	Area (km <sup>2</sup> )
-4.9	100
0	234
2	307
4.5	392

Information on the turbines used in the model is given in Table 7, and the outflow and power output against head relationships are shown in Figure 13.

Table 7: Morecambe Bay Barrage turbine information.

Diameter (m) 9	Hub Diameter (m) 3	Maximum Power Output (GW) 49.8	Maximum Outflow Rate (m <sup>3</sup> s <sup>-1</sup> ) 952
Cavitation Depth (m) 25.6	Speed (rpm) 68.18	Number of Poles 88	Rated Head (m) 6.82

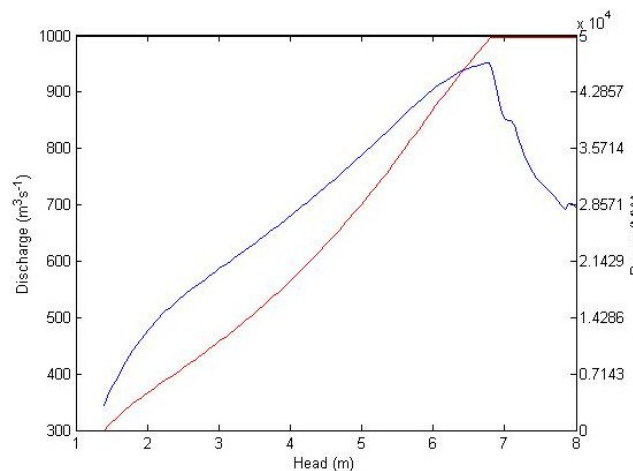


Figure 13: Characteristics of turbines used in the Morecambe Bay Barrage.

Within the barrage, 60 turbines were used together with a total effective sluice gate area of 14500m<sup>2</sup>. The annual energy output was 4.28TWh. The energy output as a function of delay is shown in Figure 14. It attains a maximum when there is a delay of 2hrs after generation can first begin.

Figure 15 shows the levels of the tide and the water within the basin impoundment. The basin level has been lifted, relative to the tidal average level, through operating in ebb generation mode. Once again, the minimum elevation is nearly always around mean water level, with little variation throughout the tidal cycle.

The power output changes significantly over the spring-neap tidal cycle, as shown in Figure 16. The maximum neap power output is about 35% of the spring value, with the total energy output for the neap tide being roughly 30% of that for the spring tide.

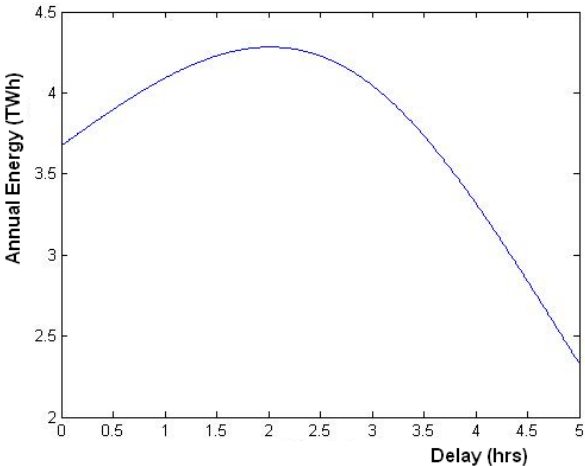


Figure 14: Annual energy output as a function of delay for the Morecambe Bay Barrage.

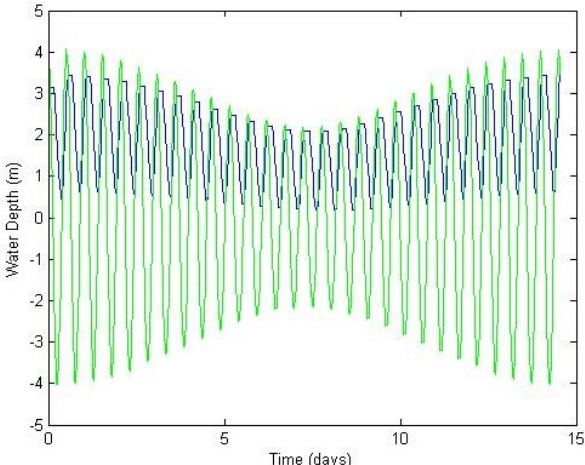


Figure 15: Basin (blue line) and tide (green line) level for the Morecambe Bay Barrage.

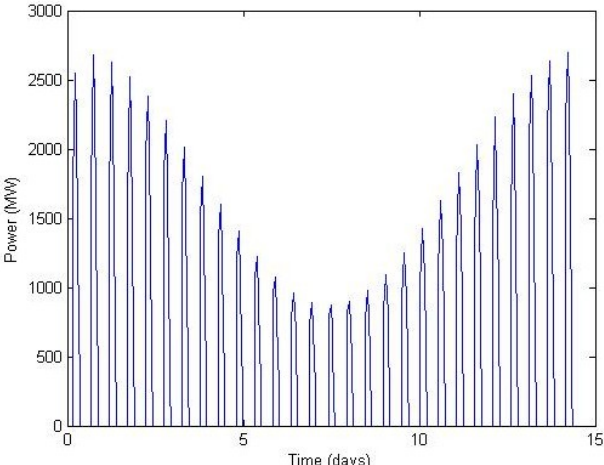


Figure 16: Power output from the Morecambe Bay Barrage.

## Solway

The Solway Barrage scheme has been modelled on the outer line. The bathymetry within the basin is summarized in Table 8. The tide had 3% and 2% reductions applied to the  $M_2$  and  $S_2$  components, respectively:

$$M_2: 2.74\text{m};$$

$$S_2: 0.86\text{m}.$$

Table 8: Elevation-area relationship for the Solway basin.

Level above OD (m)	Area (km <sup>2</sup> )
-3.7	573
0	777
3.7	887

Information on the turbines used in the model is given in Table 9, and the outflow and power output against head relationships are shown in Figure 17.

Table 9: Solway Barrage turbine information.

Diameter (m) 9	Hub Diameter (m) 3	Maximum Power Output (GW) 38.9	Maximum Outflow Rate (m <sup>3</sup> s <sup>-1</sup> ) 788
Cavitation Depth (m) 13	Speed (rpm) 55.56	Number of Poles 108	Rated Head (m) 6.03

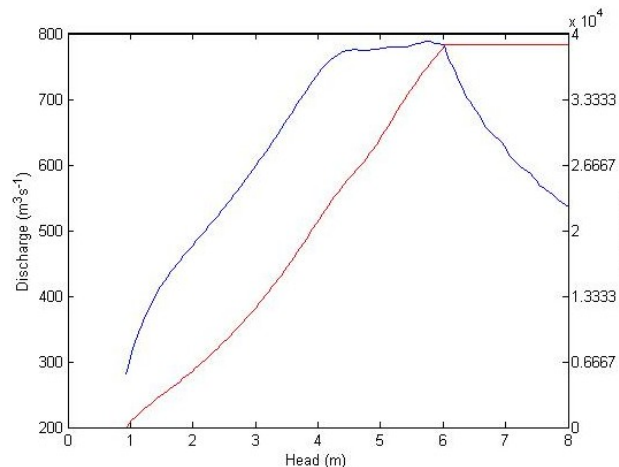


Figure 17: Characteristics of turbines used in the Solway Barrage.

Within the barrage, 180 turbines were used together with a total effective sluice gate area of 38500m<sup>2</sup>. The annual energy output was 9.82TWh. The energy output as a function of delay is shown in Figure 18. It attains a maximum when there is a delay of 2hrs 6mins after generation can first begin.

Figure 19 shows the levels of the tide and the water within the basin impoundment. The basin level has been lifted, relative to the tidal average level, through operating in ebb generation mode. As with earlier cases, the minimum elevation is nearly always around mean water level, with little variation throughout the tidal cycle.

The power output changes significantly over the spring-neap tidal cycle, as shown in Figure 20. The maximum neap power output is about 35% of the spring value, with the total energy output for the neap tide being roughly 30% of that for the spring tide.

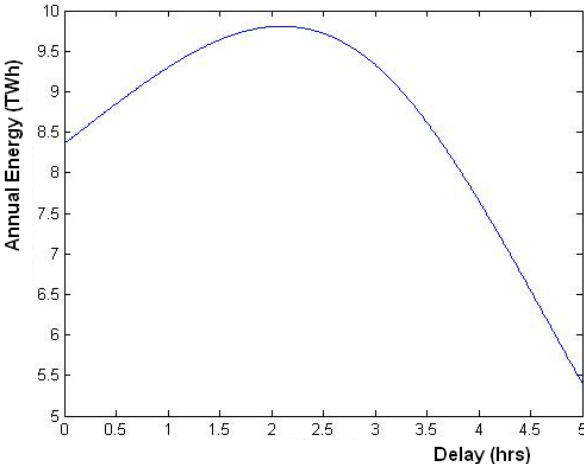


Figure 18: Annual energy output as a function of delay for the Solway Barrage.

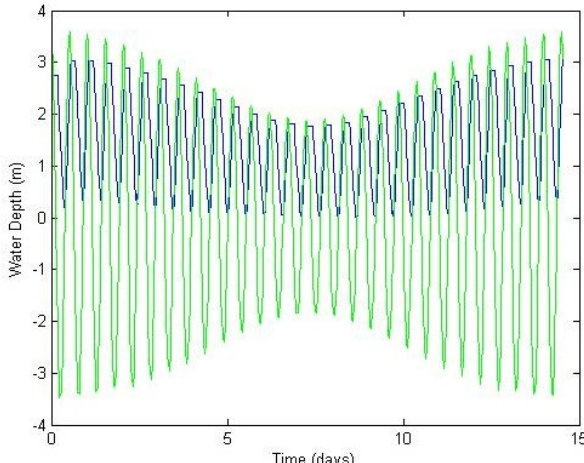


Figure 19: Basin (blue line) and tide (green line) level for the Solway Barrage.

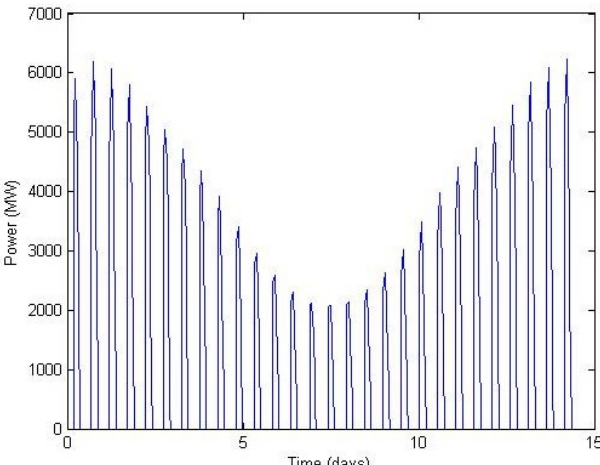


Figure 20: Power output from the Solway Barrage.

## Mersey

The Mersey Barrage scheme has been modelled on the standard line. The bathymetry within the basin is summarized in Table 10. The tidal components had no reduction applied:

$M_2$ : 3.23m;

$S_2$ : 0.98m.

Table 10: Elevation-area relationship for the Mersey basin.

Level above OD (m)	Area (km <sup>2</sup> )
-5	16.53
-2.5	33.47
0	50.4
2.5	67.34
5	84.27

Information on the turbines used in the model is given in Table 11, and the outflow and power output against head relationships are shown in Figure 21.

Table 11: Mersey Barrage turbine information.

Diameter (m) 7.6	Hub Diameter (m) 2.5	Maximum Power Output (GW) 23.7	Maximum Outflow Rate (m <sup>3</sup> s <sup>-1</sup> ) 545
Cavitation Depth (m) 12	Speed (rpm) 63.83	Number of Poles 94	Rated Head (m) 5.39

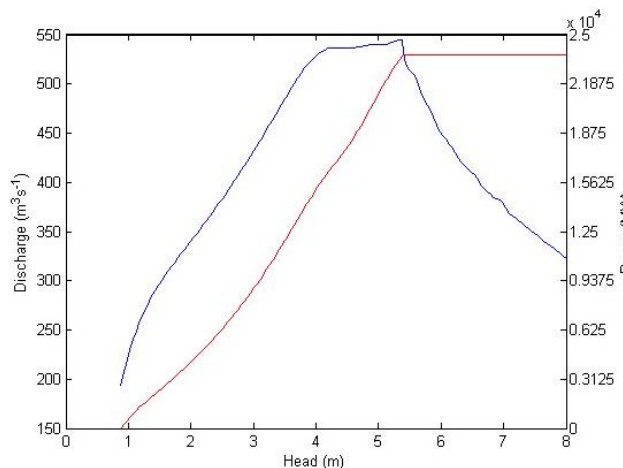


Figure 21: Characteristics of turbines used in the Mersey Barrage.

Within the barrage, 27 turbines were used together with a total effective sluice gate area of 5400m<sup>2</sup>. The total annual energy output was 1.34TWh. The energy output as a function of delay is shown in Figure 22. It attains a maximum when there is a delay of 2hrs 12mins after generation can first begin.

Figure 23 shows the levels of the tide and the water within the basin impoundment. The basin level has been lifted, relative to the tidal average level, through operating in ebb generation mode. Unsurprisingly, the minimum elevation is nearly always around mean water level, with little variation throughout the tidal cycle.

The power output changes significantly over the spring-neap tidal cycle, as shown in Figure 24. The maximum neap power output is about 45% of the spring value, with the total energy output for the neap tide being roughly 29% of that for the spring tide.

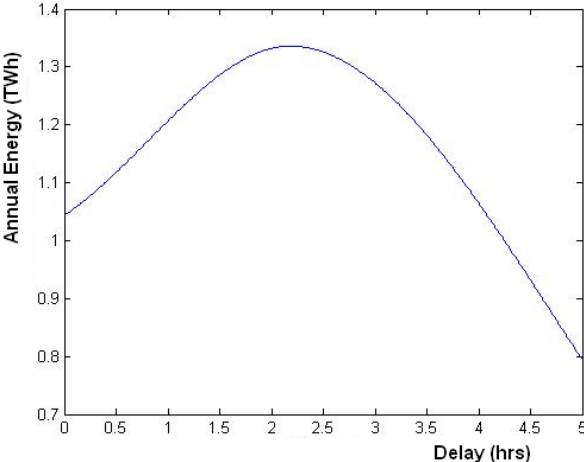


Figure 22: Annual energy output as a function of delay for the Mersey Barrage.

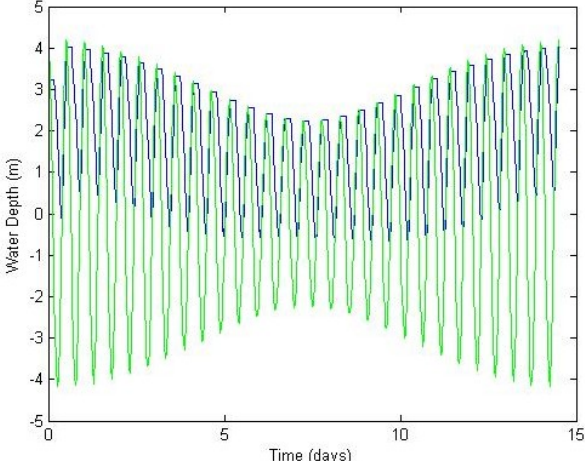


Figure 23: Basin (blue line) and tide (green line) level for the Mersey Barrage.

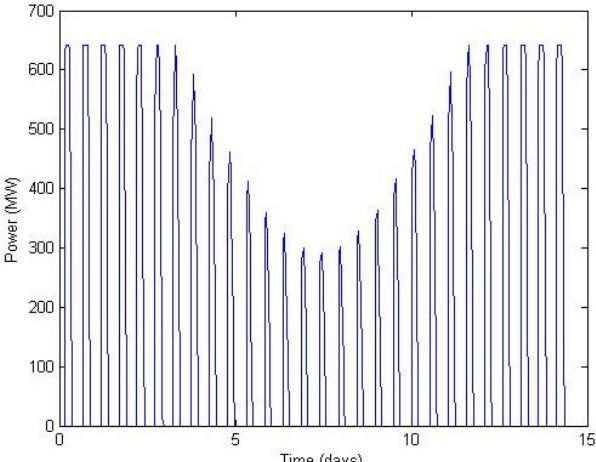


Figure 24: Power output from the Mersey Barrage.

## Humber

The Humber Barrage scheme has been modelled on the outer line. The bathymetry within the basin is summarized in Table 12. The tidal components had no reduction applied:

$$M_2: 2.05\text{m};$$

$$S_2: 0.75\text{m}.$$

Table 12: Elevation-area relationship for the Humber basin.

Level above OD (m)	Area (km <sup>2</sup> )
-3.9	171
0	228
3.9	292

Information on the turbines used in the model is given in Table 13, and the outflow and power output against head relationships are shown in Figure 25.

Table 13: Humber Barrage turbine information.

Diameter (m) 9	Hub Diameter (m) 3	Maximum Power Output (GW) 26.3	Maximum Outflow Rate (m <sup>3</sup> s <sup>-1</sup> ) 709
Cavitation Depth (m) 8.89	Speed (rpm) 50	Number of Poles 120	Rated Head (m) 4.61

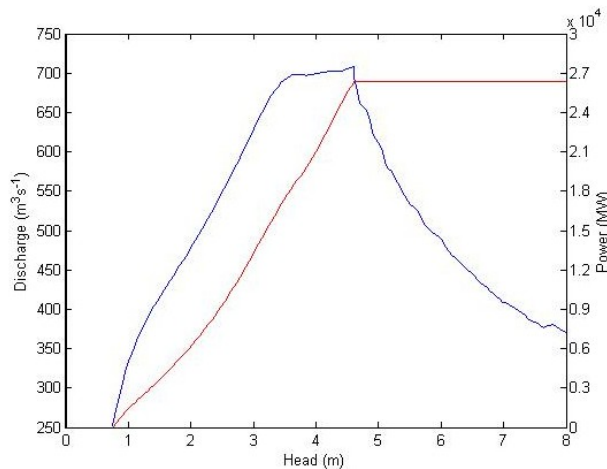


Figure 25: Characteristics of turbines used in the Humber Barrage.

Within the barrage, 40 turbines were used together with a total effective sluice gate area of 10000m<sup>2</sup>. The annual energy output was 1.55TWh. The energy output as a function of delay is shown in Figure 26. It attains a maximum when there is a delay of 1hr 36mins after generation can first begin.

Figure 27 shows the levels of the tide and the water within the basin impoundment. The basin level has been lifted, relative to the tidal average level, through operating in ebb generation mode. Predictably, the minimum elevation is nearly always around mean water level, with little variation throughout the tidal cycle.

The power output changes significantly over the spring-neap tidal cycle, as shown in Figure 28. The maximum neap power output is about 30% of the spring value, with the total energy output for the neap tide being roughly 23% of that for the spring tide.

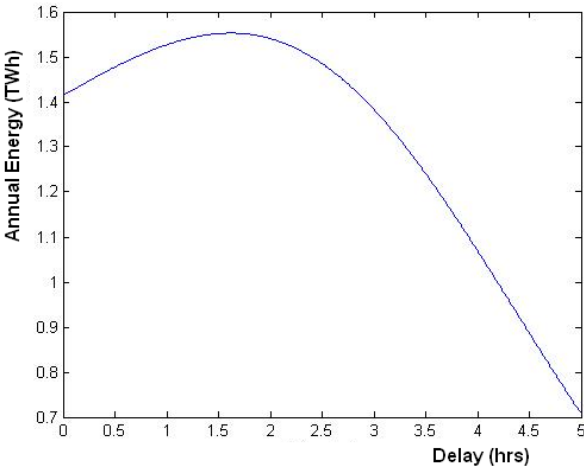


Figure 26: Annual energy output as a function of delay for the Humber Barrage.

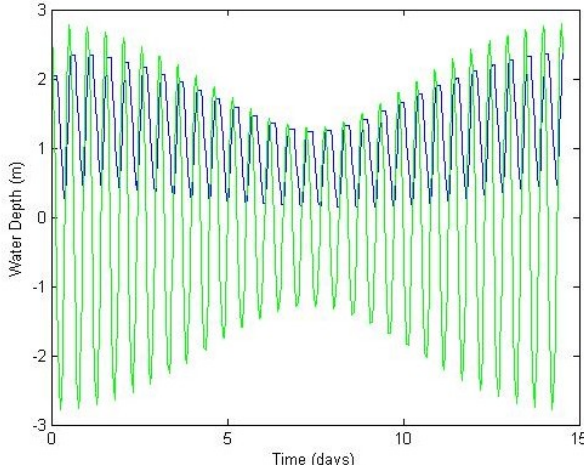


Figure 27: Basin (blue line) and tide (green line) level for the Humber Barrage.

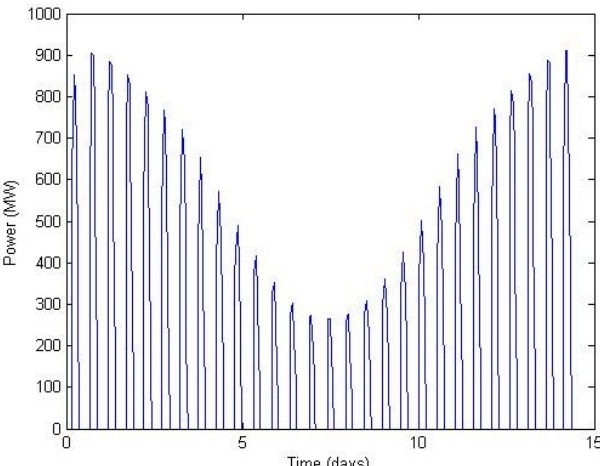


Figure 28: Power output from the Humber Barrage.

## Thames

The Thames Barrage scheme has been modelled on the outer line. The bathymetry within the basin is summarized in Table 14. The tidal components had no reduction applied:

$$M_2: 2.1\text{m};$$

$$S_2: 0.45\text{m}.$$

Table 14: Elevation-area relationship for the Thames basin.

Level above OD (m)	Area (km <sup>2</sup> )
-2.55	100
0	165
2.55	200

Information on the turbines used in the model is given in Table 15, and the outflow and power output against head relationships are shown in Figure 29.

Table 15: Thames Barrage turbine information.

Diameter (m) 9	Hub Diameter (m) 3	Maximum Power Output (GW) 28.7	Maximum Outflow Rate (m <sup>3</sup> s <sup>-1</sup> ) 721
Cavitation Depth (m) 9.5	Speed (rpm) 50.85	Number of Poles 118	Rated Head (m) 4.9

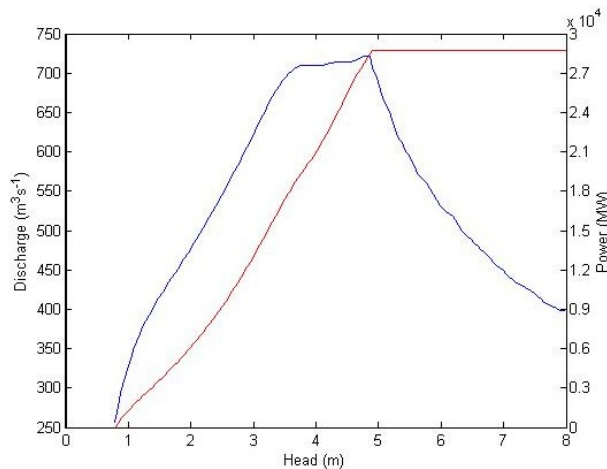


Figure 29: Characteristics of turbines used in the Thames Barrage.

Within the barrage, 40 turbines were used together with a total effective sluice gate area of 8000m<sup>2</sup>. The annual energy output was 1.3TWh. The energy output as a function of delay is shown in Figure 30. It attains a maximum when there is a delay of 2hrs 12mins after generation can first begin.

Figure 31 shows the levels of the tide and the water within the basin impoundment. The basin level has been lifted, relative to the tidal average level, through operating in ebb generation mode. As now expected, the minimum elevation is nearly always around mean water level, with little variation throughout the tidal cycle.

The power output changes significantly over the spring-neap tidal cycle, as shown in Figure 32. The maximum neap power output is about 50% of the spring value, with the total energy output for the neap tide being roughly 44% of that for the spring tide.

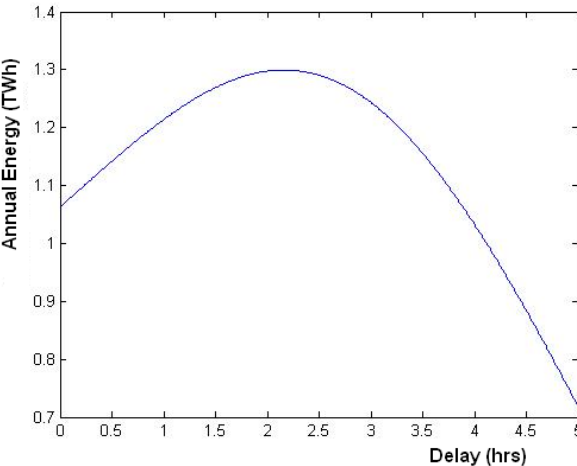


Figure 30: Annual energy output as a function of delay for the Thames Barrage.

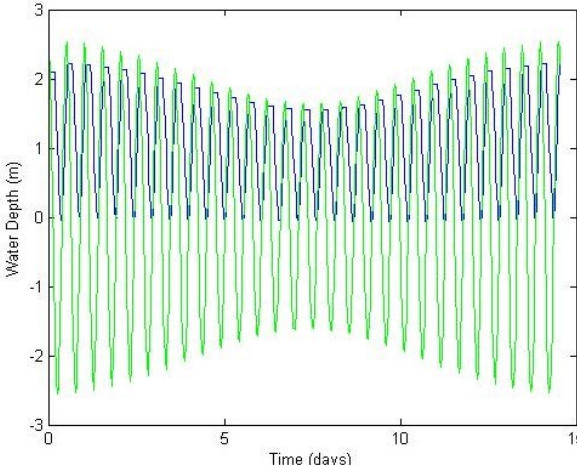


Figure 31: Basin (blue line) and tide (green line) level for the Thames barrage.

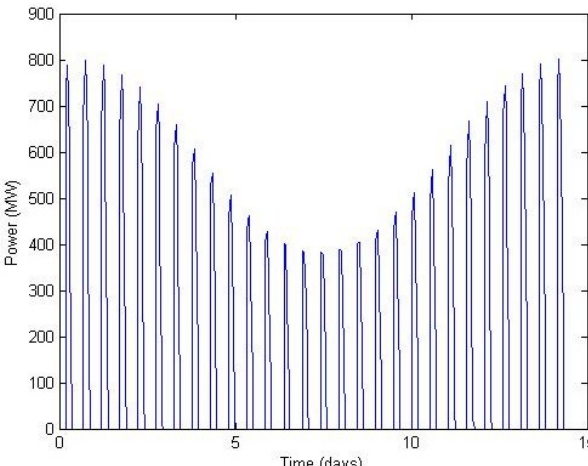


Figure 32: Power output from the Thames Barrage.

## **References**

Department of Energy (DoEn), Central Electricity Generating Board (CEGB) and Severn Tidal Power Group (STPG), 1989. The Severn Barrage Project: General Report, Energy Paper Number 57 (EP57), HMSO, London.

United Kingdom Atomic Energy Authority (UKAEA), 1980. Preliminary Survey of Tidal Energy of UK Estuaries, Severn Tidal Power Report STP-102, Binnie & Partners, London.

## Appendix A.2.5: Constructional aspects

### Introduction

This appendix considers various aspects related to the construction of barrages in the estuaries of the Eastern Irish Sea: the bathymetry, geology, hydraulic loadings, foundations, barrage sites, barrage construction, costs, and other details. It ends with concluding remarks and a set of references.

### Bathymetry

The bathymetry of the Eastern Irish Sea is shown on various Admiralty Charts at different scales. They include:

- 1:200,000 - Irish Sea, Eastern Part;
- 1:100,000 - Solway Firth and Approaches;
- 1:50,000 - Morecambe Bay and Approaches;
- 1:75,000 - Approaches to Preston;
- 1:75,000 - Great Orme's Head to Liverpool.

Details are generally poor within the estuaries.

Other available sources of information include:

- LIDAR measurements held by the Proudman Oceanographic Laboratory for the Dee, Mersey and Ribble estuaries;
- Environmental Statement Supporting Applications for an Offshore Windfarm at Robin Rigg, produced by Natural Power (2002); see Figure 1.

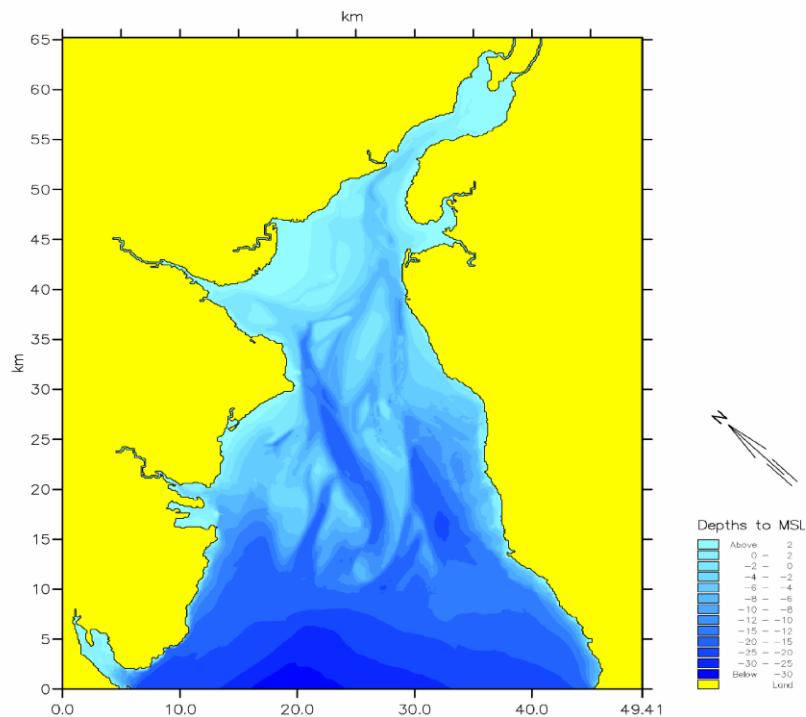


Figure 1: Solway Firth bathymetry (from Natural Power, 2002).

## Geology

Published information on the geology of the Eastern Irish Sea is scarce, although oil companies may hold significant amounts of data. Sheets published by the British Geological Survey include:

- 54N 04W: Lake District (Solid Geology);
- 54N 04W: Lake District (Seabed Sediments & Quaternary/Drift Deposits);
- 53N 04W: Liverpool Bay (Solid Geology);
- 53N 04W: Liverpool Bay (Seabed Sediments & Quaternary/Drift Deposits).

Note the separation into Solid Geology (bedrock) and Seabed Sediments and Quaternary/Drift Deposits. The Quaternary period is the most recent interval of Earth history (extending from about 2 million years ago to the present day). It is characterised by repeated extreme variations between glacial and inter-glacial climates.

There has been a very large global rise in sea level over the last 13,000 years (of the order of 60m). Tooley (1974) provides details for North West England, showing a rise of 20m during the last 9,000 years.

The general directions of bottom currents in the Eastern Irish Sea are shown in Figure 2. Together with the wave-driven currents at the coast, they strongly influence sediment transport patterns in the region. Note the tendency for sediment transport towards the estuaries. Following the large rise in sea level, estuaries have been infilling with sediment to compensate for their over-deepening during the last Ice Age.

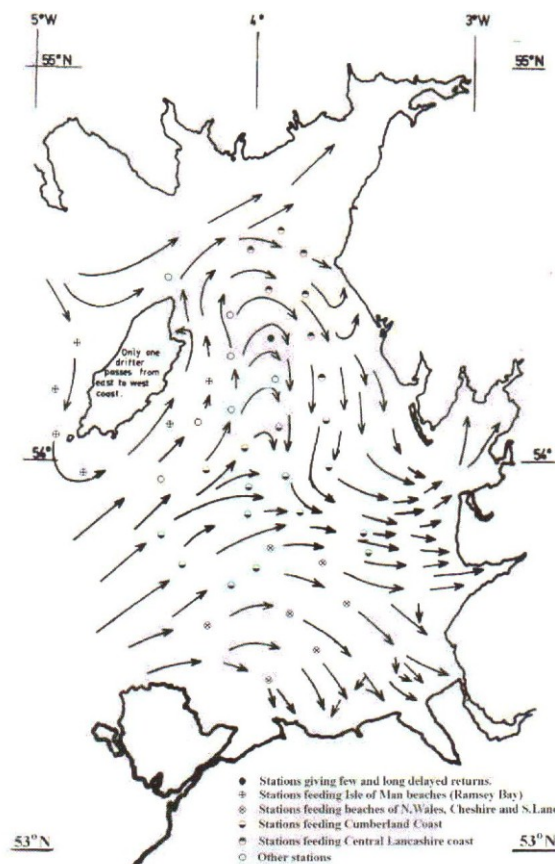


Figure 2: Bottom currents in the Eastern Irish Sea (from Sefton Council, 2003).

Figure 3 shows some available borehole information for the proposed Mersey Barrage. The boreholes confirm the soil variability implied by the periods of glaciation and the large rise in sea level over the past 9,000 years. Note the great variability in the elevation of the bedrock. It demonstrates the problem of having very few boreholes in the estuaries of the Eastern Irish Sea when attempting to define suitable barrage configurations at the conceptual stage of design.

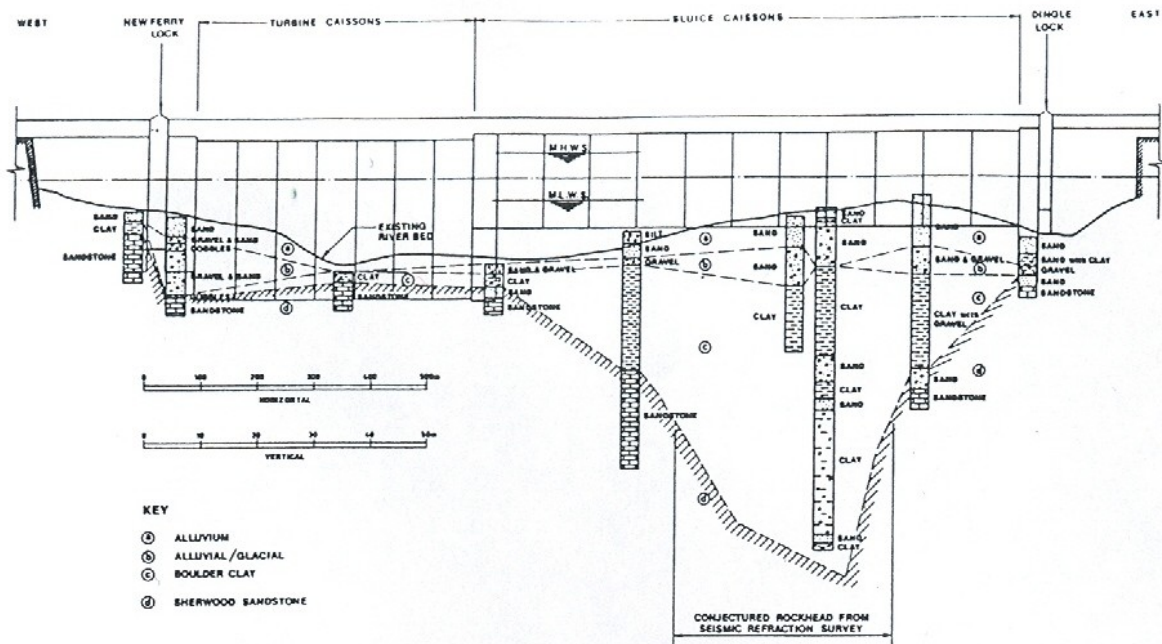


Figure 3: Borehole information for the proposed Mersey Barrage (from Jones et al, 1992).

### Hydraulic Loadings

The main hydraulic loadings on the barrages will be from tides and waves. The spring tidal range within the Eastern Irish Sea varies from less than 5m in the west of the area (e.g. at Holyhead and Port Erin) to more than 8m in the east (e.g. at Heysham and Liverpool). Whilst a large tidal range is a fundamental requirement for large power generation, it is also an engineering challenge with regard to ensuring satisfactory foundations for the various barrage elements (see later).

Barrages in the Eastern Irish Sea will be exposed mainly to wind-waves generated locally within the Irish Sea. In Liverpool Bay (Figure 4), the annual maximum significant wave height is about 5.5m. The northern end of the Eastern Irish Sea is somewhat more exposed. The extreme wave heights acting on barrage elements will depend upon local conditions, including the bathymetry.

While the strongest winds in the area are from the west, the barrages will largely be protected by Ireland from direct wave action from the Atlantic Ocean. Nevertheless, longer period waves associated with distant storms will arrive from the Atlantic Ocean through St George's Channel and the North Channel. Consequently, the structures will sometimes be subject to the action of bimodal sea conditions (Hawkes et al, 1997). The action of long period waves could have some effect on the performance of turbines and on tidal-stream devices.



Figure 4: Site location (from Reis et al, 2006).

### Foundations

Various issues must be addressed with regard to the foundations of the barrage elements, taking into account the large head differences which are expected (see schematic diagram, Figure 5). Note that the resultant loading from the head difference can be reversed, as can the direction of seepage.

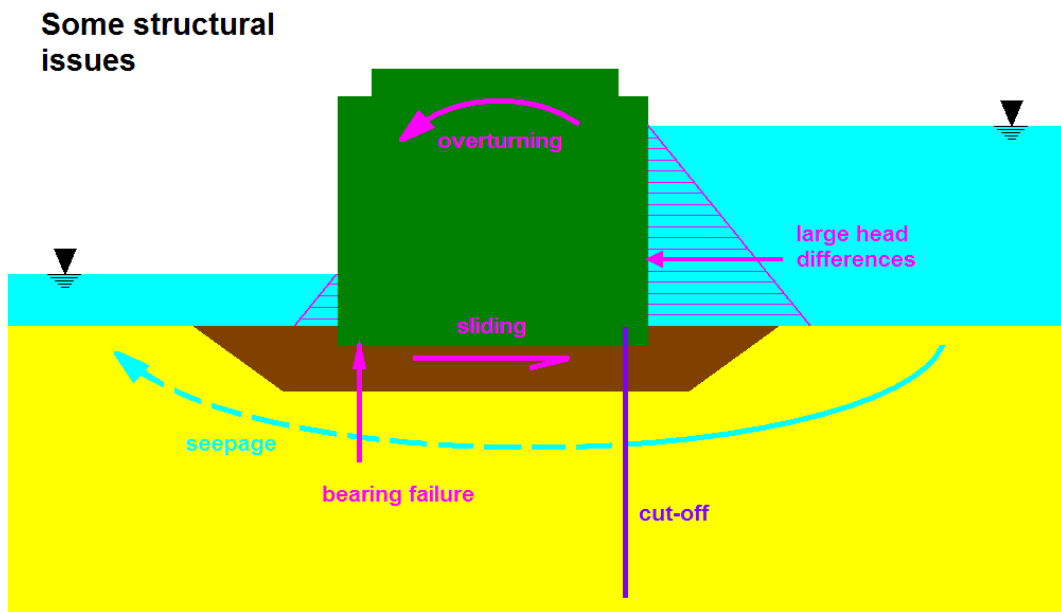


Figure 5: Some structural issues.

Most of the water available for power generation (especially in the Dee and Ribble estuaries) is above 0mOD (see schematic diagram, Figure 6). So this volume should (ideally) all be used to greatest effect. Water cannot be drained through turbines which are set too high. But the existing deep-water channels are often narrow, inhibiting the provision of turbines, sluices and locks. However, advantage may be taken of the fact that dredging is probably necessary for the foundations. Dredging will allow the turbines to be lowered. In this case, flow to and

from the turbines will widen or deepen existing channels or will scour new ones. This possibility should be borne in mind when establishing the relative locations of the turbines, sluices and locks.

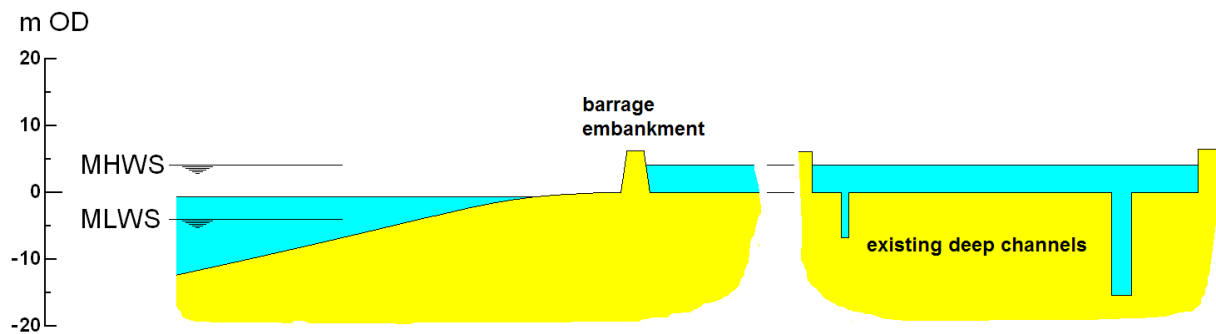


Figure 6: General bed levels in some estuaries are high, limiting the available water for power generation.

A number of possibilities exist with regard to construction of the foundations of barrage elements. They include:

- compaction of suitable existing seabed material (e.g. fine sand and coarser sediments);
- removal by dredging of unsuitable material (e.g. silt);
- protection of erodible bed material using granular filter layers and rock armour where necessary (i.e. in areas of fast flowing water or significant wave activity);
- installation of geotextile membranes beneath granular layers to reduce the required number of filter layers;
- installation of sheet pile cut-off walls or rock grouting to limit seepage beneath the barrage.

An additional benefit of the ability to dredge the estuaries is the possibility of developing sediment traps for the coarse particles at strategic locations around the barrage. A sediment trap is an area designed to collect sediment transported in run-off or during flooding of the basin from the sea. It does so by reducing the flow velocity. Sediment traps may be used to reduce more widespread siltation, but they are unlikely to trap a significant fraction of fine material.

### **Barrage Sites**

Alignments already proposed in earlier studies for the Dee, Mersey, Morecambe Bay and the Solway Firth seem appropriate (UKAEA, 1980 and 1984). Consequently, estimated power outputs using these alignments have been updated.

The estimated output for the Ribble has been checked (Section 3.4) using a north-south barrage alignment from Saltcotes to Banks. Supplementary benefits associated with transport links and flood control may be as important as (or even more important than) power generation in justifying a barrage in the shallow estuary of the Ribble.

Finally, the original alignment for the Dee estuary has been modified to include a lagoon encompassing the Great Burbo Flats and the East and West Hoyle Banks. It would provide the additional benefit of controlling wave activity and currents around any wind farm built within this envelope. Such a lagoon would also provide both a major leisure facility and significant benefits with regard to flood defence along the North Wirral coast. Wave

overtopping of well-designed lagoon embankments would generally be of little concern, whilst overtopping of coastal seawalls is a hazard to people, property and vehicles.

### ***Barrage Construction***

Barrage construction is expected to comprise reinforced concrete caissons, constructed in shore-based facilities, possibly combined with embankments armoured with rock or pre-cast concrete units protecting a core of hydraulic sand fill (or other suitable material), with filter layers to prevent leaching of the core material. Barrages would have a very noticeable effect on lee-side wave conditions, as well as moderating extreme water levels, thereby improving security from coastal flooding. Nevertheless, lee-side armour would be required on embankments to protect against waves generated within the basin. Many of the proposed barrages have substantial lee-side fetches.

Concrete caissons used in barrage construction would essentially be of three or four types, depending upon the requirements at individual sites:

- turbine caissons to house the turbine generators and associated equipment;
- sluice caissons to house gates for allowing water through the barrage;
- plain caissons, to link the others; and, if necessary,
- lock caissons for the passage of commercial shipping and pleasure craft.

Caissons would be floated to site and sunk onto prepared foundations. The crest widths of the turbine, sluice and plain caissons and of any embankments would be sufficient to accommodate transmission cables and, where appropriate, road and/or rail links. Crest levels would be chosen with regard to the need to prevent excessive wave overtopping.

Breakwaters may be required seaward of locks, depending upon the degree of natural protection which is provided within estuaries. The breakwaters may consist of plain caissons or be of rubble-mound construction. Dolphin structures, to assist in guiding vessels, would be needed adjacent to the locks.

### ***Construction Costs***

The principal physical resources needed for construction of a tidal power barrage are:

- cement and reinforcing steel;
- good quality rock as embankment armouring, aggregate for concrete, etc;
- fabricated steel for sluice gates, lock gates, etc;
- turbines and generators;
- deep-water construction sites for caissons;
- construction plant;
- labour.

Construction inflation is not the same as general inflation: it is highly dependent on demand and is also affected by specific technological advances within the industry. Nevertheless, general inflation may provide a reasonable guide to construction inflation.

Table 1: UK inflation, 1978 to 2007.

Year	UK Inflation Rate (%)	£
1978	-	1.00
1979	13.41	1.13
1980	17.97	1.34
1981	11.86	1.50
1982	8.59	1.63
1983	4.63	1.70
1984	4.95	1.78
1985	6.09	1.89
1986	3.40	1.96
1987	4.16	2.04
1988	4.91	2.14
1989	7.76	2.31
1990	9.46	2.52
1991	5.87	2.67
1992	3.75	2.77
1993	1.59	2.82
1994	2.42	2.88
1995	3.47	2.98
1996	2.41	3.06
1997	3.14	3.15
1998	3.43	3.26
1999	1.53	3.31
2000	2.96	3.41
2001	1.76	3.47
2002	1.67	3.53
2003	2.89	3.63
2004	2.98	3.74
2005	2.84	3.84
2006	3.17	3.96
2007	4.29	4.13

Table 1, derived from <<http://www.measuringworth.com/inflation/>>, shows that between the beginning of 1979 and the beginning of 1983, general costs increased by a factor of 1.63, consistent with the updating of scheme costs in the Preliminary Study of Small Scale Tidal Energy (UKAEA, 1984). This report gave cost escalation factors ranging from 1.494 (for turbines and transmissions) to 1.663 (for embankments) in order to update costs from March 1979 to January 1983. The estimated costs, at January 1983 prices, of various proposed schemes are given in Table 11.2 of Tidal Power (Baker, 1991). To update costs from 1983 to 1990, Baker suggested a multiplication factor of 1.6. General inflation would suggest a cost escalation factor of  $2.52/1.63 = 1.55$  between January 1983 (the end of 1982) and December 1990, in good agreement with Baker's estimate. Likewise, between the beginning of 1988 (the end of 1987) and the end of 2001, the cost escalation factor would be  $3.47/2.04 = 1.70$ . This figure is only a little higher than the range 1.4 to 1.6 given in the ETSU Report (Taylor, 2002) to update EP57 costs for the Severn Barrage (Department of Energy, Central Electricity Generating Board and the Severn Tidal Power Group, 1989), estimated in April 1988 according to EP57 (but January 1988 according to the ETSU Report). The most recent updating of construction costs for the Severn (Cardiff-Weston) Barrage was given by the Sustainable Development Commission (2007): £15,066M at 2006 prices. This figure may be compared with the EP57 estimated cost, in April 1988 money terms, of £8,280M, giving a cost escalation factor of  $15,066/8,280 = 1.82$ . According to Table 1, general costs rose in a similar period, the end of 1987 to the end of 2005, by a factor of  $3.84/2.04 = 1.89$  and from the end of 1988 to the end of 2006 by a factor of  $3.96/2.14 = 1.85$ . Thus updating costs for

the Severn barrage to January 2008 on the basis of general UK inflation rates seems reasonable, resulting in:

Table 2: Severn barrage construction costs.

Scheme	Cost in 2006 (£M)	Cost in 2008 (£M)
Severn	15,066	16,210

Updating the January 1983 costs of barrage construction given by Baker for north-west schemes provides the following figures (Table 3) for January 2008 (assuming a cost escalation factor of  $4.13/1.63 \approx 2.53$ ):

Table 3: North West barrage construction costs.

Scheme	Cost in 1983 (£M)	Cost in 2008 (£M)
Solway Firth	7,480	18,950
Morecambe Bay	3,610	9,145
Mersey	697	1,765
Dee	1,230	3,115

### **Other Costs**

Besides construction costs directly associated with barrages, there would be additional costs needed to reinforce the electricity transmission system. However, this reinforcement would benefit the transmission grid as a whole. Consequently, there is particular difficulty in assigning grid reinforcement costs to individual schemes.

There would also be annual operating, maintenance, repair and replacement costs. Costs associated with public road access or other transport links would also be extra, the exact amount depending upon the required links to existing infrastructure.

### **Other Benefits**

Barrages could also offer major socio-economic benefits to the North West of England and, in the case of the Solway Firth, to Dumfries and Galloway. Potential benefits include:

- improvements in flood defence (see Section 5.7);
- potential improvements in transport links;
- associated increases in land values;
- employment creation from barrage construction; and
- a regenerative effect on the region, including tourism.

Furthermore, whilst construction of barrages would be certain to have ecological impacts on the estuaries, and some of these impacts may be harmful (at least in the short term), others could be beneficial. For example, a reduction in wave activity in the lee of a barrage may lead to significant improvements in salt marshes.

### **Cost, Price, Value or Worth and Issues Related to Discounting**

The cost of a product or service is the amount which is spent to produce it. The price is the financial reward for providing the product or service, whilst the value is what the customer believes the product or service is worth to them. The price of electricity depends principally on demand. Industrialised countries have a high demand for electricity. In contrast, people

exist in many parts of the world with little or no access to electricity and little ability to pay for it, even if it were available. It is assumed that households in the UK will always give a high priority to using electricity, almost regardless of price.

Discounting is used to compare alternative investments which have different cash flows (i.e. costs and incomes arising at different times). If £100 is deposited in a bank at 5% interest rate, then it will pay for something costing  $£100 \times 1.05 = £105.00$  in a year's time, for something costing  $£100 \times 1.05^2 = £110.25$  in two years' time, or  $£100 \times 1.05^n$  in n years' time. In the same way, present values can be attributed to future income (i.e. the future income can be 'discounted' to a present worth). Thus, £100 income in one year's time is worth  $£100/1.05 = £95.24$  if the discount rate is 5%, or  $£100/1.10 = £90.91$  if the discount rate is 10%. More generally, the present worth, P, of a future sum, S, arising in n years' time is given by  $P = S/(1+r)^n$ , where r is the discount rate.

It follows from the above calculations that the higher the discount rate, the lower is the present worth of future income. As a consequence, the economics of long-term investments tend to be dominated by the selected discount rate. A high discount rate will tend to favour power-generating plant with lower initial costs, even though it may have high running costs and a short life, over plant with high initial costs, low running costs and a long life.

A tidal power station uses a renewable and reliable source of energy and should have a long working life. But the discounting process might attribute little value to these advantages because electricity produced in 50 or 100 years' time appears to have little present worth at high discount rates, whereas the real value of electricity could be very large in a future where oil and gas are in short supply and there are concerns about the greenhouse effects of CO<sub>2</sub> discharges. To account for the advantages of a reliable and renewable resource, additional value (beyond that attributed using high discount rates) might be assigned to the generation of electricity by a tidal power station. Alternatively, a lower discount rate could be adopted than for normal commercial purposes when assessing projects of low risk with a guaranteed source of revenue (see, also, Sustainable Development Commission, 2007).

### **Costs of Barrage Elements**

Table 2.1 in EP57 for the Severn Barrage gives the estimated costs of construction in £M at 1988 prices. Costs are broken down as follows:

- civil works, including caisson construction, dredging, foundations, caisson installation, embankments and breakwaters, substations, service roads, and contingencies;
- turbines, generators and ancillary plant, including design, capital plant, manufacturing, transport to site, installation and commissioning, and contingencies;
- on-barrage transmission and control including manufacturing, delivery, installation, commissioning and contingencies;
- associated activities, including feasibility studies, parliamentary and environmental issues, land and urban drainage, sea defence, effluent discharge, port works and compensation.

The figures for civil works alone are as follows:

	£M (1988 figures)
<b>Caisson construction</b>	
• construction yards	339
• turbine-generator caissons (54 no., 4.3km)	1,082
• sluice caissons (46no., 4.1km)	326
• plain caissons	270

• lock caissons	81
• breakwater caissons	86
• steelwork fabrication and installation	580
Dredging	380
Foundations	377
Caisson installation	148
Embankments and breakwaters	382
Substations	65
Service roads	141
Contingencies (15% of above costs)	639
CIVIL WORKS TOTAL =	4,896

The 54 turbine-generator caissons would house 216 turbine-generator sets with the following costs, including installation and commissioning:

	£M (1988 figures)
Turbines, generators and ancillary plant	2,302
Contingencies (5% of above costs)	115
TURBINES/GENERATORS TOTAL =	2,417

Thus, the total cost of turbine-generator provision, including caisson housing but excluding the cost of construction yards, dredging, foundation works and installation (which are required regardless of caisson type), is £1,082M + £2,302M = £3,384M. Assuming that all of the steel fabrication and installation costs relate solely to the sluice gates (some will relate to locks, etc), then the cost of completed sluice caissons, again excluding construction yards, dredging, foundation works and installation, is £326M + £580 = £906M. The equivalent cost for plain caissons is £270M. This gives cost ratios for the three completed types of caisson as: £3,384M: £906M: £270M (16.35: 4.38: 1.00).

The lengths of the various forms of construction are given as: turbine-generator caissons, 4.3km; sluice caissons, 4.1km; 'other' caissons (taken to include plain and lock caissons, but excluding breakwater caissons), 3.9km; and embankments, 3.6km. The total length of the barrage is given as 4.3km + 4.1km + 3.9km + 3.6km = 15.9km. Thus, the costs per kilometre of finished construction (again excluding the cost of construction yards, dredging, foundation works and caisson installation) are: turbine-generator caissons, £3,384M / 4.3km = £786.98M/km; sluice caissons, £906M / 4.1km = £220.98M/km; other caissons, (£270M + £81M) / 3.9km = £90.00M/km; and embankments, £382M / 3.6km = £106.11M/km. In terms of cost ratios per kilometre of construction, the above figures give 8.74: 2.46: 1.00: 1.18. Note that the figure for embankments is conservative as any cost associated with breakwaters under the heading 'Embankments and breakwaters' has been ignored on the assumption that most breakwater construction will involve breakwater caissons which were excluded from the sum for 'other' caissons. Note also that embankment construction is limited to the relatively shallow depths at the landward ends of the barrage whilst the breakwaters would be in deeper waters.

The dominance of the costs for the turbine-generator sets and the associated caissons over the other elements of barrage construction shows that correctly establishing the number of turbine-generator sets is fundamental to the economics of tidal barrage schemes.

Figure 11.1 in Tidal Power (Baker, 1991) gives a good indication of the number,  $N$ , of sets required once the runner diameter,  $D$ , is established from the minimum depth of water at the barrage site if schemes are to provide electricity at minimum unit cost (which formed the basis of the 1980's studies). Note, however, that providing electricity at minimum unit cost may not be the correct goal in an era in which there are growing concerns about the greenhouse effects of CO<sub>2</sub> discharges.

### **Concluding Remarks**

- Construction of barrages in the Eastern Irish Sea would have major socio-economic benefits for the North West of England and, in the case of the Solway Firth, for Dumfries and Galloway.
- Barrage construction is expected to comprise reinforced concrete caissons combined with embankments armoured with rock or pre-cast concrete units protecting a core of sand fill, with filter layers to prevent leaching of the sand.
- All potential barrage sites in the Eastern Irish Sea would be in locations affected by glaciations and have superficial (and possibly extensive) alluvial deposits. Dredging and/or seabed treatment such as vibro-compaction would be necessary for the structural integrity of the barrage elements at all locations and may be extensive at many locations. However, dredging may also make it possible to accommodate turbine, sluice and lock arrangements which are more convenient than those originally proposed. Such opportunities would be limited only by the solid geology (i.e. the bedrock), as in the case of the Mersey.
- Suitable dredged material would be required for construction of barrage embankments, for ballasting caissons, etc. Considerable amounts of rock or other armour would also be needed to cope with the present annual maximum significant wave height in the Eastern Irish Sea of 5.5m or more.
- Wind wave and swell activity may have important implications for the vertical location of the turbines. Allowances would need to be made for expected changes in water levels and wave activity over the lifetime of each barrage.
- The barrage lines originally proposed for the Dee, Mersey, Morecambe Bay and Solway Firth appear appropriate and the original estimated power outputs using these alignments have been updated (see elsewhere in the report).
- The costs of various barrage schemes have been updated to January 2008 using UK general inflation rates. This approach results in costs which are generally consistent with earlier updates, despite the fact that construction inflation is not the same as general inflation: it is highly dependent on demand and is also affected by specific technological advances within the industry.
- Tidal power stations use a renewable and reliable source of energy and should have a long working life. But the process of discounting in the economic evaluation of schemes may attribute little value to these advantages. To account for the advantages of a reliable and renewable resource, additional value might be assigned to the generation of electricity by a tidal power station. Alternatively, a lower discount rate could be adopted than for normal commercial purposes when assessing projects of low risk with a guaranteed source of revenue.
- The dominance of the costs for turbine-generator provision, including caisson housing, over the other elements of barrage construction shows that correctly establishing the number of turbine-generator sets is fundamental to the economics of tidal barrage schemes.

- Construction of barrages in the estuaries of the Eastern Irish Sea would have ecological impacts on the estuaries. Some impacts may be harmful (at least in the short term) whilst others may be beneficial.
- There would be other significant non-energy benefits associated with the construction of barrages, including potential improvements in transport links, associated increases in land values, employment creation from barrage construction and a regenerative effect on the region, including tourism.

## **References**

- Baker AC, 1991. Tidal Power, Institution of Electrical Engineers Energy Series 5, Peter Peregrinus Ltd, London.
- Department of Energy (DoEn), Central Electricity Generating Board (CEGB) and Severn Tidal Power Group (STPG), 1989. The Severn Barrage Project: General Report, Energy Paper Number 57 (EP57), HMSO, London.
- Hawkes PJ, Bagenholm C, Gouldby BP and Ewing J, 1997. Swell and Bi-Modal Wave Climate Around the Coast of England and Wales, Report SR409, HR Wallingford: Wallingford.
- Jones BI, Morgan CDI, Phillips D and Pinkney MW, 1992. Tidal Power: Trends and Developments (ed. Clare R), Institution of Civil Engineers, London, 27-47.
- MeasuringWorth.com, 2008. <<http://www.measuringworth.com/inflation/>>, accessed 05-August-2008.
- Natural Power, 2002. Environmental Statement Supporting Applications for an Offshore Windfarm at Robin Rigg.
- Reis MT, Hedges TS, Williams A and Keating K, 2006. Specifying seawall crest levels using a probabilistic method, Proceedings of the Institution of Civil Engineers, Maritime Engineering, 159(MA4), 137-145.
- Sefton Council, 2003. Guide to the Sefton Coast Database, <<http://www.sefton.gov.uk/default.aspx?page=4730>>, accessed 05-August-2008.
- Sustainable Development Commission (SDC), 2007. Turning the Tide: Tidal Power in the UK, Sustainable Development Commission, London, <[www.sd-commission.org.uk](http://www.sd-commission.org.uk)>.
- Taylor SJ, 2002. The Severn Barrage - Definition Study for a New Appraisal of the Project, ETSU Report No. T/09/00212/00/REP, Department of Trade and Industry.
- Tooley MJ, 1974. Sea-Level Changes During the Last 9000 Years in North-West England, The Geographical Journal, 140(1), 18-42.
- United Kingdom Atomic Energy Authority (UKAEA), 1980. Preliminary Survey of Tidal Energy of UK Estuaries, Severn Tidal Power Report STP-102, Binnie & Partners, London.
- United Kingdom Atomic Energy Authority (UKAEA), 1984. Preliminary Survey of Small Scale Tidal Energy, Severn Tidal Power Report STP-4035 C, Binnie & Partners, London.

# **Tapping the Tidal Power Potential of the Eastern Irish Sea**

## **APPENDIX 3**

comprising three separate documents:

- A.3.1 Barrage lines, cross sections and bathymetries
- A.3.2 Energy computation spreadsheets
- A.3.3 Costing calculations

**March 2009**

**[www.liv.ac.uk/engdept/tidalpower](http://www.liv.ac.uk/engdept/tidalpower)**

### A.3.1 Barrage lines, cross sections and bathymetries

#### Dee Estuary and Dee-Wirral Lagoon schemes

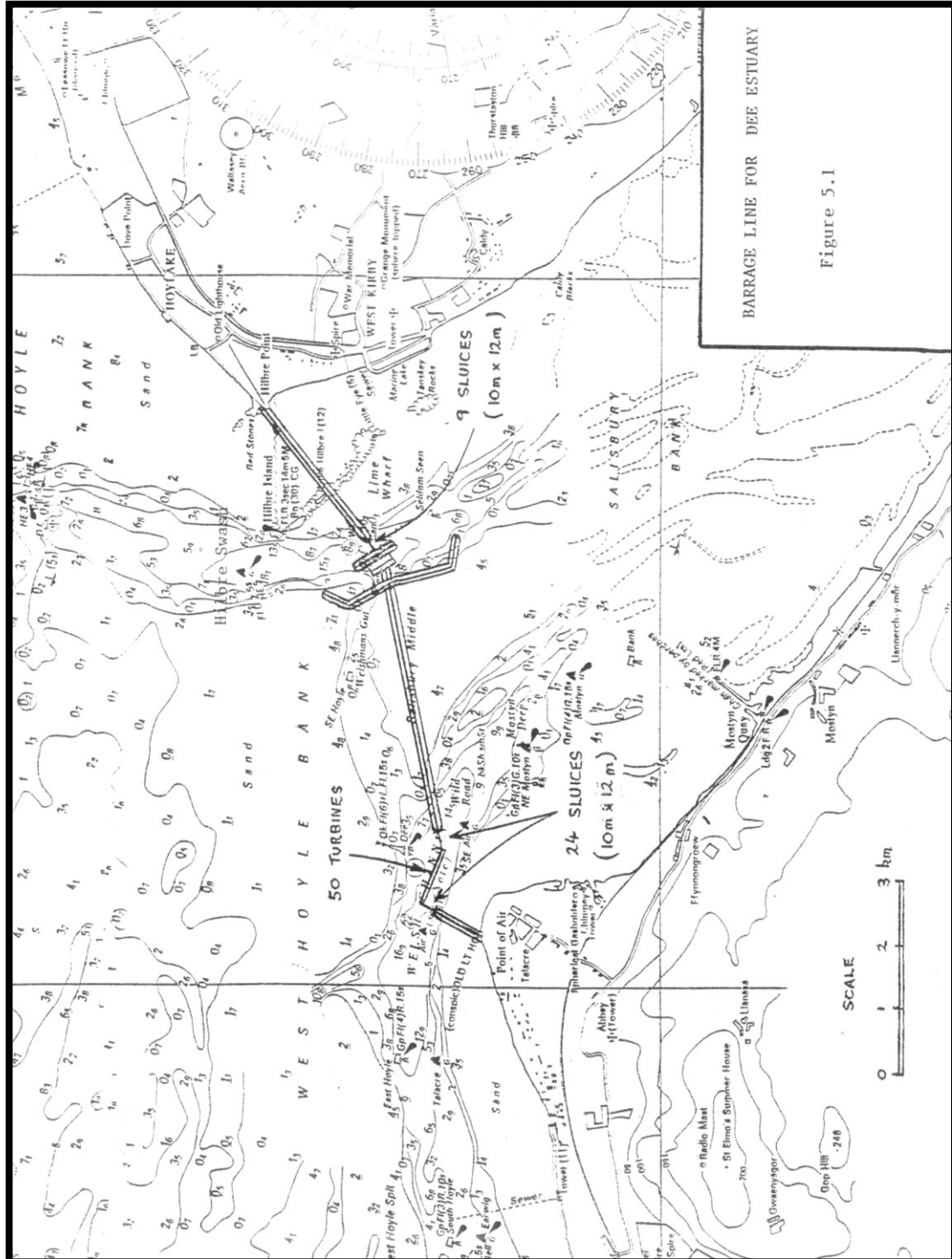


Figure 1: Dee (Inner) Barrage line from UKAEA (1980) report.

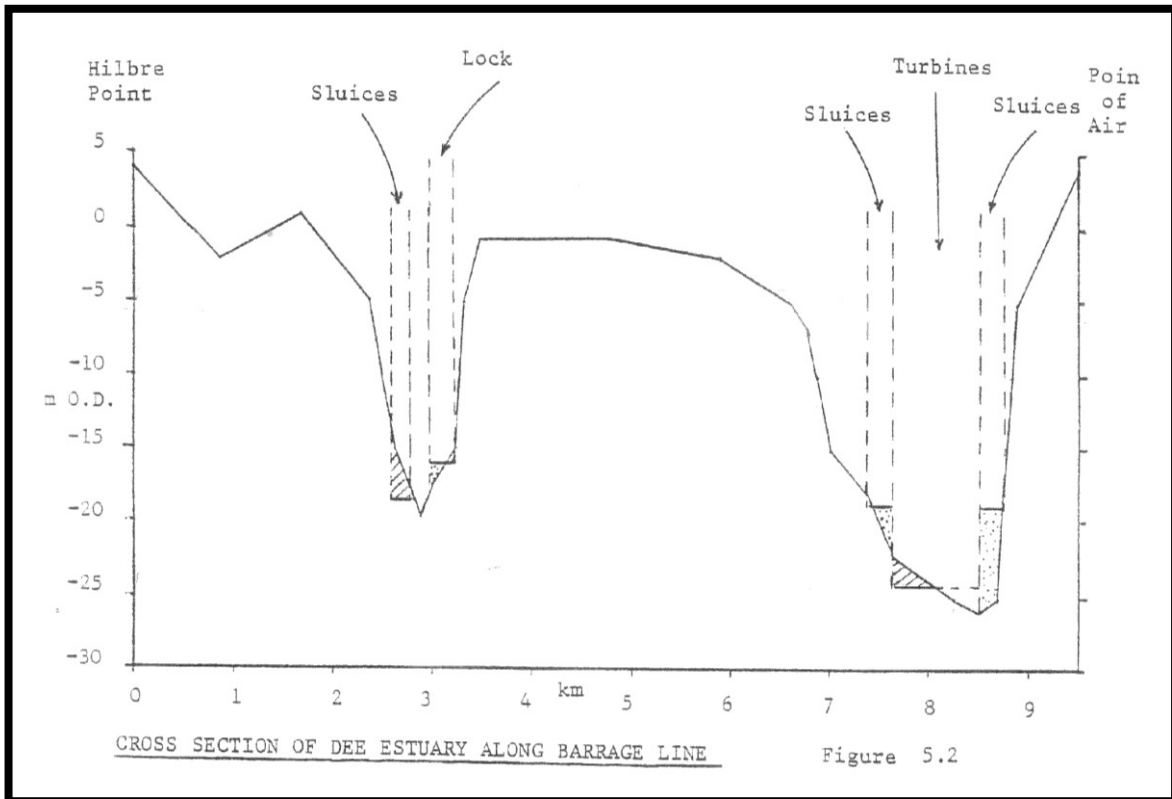


Figure 2: Dee (Inner) cross section along barrage line from UKAEA (1980) report.

Table 1: Dee (Inner) bathymetry from 2003 Lidar study.

Level above OD (m)	Surface area of water (km <sup>2</sup> )
-5	12.55
-4	16.48
-3	21.02
-2	28.85
-1	36.84
0	50.44
1	61.42
2	78.04
3	94.23
4	103.98
5	129.05

Table 2: Dee (Outer) / Dee-Wirral Lagoon bathymetry.

Level above OD (m)	Surface area of water (km <sup>2</sup> )
-5	103.51
-4	132.11
-3	159.03
-2	179.52
-1	193.8
0	210.65
1	223.15
2	241.04
3	258.72
4	269.85
5	295.2

Table 3: Dee (Inner) bathymetry from UKAEA (1980) study.

Level above OD (m)	Surface area of water (km <sup>2</sup> )
-2	27
0	50
+2	76
+4	109

# Mersey Estuary

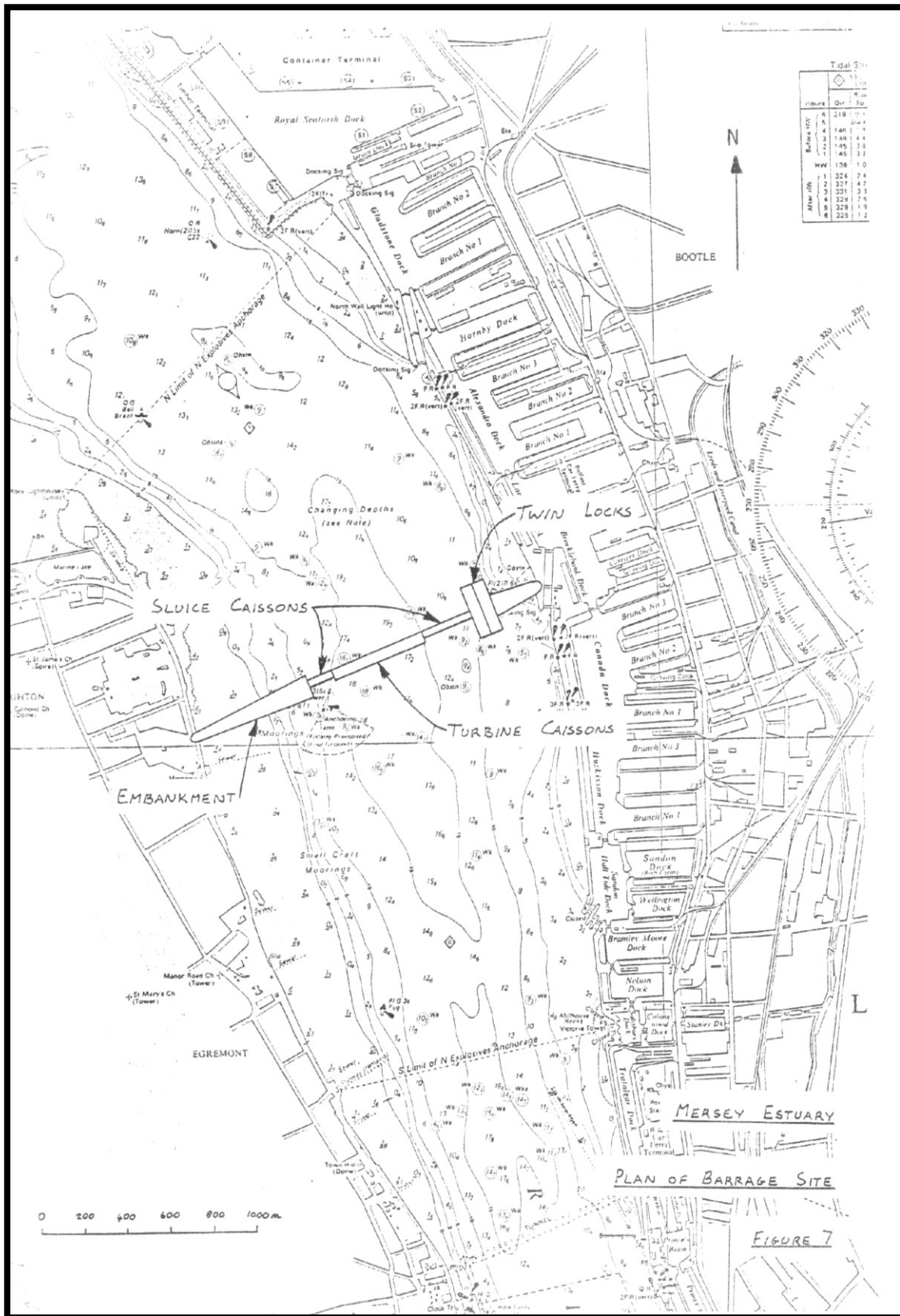


Figure 3: Mersey Barrage line from UKAEA (1984) report.

Table 4: Mersey bathymetry from 2003 Lidar study.

Level above OD (m)	Surface area of water (km <sup>2</sup> )
-5	5.97
-4	8.87
-3	13.71
-2	20.86
-1	28.95
0	38.48
1	47.1
2	53.37
3	59.75
4	63.13
5	66.37

Table 5: Mersey bathymetry from UKAEA (1984) study.

Level above OD (m)	Surface area of water (km <sup>2</sup> )
-5	16.53
-2.5	33.47
0	50.4
+2.5	67.34
+5.0	84.27

## ***Ribble Estuary***

Table 6: Ribble bathymetry.

Level above OD (m)	Surface area of water (km <sup>2</sup> )
-5	0
-4	0
-3	0.02
-2	0.45
-1	1.02
0	1.68
1	2.37
2	3.3
3	3.96
4	8.65
5	27

**Morecambe Bay**

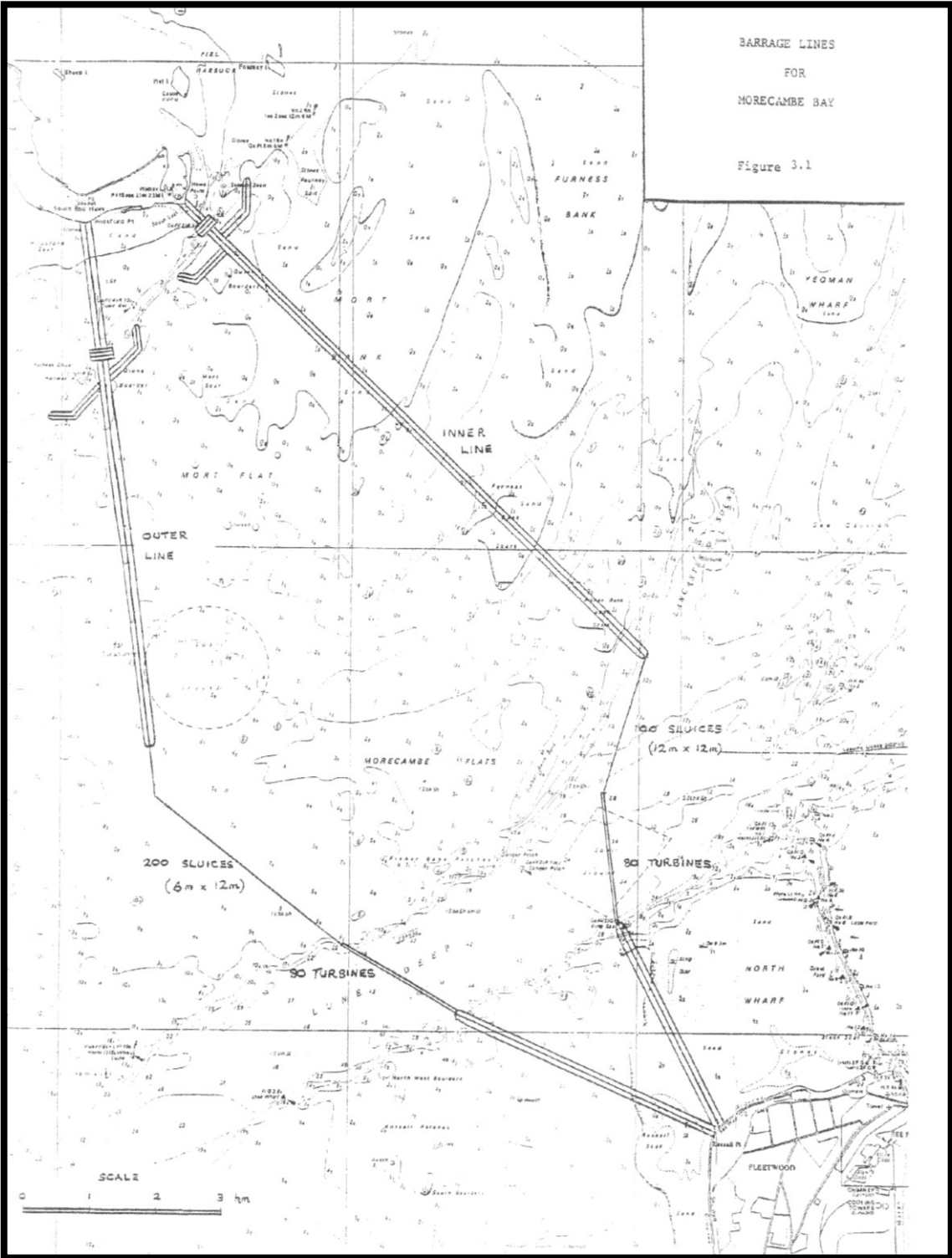


Figure 4: Morecambe Bay Barrage lines from UKAEA (1980) report.

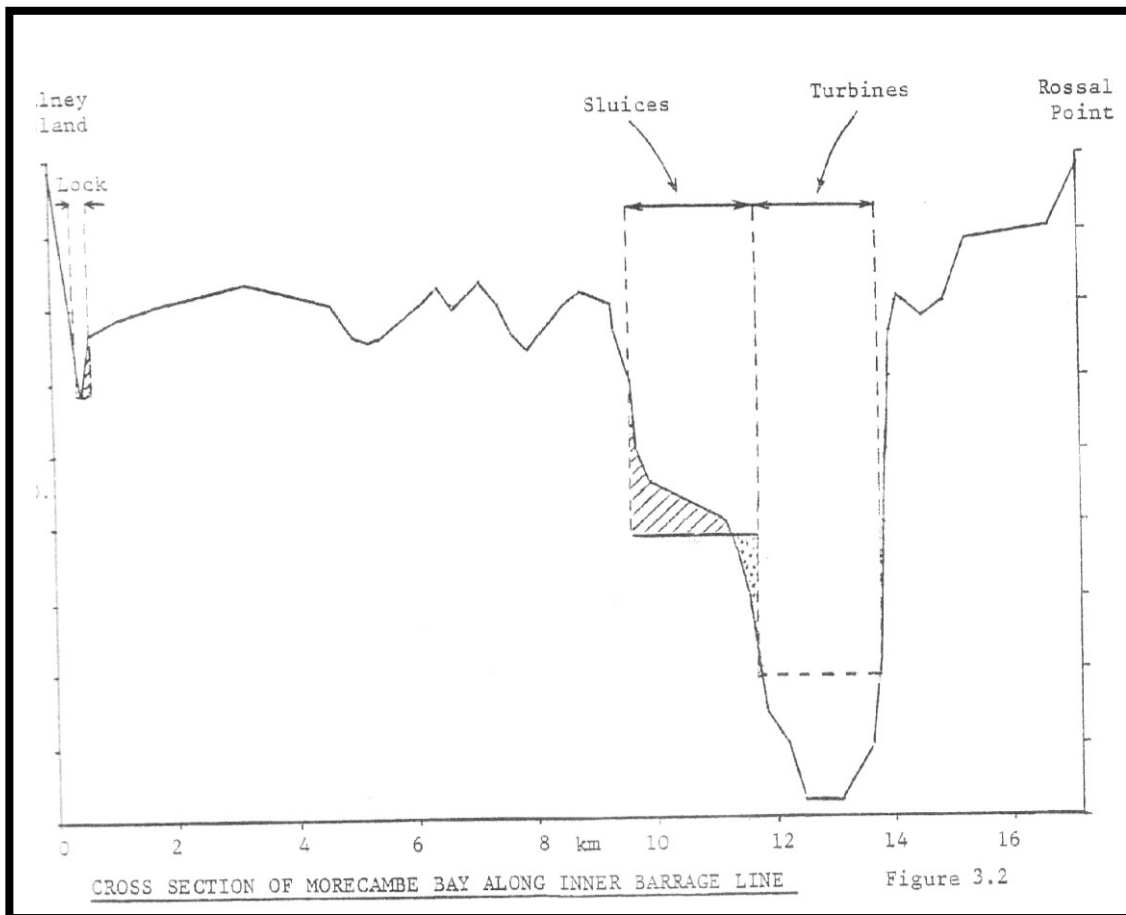


Figure 5: Morecambe Bay (Inner) cross section along barrage line from UKAEA (1980) report.

Table 7: Morecambe Bay (Outer) bathymetry from BODC data set.

Level above OD (m)	Surface area of water (km <sup>2</sup> )
-5	199.36
-4	221.84
-3	253.78
-2	291.66
-1	311.83
0	457.18
1	469.99
2	471.37
3	471.37
4	471.37
5	471.37

Table 8: Morecambe Bay (Outer) bathymetry from UKAEA (1980) study.

Level above OD (m)	Surface area of water (km <sup>2</sup> )
-4.9	157
0	297
+2.0	370
+4.5	455

# Solway Firth

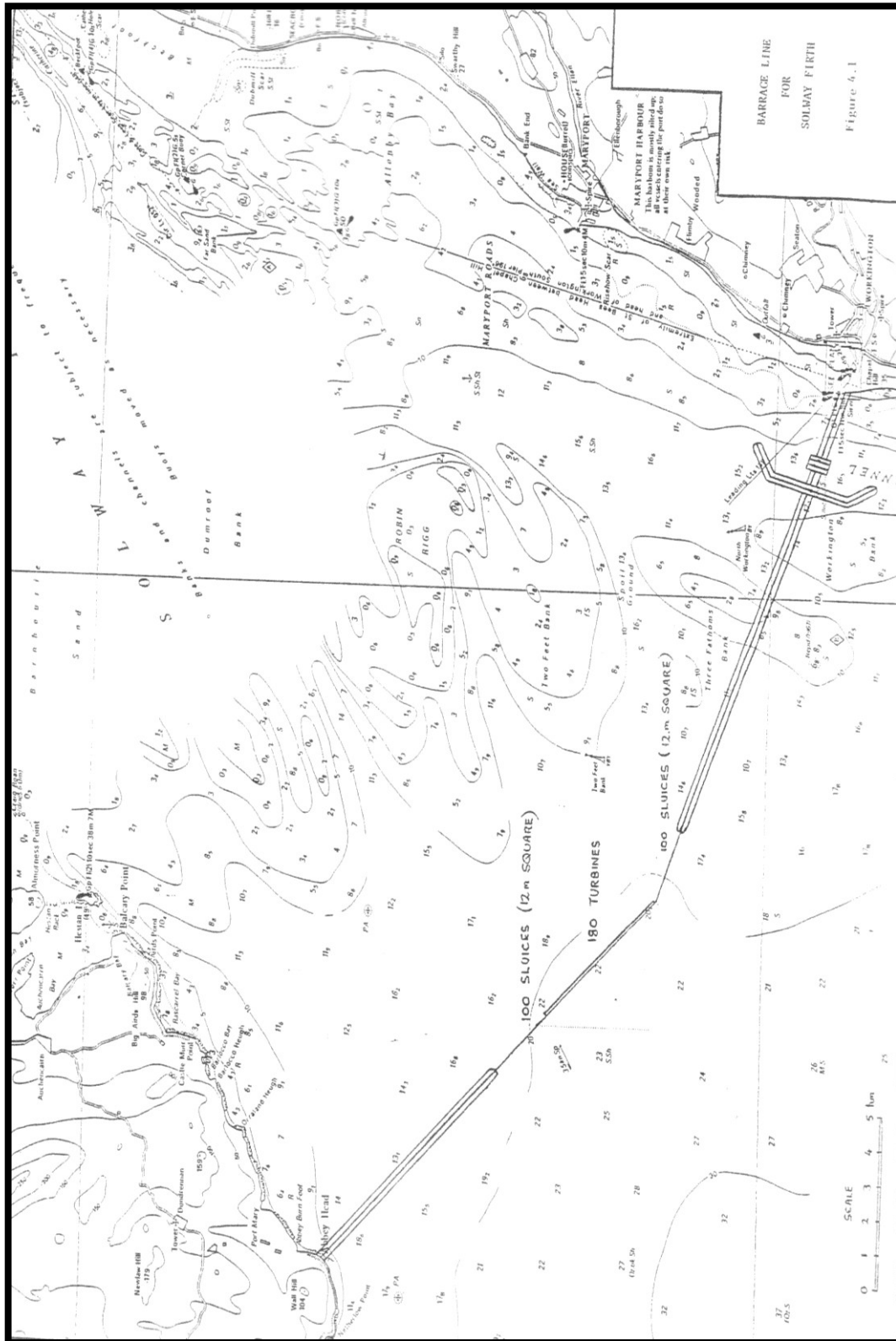


Figure 6: Solway Firth Barrage line from UKAEA (1980) report.

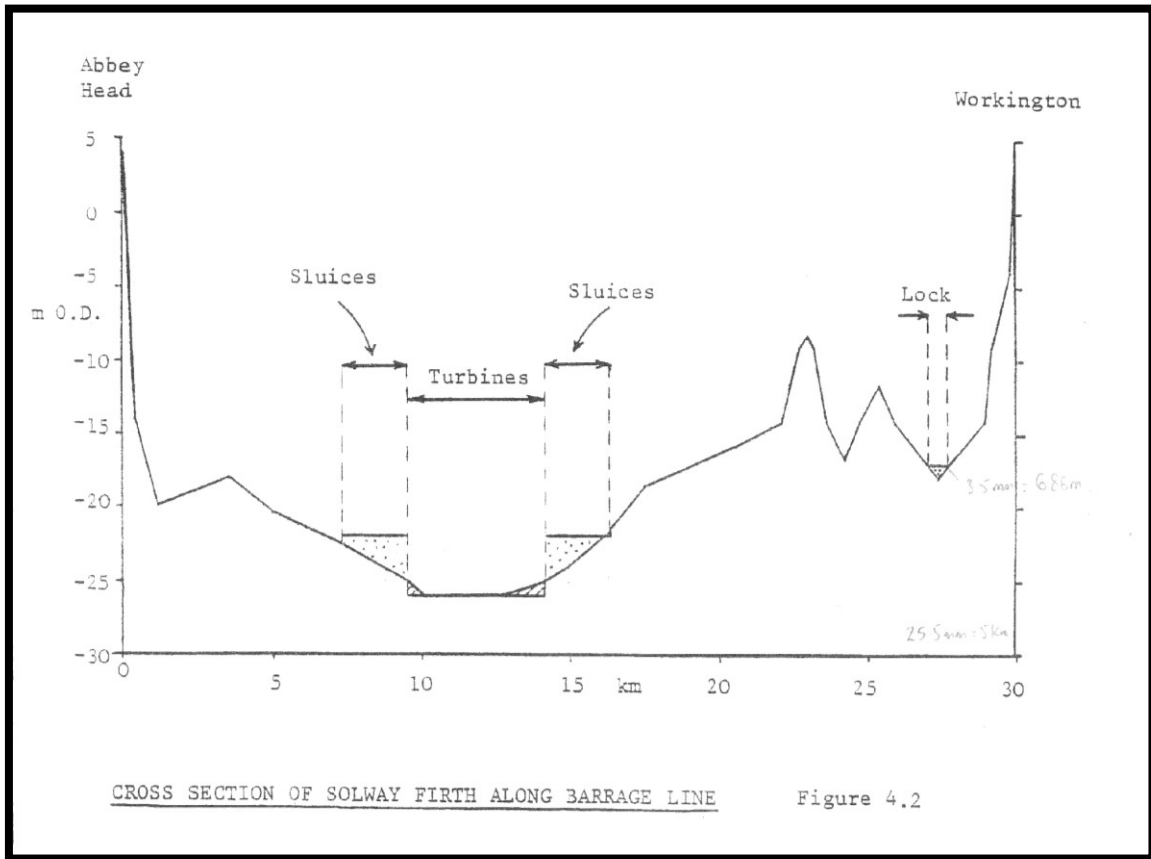


Figure 7: Solway Firth cross section along barrage line from UKAEA (1980) report.

Table 9: Solway Firth bathymetry from BODC data set.

Level above OD (m)	Surface area of water (km <sup>2</sup> )
-5	627.16
-4	739.82
-3	810.22
-2	885.88
-1	905.49
0	916.28
1	916.28
2	916.28
3	916.28
4	916.28
5	916.28

Table 10: Solway Firth bathymetry from UKAEA (1980) study.

Level above OD (m)	Surface area of water (km <sup>2</sup> )
-3.7	573
0	777
+3.7	887

**References**

United Kingdom Atomic Energy Authority (UKAEA), 1980. Preliminary Survey of Tidal Energy of UK Estuaries, Severn Tidal Power Report STP-102, Binnie & Partners, London.

United Kingdom Atomic Energy Authority (UKAEA), 1984. Preliminary Survey of Small Scale Tidal Energy, Severn Tidal Power Report STP-4035 C, Binnie & Partners, London.

### A.3.2 Energy computation spreadsheets

Table 1: Excel files containing data used in Section 3 of the report.

Location	File name	
Dee Estuary	Dee_costs	See Section 3.2.
	Dee_energy	
Mersey Estuary	Mersey_costs	See Section 3.3.
	Mersey_energy	
Ribble Estuary	Ribble_energy	See Section 3.4.
Morecambe Bay	Morecambe_costs	See Section 3.5.
	Morecambe_energy	
Solway Firth	Solway_costs	See Section 3.6.
	Solway_energy	

### A.3.3 Costing calculations

#### **General Comments**

To calculate the 2008 barrage and electricity costs from scratch would have been a complex and time-consuming exercise. A complete costing would require knowledge of the current prices for concrete, turbines etc., and also details of the ROC rate (Renewable Obligation Certificate) applicable to tidal energy, which is currently subject to some uncertainty. In addition, any such costs would have been out-of-date almost as soon as they had been assessed, due to the recent decline in economic activity and, hence, fall in commodity prices.

In order to give indicative unit costs of electricity and, hence, allow comparisons, barrage costs were taken from existing UK Atomic Energy Authority Reports (UKAEA, 1980 and 1984). Costs for the Mersey were taken from the 1984 report; the other estuaries were taken from the 1980 report. The costs for the Ribble were estimated from the 1984 report. Barrage costs were scaled for configurations different from the base UKAEA schemes, with embankment costs being altered to account for the length of additional sluices or turbines. Energy outputs for the barrage were those calculated in this study.

For calculations with turbine generators smaller than the UKAEA schemes, the turbine generator costs were reduced by the ratio of the generator power to the UKAEA specified power. The transmission costs were similarly reduced. For dual mode operation schemes, the turbine caisson, turbine and turbine generator costs were increased by 20%, in line with the 1981 Department of Energy study of the Severn (DoEn, 1981).

The 2007 unit cost of electricity was derived using the following formula:

$$\begin{aligned} & (\text{Cost of Barrage} / \text{Cost of UKAEA Barrage}) \times \\ & (\text{UKAEA Energy Output} / \text{Energy Output of Barrage in this study}) \times \\ & (\text{UKAEA Unit Cost of Electricity} / \text{Cost of Electricity of Severn Cardiff-Weston Line}) \times \\ & \text{SDC 2007 Unit Cost of Electricity for the Severn.} \end{aligned}$$

The Severn unit cost of electricity was taken as 3.56p/kWh, this being the price with a 3.5% discount rate and 5 year construction period.

No allowance was made for barrage maintenance costs in calculating the unit cost of electricity.

#### **Treatment of Specific Items**

Unless otherwise stated, all costs were taken from the 1980 UKAEA report (UKAEA, 1980).

##### Embankment costs

The length of an embankment was derived from the total length of the barrage in the UKAEA studies. The overall lengths of the turbine caissons, sluice caissons and locks were deducted from the barrage length to give the extent of the embankment, and hence the cost per unit length of the structure. This base length and cost were then reduced or increased in line with changes to the overall lengths of the turbine or sluice caissons. Lock lengths were estimated from the schematics in the UKAEA studies (see Appendix A.3.1).

The lengths of individual turbine caissons are noted in Table 1. Lengths not listed were derived by interpolation. The lengths of sluice caissons are given in Table 2.

Table 1: Lengths of individual turbine caissons (from the 1980 UKAEA report).

Turbine Diameter (m)	Caisson Length (m)
9	50
7.5	43
6	35

Table 2: Lengths of sluice caissons (from the 1980 UKAEA report).

Sluice Size	Sluice Caisson Length (m)
12m x 12m	64.5
10m x 12m	64.5
8m x 12m	64.5
6m x 12m	64.5

### Turbine costs

The UKAEA quoted a 1980 cost of £5M for a 9m diameter 60MW turbine, with 2/3 (£3.33M) for the turbine and 1/3 (£1.67M) for the generator. For turbines with different diameters, the turbine cost is assumed to be proportional to the ratio of the diameters. For different generators, the cost is taken as proportional to the rated power.

### Turbine gate costs

The 1980 UKAEA cost is £0.33M for a 12m x 12m gate suitable for a 9m diameter turbine. For smaller gates, the cost is assumed to be proportional to the square of the turbine diameter (i.e. scale with area).

### Sluice gate costs

The 1980 UKAEA cost is £0.33M for a 12m x 12m sluice gate. For smaller gates, the cost is taken to be proportional to the ratio of the area of the gates.

## ***Estuary Specific Treatments***

### Dee Estuary

The UKAEA costs were based on a 6m diameter turbine. It has been found that an 8m turbine was better conditioned, and so most of the runs were performed using this size of turbine. In order to amend the costs, the following adjustments were made:

- turbine caisson costs are expected to scale with volume, and so the costs were scaled by  $(\text{Length } 8\text{m caisson} / \text{Length } 6\text{m caisson})^3$ ;
- turbine costs were scaled on the ratio of the diameter;
- turbine gate costs were scaled on the square of the turbine diameter.

### Mersey Estuary

The 1984 UKAEA study gave no breakdown of the turbine costs into separate turbine and turbine generator components; nor did it split the gate costs for turbine and sluice gates. These were derived by apportioning the 1984 total cost on the ratio of what these items would have cost in 1980.

## **References**

Department of Energy (DoEn), 1981. Tidal Power From the Severn Estuary, Energy Paper No. 46, HMSO, London.

Sustainable Development Commission (SDC), 2007. Turning the Tide: Tidal Power in the UK, Sustainable Development Commission, London, <[www.sd-commission.org.uk](http://www.sd-commission.org.uk)>.

United Kingdom Atomic Energy Authority (UKAEA), 1980. Preliminary Survey of Tidal Energy of UK Estuaries, Severn Tidal Power Report STP-102, Binnie & Partners, London.

United Kingdom Atomic Energy Authority (UKAEA), 1984. Preliminary Survey of Small Scale Tidal Energy, Severn Tidal Power Report STP-4035 C, Binnie & Partners, London.

# **Tapping the Tidal Power Potential of the Eastern Irish Sea**

## **APPENDIX 4**

comprising one document in four parts:

- A.4.1 ADCIRC background
- A.4.2 Barrage operation in ADCIRC
- A.4.3 Tidal stream farms in ADCIRC
- A.4.4 Validation of simulation grid

**March 2009**

**[www.liv.ac.uk/engdept/tidalpower](http://www.liv.ac.uk/engdept/tidalpower)**

## **A.4.1 ADCIRC background**

### ***Introduction***

The ADCIRC model used is a 2-D depth-integrated shallow water model. Formulated in the generalized wave continuity form, it is solved using an unstructured grid approach for the discretisation of the mass equation and the momentum equation. The model was developed by Rick Leutlich and others (see Hench and Leutlich, 2003; Leutlich and Westerink, 1995) and is in widespread usage throughout the world. It has a particularly large user group in the USA where the US Navy are amongst the supporters of its development for tide and tidal surge predictions. ADCIRC is in constant development, with work ongoing in the areas of adaptive grids, sediment transport and biological processes.

The use of unstructured grids permits a large variation in the scale in regions of interest. Thus, it is easily possible to examine the effects of the tide within an estuary whilst applying the forcing in the deep ocean. The progression of the tide across the shelf and into the estuary may be followed throughout its course. A structured grid would restrict the grid scale to that of the estuary, which may be less than 50m, and this would make such a large study area impractical due to the computational cost.

In this study, the region of interest covers the Irish and Celtic Seas and, specifically for tidal range power production, the Severn and other major estuaries adjacent to these seas. Due to the impact of barrages and their influence upon the tidal hydrodynamics of the region, the forced boundaries must be far from the Irish and Celtic Seas. The effect of the barrages will be seen at their greatest within the estuaries in which they are placed and these must be accurately modelled. This requirement introduces a range of scales, from the order of 10km down to the order of 10m, which suggests the use of an unstructured grid. An unstructured grid also permits a high resolution in regions where tidal stream devices may be considered, such as off coastal headlands.

As this current study is based primarily upon the maximum potential tidal power yield from the Irish Sea, it was considered unnecessary to use a 3-D model, as the maximum potential power will be provided through tidal range devices (see the results in Section 4 and RSK Environmental Ltd, 2007). The operation of these devices is modelled accurately, in terms of power production, using only a 2-D model to obtain an accurate prediction of the varying water levels at the barrage sites. The extra computational time and cost involved using a fully 3-D model would not be justified by any increased accuracy of the results. In contrast, the potential output from tidal stream devices requires knowledge of the water velocities at their location and, due to the use of depth-averaged velocities, these will not be exactly captured. Nevertheless, the predicted power from these devices using a 2-D model is adequate for the purposes of the present study.

ADCIRC does not provide an inbuilt mechanism for modelling tidal range or tidal stream devices. As part of this project, the ability to simulate the operation of these devices has been added to the ADCIRC model. In the next section, a description is given of the process of model preparation. Descriptions of the methods used to simulate tidal range and tidal stream devices are then presented, together with some preliminary studies which provide some validation and proof of concept of the new additional simulation capabilities.

### ***Model Preparation***

The model preparation proceeds through a number of distinct steps. Initially the area of interest is defined and a range of datasets concerning this area are obtained. These datasets include the area's bathymetry (as shown in Figure 1), the tidal forcing conditions and the operational procedures and characteristic data for the tidal devices under consideration (as shown in Figure 2 for a tidal barrage turbine).

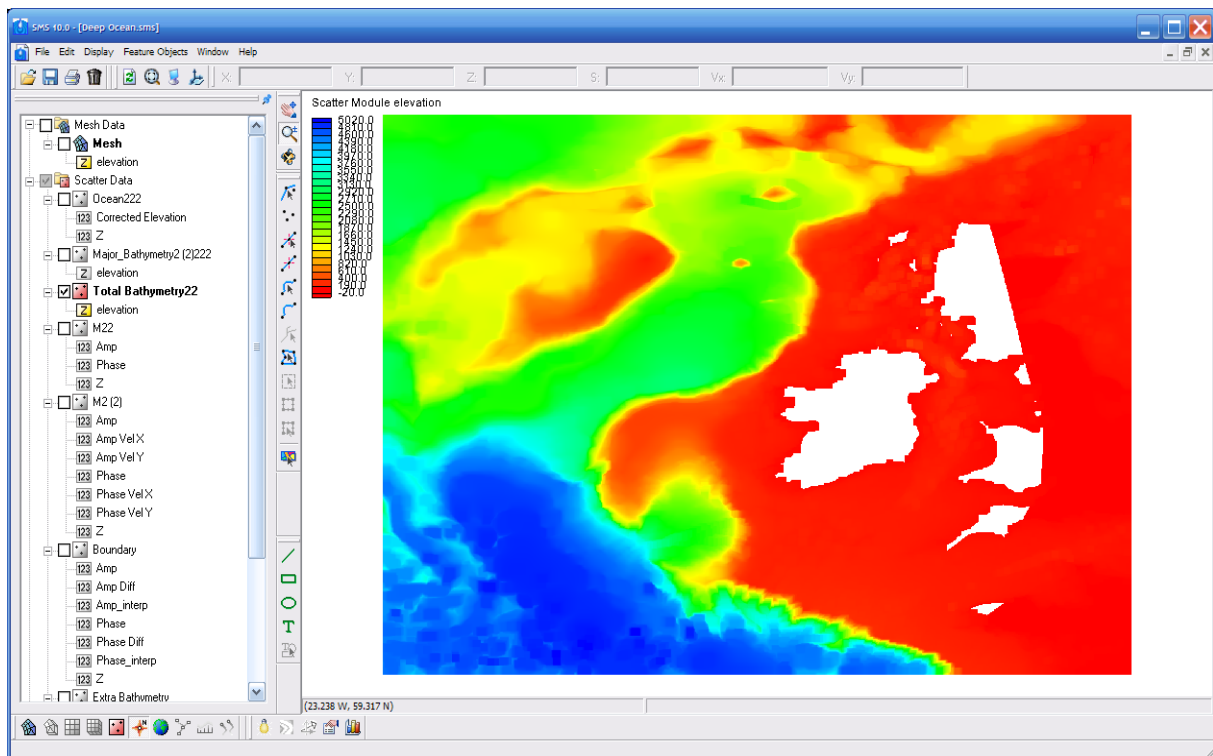


Figure 1: Bathymetry of area as seen in SMS.

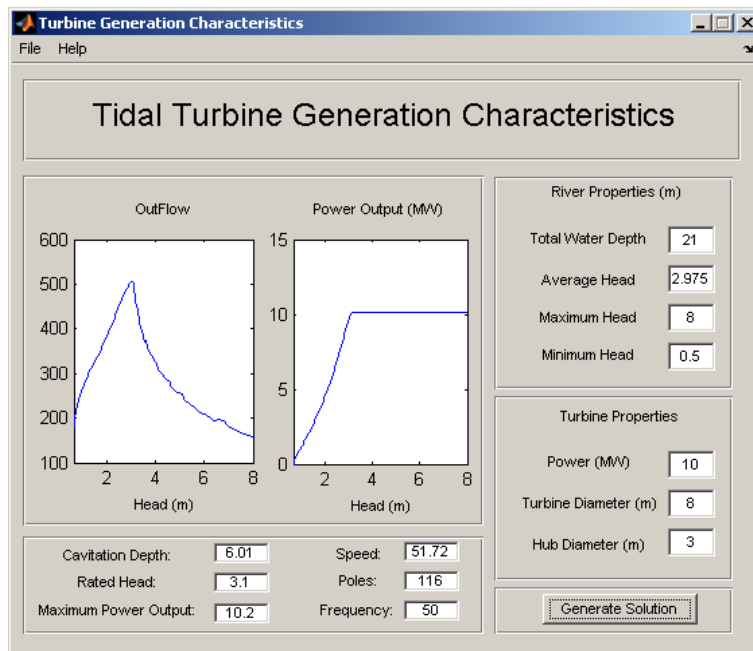


Figure 2: Turbine characteristics for use within a barrage.

The bathymetry, tidal forcing and area of interest are loaded into a piece of software called SMS, as shown in Figure 1. SMS is commercial software which provides a graphical user interface to simplify the pre- and post-processing of much of the data used to generate a suitable grid for use in the simulations. Using the bathymetry, forcing and area information, the software constructs a grid upon which a tidal prediction can be performed.

The tidal device characteristics are obtained, in the case of a barrage turbine, using the program Turgency. This Matlab program generates the operating characteristics of a turbine, given information about its maximum power, diameter and available water depths, utilizing a performance hill chart, as shown in Baker (1991). More details of the program Turgency can be found in Appendix 2.1. Figure 2 is a screen shot of the program after calculating the turbine operating characteristics for the shown input parameters.

At this point, a validation exercise is undertaken which compares the prediction obtained using the newly-generated grid with any available tidal information. When sufficient agreement is obtained, then the grid may be edited to incorporate any tidal range devices and the position of any tidal stream devices is noted (see Appendix A.4.3). Figure 3 shows the incorporation of the Mersey Barrage. Here, the grid portion containing the barrage is removed and regenerated so that the barrage is now included and the rest of the grid remains the same.

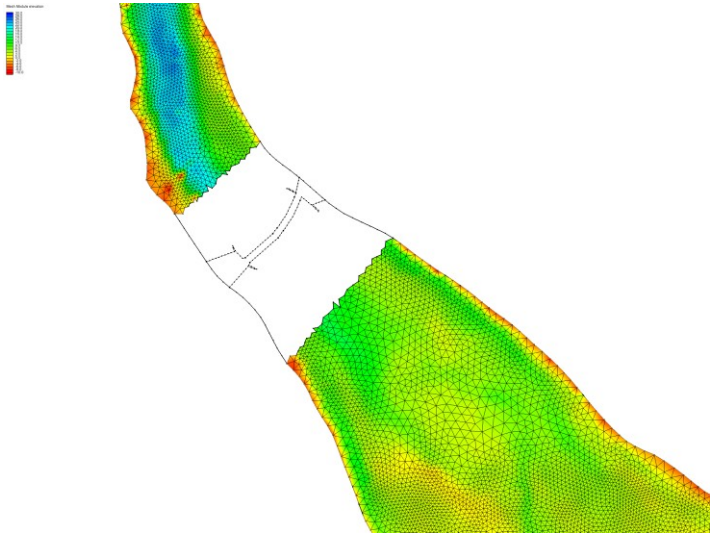


Figure 3: Grid cutout for barrage insertion.

The tidal range devices must have appropriate boundary conditions selected for all the various turbine and sluice sections. Once these have been selected, the grid is loaded into another piece of Matlab software that gives a graphical user interface for the selection of operating mode, sluice gate area and turbine characteristics. This software produces a parameter file which is read into ADCIRC and used within the calculation to simulate the operation of the tidal range device.

At present, the ADCIRC input parameter file for tidal stream devices must be generated by hand. This requires the tidal stream farm nodes to be listed, together with the rated power and speed. More information on the simulation of tidal stream devices within the ADCIRC model is given in Appendix 4.3.

The ADCIRC model is then run with the inclusion of the tidal devices; and the power produced from each tidal device is output as a time series. Any change to the hydrodynamics of the area can be obtained through comparison with the validated model results previously obtained.

## A.4.2 Barrage operation in ADCIRC

### ***Barrage Simulation***

The operation of a barrage is not directly modelled by the standard ADCIRC software. Simulation of barrage operation was added by making alterations to an existing boundary condition. Within ADCIRC, a boundary condition exists called an interior boundary, or weir, which is set to a finite height. If the water rises above the specified height, overtopping occurs. Included within this boundary condition is a leaky option, which models the addition of pipes through the barrier. These pipes are supposedly modelled using the standard rate for potential flow. Unfortunately, the pipe flow is incorrectly modelled within ADCIRC. Thus, a correction was applied at the same time as the addition of the barrage simulation capabilities. The problem in ADCIRC is that the pipe flow should be modelled as point flux sources, whereas they are actually modelled as distributed fluxes along the element edges. To correct the problem, a division by the approximate length of the element was performed which, due to the linear nature of the interpolation and quadrature used within ADCIRC, produces accurate results.

The barrage sluices and turbines must be adopted as a boundary condition. This is the standard internal leaky barrier boundary condition, which is then augmented by an input parameter file which provides information regarding the barrage operation.

Within a barrage, there are 3 possible flow regimes to be modelled. Firstly, there are the sluices which are modelled by free flow and only the total effective gate area is needed as an input parameter for modelling. Secondly, there are turbines which are modelled through a defined head-outflow relationship. The power produced for a given outflow must also be known if any estimate of the power production from a barrage is to be obtained. Therefore, to model the turbine flow, the head-outflow and head-power relationships must be provided as input. The final flow regime is that of pumping, which is modelled after the manner of the turbines. Thus the pump-outflow and pump-power usage relationships must be provided.

The actual turbine characteristic curves for the head-outflow and head-power relationships are produced by the Turgency software, which uses a specific hill chart to determine these curves, details of which can be found in Appendix A.2.1.

To simulate the operation of a barrage, information regarding its operating mode and any associated delays must be provided. Thus, for each barrage a set of input parameters must be supplied, declaring whether the barrage is operating in ebb, flood or dual mode and the time delay in generation after reaching the minimum head for power production.

To make an informed judgement on the best operating mode and delays, judicious use may be made of the Generation 0-D model (see Appendix A.2.1) before work is undertaken on the 2-D model. This will provide a quick estimate of power production for any operating mode and various delays. Having optimised these choices, they may then be passed into the ADCIRC model.

All this information must be linked to the relevant barrages modelled within ADCIRC. Thus, the pre-selected boundary conditions are coupled within the software to a specific barrage and its operating mode. The actual type of each boundary condition, whether it is a turbine or a sluice, is also included within the parameter file and is linked at the same time as the operating mode. This is done through the use of the newly-defined fort.101 file, the structure of which is detailed below.

*NoOfBarrages*

*NoOfPipes*

*Do i=1,NoOfPipes*

*GroupNo*

```

Type
BasinSide
If(Type = Sluice)
    ScaleSluice
Else
    ScaleSluice ScaleTurbine
Filename

Do i=1,NoOfBarrages
    OppMode
    If(OppMode=Ebb | Flood)
        MinHeadStart
        Delay
        MinHeadStop
        SluiceWait
    Else If(OppMode=Dual)
        MinHeadStartEbb
        DelayEbb
        MinHeadStopEbb
        SluiceWait
        MinHeadStartFlood
        DelayFlood
        MinHeadStopFlood
        FloodEff
    RampGen
    OutputSteps

```

*NoOfBarrages* - The number of barrages to be modelled.

*NoOfPipes* - The number of sluice and turbine boundary condition sections selected throughout the grid.

*GroupNo* – The barrage group that the pipe belongs to.

*Type* - What type of culvert this pipe is, either a sluice, a turbine or a pump.

*BasinSide* - Tells the program which side is the basin and which is the ocean so that the operating mode knows when to change states.

*ScaleSluice* - The correction to the cross barrage flux for the sluices. This number will correct for the modelled area and integration error implicit in the ADCIRC model.

*ScaleTurbine* – The correction.

*Filename* - This states the file which contains the head-outflow/power relationship. If the word 'Sluice' is used then the standard formulae are used.

*OppMode* - The barrage operating mode.

If the *OppMode* is either ebb or flood then:

*MinHeadStart* - The minimum head across the barrage at which generation can occur.

*Delay* - The time after the minimum head has been reached before generation actually begins. This is altered to produce optimum power output.

*MinHeadStop* – The head across the barrage at which generation will cease.

*SluiceWait* - A parameter which forces the computer to open the sluices at least this long. This removes the problem of waves and the non-monotonic head difference across the barrage.

In dual mode operation the four parameters defined for ebb and flood mode are required but they are supplemented by four more parameters:

*MinHeadStartFlood* – The minimum head at which generation may occur in the flood phase.

*DelayFlood* – The delay to start generating on the flood phase.

*MinHeadStopFlood* – The head at which generation will cease for the flood phase.

*GenEff* – The operating efficiency of the turbines in flood phase compared to ebb phase.

*RampGen* – The time over which the turbines ramp up from off to fully on.

*OutputSteps* – The number of timesteps between writing of barrage power output.

At the end of the model run, a fort.102 file is generated which provides the power output for each barrage at the predefined timesteps. This can be read into any appropriate software and analysed further to give energy production and subsequently annual energy output.

### ***ADCIRC Barrage Modelling Results***

A simple grid, shown in Figure 4, representing a basic river estuary, was generated so that barrages incorporated within the ADCIRC model could be validated against the 0-D Generation model and any indicative effects of tidal barrages on the wider hydrodynamics might be seen. The bottom friction was set at 0.0025 across the entire domain and the whole area had a constant water depth of 30m. The river section (running westwards towards the sea) was 20km long and 5km wide, with the 100m-wide barrage being situated 1km upstream from the mouth, leaving a basin of 18.9km by 5km. The semi-circular open boundary had a radius of 40km and the model was forced by a single  $M_2$  tidal constituent of 3m amplitude, with no phase difference around the boundary. The undisturbed  $M_2$  amplitude within the modelled area is shown in Figure 5. It can be seen to monotonically increase from 3m at the forced boundary to 3.11m at the head of the river section.

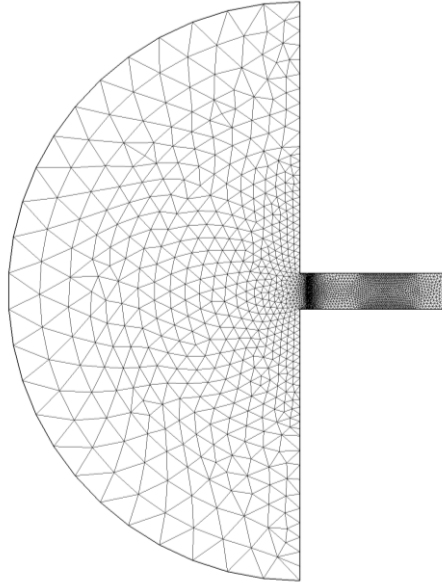


Figure 4: Barrage test grid. The barrage is located in the mouth of the river section.

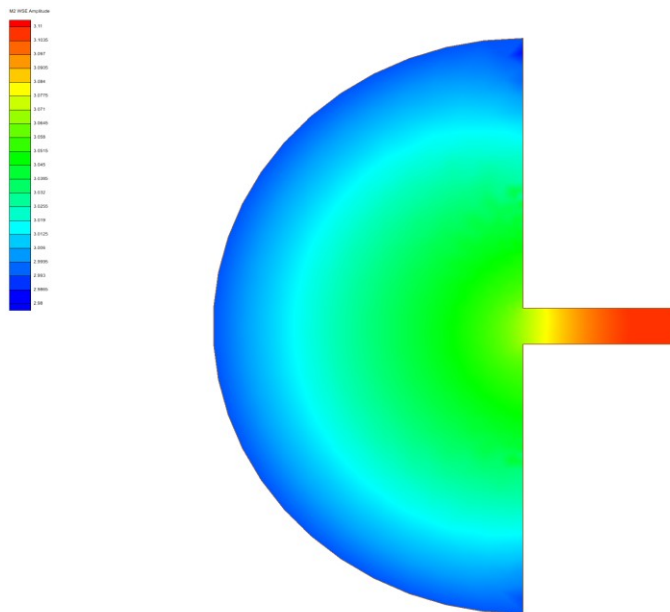


Figure 5: Contour plot of the basic  $M_2$  tidal amplitude.

Figure 6 shows a contour plot of the bottom stress,  $c_d|\mathbf{u}|^2$ , where  $c_d$  is the drag coefficient of 0.0025 and  $\mathbf{u}$  is the velocity vector. The figure shows where the energy from the tides is dissipated within the model. There is a large bottom stress at the boundary, which decreases until the river mouth is reached. At the mouth, the bottom stress increases and at the sharp, and unrealistic, corners into the river there is a large increase in bottom stress. Up-river, the stress again reduces to very small values.

The residual currents around the mouth of the river are shown in Figure 7, where the maximum plotted speed is 16.2cm/s. There are two pairs of counter-rotating gyres at the mouth of the river. The flow upriver of the pair of gyres in the river is directed seaward and enters the gyres through narrow currents along the river banks. The flow at the centre of the river mouth is directed upstream.

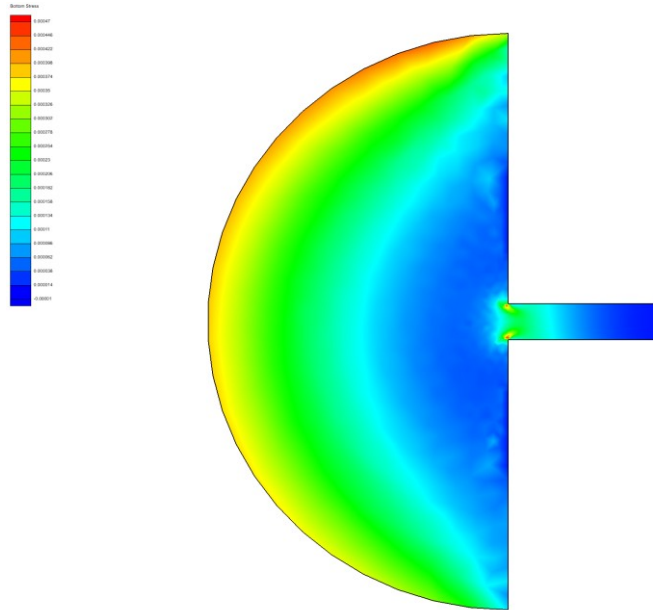


Figure 6: Contour plot of the bottom stress in the basic system.

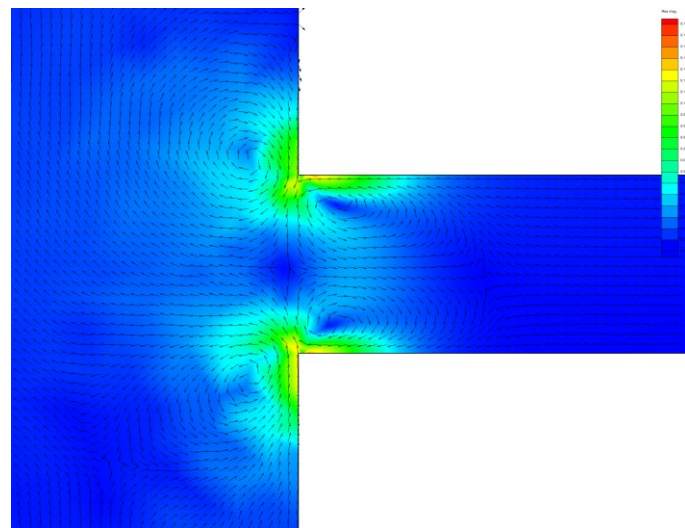


Figure 7: Plot of the residual currents in the mouth of the river.

To consider the performance and hydrodynamic implications of the ADCIRC barrage model, two simulations were run. The first was an ebb mode scheme with 60 turbines in the centre of the barrage and two identical sets of sluices on either side with a combined gate area of 7012m<sup>2</sup>. The turbines used were rated at 13MW, had a 9m diameter and a rated head of 2.97m, which matches well with the M<sub>2</sub> amplitude at the site of just over 3m. A delay of 2 hours was prescribed using a minimum start and end head of 1m, and the generators were ramped up over a 15 minute period. The second simulation was a dual run with 184 turbines, configured with 60 in the middle and 62 on either side, replacing the sluice gates of the ebb run. The turbines used remained the same as for the ebb mode run and no extra sluices were included. The only changes in parameters from the ebb simulation were that a delay of 3 hours was used rather than 2 hours and a turbine efficiency of 79% was used during the flood phase.

The change in M<sub>2</sub> amplitude outside the barrage was small and reached its maximum reduction of 1.5cm at the barrage site. The basin had a much larger reduction in tidal amplitude of just over 1.3m throughout. The phase outside the barrage was delayed slightly

by less than 0.2 degrees. However, the phase delay within the barrage was almost 60 degrees, reflecting the delay utilized to hold back the water and create a larger head for power generation.

The changes in bottom stress associated with the introduction of the barrage are shown in Figure 8. The plot is centered upon the barrage area, as the changes in bottom stress are negligible in the rest of the modelled domain. The striking features are the reduction in stress near the sluice gates and the increase in stress in the turbine region. The increased bottom stress is entirely localised next to the barrage whereas the drop in stress, due to the sluices, affects a region stretching up to 2km from the barrage. The changes in bottom stress are up to 60% of the undisturbed values.

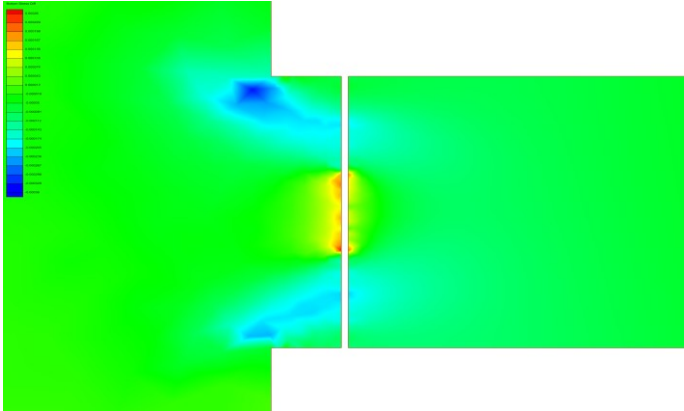


Figure 8: Contour plot of change in bottom stress associated with the barrage operating in ebb mode.

The residual flows around the barrage are shown in Figure 9, where the maximum residual current speed is 16.4cm/s. Water enters the basin through the sluices and exits by way of the turbines, and a seaward current is seen directly in front of the turbines. Within the basin, there is a preference for the flow to be seaward near the northern bank of the river, with some reverse flow in the south. When the residual current pattern is compared with that in the base (undisturbed) model (Figure 7), large changes can be seen. No longer is there a dual pairing of gyres at the mouth of the river; now an outward jet, fed by a circulation into the turbines from the sluices, dominates the flow.

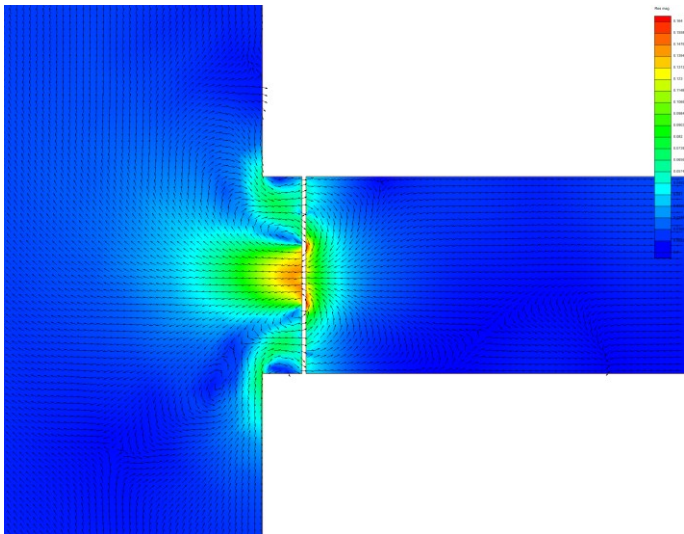


Figure 9: Residual currents with a barrage operating in ebb mode.

The water levels in front of and behind the barrage, in both the Generation and ADCIRC programs, are plotted in Figure 10. There is good agreement between the 0-D and 2-D models. The initial difference in the basin levels is due to the 2-D model not having reached a complete spin-up state. Thereafter, the differences are caused by the hydrodynamics being accurately modelled in ADCIRC. The water levels on the seaward side of the barrage can be seen to be in very close agreement and suggests that, for this configuration, the detailed modelling of the hydrodynamics has little impact on the water levels on either side of the barrage.

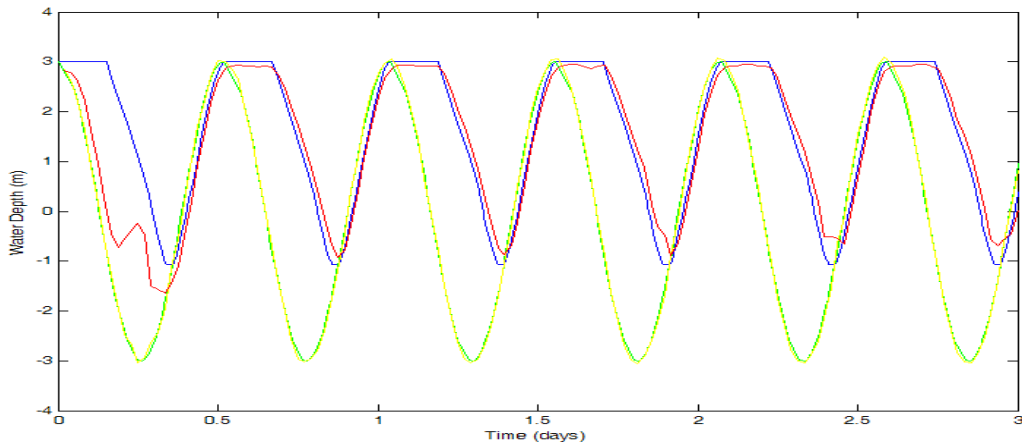


Figure 10: Plot of the water levels in front of and behind the barrage from the Generation and ADCIRC models. The seaward water levels in the Generation and ADCIRC models are plotted in green and yellow, respectively, and the basin levels in blue and red, respectively.

Figure 11 illustrates the predicted power output from the barrage. Here again, as for the water levels, the results from the two models are in good agreement. The annual energy output predicted by the Generation model is 1.92TWh, whilst ADCIRC predicts 1.95TWh. The maximum available energy from this site is 6.83TWh. Thus, ebb generation is extracting 28% of the available energy, comparable to the extraction rates of real proposed schemes.

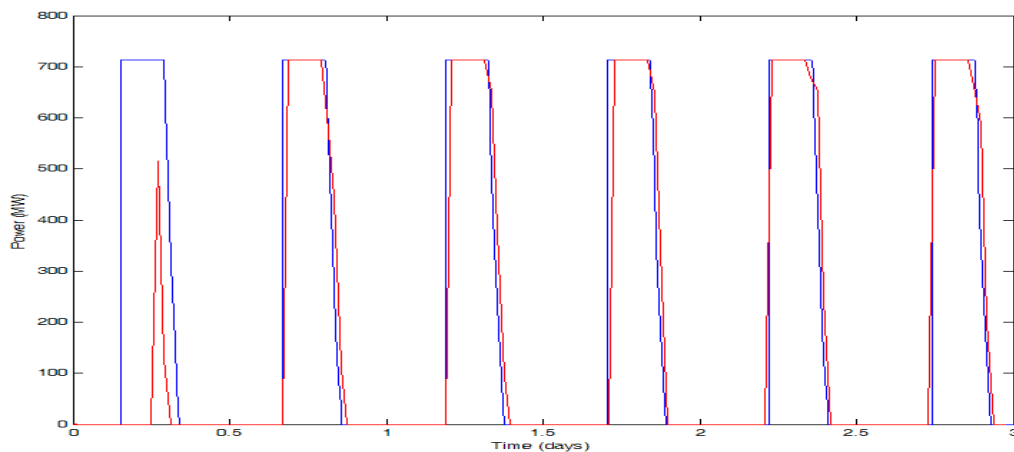


Figure 11: Power output from the Generation model, in blue, and the ADCIRC model, in red.

The second barrage configuration was for a dual mode scheme with approximately 3 times the number of turbines. The  $M_2$  tidal amplitude within the open sea again changed only slightly due to the presence of the barrage, with a maximum reduction of up to 3cm at the barrage line. However, the amplitude was not constant along the line of the barrage, but varied by up to 2cm. Within the basin, the tidal amplitude actually increased, probably due to reflection.

The difference in bottom stress produced by the dual mode operation is plotted in Figure 12. There is an increase in bottom stress at each turbine site, although the central turbine section has an increase along its entire length, whereas the outer turbine sets have only localized increases. A large increase is also seen near the southern corner of the river mouth. This increase in bottom stress is in marked contrast to the decrease in stress seen in ebb mode operation (Figure 8) associated with the sluices. However, outside of the local region around the barrage there is negligible change in the bottom stress.

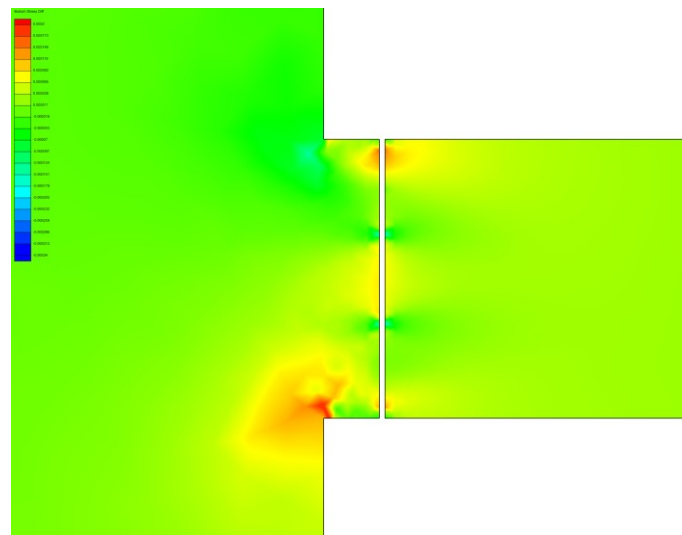


Figure 12: Change in bottom stress around the barrage with approximately 3 times dual mode configuration compared to the base (undisturbed) case.

The residual currents, shown in Figure 13, reveal a very different flow pattern from those for the undisturbed model and for the barrage operating in ebb mode. Now, there is a residual flow out of the basin along the whole length of the structure. Nowhere is there a residual flow into the basin. However, the outward flow is not uniform: it varies along the barrage line. Seaward of the barrage, the residual flow is mainly westwards along the estuary centre-line, with a pair of contra-rotating gyres visible to the north and south, and a smaller clockwise gyre near the south end of the barrage. Thus, dual mode operation of the barrage with the associated increased number of turbines has produced large changes in the residual current circulation. The maximum residual current is 19cm/s.

The predicted water levels within the basin and seaward of the barrage are plotted in Figure 14, for both the 0-D and 2-D models. The two models are generally in good agreement, although agreement is not as good as for ebb mode operation. However, there are differences in the basin water levels during the delay period, with the appearance of spikes in the water elevation predicted by ADCIRC, owing to the hydrodynamics of the basin. These spikes explain the predicted increase in the  $M_2$  amplitude, as shorter waves propagating within the basin would act to increase the maximum water level and decrease the minimum level.

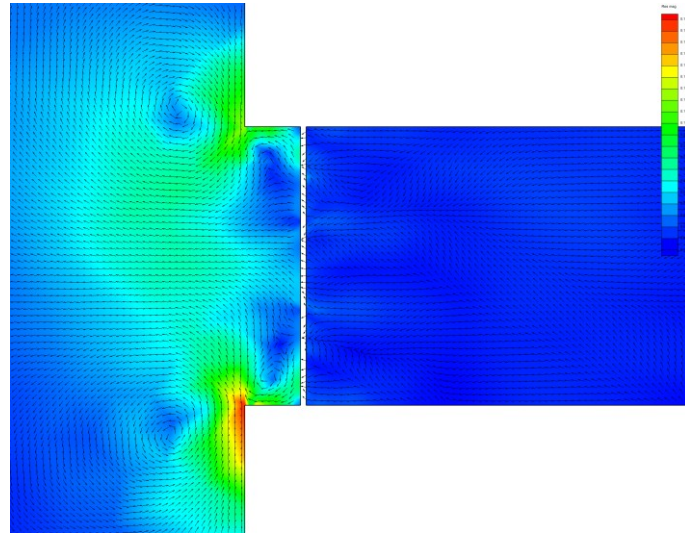


Figure 13: Residual currents associated with the barrage with approximately 3 times dual mode configuration.

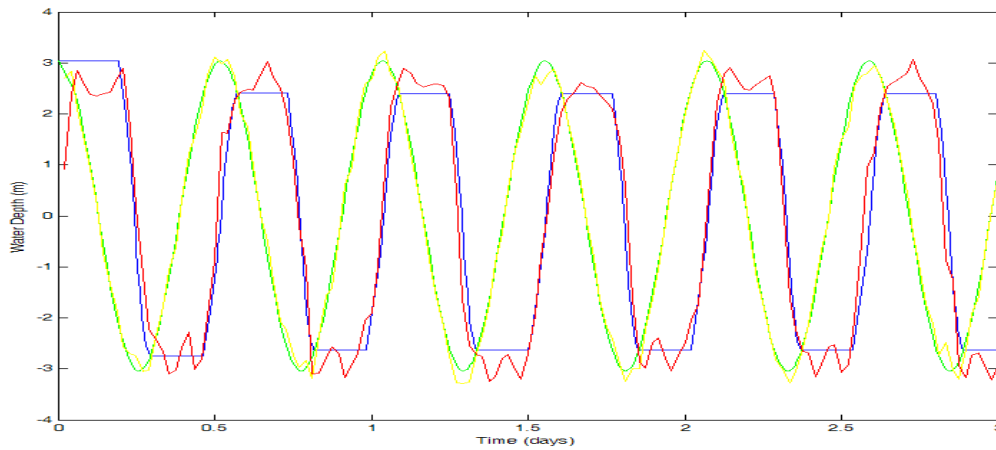


Figure 14: Plot of the predicted water levels within the basin and seaward of the barrage using the Generation and ADCIRC models. The colour scheme is the same as in Figure 10.

The power output predictions, plotted in Figure 15, show that the two models are in good agreement. The change in power output associated with the reduction in turbine efficiency during the flood phases is clearly seen in both models, as ebb power generation is significantly greater than flood power generation. In reality, the change in water volume within the basin, due to the bathymetry, would also have an impact, but this aspect is not relevant here due to the flat bottom bathymetry being used.

The annual energy output from the barrage under this mode of operation is predicted as 4.02TWh by Generation, which is 58% of the total available power, and as 4.77TWh by ADCIRC, which is 69% of the total available power. The greater power output is seen in the wider generation windows within the ADCIRC model.

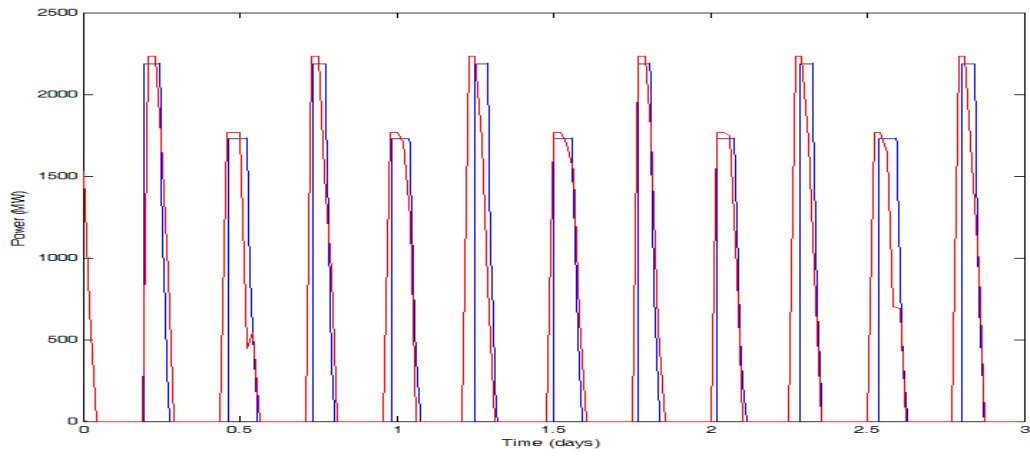


Figure 15: Plot of the power output as predicted by Generation, in blue, and by ADCIRC, in red.

### A.4.3 Tidal stream farms in ADCIRC

#### **Background**

Utilising the simple concept of representing the energy dissipation associated with tidal stream devices as an increase in the quadratic bottom friction parameter, Sutherland et al (2007) modelled the effect of a tidal stream farm on the circulation within the Johnstone Strait, off Vancouver Island. This simple approach is adopted here and applied to the ADCIRC ocean model.

#### **Tidal Stream Simulation**

Within the model, an area is selected for the tidal stream farm and an appropriate drag coefficient is calculated which corresponds to the amount of energy extracted from the system by the tidal stream devices. The energy dissipation rate is given by:

$$P = \iint_A \rho(k_o + k_t) |u^3| dA$$

where  $\rho$  is the water density,  $k_o$  and  $k_t$  are the drag coefficients associated with the natural bottom and tidal stream devices, respectively,  $u$  is the water velocity and  $A$  is the area over which the tidal stream devices are located. The approximation used within the model to calculate the power associated with the tidal stream farm is given by:

$$P_t = \sum_n \frac{1}{3} \rho k_t |u_n^3| A_n$$

where  $n$  is a node within the farm and  $A_n$  is the total area of all elements attached to the node  $n$ . At this point, it should be noted that the energy dissipated by the tidal stream devices will not all be converted into useful electrical power and for a more detailed study this should be considered. However, here we are not considering directly the amount of electricity generated but merely the effect upon the ocean circulation. Thus, we do not need to consider any losses through conversion. It will be possible, in general, to simply apply a correction factor in post-processing to obtain a reasonable estimate of the electricity produced by any given tidal stream farm.

From a practical point of view, it is unlikely that the drag coefficient associated with the energy dissipation will be known for any given tidal stream farm. It is the theoretical power output from the tidal stream devices at a rated velocity which will be known. Using these values, we can calculate the drag coefficient using:

$$k_t = \frac{P_{rt}}{\sum_n \frac{1}{3} \rho |u_m^3| A_n}$$

where subscript  $r$  denotes the rated values for the tidal stream devices used with the farm.

The parameter input file used for the ADCIRC model has the following structure:

*NoOfFarms*

*Do i=1, NoOfFarms*

*FarmName*

*Rated Power*

*Rated Speed*

*OutputSteps*  
*NoOfNodes*  
*Do i=1,NoOfNodes*  
*NodeNumber*

*NoOfFarms* – The number of tidal stream farms that are listed in the file.

*FarmName* – The name of this tidal stream farm. The power output will be in a file whose name is based upon this name.

*Rated Power* – The maximum power output from the farm as a whole.

*Rated Speed* – The speed at which the maximum power is first reached.

*OutputSteps* – The number of timesteps between each successive writing to the output file of the power generated by the farm.

*NoOfNodes* – The number of nodes that the farm is defined over.

*NodeNumber* – The number of the node from the grid at which the increased bottom friction will be applied.

The increased friction associated with the tidal stream devices, as calculated using the above equations, is then applied as a constant value across all the nodes in the given farm.

### ***ADCIRC Tidal Stream Modelling Results***

A simple grid, shown in Figure 16, was generated so that the impacts of the addition of tidal stream farms might be explored. The grid had an outer ocean area and an inner river portion. The semi-circular edge was forced with an  $M_2$  tidal component of 3m amplitude with the same phase around the whole edge. The bottom friction was set at 0.0025 across the entire domain and the whole area had a constant water depth of 30m. The river portion was 20km long and 5km wide, and the ocean region had a radius of 20km.

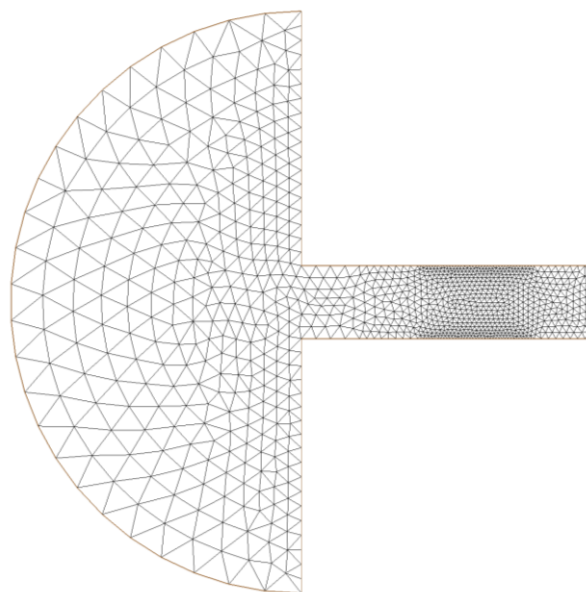


Figure 16: Grid used for test runs.

The  $M_2$  amplitude is shown in Figure 17. The minimum amplitude is 3m and the maximum amplitude, found at the furthest reaches of the river, is 3.06m. The  $M_2$  current amplitude has a maximum of about 30cm/s at the mouth of the river (Figure 18).

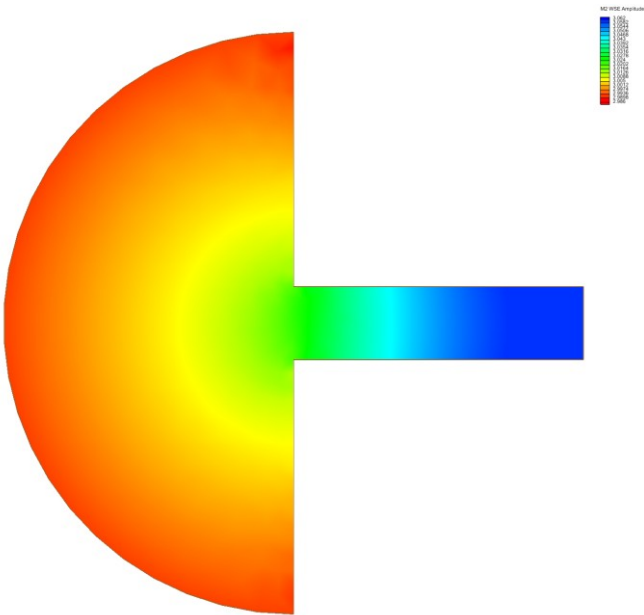


Figure 17:  $M_2$  tidal amplitude in base (undisturbed) case.

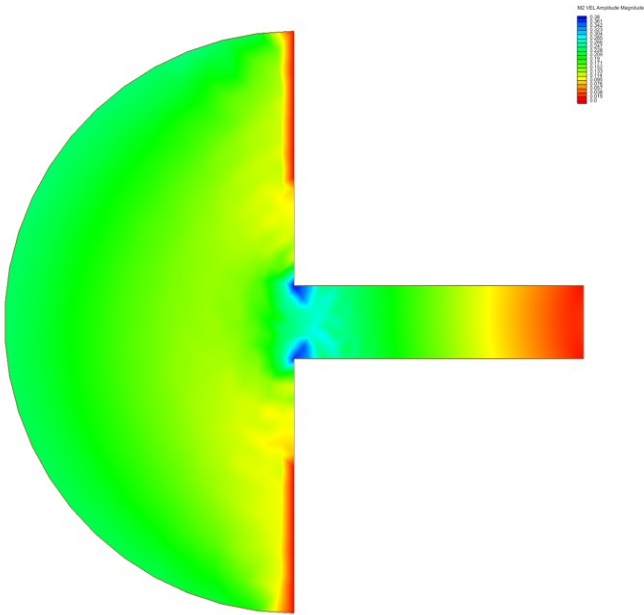


Figure 18:  $M_2$  current amplitude in base (undisturbed) case.

The tidal stream farm was situated in a region of the greatest flow in the river mouth, shown in Figure 19 by the red dots. The current amplitude in the farm area was about 26.75cm/s. This speed is far too small to be of any real use but, in these tests, we were more interested in the effects of a tidal stream farm rather than on realistic power output. Attention was centred on three runs (runs 1, 2 and 3) corresponding to the three significant impact factors (SIFs) shown in Table 1. The SIF denotes the limit on the percentage of the incident kinetic energy to be extracted through the chosen installed capacity.

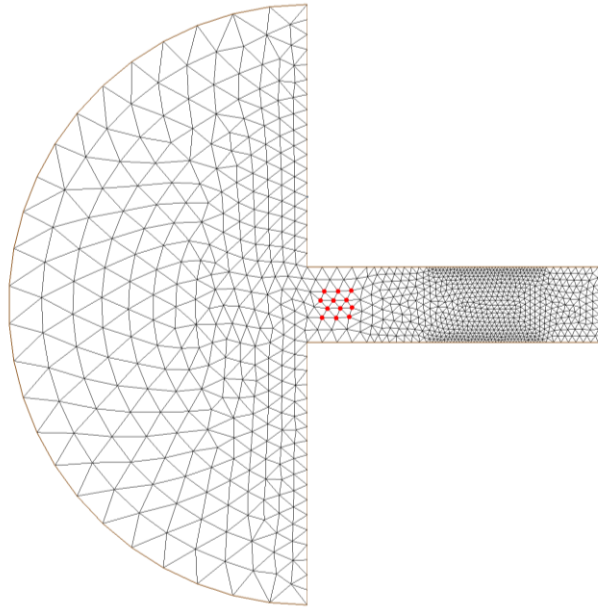


Figure 19: Site of tidal stream farm (shown as red dots).

Table 1: SIF used for each test case.

Run*	1 and 4	2 and 5	3 and 6
SIF	10%	20%	40%

\* Runs 1, 2 and 3 relate to a farm occupying part of the river width (Figure 19).  
Runs 4, 5 and 6 are for a farm occupying the full river width (Figure 28, later).

The farm in runs 1, 2 and 3 had a width of 1.757km, located in a depth of 30m. Thus, the instantaneous maximum power available at the site was 0.5MW. The rated power for the three runs was 0.05MW, 0.1MW and 0.2MW, respectively. The rated velocity to achieve this power was set as 26.75cm/s for all cases. The farm covered an area of just over 10km<sup>2</sup> and so the associated drag coefficient for the runs was 0.00079, 0.00158 and 0.00316, respectively, the associated bottom friction enhancement in the three cases thus being about 32%, 63% and 126% of the natural bottom friction.

We can see from Figure 20 that the main effect of the tidal stream farm is to create a generating head across the farm. It tends to increase the tidal amplitude upstream of the farm within the river. However, the scale of the changes is small. The maximum increase is about 4mm with a maximum decrease seaward of the farm of about 1mm.

The changes in the flow speed are shown in Figure 21, and we can see that the major effects are all localised around the tidal stream farm. The flow through the mouth of the river has changed due to the presence of the farm, so that a large proportion of the flow goes around the farm rather than through it. The flow around the edges has increased by up to 14cm/s and the flow through the farm has decreased by up to 12cm/s. This has meant that the instantaneous power available at the farm site has dropped to 0.14MW, less than 30% of that originally available, and the power pulses extracted in run 1 (with SIF = 10%) are shown later in Figure 26.

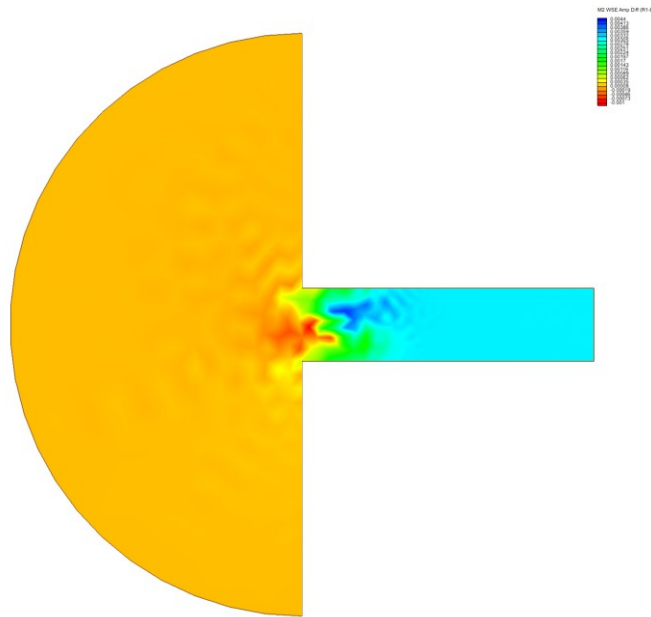


Figure 20: Differences in  $M_2$  amplitude between run 1 and base case.

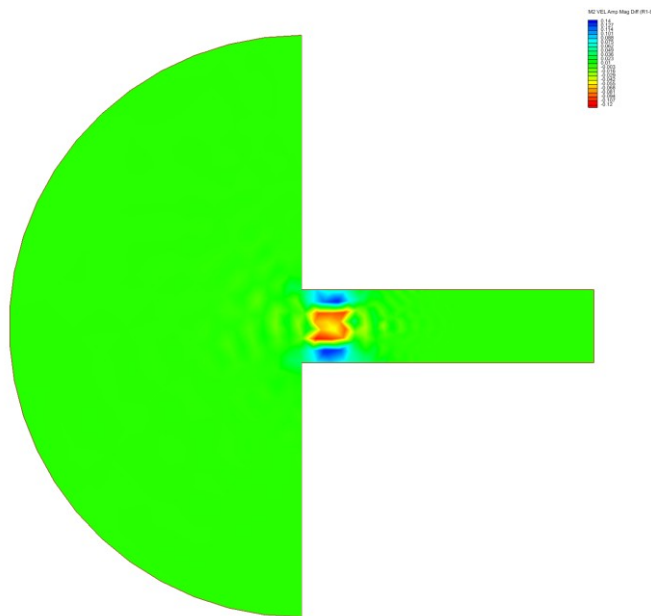


Figure 21: Differences in  $M_2$  current amplitude between run 1 and base case.

Figure 22 shows the differences in tidal amplitude between run 2 and the base (undisturbed) case. The effect on the tidal amplitude is generally the same as for run 1, but now the maximum increase is 7mm and the largest reduction is 2.5mm.

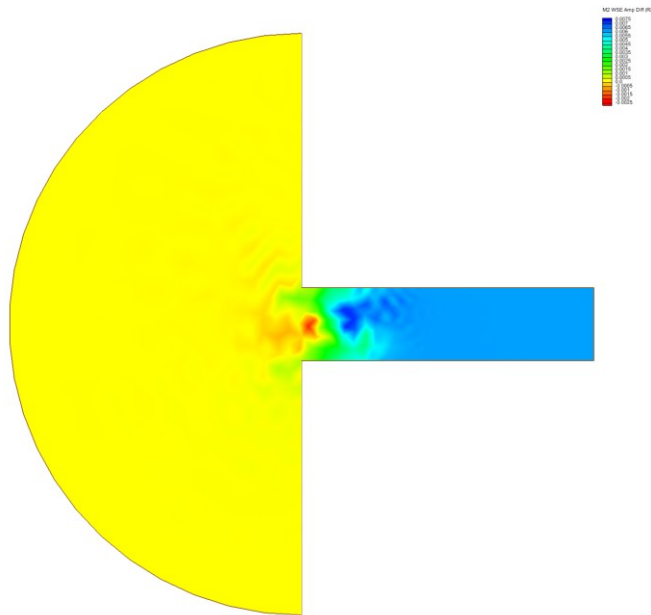


Figure 22: Differences in  $M_2$  tidal amplitude between run 2 and base case.

Figure 23 shows that the changes in tidal current amplitude in run 2 are similar to those in the first run (Figure 21). However, the magnitude of the changes in this run is again significantly greater. The current amplitude around the farm has increased by up to 21cm/s and through the farm the reduction has been up to 17cm/s. The power available at the farm site has now dropped to 0.04MW, and the power pulses extracted in run 2 (with SIF = 20%) are shown later in Figure 26.

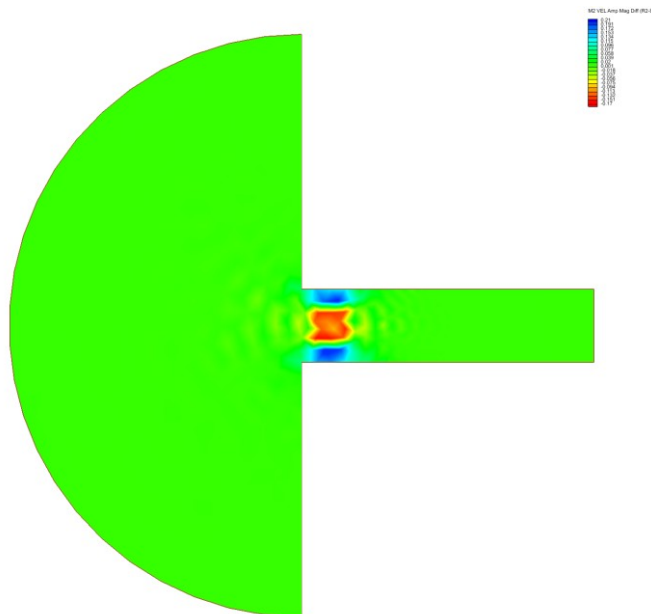


Figure 23: Differences in  $M_2$  current amplitude between run 2 and base case.

As in the previous runs, the changes in tidal amplitude in run 3 show the same general pattern although, once again, there is an increase in magnitude (Figure 24). This time the changes are up to 1cm, although this is still small compared to the natural tidal amplitude of over 3m.

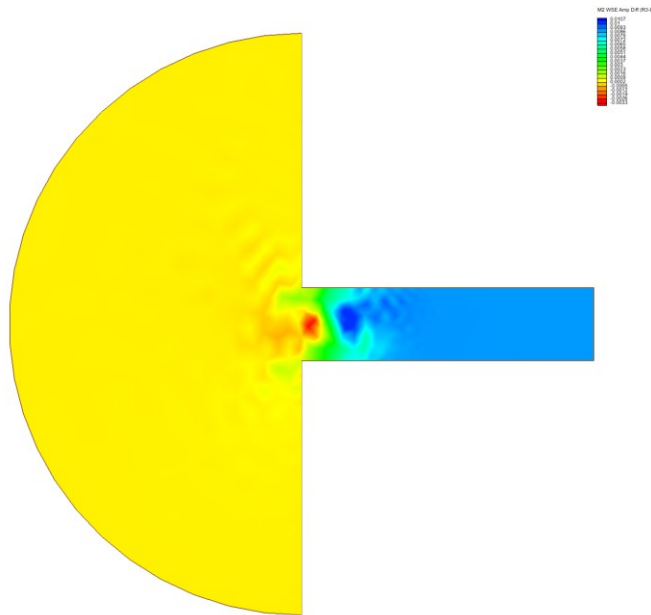


Figure 24: Differences in  $M_2$  amplitude between run 3 and base case.

The changes in current amplitude are shown in Figure 25 and can be seen to be similar to previous runs. Now, the changes in speed are very large and the increase in current amplitude around the farm is up to 26cm/s. The current amplitude within the farm has dropped by up to 21cm/s. This has a significant impact upon the power available from the site, which is now just 0.009MW, only 1.8% of the originally available value.

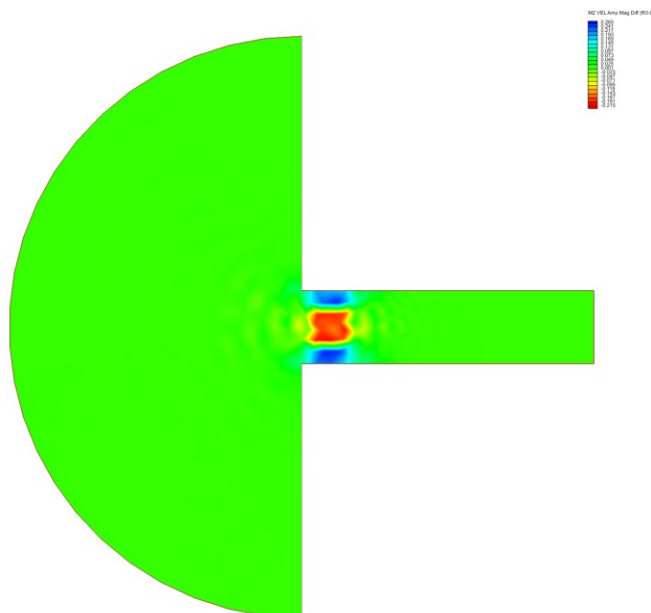


Figure 25: Differences in  $M_2$  current amplitude between run 3 and base case.

Figure 26 shows the power generated by the tidal stream farm during each run. The maximum power return has been generated in the first run. There is also unevenness in the power production on the flood and ebb tides. The flood tide generates the greater power in this model, with the peak ebb power output being about 70% of the peak flood power output.

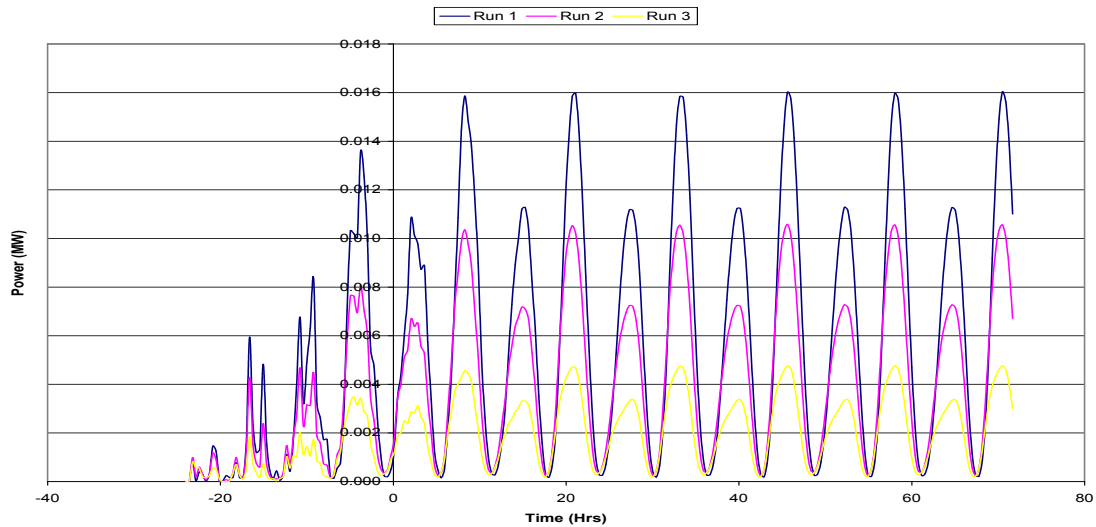


Figure 26: Plots of power outputs in runs 1, 2 and 3.

The annual energy production for the tidal stream farm, for varying SIF, is shown in Figure 27. It shows that the SIF values used to test the impacts on the hydrodynamics are in the region of decreasing production. From consideration of environmental impacts, from which the concept of the SIF is derived, a SIF of about 20% is usually targeted. However, this does not necessarily produce an optimum for power production and, indeed, having a lower impact factor would not only result in less environmental impact but also produce greater annual energy. Previous studies have, in general, focused upon farms which extract from the entire flow in an enclosed channel. This was not the case in the above runs, where the water could flow around the farm, more consistent with an open ocean current. The maximum annual energy was achieved with an impact factor of about 9%, which leads to a tidal stream farm with an installed capacity of about 45.5kW.

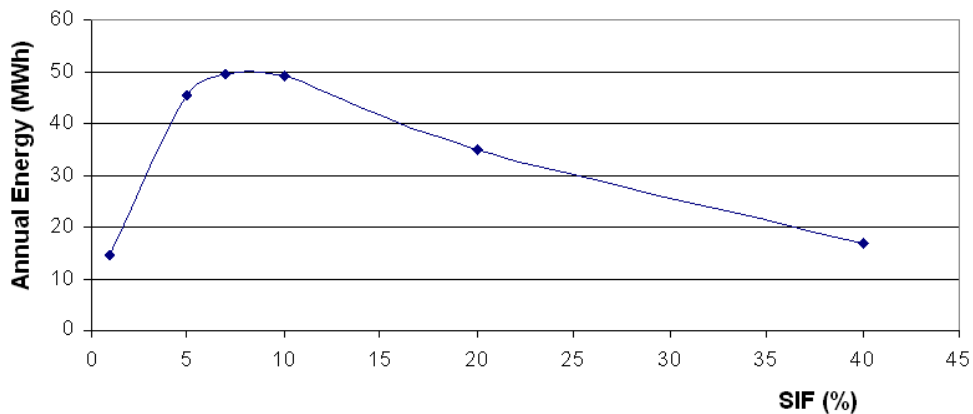


Figure 27: Plot of annual energy output against SIF (partial-width farm).

Next, we will consider the impact of a tidal stream farm covering the full width of the river. The extent of the tidal stream farm for this second set of runs (runs 4, 5 and 6) is shown in Figure 28. Flow entering the channel must now pass through the farm, generating power rather than being diverted to either side. Within the extended farm, the maximum instantaneous available power is just over 2MW. So that comparisons can be made between the two alternative farm configurations, the same significant impact factors are used for the full-width farm as for the partial-width arrangement (see Table 1).

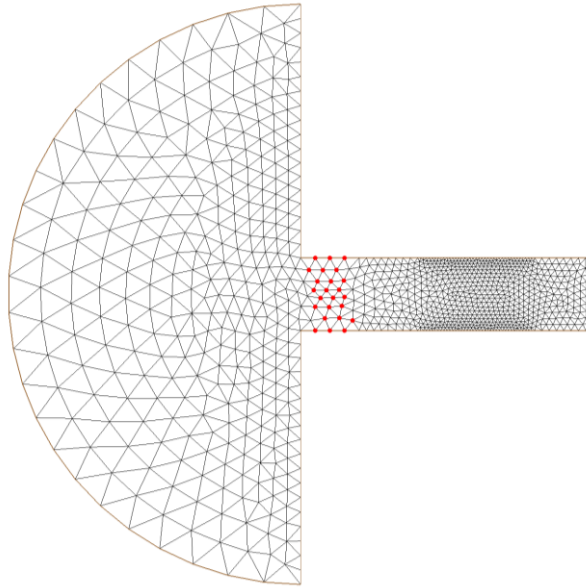


Figure 28: Plot showing the location of the extended farm so that the full width of the channel is covered.

The change in tidal amplitude resulting from the presence of the extended farm is shown in Figure 29. There is a slight increase in tidal amplitude behind the farm of the order of 1mm. The maximum increase in amplitude, 4mm, is seen at the farm. The greatest decrease in tidal amplitude, seen at the mouth of the river, is 1.6mm. Unlike for the partial-width tidal stream farm, there is negligible effect upstream.

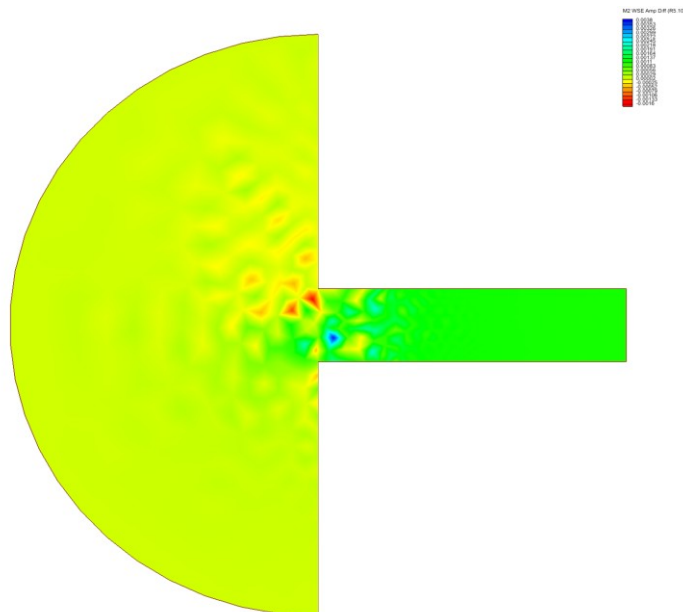


Figure 29: Differences in  $M_2$  amplitude between run 4 and base case.

Figure 30 shows the changes in current amplitude from the base (undisturbed) case as a consequence of the presence of the tidal stream farm. Most of the changes are immediately either side of the farm.

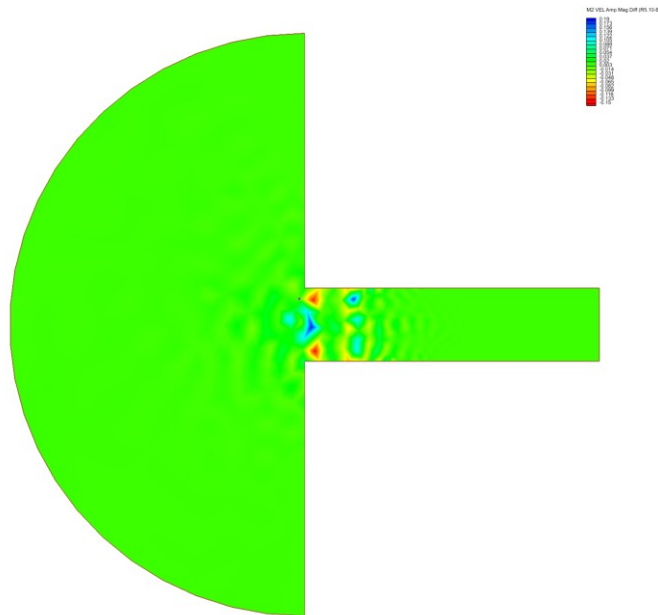


Figure 30: Differences in  $M_2$  current amplitude between run 4 and base case.

The change in current amplitude through the farm is a reduction of just 1.9cm/s. This is in marked contrast to the previous farm configuration, where the water changed course to flow around the farm, with the flow through the farm significantly reduced, affecting the extractable energy from the site. Further upstream of the farm, the current amplitude is changed by around 1mm/s or less. The power available at the farm site is now 1.2MW, which is 60% of the undisturbed original power. The power pulses extracted in run 4 (with SIF = 10%) are shown later in Figure 35.

As in run 4, the change in tidal amplitude in run 5, due to the presence of the tidal stream farm, is quite small and generally localised to the region in front of and behind the farm (Figure 31).

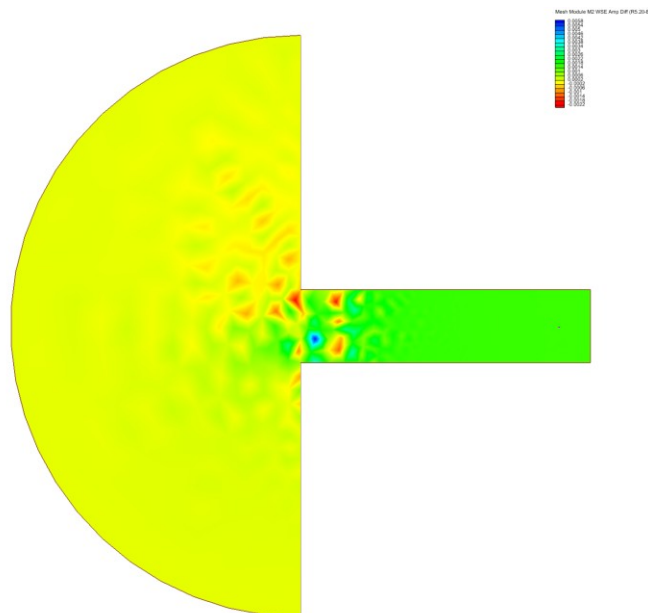


Figure 31: Differences in  $M_2$  amplitude between run 5 and base case.

The flow is again changed primarily in the vicinity of the tidal stream farm (Figure 32). The maximum increase in current amplitude is almost 28cm/s and the maximum decrease is about 20cm/s. The power available at the farm site is now 0.97MW, 48% of the potential power available at the site. The power pulses extracted in run 5 (with SIF = 20%) are shown later in Figure 35.

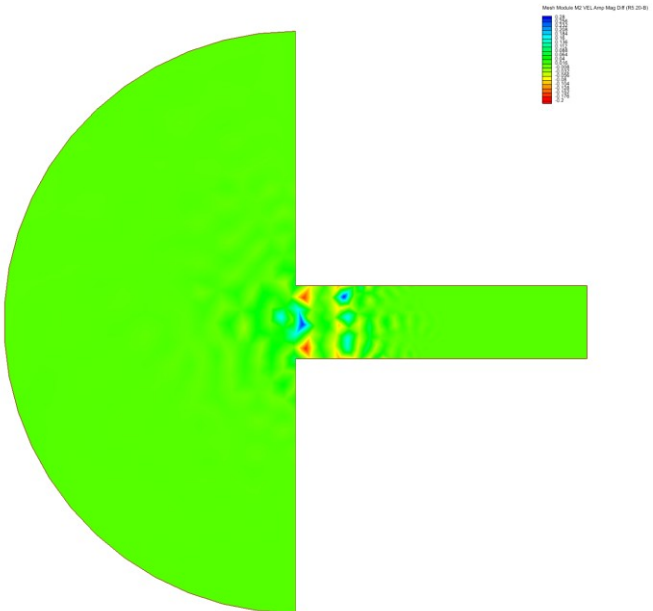


Figure 32: Differences in  $M_2$  current amplitude between run 5 and base case.

In a similar manner to the previous runs, the changes due to the SIF of 40% (run 6) are centred about the tidal stream farm. The changes to the  $M_2$  tidal amplitude and current amplitude are shown in Figures 33 and 34, respectively. The maximum increase in current amplitude is 40cm/s and the maximum decrease is about 22cm/s. The power available at the farm site has now dropped to 0.74MW, 37% of the undisturbed instantaneous power available.

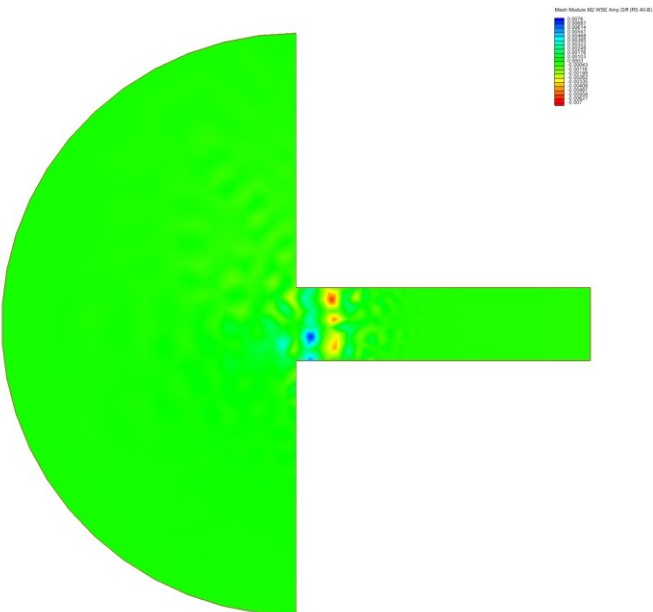


Figure 33: Differences in  $M_2$  amplitude between run 6 and base case.

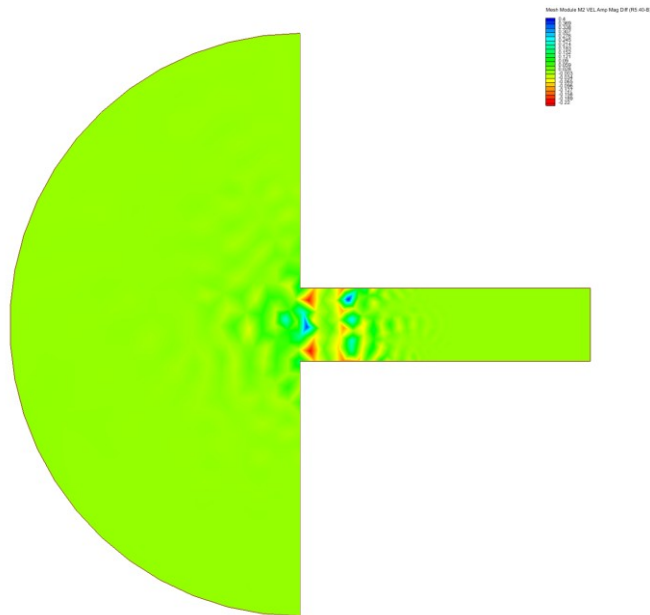


Figure 34: Differences in  $M_2$  current amplitude between run 6 and base case.

The power output from the extended tidal stream farm is shown in Figure 35. In contrast to the partial-width tidal stream farm, by increasing the SIF in the range of values explored here, the energy output from the farm also increases.

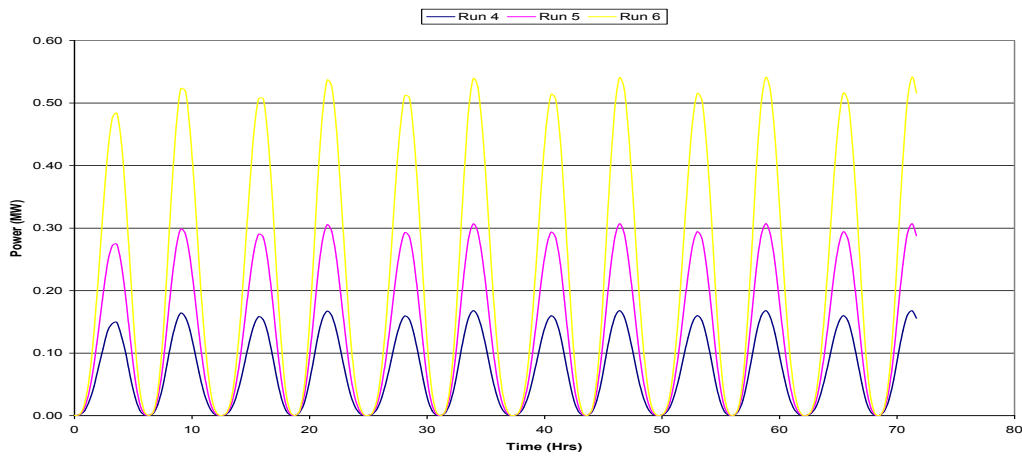


Figure 35: Plot showing power output from the tidal stream farm for runs 4, 5 and 6.

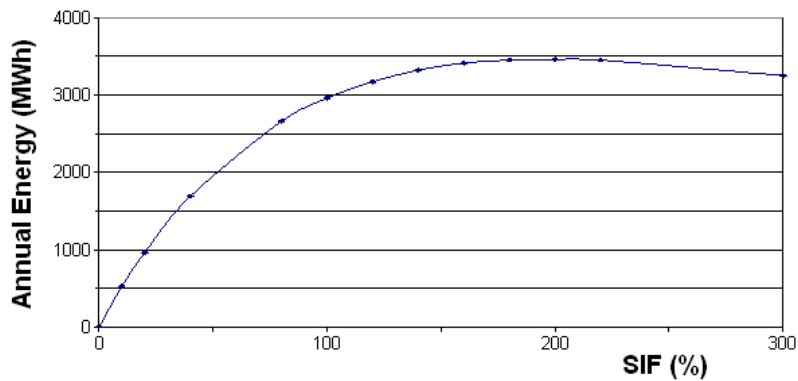


Figure 36: Plot of annual energy output against SIF (full-width farm).

The annual energy output from the full-width tidal stream farm for increasing SIF is plotted in Figure 36. The maximum annual output is seen at a SIF of around 200%. Comparing the full-width farm with the partial-width configuration, the maximum annual energy output increases from about 50MWh to nearly 3500MWh.

For the maximum annual energy output, the changes in  $M_2$  tidal amplitude and current amplitude are shown in Figures 37 and 38, respectively. The maximum increase in tidal amplitude is 1cm and the largest decrease is about 7cm. The increase in current amplitude has a maximum of 86cm/s, whilst the maximum decrease is around 30cm/s. The maximum instantaneous power available from the kinetic energy now approaching the farm with the SIF of 200% is 0.24MW, only 12% of the 2MW originally available, demonstrating that the farm is now also capturing significant potential energy.

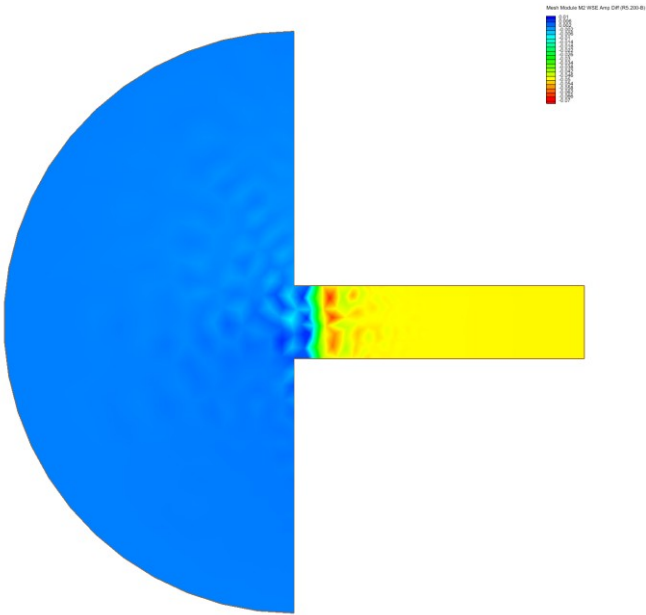


Figure 37: Differences in  $M_2$  amplitude for full-width farm with SIF = 200%.

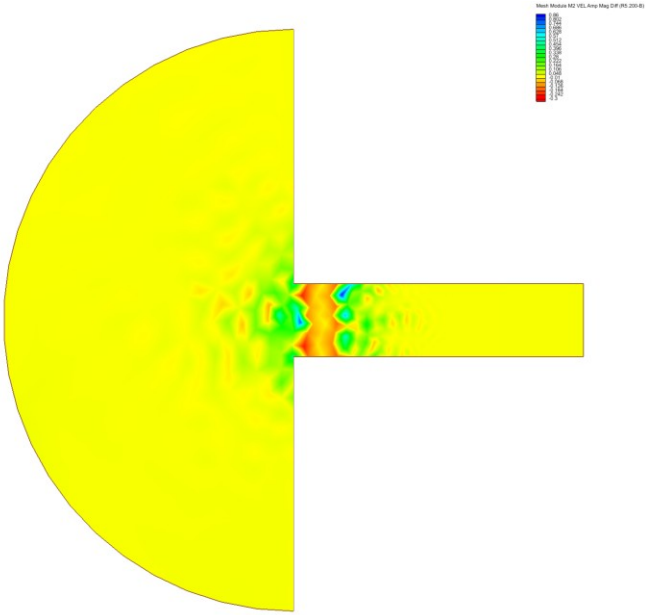


Figure 38: Differences in  $M_2$  current amplitude for full-width farm with SIF = 200%.

#### A.4.4 Validation of simulation grid

A grid was generated to model the tides in the Irish Sea. This grid had a boundary in deep water so that the tidal boundary conditions applied were as close as possible to sinusoidal. It also meant that any effects generated due to the presence of the tidal barrages or tidal stream devices should not propagate to the forced boundaries and, therefore, the forcing conditions would remain valid and the grid be kept stable during any prediction runs. The grid had over 750,000 elements with a resolution ranging from 15km near the deep water open boundaries to 50m in some shallow estuaries, such as the Dee.

The bathymetry used within the model came from a number of different sources. The bathymetry in the Irish and Celtic Seas was from the POL Irish Sea model and had been used extensively within the POLCOMS computational framework. LIDAR data were used where available. This was in three estuaries: the Dee, Mersey and Ribble. The high resolution data were filtered so that the large datasets associated with LIDAR bathymetry could be reduced to a reasonable size. However, the data were not interpolated onto the grid using a volume conservation method, which may be desirable in any future work. The outer bathymetry was again obtained from POL computational models.

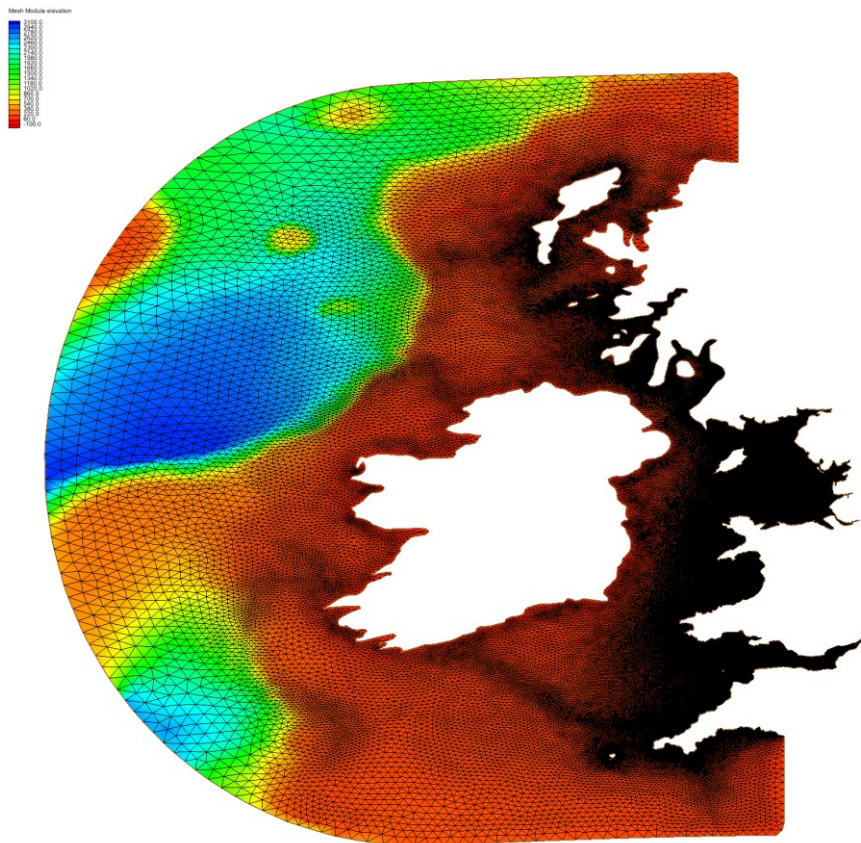


Figure 39: Grid used to model the tides in the Irish Sea.

The tidal boundary forcing conditions were obtained from the TPXO7.1 tidal model developed by OSU for ESR (Egbert and Erofeeva, 2002). Five tidal constituents were used to force the model at the ocean boundaries, these being  $M_2$ ,  $S_2$ ,  $N_2$ ,  $K_1$  and  $O_1$ . Two observation data sets were employed for validation purposes. The first was a general set, comprising 70 observation locations across a large part of the grid, including the western coast of Ireland. The second was a larger, more concentrated set, comprising 212

observation locations centered upon the Irish and Celtic Seas. There was some overlap in the port data between the two sets.

The model was run with a timestep of 1 second and a quadratic bottom friction parameter of 0.002 over the entire domain, except within the Severn Estuary where this was increased to 0.003. Figure 40 shows the errors in the  $M_2$  tidal amplitude and phase as a scatter plot for the observation sites listed in Table 6, under Data Tables (see below).

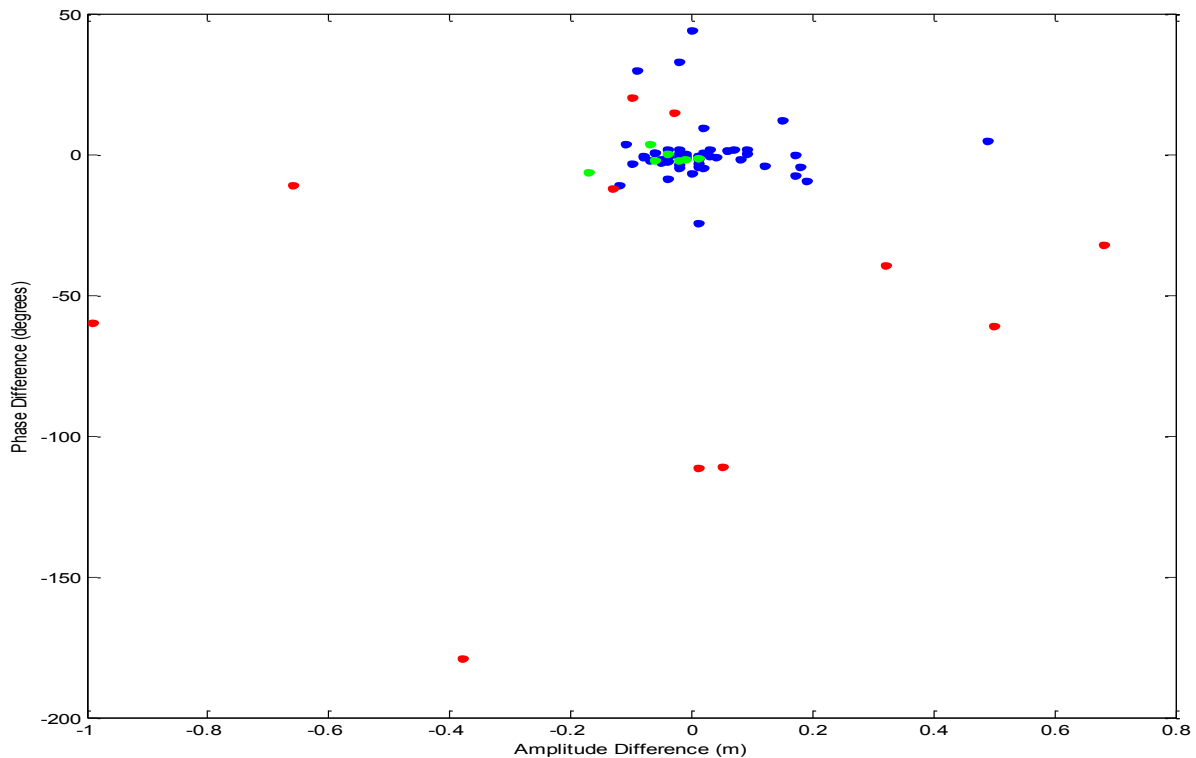


Figure 40: Scatter plot of differences (observed - simulation) in the  $M_2$  tidal amplitude and phase using dataset 1.

The red points show error values for places which are not explicitly modelled by the simulation, such as river ports or sea lochs, but for which model values have been obtained by extrapolation. The green points show locations with insufficient water depth to model the full observed tidal curve (i.e. they are subject to wetting and drying). To provide a suitable comparison, a search was done to find the closest modelled point which had the requisite water depth. Blue points are sites modelled within the simulation which have deep enough water to model the observed  $M_2$  tidal amplitude.

There were 11 unusable observation sites from dataset 1, due to the locations not being modelled within the present grid, and a further 7, shown in Table 2, which were corrected due to the lack of water depth at the observation site within the simulation. It can be seen that of those points which were modelled, shown in blue, the vast majority have only small errors in both amplitude and phase.

Table 2: Original and corrected values for dataset 1 where the simulated site does not have the requisite depth to model the  $M_2$  tidal curve without drying.

Observation Site Name	Site $h_c$ (m)	Site $g_c$	Corrected $h_c$ (m)	Corrected $g_c$	Distance (m)
Avonmouth	0.17	189.00	4.28	199.46	800
Hilbre Island	0.57	308.60	2.91	315.61	750
Barrow (Furness)	2.40	331.15	2.98	333.57	750
Birkenhead	2.09	317.71	3.11	323.62	350
Eastham	0.55	224.53	3.16	327.20	900
Fleetwood	2.09	324.66	3.03	324.26	700
Greenock	0.01	173.61	1.00	340.00	500

The second dataset was larger than dataset 1, but with a more restricted coverage. As for the first dataset, the errors in the  $M_2$  tidal amplitude and phase for the majority of modelled points lie within a small region around the origin (Figure 41).

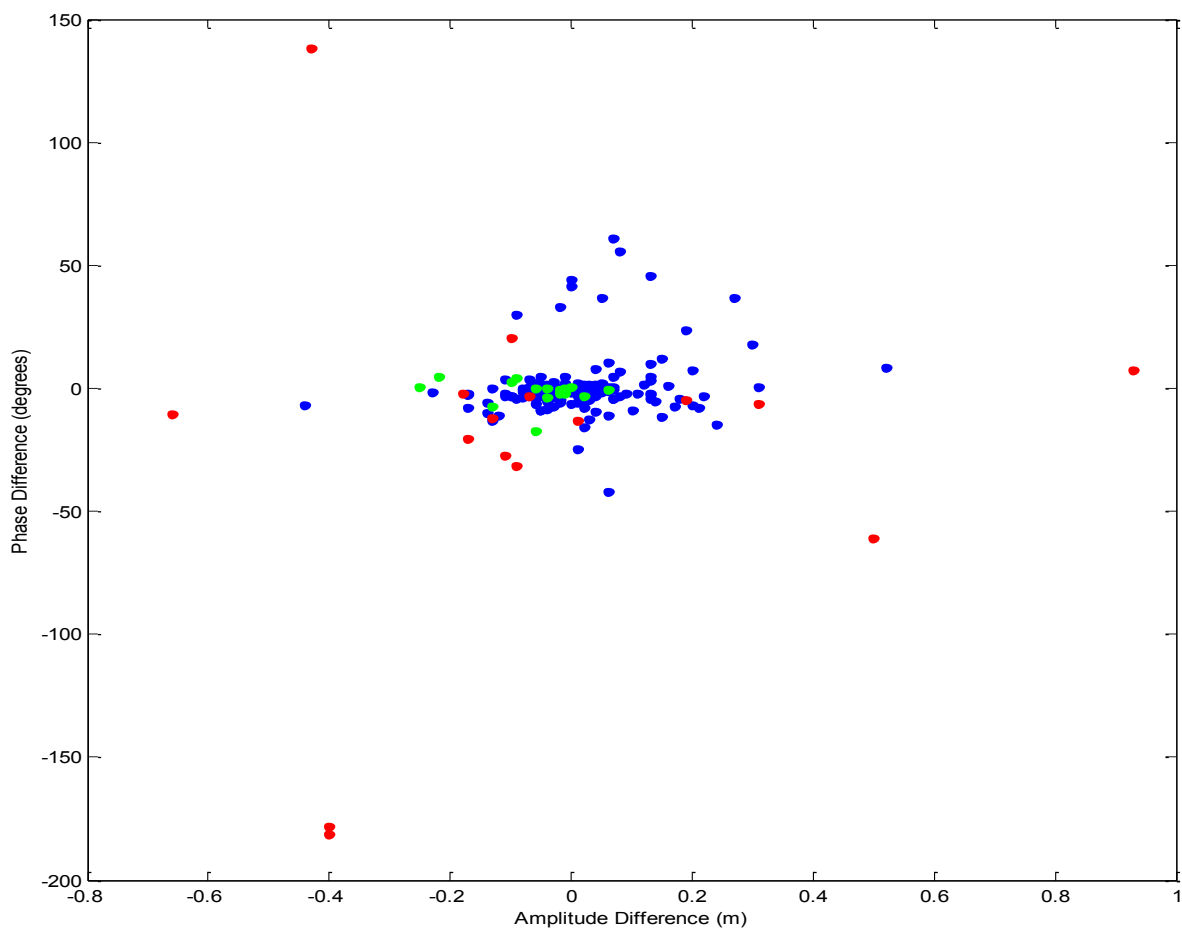


Figure 41: Scatter plot of differences (observation - simulation) in  $M_2$  tidal amplitude and phase using dataset 2. Plot colour scheme as in Figure 40.

There were 16 observation sites within this dataset which required attention due to the locations not having the necessary water depths to accurately model the  $M_2$  tidal constituent. These sites are shown below in Table 3. There were 18 observation sites which were not modelled within the simulation for dataset 2.

Table 3: Original and corrected values for dataset 2 where the simulated site does not have the requisite depth to model the  $M_2$  tidal curve without drying.

Observation Site Name	Site $h_c$ (m)	Site $g_c$	Corrected $h_c$ (m)	Corrected $g_c$	Distance (m)
Aust	0.18	197.79	4.02	202.78	650
Avonmouth	1.27	196.80	4.28	199.46	800
Barrow RI	2.18	329.22	2.97	333.34	1150
Barrow (Furness)	2.40	331.15	2.98	333.57	750
Birkenhead	2.09	317.71	3.11	323.62	350
Burry Port	1.84	170.97	2.76	171.34	500
Cardiff	3.11	189.97	3.98	191.38	550
Eastham Lock	0.55	224.53	3.16	327.20	900
Fleetwood	2.09	324.66	3.03	324.26	700
Formby	2.85	316.48	2.88	316.58	150
Hilbre Island	0.57	308.60	2.91	315.61	750
Inward Rocks	1.21	231.02	3.88	205.47	3450
Liverpool (Gladstone)	0.65	312.79	3.04	321.60	100
Liverpool (Princes)	0.40	194.07	3.08	323.28	150
Morecambe	2.40	335.42	2.86	330.73	1400
Port of Bristol	1.36	193.92	4.28	198.19	550

A mean and a root-mean-square error were calculated for both amplitude and phase for both datasets, using only those points modelled in the simulation. A further average error,  $H_s$ , the magnitude of the vector difference between observation and simulation, was also calculated. All the errors are shown in Table 4, together with the same errors from three other models of the Irish and Celtic sea regions for comparison.

Table 4: Mean and RMS errors (model minus observation) from a comparison with harmonic analysis of the  $M_2$  constituent from tide gauge data around the Irish and Celtic Seas. The Jones' values are from Jones et al. (2009), and the POLCOMS values are from Holt et al. (2001).

	Dataset 1 (59)	Dataset 2 (198)	Jones ADCIRC (198)	Jones Telemac (198)	POLCOMS (257)
Amplitude Mean (cm)	1.04	0.41	6.41	3.85	-4.99
Amplitude RMS (cm)	9.89	10.15	17.14	23.97	14.90
Phase Mean (degrees)	0.30	0.29	-1.07	0.28	-1.00
Phase RMS (degrees)	9.59	11.53	17.62	41.08	14.76
$H_s$ (cm)	11.09	14.42	31.50	36.05	21.61

Values in brackets indicate the size of the dataset.

The errors associated with the two unstructured grid models labelled as Jones are calculated using dataset 2 and, thus, are directly comparable with the present model. The POLCOMS model data come from analysis performed on a European shelf model. That model domain is not identical to the present area, although the present domain is covered by the European shelf model.

Figure 42 shows the errors associated with the  $S_2$  tidal component predictions. The same corrections were applied to the data as those applied to the  $M_2$  datasets. Again a clustering of results is seen around the origin.

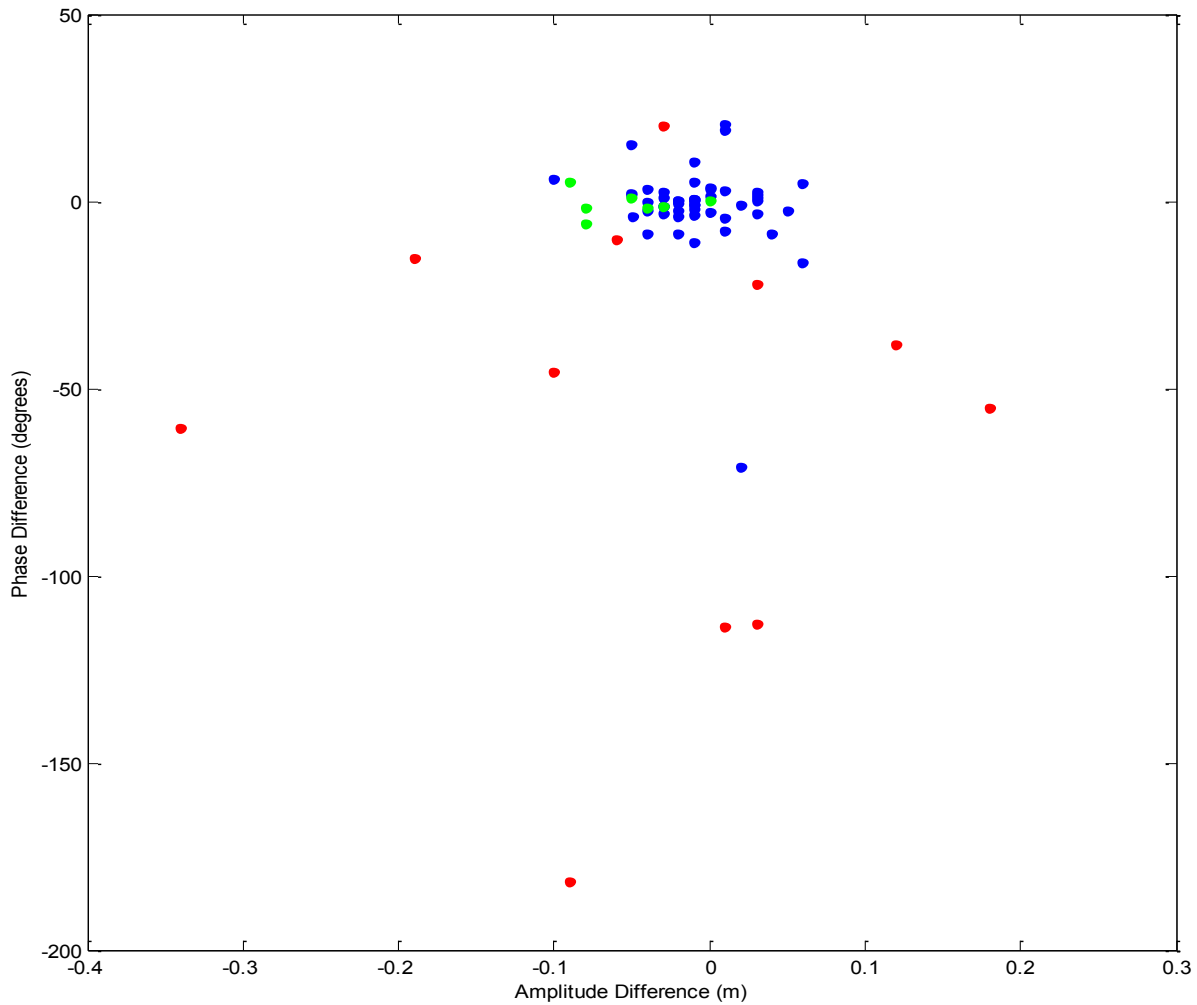


Figure 42: Scatter plot of differences (observation - simulation) in  $S_2$  tidal amplitude and phase using dataset 2. Plot colour scheme as in Figure 40.

Table 5 shows the mean, root-mean-square and  $H_s$  errors for the amplitude and phase of the  $S_2$  tidal constituent. They confirm that the model is performing well in predicting the  $S_2$  tidal component as well as the main  $M_2$  component, although the number of observation data points used for this comparison is limited.

Table 5: Mean and RMS errors (model minus observation) from a comparison with harmonic analysis of the  $S_2$  constituent from tide gauge data around the Irish and Celtic Seas.

	Amplitude Mean (cm)	Amplitude RMS (cm)	Phase Mean (degrees)	Phase RMS (degrees)	$H_s$ (cm)
POLCOMS	-3.83	7.64	5.31	22.55	12.04
Dataset 1	-1.31	3.66	-1.03	11.06	4.45

Some important baseline predictions made using the validated model are shown below. They are the amplitude and phase for the tidal components  $M_2$  and  $S_2$ , the residual currents, the bottom stress parameter and the mixing parameter, defined as  $\log_{10}(h/u^3)$ .

The co-tidal chart for the  $M_2$  tidal constituent is plotted in Figure 43. The tidal amplitude is shown in green and the phase is plotted in red. The two amphidromic points off the east and north coasts of Ireland are clearly visible. Figure 44 shows the co-tidal chart for the  $S_2$  tidal component.

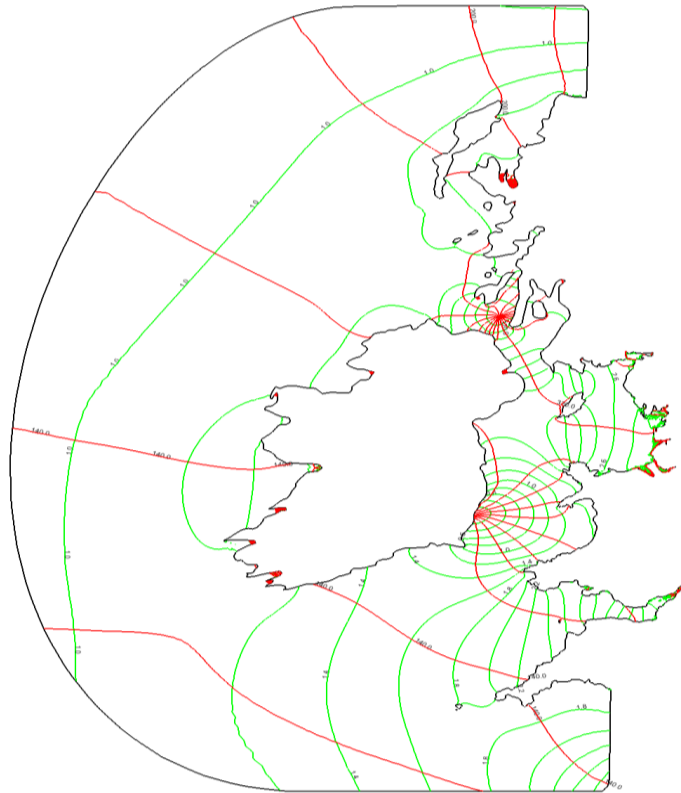


Figure 43:  $M_2$  tidal amplitude and phase co-tidal chart. Amplitudes shown in green, 20cm contours; phases in red, 20 degree contours.

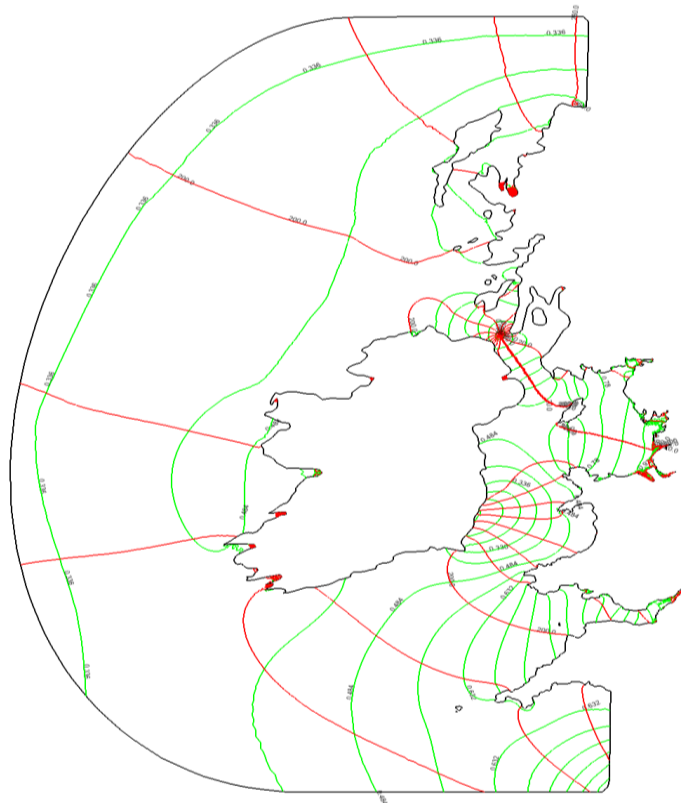


Figure 44: Contour plot of  $S_2$  amplitudes and phases. Contours as in Figure 43.

The residual currents across the domain are plotted in Figure 45. The speeds of the residual currents are plotted as the background colour and the directions are shown by the vectors. The residual currents follow a clockwise route around Ireland, and at the shelf edge they flow northwards, following the depth contours. The maximum plotted speed is 20cm/s, although a number of sites throughout the model have larger residual current speeds.

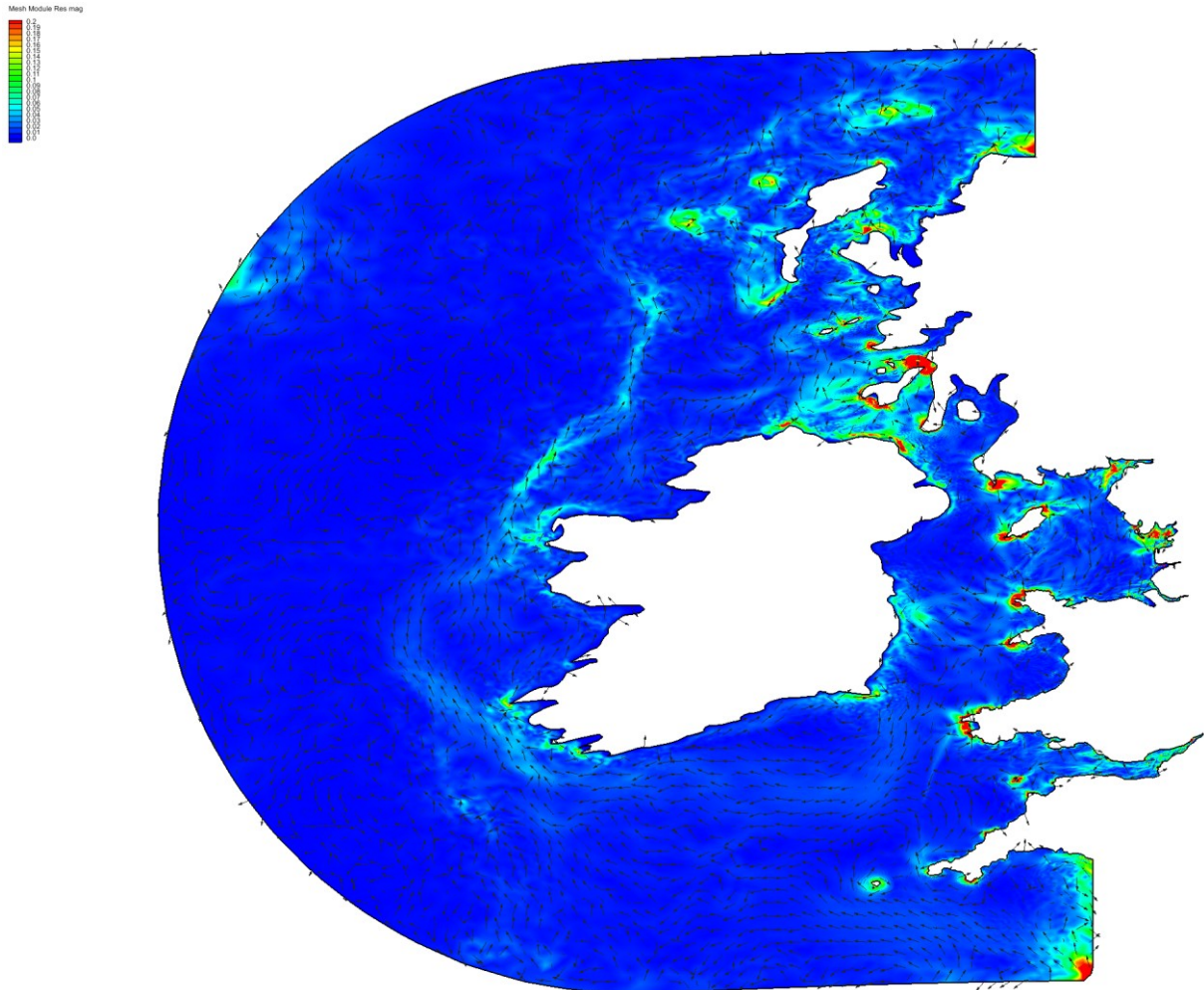


Figure 45: Residual currents within the modelled area. Maximum plotted speed is 20cm/s.

Figure 46 shows the residual currents within the Irish Sea. A number of features stand out in this plot. There is a broad southward current between the Isle of Man and the English North West, which feeds into a clockwise gyre off the north coast of Anglesey. A similar clockwise gyre can be seen off the north-east coast of the Isle of Man and a smaller anticlockwise gyre is visible south of the island. All of these features have been reported previously in a number of models of the Irish Sea; see Jones and Davies (2007). An interesting feature of the residual currents is an offshore 'jet' associated with headlands, as can be seen flowing westward from Holyhead towards Ireland.

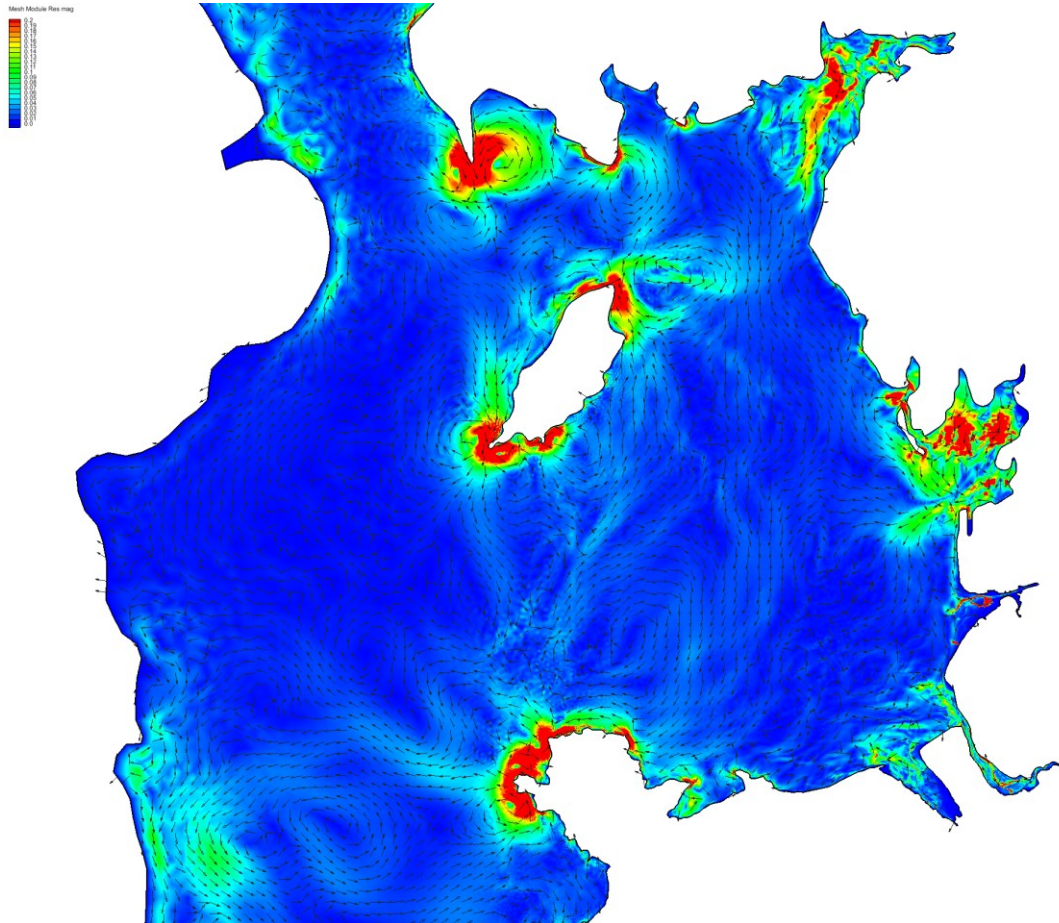


Figure 46: Residual currents within the Irish Sea.

The bottom stress parameter, shown in Figure 47, reveals the distribution of energy dissipation throughout the Irish and Celtic Seas. At the mouth of the Severn Estuary, the jump in bottom stress is clearly visible where the friction parameter is changed from  $2 \cdot 10^{-3}$  to  $3 \cdot 10^{-3}$ .

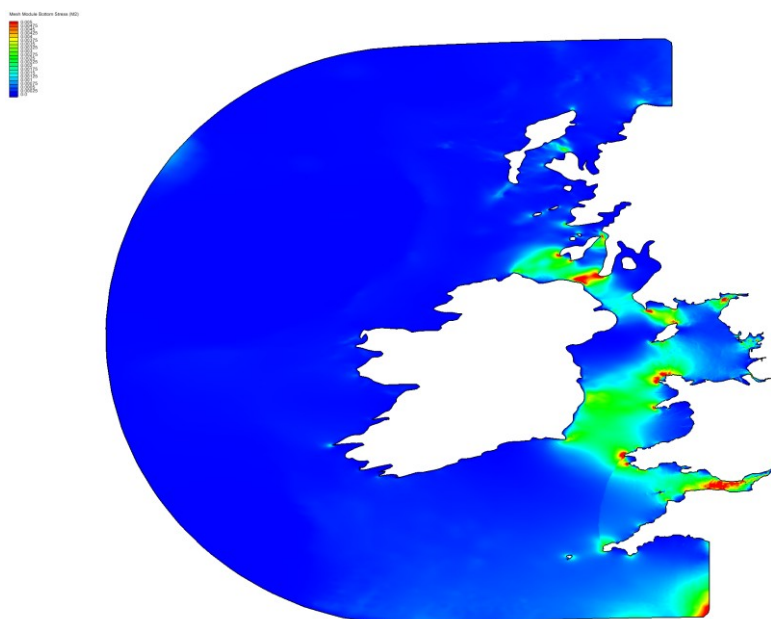


Figure 47: Plot of bottom stress. Maximum is  $5 \cdot 10^{-3}$  in 21 steps of  $2.5 \cdot 10^{-4}$ .

The stratification parameter,  $\log_{10}(h/|\mathbf{u}|^3)$ , is plotted in Figure 48. The stratification parameter shows the amount of stratification at a given location. If the parameter is larger than 3 then the water column is stratified; and if it is less than 2.4 then the water column is mixed throughout its depth. Figure 48 shows the location of tidal-induced mixing fronts in light blue. The colour scale is from 2 to 5 in 21 steps of 0.15.

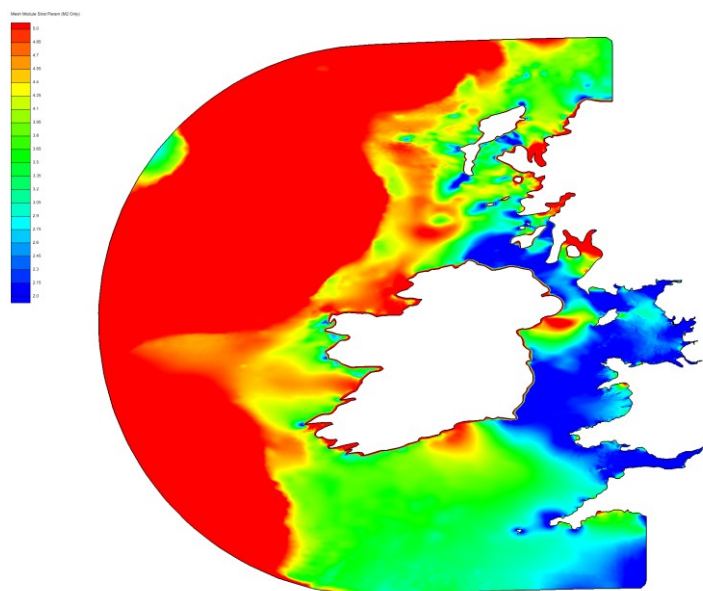


Figure 48: Contour plot of the stratification parameter  $\log_{10}(h/|\mathbf{u}|^3)$ .

### Data Tables

Tables 6, 7 and 8 contain data on the observed and simulated amplitudes and phases for tidal constituents at various sites.

Table 6:  $M_2$  tidal component at observation points in dataset 1. Observation sites marked with \* are not modelled in the grid.

No	Name	Location		$M_2$			
		Lat	Lon	Observed		Simulated	
				Amp (m)	Phase (degrees)	Amp (m)	Phase (degrees)
1	ARKLOW	52.80	-6.15	0.29	288.9	0.27	321.8
2	AUGHRIS HEAD	54.28	-8.75	1.16	155.9	1.25	156.0
3	AVONMOUTH	51.51	-2.71	4.27	200.7	4.28	199.5
4	BAGINBUN	52.17	-6.83	1.27	150.2	1.29	145.2
5	BALLYCASTLE	55.22	-6.23	0.31	230.5	0.46	242.7
6	HILBRE ISLAND	53.38	-3.22	2.92	317.5	2.91	315.6
7	BANGOR	54.66	-5.67	1.17	317.6	1.18	313.0
8	BARMOUTH	52.72	-4.05	1.45	238.9	1.43	234.0
9	BARROW BRIDGE*	52.38	-6.93	1.45	157.1	1.32	145.0
10	BARROW (FURNESS)	54.10	-3.20	3.05	330	2.98	333.6
11	BELFAST*	54.60	-5.92	1.18	315.5	0.80	136.6
12	BIRKENHEAD (ALFRED DOCK)	53.40	-3.02	3.15	323.6	3.11	323.6
13	CARLOWAY	58.27	-6.78	1.19	190	1.21	190.6
14	CASTLETOWNSEND	51.53	-9.17	1.18	139.2	1.21	138.5
15	COBH	51.85	-8.30	1.41	147.4	1.39	143.8
16	CONSLEX SA6	57.32	-9.87	1.02	169.4	1.03	169.0
17	CONWY*	53.28	-3.83	2.41	318.4	1.75	307.6
18	CORK CITY*	51.90	-8.45	1.47	123.2	1.37	143.6
19	COURTOWN	52.65	-6.22	0.14	239.4	0.05	269.3
20	DOUGLAS	54.15	-4.47	2.31	326.7	2.30	326.2
21	DUBLIN (NORTH WA)	53.35	-6.22	1.33	325.4	1.32	324.1

22	EASTHAM	53.32	-2.95	3.22	329.5	3.16	327.2
23	FISHGUARD	52.01	-4.98	1.35	207.4	1.31	205.0
24	FLATHOLM	51.38	-3.12	3.90	190	3.94	189.2
25	FLEETWOOD	53.92	-3.01	3.05	326.4	3.03	324.3
26	GALWAY	53.27	-9.05	1.53	140.5	1.55	150.0
27	GREENOCK	55.95	-4.77	1.17	346.5	1.00	340.0
28	GRIMINISH POINT	57.67	-7.48	1.20	177.1	1.27	178.8
29	HEYSHAM	54.03	-2.92	3.17	325.7	3.15	327.3
30	HINKLEY POINT	51.22	-3.13	3.91	182.6	3.87	184.3
31	HOLYHEAD	53.31	-4.62	1.81	291.9	1.77	291.4
32	ILFRACOMBE	51.21	-4.11	3.04	162.3	2.98	162.8
33	INVERGORDON*	57.68	-4.17	1.35	337.1	1.36	225.9
34	ISLAY (PORT ELLEN)	55.63	-6.19	0.16	89.1	0.16	133.0
35	KINLOCHBERVIE	58.46	-5.05	1.44	208	1.47	209.6
36	LARNE	54.85	-5.78	0.97	316.9	0.97	310.2
37	LEITH*	55.99	-3.18	1.80	55.4	2.48	23.4
38	LLANDUDNO	53.33	-3.83	2.69	309.9	2.67	309.1
39	LONDONDERRY*	55.00	-7.32	0.79	232.3	1.29	171.3
40	MACRAHANISH	55.43	-5.75	0.20	30.8	0.21	27.7
41	MALIN HEAD	55.38	-7.40	1.08	177.7	1.26	173.4
42	MILFORD HAVEN	51.71	-5.05	2.22	172.7	2.17	169.9
43	MILLPORT	55.75	-4.91	1.12	342.7	1.02	339.4
44	MORAY FIRTH*	57.60	-4.00	1.30	336.9	1.35	226.1
45	MUMBLES	51.57	-3.98	3.12	172.2	3.06	172.7
46	NEWLYN	50.10	-5.54	1.72	133.4	1.68	132.5
47	NEWPORT	51.55	-2.99	4.13	195	4.14	194.4
48	OBAN	56.41	-5.48	1.09	163.7	0.97	152.8
49	PORT ERIN	54.09	-4.77	1.83	321.7	1.78	319.9
50	PORTPATRICK	54.84	-5.12	1.34	332.2	1.27	329.9
51	PORTRUSH	55.21	-6.66	0.54	197.4	0.71	197.2
52	RINGASKIDDY	51.83	-8.32	1.43	152.3	1.39	143.8
53	RIVER SHANNON (T)*	52.58	-9.37	1.64	153.4	0.65	93.5
54	RIVER FOYLE (LIS)*	55.05	-7.27	0.77	221.3	1.09	181.8
55	ROA ISLAND	54.07	-3.17	3.06	328.6	2.95	332.2
56	ROSSAVEEL	53.27	-9.57	1.46	141.5	1.54	139.8
57	ROSSLARE	52.25	-6.35	0.56	156.9	0.73	149.5
58	ROSYTH*	56.02	-3.45	1.88	55.9	1.85	70.6
59	SCOLPAIG BAY	57.65	-7.50	1.19	176.5	1.28	178.1
60	STRANRAER	54.92	-5.03	1.10	339.2	1.29	329.9
61	STORNOWAY	58.21	-6.39	1.39	197.6	1.45	198.8
62	SWANSEA	51.62	-3.92	3.17	173.6	3.09	173.0
63	TENBY	51.67	-4.70	2.72	171.5	2.64	170.5
64	TOBERMORY	56.62	-6.06	1.30	168.6	1.42	164.5
65	TOR HEAD	55.20	-6.07	0.43	309.3	0.44	284.7
66	ULLAPOOL	57.90	-5.16	1.50	200.8	1.56	202.0
67	VALENTIA	51.88	-10.37	1.17	123.4	1.18	121.8
68	WICKLOW	53.00	-6.05	0.33	323.5	0.82	328.2
69	WORKINGTON	54.65	-3.57	2.73	332	2.72	332.2
70	YN	57.17	-10.10	1.04	167.7	1.02	167.7

Table 7: S<sub>2</sub> tidal component at observation points in dataset 1. Observation sites marked with \* are not modelled in the grid.

No	Name	Location		S <sub>2</sub>			
		Lat	Lon	Observed		Simulated	
				Amp (m)	Phase (degrees)	Amp (m)	Phase (degrees)
1	ARKLOW	52.80	-6.15	0.17	291.9	0.12	307.1
2	AUGHRIS HEAD	54.28	-8.75	0.43	188.9	0.46	189.8
3	AVONMOUTH	51.51	-2.71	1.51	260	1.51	260.3
4	BAGINBUN	52.17	-6.83	0.43	200.7	0.42	196.9
5	BALLYCASTLE	55.22	-6.23	0.14	217.8	0.15	238.6
6	HILBRE ISLAND	53.38	-3.22	0.95	0.1	0.91	358.4
7	BANGOR	54.66	-5.67	0.29	359.5	0.30	351.6
8	BARMOUTH	52.72	-4.05	0.54	277.4	0.55	272.8
9	BARROW BRIDGE*	52.38	-6.93	0.49	206.4	0.43	196.2
10	BARROW (FURNESS)	54.10	-3.20	0.98	14.3	0.89	19.5
11	BELFAST*	54.60	-5.92	0.29	358.7	0.20	176.9
12	BIRKENHEAD (ALFRED DOCK)	53.40	-3.02	1.02	8.8	0.97	9.7
13	CARLOWAY	58.27	-6.78	0.49	225	0.46	225.9
14	CASTLETOWNSEND	51.53	-9.17	0.36	175.4	0.36	176.7
15	COBH	51.85	-8.30	0.44	192.7	0.42	188.5
16	CONSLEX SA6	57.32	-9.87	0.39	203.7	0.38	203.9

17	CONWY*	53.28	-3.83	0.70	2.9	0.51	347.9
18	CORK CITY*	51.90	-8.45	0.45	167.7	0.42	187.9
19	COURTOWN	52.65	-6.22	0.14	269.6	0.11	268.4
20	DOUGLAS	54.15	-4.47	0.72	7	0.71	7.6
21	DUBLIN (NORTH WA)	53.35	-6.22	0.39	358.5	0.39	355.8
22	EASTHAM	53.32	-2.95	1.04	16.1	0.96	14.5
23	FISHGUARD	52.01	-4.98	0.53	248.4	0.50	246.9
24	FLATHOLM	51.38	-3.12	1.35	245.6	1.38	246.0
25	FLEETWOOD	53.92	-3.01	0.97	8.9	0.94	7.7
26	GALWAY	53.27	-9.05	0.56	172.7	0.55	183.3
27	GREENOCK	55.95	-4.77	0.31	38.7	0.23	32.7
28	GRIMINISH POINT	57.67	-7.48	0.45	211.2	0.48	213.6
29	HEYSHAM	54.03	-2.92	1.03	8.7	1.00	11.3
30	HINKLEY POINT	51.22	-3.13	1.40	236.8	1.36	240.1
31	HOLYHEAD	53.31	-4.62	0.59	328.7	0.57	328.7
32	ILFRACOMBE	51.21	-4.11	1.10	209.3	1.05	211.0
33	INVERGORDON*	57.68	-4.17	0.47	15.5	0.48	262.0
34	ISLAY (PORT ELLEN)	55.63	-6.19	0.14	154.2	0.15	173.4
35	KINLOCHBERVIE	58.46	-5.05	0.55	242.1	0.55	245.6
36	LARNE	54.85	-5.78	0.23	359.3	0.22	348.4
37	LEITH*	55.99	-3.18	0.61	95.7	0.69	73.7
38	LLANDUDNO	53.33	-3.83	0.87	351.1	0.85	350.4
39	LONDONDERRY*	55.00	-7.32	0.30	257.1	0.48	201.7
40	MACRAHANISH	55.43	-5.75	0.11	134	0.10	131.8
41	MALIN HEAD	55.38	-7.40	0.42	206.1	0.47	203.5
42	MILFORD HAVEN	51.71	-5.05	0.81	217.3	0.77	214.9
43	MILLPORT	55.75	-4.91	0.30	35.1	0.25	31.0
44	MORAY FIRTH*	57.60	-4.00	0.45	15.1	0.48	262.0
45	MUMBLES	51.57	-3.98	1.12	219.8	1.07	221.8
46	NEWLYN	50.10	-5.54	0.57	177.7	0.56	176.8
47	NEWPORT	51.55	-2.99	1.47	252.7	1.46	253.1
48	OBAN	56.41	-5.48	0.47	198.9	0.43	190.4
49	PORT ERIN	54.09	-4.77	0.56	1.1	0.54	358.8
50	PORTPATRICK	54.84	-5.12	0.37	16.5	0.34	13.4
51	PORTRUSH	55.21	-6.66	0.23	211.4	0.29	216.0
52	RINGASKIDDY	51.83	-8.32	0.44	197.2	0.42	188.6
53	RIVER SHANNON (T)*	52.58	-9.37	0.57	188.6	0.23	127.9
54	RIVER FOYLE (LIS)*	55.05	-7.27	0.30	247	0.42	208.6
55	ROA ISLAND	54.07	-3.17	0.98	11.8	0.88	17.7
56	ROSSAVEEL	53.27	-9.57	0.53	173.8	0.55	172.7
57	ROSSLARE	52.25	-6.35	0.24	219.8	0.28	211.0
58	ROSYTH*	56.02	-3.45	0.64	96.8	0.54	51.4
59	SCOLPAIG BAY	57.65	-7.50	0.45	211.1	0.48	212.8
60	STRANRAER	54.92	-5.03	0.29	29.6	0.35	13.1
61	STORNOWAY	58.21	-6.39	0.55	231.2	0.55	234.3
62	SWANSEA	51.62	-3.92	1.12	222.3	1.08	222.2
63	TENBY	51.67	-4.70	0.97	217.2	0.93	217.2
64	TOBERMORY	56.62	-6.06	0.53	205	0.56	201.6
65	TOR HEAD	55.20	-6.07	0.05	355	0.07	284.0
66	ULLAPOOL	57.90	-5.16	0.59	235	0.60	237.9
67	VALENTIA	51.88	-10.37	0.41	154.5	0.40	153.5
68	WICKLOW	53.00	-6.05	0.25	344.2	0.24	349.5
69	WORKINGTON	54.65	-3.57	0.87	15.5	0.85	15.7
70	YN	57.17	-10.10	0.39	202.3	0.38	202.7

Table 8: M<sub>2</sub> tidal component at observation points in dataset 2. Observation sites marked with \* are not modelled in the grid.

No	Name	Location		M <sub>2</sub>			
		Lat	Lon	Observed		Simulated	
				Amp (m)	Phase (degrees)	Amp (m)	Phase (degrees)
1	ABERDARON	-4.72	52.80	1.41	245.0	1.30	242.9
2	ABERDOVEY	-4.05	52.53	1.45	237.0	1.41	228.7
3	ABERPORTH	-4.53	52.15	1.41	218.4	1.33	217.8
4	ABERYSTWYTH	-4.09	52.42	1.51	229.5	1.41	226.3
5	AMLWCH	-4.33	53.42	2.35	305.0	2.31	303.8
6	APPLEDORE	-4.20	51.05	2.54	165.0	2.75	157.1
7	ARDMINISH BAY	-5.73	55.68	0.19	81.0	0.24	117.7
8	ARDNAVE POINT	-6.33	55.87	1.01	163.0	1.03	155.0
9	ARDROSSAN	-4.82	55.63	1.07	343.0	1.01	339.0
10	ARKLOW	-6.15	52.80	0.29	288.9	0.27	321.8
11	AUST	-2.63	51.60	4.15	210.0	0.18	197.8

12	AVONMOUTH	-2.71	51.51	4.30	200.2	1.27	196.8
13	BAGINBUN	-6.83	52.17	1.27	150.2	1.29	145.2
14	BALLYCASTLE	-6.23	55.22	0.31	230.5	0.46	242.7
15	BALTIMORE	-9.38	51.48	1.14	140.0	1.16	135.9
16	BANGOR	-5.67	54.67	1.15	317.5	1.18	313.0
17	BARMOUTH	-4.04	52.72	1.47	238.8	1.43	234.0
18	BARROW (RAMSDEN)	-3.22	54.09	3.08	330.9	3.01	334.3
19	BARROW BRIDGE*	-6.93	52.38	1.45	157.1	1.32	144.9
20	BARROW HP	-3.17	54.07	2.92	327.0	3.05	331.6
21	BARROW HS	-3.18	54.02	2.97	325.0	2.96	325.3
22	BARROW RI	-3.17	54.08	3.06	329.0	2.18	329.2
23	BARROW(FURNESS)	-3.20	54.10	3.08	331.1	2.40	331.2
24	BARRY	-3.27	51.38	3.82	186.0	3.78	186.7
25	BEACHLEY PIER	-2.65	51.62	4.17	211.0	4.00	203.0
26	BEAUMARIS	-4.10	53.27	2.54	311.7	2.63	309.5
27	BELFAST*	-5.92	54.61	1.20	316.4	0.80	135.1
28	BELFAST HARBOUR*	-5.92	54.60	1.20	314.6	0.80	136.6
29	BIRKENHEAD	-3.02	53.40	3.12	323.9	2.09	317.7
30	BIRNBECK ISLAND	-3.00	51.35	3.95	180.6	3.99	188.2
31	BOSCASTLE	-4.70	50.70	2.36	143.0	2.43	147.9
32	BRODICK BAY	-5.13	55.58	1.04	347.0	1.01	339.9
33	BRUICHLADDICH	-6.37	55.77	0.40	131.0	0.46	141.7
34	BURRY PORT	-4.25	51.67	2.80	175.0	1.84	171.0
35	BURTON PORT	-8.43	54.98	1.13	168.0	1.23	159.0
36	CAERNARVON*	-4.30	53.15	1.61	292.0	1.44	271.6
37	CAMPBELTOWN	-5.58	55.42	0.92	349.0	0.90	343.1
38	CARDIFF	-3.15	51.45	3.92	192.0	3.11	190.0
39	CARRICKFERGUS	-5.80	54.72	1.14	317.0	1.18	307.4
40	CARSAIG BAY	-5.63	56.05	0.46	109.0	0.73	145.9
41	CASTLE BAY	-7.48	56.95	1.13	174.0	1.24	171.8
42	CASTLETOWNSEND	-9.17	51.53	1.18	139.2	1.21	138.5
43	CELTIC SEA B78	-6.60	51.75	1.44	154.1	1.41	151.6
44	CELTIC SEA C78	-6.50	51.33	1.65	151.5	1.62	149.6
45	CELTIC SEA D78	-6.17	50.58	1.89	142.4	1.88	140.8
46	CELTIC SEA E78	-7.85	51.45	1.41	144.5	1.43	142.2
47	CELTIC SEA E80	-8.52	51.35	1.29	140.7	1.34	138.9
48	CELTIC SEA F78	-7.53	50.55	1.56	136.2	1.56	135.2
49	CELTIC SEA F80	-7.62	50.53	1.52	136.1	1.55	134.7
50	CELTIC SEA G78	-8.62	49.60	1.38	121.6	1.37	121.6
51	CELTIC SEA G80	-8.53	49.67	1.36	123.0	1.39	122.5
52	CELTIC SEA H78	-9.35	48.92	1.23	112.0	1.21	112.1
53	CELTIC SEA K80	-9.82	50.50	1.20	125.2	1.23	124.4
54	CELTIC SEA L80	-7.02	48.80	1.50	117.3	1.55	117.2
55	CELTIC SEA M80	-9.80	51.13	1.14	129.2	1.18	128.2
56	CLEVEDON	-2.85	51.45	4.15	196.0	4.17	194.2
57	COBH	-8.30	51.83	1.38	149.6	1.39	143.8
58	COLERAINE	-6.77	55.17	0.56	198.2	0.78	194.8
59	CONWY*	-3.83	53.28	2.41	318.4	1.75	307.6
60	CORK CITY*	-8.45	51.90	1.47	123.2	1.37	143.6
61	COULPORT*	-4.88	56.05	1.22	342.0	1.04	339.6
62	COURTOWN	-6.22	52.65	0.14	239.4	0.05	269.3
63	COVERAK	-5.08	50.02	1.63	143.0	1.65	142.3
64	CRAIGHOUSE	-5.95	55.83	0.23	85.0	0.30	145.9
65	CRAIGNURE	-5.70	56.47	1.10	167.0	0.97	153.6
66	CREETOWN	-4.40	54.87	2.33	342.5	2.46	339.7
67	CRICCIETH	-4.23	52.92	1.48	239.0	1.43	236.8
68	CROOKHAVEN	-9.72	51.47	1.09	132.9	1.10	130.7
69	CUSHENDUN	-6.03	55.12	0.59	311.0	0.62	298.4
70	DEVONPORT	-4.18	50.37	1.69	154.4	1.67	149.6
71	DOUGLAS	-4.47	54.15	2.31	326.7	2.30	326.2
72	DUBLIN (NORTH WA)	-6.22	53.35	1.34	326.1	1.32	324.1
73	E LOCH TARBERT	-5.40	55.87	1.16	346.0	1.02	340.4
74	EASTHAM LOCK	-2.95	53.32	3.22	327.2	0.55	224.5
75	FALMOUTH	-5.05	50.15	1.64	147.0	1.67	144.4
76	FANAD HEAD	-7.63	55.27	1.16	172.0	1.29	170.0
77	FISHGUARD	-4.97	52.00	1.36	207.6	1.32	205.1
78	FLATHOLM	-3.12	51.38	3.90	190.0	3.94	189.2
79	FLEETWOOD	-3.01	53.92	3.05	326.4	2.09	324.7
80	FORMBY	-3.12	53.57	3.13	315.9	2.85	316.5
81	FORT BELAN	-4.33	53.13	1.43	285.0	1.44	271.6
82	FOWEY	-4.63	50.33	1.66	148.0	1.69	147.2
83	GIRVAN	-4.87	55.25	1.05	340.0	0.97	336.1
84	GLENGARRISDALE	-5.78	56.10	1.06	163.0	0.89	160.2
85	GOUROCK	-4.82	55.97	1.17	342.0	1.00	340.0

86	GREENOCK	-4.82	55.97	1.17	342.0	1.00	340.0
87	HALFWAY SHOALS	-3.19	54.03	2.96	324.3	2.95	325.5
88	HESTAN ISLAND	-3.80	54.83	2.76	339.0	2.69	337.8
89	HEYSHAM	-2.92	54.03	3.16	325.6	3.13	327.3
90	HILBRE ISLAND	-3.22	53.38	2.92	317.5	0.57	308.6
91	HINKLEY	-3.13	51.22	3.80	184.9	3.87	184.4
92	HINKLEY POINT	-3.13	51.22	3.92	183.0	3.87	184.4
93	HOLYHEAD	-4.63	53.31	1.81	291.9	1.75	291.4
94	HOWTH	-6.07	53.38	1.38	325.0	1.38	323.1
95	HUNTERSTON	-4.83	55.72	1.09	342.3	1.02	339.2
96	ILFRACOMBE	-4.11	51.21	3.05	162.3	2.98	162.8
97	INSTOW	-4.17	51.07	2.51	172.0	2.75	157.2
98	INWARD ROCKS	-2.62	51.65	3.94	223.0	1.21	231.0
99	IONA	-6.38	56.32	1.14	165.0	1.20	153.8
100	ISLAY (PORT ELLEN)	-6.19	55.63	0.16	89.00	0.16	133.2
101	ISLE OF WHITHORN	-4.37	54.70	2.36	334.0	2.37	336.2
102	KILKEEL	-5.98	54.05	1.54	330.0	1.69	318.4
103	KILLYBEGS	-8.43	54.63	1.21	157.4	1.28	157.7
104	KINSALE	-8.52	51.70	1.30	146.0	1.34	142.8
105	LARNE	-5.78	54.85	0.97	316.6	0.97	310.2
106	LAVERNOCK POINT	-3.17	51.40	3.93	189.5	3.91	189.4
107	LITTLE HAVEN	-5.10	51.77	1.66	183.0	1.86	176.4
108	LIVERPOOL (GLADSTONE DOCK)	-3.02	53.45	3.04	321.2	0.65	312.8
109	LIVERPOOL (PRINCES DOCK)	-3.00	53.41	3.12	323.5	0.40	194.1
110	LIVERPOOL BAY	-3.25	53.48	2.62	315.0	2.93	315.3
111	LIZARD POINT	-5.20	49.95	1.62	137.0	1.65	137.7
112	LLANDUDNO	-3.82	53.33	2.68	310.1	2.67	309.1
113	LOCH BEAG	-5.60	56.15	0.61	125.0	0.80	148.8
114	LOCH INVER*	-5.25	56.15	1.46	202.0	1.03	340.3
115	LOCH RANZA	-5.30	55.72	1.07	342.0	1.01	340.2
116	LONDONDERRY*	-7.32	55.00	0.79	232.3	1.29	171.3
117	LOWERLOCHCRERAN*	-5.32	56.48	1.10	180.4	0.99	153.1
118	LUNDY	-4.67	51.18	2.58	162.6	2.56	160.0
119	MACRAHANISH	-5.75	55.43	0.20	30.80	0.21	27.7
120	MALIN HEAD	-7.40	55.38	1.08	177.7	1.26	173.4
121	MARTINS HAVEN	-5.25	51.73	1.84	180.0	1.98	174.6
122	MENAI BRIDGE*	-4.15	53.22	2.33	316.0	2.64	309.5
123	MEVAGISSEY	-4.78	50.27	1.62	151.0	1.69	146.9
124	MILFORD HAVEN*	-5.01	51.70	2.24	173.0	2.17	169.8
125	MILLPORT	-4.93	55.75	1.12	342.7	1.02	339.5
126	MINEHEAD	-3.47	51.22	3.61	179.5	3.61	177.9
127	MINEHEAD SEVEST	-3.47	51.22	3.61	179.5	3.62	178.0
128	MORECAMBE	-2.88	54.08	3.08	326.0	2.40	335.4
129	MUMBLES	-3.97	51.57	3.17	175.6	3.06	172.6
130	MUMBLES	-3.98	51.57	3.11	172.9	3.06	172.7
131	NEFYN	-4.57	52.95	1.40	269.5	1.36	267.4
132	NEW BRIGHTON	-3.03	53.45	3.06	318.8	3.03	321.2
133	NEWLYN	-5.54	50.10	1.72	133.2	1.68	132.5
134	NEWPORT	-2.98	51.55	4.20	197.6	4.15	194.4
135	OBAN	-5.48	56.41	1.09	163.7	0.97	152.8
136	OSTG	-7.00	51.05	1.63	144.2	1.60	143.0
137	OSTG	-3.22	53.50	2.90	315.6	2.94	315.8
138	OSTG-	-5.37	53.43	1.38	309.2	1.41	307.7
139	OSTG-33J	-5.78	52.07	1.12	183.8	1.07	174.9
140	PADSTOW	-4.93	50.55	2.45	149.0	2.36	145.0
141	PEEL	-4.70	54.23	1.74	318.6	1.75	319.9
142	PEMBROKE DOCK*	-4.93	51.70	2.29	174.0	2.48	169.5
143	PLYMOUTH (DEVONPORT)	-4.18	50.37	1.69	154.1	1.67	149.6
144	PORLOCK	-3.63	51.22	3.42	189.0	3.44	173.4
145	PORT APPIN	-5.42	56.55	1.13	163.0	0.99	153.1
146	PORT ASKAIG	-6.10	55.85	0.51	149.0	1.03	157.4
147	PORT DINORWIC*	-4.22	53.18	1.71	302.0	2.64	309.5
148	PORT ELLEN	-6.18	55.63	0.16	92.20	0.16	133.6
149	PORT ELLEN (ISLAY)	-6.18	55.63	0.16	92.20	0.16	133.6
150	PORT ERIN	-4.77	54.09	1.83	321.8	1.78	319.9
151	PORT ISAAC	-4.83	50.58	2.44	142.0	2.39	146.5
152	PORT MORE	-7.23	55.43	0.97	175.0	1.10	177.9
153	PORT OF BRISTOL	-2.72	51.50	4.26	201.5	1.36	193.9
154	PORT RUSH	-6.65	55.20	0.51	190.0	0.71	197.5
155	PORT ST MARY	-4.73	54.08	1.95	325.0	1.99	323.2
156	PORT TALBOT	-3.82	51.58	3.15	173.0	3.11	173.0
157	PORTAVOGIE	-5.43	54.47	1.56	316.0	1.55	316.7
158	PORTH YSGADAN	-4.65	52.90	1.38	265.0	1.30	264.4
159	PORTHCAWL	-3.70	51.47	3.17	173.0	3.22	175.0

160	PORTHGAIN	-5.18	51.95	1.33	197.0	1.41	193.6
161	PORTHLEVEN	-5.32	50.08	1.65	135.0	1.67	133.4
162	PORTNAHAVEN	-6.52	55.68	0.49	141.0	0.62	151.1
163	PORTPATRICK	-5.12	54.84	1.33	332.4	1.27	329.9
164	PORTRUSH	-6.65	55.20	0.55	196.4	0.71	197.5
165	POSITION 14	-8.58	56.02	1.12	162.8	1.14	164.1
166	PWLLHELI	-4.40	52.88	1.47	241.0	1.42	237.6
167	QUEENS CHANNEL	-3.20	53.52	2.97	316.2	2.94	316.2
168	RAMSAY	-4.37	54.32	2.62	328.0	2.39	326.6
169	RHOSSILI	-4.32	51.57	2.79	170.6	2.77	169.2
170	RINGASKIDDY	-8.32	51.83	1.43	152.3	1.39	143.8
171	RIVER YEALM	-4.07	50.30	1.63	155.0	1.66	150.0
172	ROA ISLAND	-3.17	54.07	3.06	328.6	2.95	332.2
173	ROBERTS COVE	-8.32	51.73	1.37	144.9	1.37	143.6
174	ROSCOFF	-3.97	48.72	2.68	142.2	2.62	135.6
175	ROSSLARE HARBOUR	-6.35	52.25	0.56	157.1	0.73	149.5
176	ROTHESAY BAY	-5.05	55.85	1.16	340.0	1.03	339.7
177	RUBHA BODACH	-5.15	55.92	1.00	340.0	1.02	340.2
178	RUDHA MHAIL	-6.12	55.93	1.01	162.0	1.03	157.3
179	SCARINISH	-6.80	56.50	1.18	166.0	1.24	165.0
180	SEIL SOUND	-5.58	56.30	0.65	135.0	0.95	152.7
181	SKULL	-9.53	51.52	1.10	131.0	1.13	132.7
182	SOLVE	-5.20	51.87	1.89	178.0	1.87	177.1
183	SOUTHENDKINTYRE	-5.63	55.32	0.66	337.0	0.74	343.7
184	ST IVES	-5.47	50.20	2.20	137.6	2.17	136.7
185	ST. MARY'S	-6.32	49.92	1.77	130.1	1.73	130.3
186	ST.TUDWALSROADS	-4.48	52.82	1.45	236.0	1.39	238.3
187	STACKPOLE QUAY	-4.90	51.62	2.48	167.5	2.47	169.5
188	STATION BC3	-5.02	51.42	2.33	162.3	2.29	163.7
189	STATION BC4	-5.00	50.92	2.36	149.9	2.32	151.4
190	STATION S13	-8.58	56.92	1.09	168.3	1.13	167.8
191	STD IRISH SEA	-4.12	53.77	2.36	317.2	2.39	315.7
192	STDAVIDSLBLSLIP	-5.32	51.88	1.55	187.0	1.62	183.0
193	STEEPHOLME	-3.10	51.33	3.88	186.1	3.92	187.6
194	STN B N.CHANNEL	-5.60	54.97	0.97	325.3	0.93	319.8
195	STN D N.CHANNEL	-5.73	55.87	0.26	87.0	0.39	132.6
196	STN E N.CHANNEL	-6.17	55.47	0.07	125.3	0.15	180.9
197	STN10 IRISHSEA	-3.72	53.77	2.62	318.2	2.64	317.3
198	STN34 IRISHSEA	-3.67	54.15	2.64	324.7	2.66	324.7
199	STN35 IRISHSEA	-3.92	54.65	2.56	332.8	2.56	332.8
200	SWANSEA	-3.92	51.61	3.17	172.8	3.09	173.0
201	TENBY	-4.70	51.67	2.72	171.5	2.64	170.5
202	TIGNHA BRUICH	-5.22	55.92	1.05	344.0	1.02	340.2
203	TOBERMORY	-6.08	56.62	1.29	168.8	1.42	164.5
204	TOR HEAD	-6.07	55.20	0.43	309.3	0.44	284.7
205	TREARDDUR BAY	-4.62	53.27	1.57	286.0	1.52	277.3
206	TREVOR	-4.42	53.00	1.48	272.0	1.41	270.5
207	TROON	-4.68	55.55	1.09	340.0	1.01	338.5
208	UPPERLOCHCRERAN*	-5.28	56.50	1.08	184.8	0.99	153.1
209	WATCHET	-3.33	51.18	3.62	179.0	3.74	180.5
210	WESTON-S-MARE	-2.98	51.35	4.43	195.0	3.99	188.2
211	WEXFORD	-6.45	52.33	0.49	188.0	0.55	146.0
212	WICKLOW	-6.05	53.00	0.83	323.5	0.82	328.2
213	WORKINGTON	-3.57	54.65	2.74	332.5	2.72	332.2
214	WYLFA HEAD	-4.47	53.42	2.07	300.0	2.13	300.6

## References

- Baker AC, 1991. Tidal Power, Institution of Electrical Engineers Energy Series 5, Peter Peregrinus Ltd, London.
- Egbert GD and Erofeeva SY, 2002. 'Efficient inverse modeling of barotropic ocean tides', Journal of Atmospheric and Oceanic Technology, 19(2), 183-204.
- Hench JL and Luetlich RA, 2003. 'Transient tidal circulation and momentum balances at a shallow inlet', Journal of Physical Oceanography, 33, 913-932.
- Holt JT, James ID and Jones JE, 2001. 'An s coordinate density evolving model of the northwest European continental shelf 2, Seasonal currents and tides', Journal of Geophysical Research, 106(C7), 14035-14053.

- Jones JE and Davies AM, 2007. 'On the sensitivity of tidal residuals off the west coast of Britain to mesh resolution', *Continental Shelf Research*, 27, 64-81.
- Jones, JE, Hall P and Davies AM, 2009. 'An intercomparison of tidal solutions computed with a range of unstructured grid models of the Irish and Celtic Sea Regions', *Ocean Dynamics*, 59(6), 997-1023.
- Leutlich RA and Westerink JJ, 1995. 'Continental shelf scale convergence studies with a barotropic tidal model', in *Quantitative Skill Assessment for Coastal Ocean Models* (Lynch DR and Davies AM, eds.), American Geophysical Union, 349-411.
- RSK Environmental Ltd, 2007. *Mersey Tidal Power Study: an Exploration of the Potential for Renewable Energy*, Full report, <[www.merseytidalpower.co.uk](http://www.merseytidalpower.co.uk)>.
- Sutherland G, Foreman M and Garrett C, 2007. 'Tidal current energy assessment for Johnstone Strait, Vancouver Island', *Proceedings of the Institution of Mechanical Engineers, Part A: Journal of Power and Energy*, 221(2), 147-157.